The Effect of Heterozygous Loss of Progranulin on Alzheimer's Disease

by
Craig Thomas Vollert

A dissertation submitted to the Department of Pharmacological and Pharmaceutical Sciences,
College of Pharmacy
in partial fulfillment of the requirements for the degree of

DOCTOR OF PHILOSOPHY

in Pharmacology

Chair of Committee: Jason Eriksen, Ph.D.

Committee Member: Samina Salim, Ph.D.

Committee Member: Karim Alkadhi, Ph.D.

Committee Member: J. Leigh Leasure, Ph.D.

Committee Member: Guilio Taglialatela, Ph.D.

University of Houston
July 2021

Dedicated to Champey

ACKNOWLEDGMENTS

This work would not have been possible without the help and support of many people in many ways.

First, I would like to thank my amazing wife, Mary, her unconditional love and support over the years has meant so much to me. From listening to me drivel on about research to providing advice and motivation at every turn. In many ways she is as important to this work getting done as I was. I am blessed to have her as my wife.

To my advisor, Dr. Eriksen, whose guidance and mentorship over the years has helped me realize my full potential. His support in pursuing projects and opportunities outside of this work has helped me better understand the type of scientist and person I wanted to be and then develop towards it.

To my committee members, Dr. Samina Salim, Dr. Karim Alkadhi, Dr. J. Leigh Leasure and Dr. Giulio Taglialatela, thank you for taking the time to give helpful comments and feedback that have undoubtedly improved this work. Specifically, I would like to thank Dr. Karim Alkadhi for his mentorship and guidance over the years, Dr. J. Leigh Leasure for her insightful comments and suggestions regarding behavioral and statistical analysis, and Dr. Giulio Taglialatela for his feedback and input that has helped me better analyze my results within a wider context of the literature.

My deepest gratitude to Dr. Samina Salim who gave me my first opportunity in research. From the very beginning her technical support, guidance, and trust placed on myself inspired me to pursue research and laid the foundation for the scientist that I am today and will be in the future.

To Dr. Tahir Hussain who played an instrumental part in my decision to pursue research by connecting me with Dr. Samina Salim. I still have a copy of the angiotension II book he originally loaned me in which I formed my first research hypothesis and will never forget our initial conversations that sparked my interest in research.

To Dr. C. “Chip” Raymond Knee, Dr. Amy (Bush) Amspoker, and Dr. Linsey Rodriguez for their guidance and support while pursuing research in social psychology on relationship-contingent self-esteem. Specifically, to Dr. Amspoker for her mentorship and dedication to supporting undergraduate research which taught me important lessons that I will never forget.

To Dr. Jan-Ake Gustafsson, Dr. Wanfu Wu, and Dr. Yubing Dai at the Center for Nuclear Receptors and Cell Signaling for the opportunity to rotate in their lab. Their

patience and technical guidance have helped me greatly in learning the technical aspects of immunostaining and in validating new antibodies.

To all the past and current members of Dr. Eriksens lab, especially Dr. Odochi Ohia, Saghi Montazari, Monika Schmidt, Kim Ngo, and Steven Gregory for their dedication to this and other projects in the lab.

To Dr. Maria V. Tejada-Simon and Dr. Luis Martinez whose technical guidance and assistance in electrophysiology and behavioral modeling for this work was a lifesaver.

To Dr. George L. Gerton who provided the $Grn^{+/-}$ transgenic mouse model which was the foundation for this work.

To Dr. Michael Paul Murphy and Tina L. Beckett for their technical guidance and assistance in performing Aβ Sandwich ELISA.

To all the professors in the PPS department for their teaching and guidance; administrative and animal care facility staff for their support; and all the PPS students past and present for their help and support during my study.

To my parents, Terri and Johnie Vollert, and brothers, Mark and Ryan, for their encouragement throughout my life and the opportunity to pursue higher education.

Lastly, I would like to thank the leadership at the University of Houston. Since I first arrived, the University of Houston has grown tremendously, and I have undoubtedly benefited from this. From SURF, RED labs, regional and national NSF I-Corps, Cougar Venture Fund, and Bioventures have all helped me become a better scientist.

ABSTRACT

Haploinsufficient loss of progranulin (PGRN) is implicated in both frontotemporal lobar dementia (FTD) and Alzheimer's disease (AD). Furthermore, *Grn* polymorphisms have been linked to various other neurodegenerative diseases suggesting PGRN plays an important role in neurodegenerative disease pathways. Although genetic studies have demonstrated that partial loss of PGRN increases the risk of AD there are conflicting reports in mouse studies examining the loss of PGRN and it is unclear how the loss of PGRN modulates AD pathophysiology. Therefore, the present study was designed to elucidate the effect of haploinsufficiency loss of PGRN on the pathophysiology of AD.

To this end, we characterized a novel PGRN haploinsufficient mouse model ($Grn^{+/-}$) across age. Utilizing a battery of cognitive and non-cognitive behavior tests we observed key FTD-related behavior deficits in $Grn^{+/-}$ mice across age in the absence of FTD-related pathology including neuroinflammation and TDP-43 proteinopathy as measured by immunohistochemical and western blot techniques. We observed functional deficits in $Grn^{+/-}$ mice, including impaired long-term potentiation and reduced numbers of GABAergic interneurons. Next, we investigated the role of happloinsufficiency PGRN loss on tau pathology by crossing $Grn^{+/-}$ mice with the P301S tau transgenic mouse model. There were slight differences in tau-related non-cognitive behavior deficits and reduced AT8 tau phosphorylation in the brain and spinal cord measured by western blot techniques. While we did not observe differences in microglial activation, we observed alterations in the Akt signaling pathway. Lastly, we investigated the role

of haploinsufficiency PGRN loss on amyloid pathology by crossing $Grn^{+/-}$ mice with the APdE9 amyloid transgenic mouse model. We observed exacerbated deficits in AD-related cognitive and non-cognitive behavior, including worsened cognitive learning and memory and motor coordination. We also observed biochemical and morphological changes in amyloid pathology. While we did not observe differences in microglial activation, we did observe deficits in synaptic plasticity and loss of GABAergic interneurons with loss of PGRN.

In summary, several conclusions can be drawn from the present study. First, heterozygous loss of global progranulin across age replicates critical frontotemporal dementia-related behavioral and functional deficits in the absence of detectable neuroinflammation. Secondly, heterozygous loss of progranulin reduces tau hyperphosphorylation in an Alzheimer's transgenic mouse model suggesting that loss of progranulin, at least in the context of tau pathology, may be beneficial. Lastly, heterozygous loss of progranulin exacerbates Alzheimer's disease- related behavior and amyloid-beta pathology in an Alzheimer's transgenic mouse model, suggesting that loss of progranulin, at least in the context of amyloid pathology, may be detrimental. Our results suggest a dissociation of behavioral and functional deficits from microglial activation, suggesting an essential effect of progranulin deficiency on neurons driving key FTD-related behavioral deficits and potential underlying mechanisms. While progranulin has been suggested to be a potential therapeutic target for Alzheimer's disease our results suggest this may not be the case due to differential effects on Alzheimer's' disease pathology.

TABLE OF CONTENTS

LIST OF ABBREVIATIONS

Aβ	Amyloid beta
AD	Alzheimer's disease
Akt	Protein kinase B
APdE9	APP_{SWE}/PS1dE9 amyloid transgenic mice
APdE9-$Grn^{+/-}$	APdE9 mice crossed with $Grn^{+/-}$ mice
CAA	Cerebral amyloid angiopathy
CAMKII	calmodulin-dependent protein kinase-II
CDK5	Cyclin dependent protein kinase 5
CNS	Central nervous system
CSF	Cerebral spinal fluid
CTFα	C-terminal fragment of APP after α-secretase processing
CTFβ	C-terminal fragment of APP after β-secretase processing
FAD	Familial Alzheimer's disease
FTD	Frontotemporal dementia
FTLD	Frontotemporal lobar degeneration
$Grn^{+/-}$	Progranulin haploinsufficient mice
$Grn^{-/-}$	Progranulin knockout mice
GSK-3β	Glycogen synthase kinase-3β
HFS	High frequency stimulus
LOAD	Late-onset Alzheimer's disease

LPS	Lipopolysaccharide
LTD	Long-term potentiation
MWM	Morris water maze
NCL	Neuronal ceroid lipofuscinosis
NFT	Neurofibrillary tangles
NMDA	n-methyl-D-aspartic acid
NTg	Non-transgenic
P301S	P301S tau transgenic mice
P301S-Grn$^{+/-}$	P301S mice crossed with Grn$^{+/-}$ mice
PDPK	Proline-directed protein kinase
PGRN	Progranulin
RIPA	radioimmune precipitation buffer
sAPPα	Soluble alpha-amyloid precursor protein
sAPPβ	Soluble beta-amyloid precursor protein
TDP-43	Trans-activating DNA binding protein with molecular weight 43kDa
TNF	Tumor necrosis factor

LIST OF FIGURES

CHAPTER 1: INTRODUCTION AND STATEMENT OF PROBLEM

Alzheimer's disease (AD) is the leading cause of dementia, affecting more than 35 million people worldwide (Prince et al., 2013). AD is a devastating neurodegenerative disease marked by progressive memory loss behaviorally and the accumulation of intracellular neurofibrillary tangles (NFTs) composed of hyperphosphorylated tau and extracellular amyloid-beta plaques composed of amyloid β (Aβ) in the central nervous system (Bertram et al., 2010). While Aβ is predominately only seen in AD, tau accumulation occurs in other diseases collectively known as tauopathies, including frontotemporal dementia (FTD), Pick's disease, progressive supranuclear palsy and corticobasal degeneration (Goedert and Jakes, 2005).

Due to AD and tauopathies' high societal and economic costs, there is a significant need to discover new pathways and develop new treatments that either delay or prevent disease progression. If left untreated AD is expected to become an enormous economic burden, with the cost of caring for patients with AD and dementia is expected to rise to $2 trillion by 2030. Few treatments have been approved for AD and the ones that have do not alter disease progression, and only temporarily relieving symptoms (Karakaya et al., 2012; Anand et al., 2014). There are only five FDA-approved treatments for AD and the ones that have do not alter disease progression, but only temporarily relieve symptoms associated with memory loss (Karakaya et al., 2012; Anand et al., 2014). There are no approved treatments for tauopathies. Despite many efforts towards developing disease-

modifying therapies that can block AD disease progression, drug candidates have 99.6% failure rate, one of the highest of any disease area (Cummings et al., 2014).

PGRN, a secreted pleiotropic growth factor, has been implicated in AD pathophysiology, with several studies suggesting genetic variability in PGRN is a risk factor for AD (Brouwers et al., 2008; Cortini et al., 2008; Viswanathan et al., 2009). The PGRN polymorphism rs5848, which causes up to a 20% reduction of PGRN levels, increases the risk for AD (Rademakers et al., 2008; Lee et al., 2011; Sheng et al., 2014; Xu et al., 2016). Additionally, individuals with a single base-pair deletion causing a frameshift mutation in *Grn* have been reported to have clinical presentations unique to AD, including prominent early memory impairment (Kelley et al., 2010). Lastly, *Grn* mutation carriers expressing the apolipoprotein E4 isoform have been reported to exhibit both plaques and tau-positive neurofibrillary tangles (Perry et al., 2013). Despite growing evidence that *GRN* mutations lead to neurodegeneration and affect AD via haploinsufficiency exactly how is unknown.

Loss-of-function mutations in the *GRN* gene resulting in PGRN haploinsufficiency represent a significant cause of familial frontotemporal lobar dementia (FTLD) with TAR DNA-binding protein 43-positive inclusions and has been implicated in various other neurodegenerative diseases (Baker et al., 2006; Cruts et al., 2006b; Gass et al., 2006). While the exact function of PGRN in the central nervous system remains unclear, PGRN is expressed in neurons and dynamically in microglia (Daniel et al., 2000; Daniel et al., 2003; Petkau et al., 2010). Studies using mouse models of PGRN deficiency have suggested both

neurotrophic and neuroprotective effects, with mice displaying abnormal behavioral and pathological phenotypes related to FTLD (Yin et al., 2010b; Martens et al., 2012; Petkau et al., 2012; Filiano et al., 2013).

Exactly how haploinsufficient loss of PGRN modifies AD pathophysiology remains poorly understood. Two previous studies have focused on PGRN's role in modulating neuroinflammation concerning AD (Minami et al., 2014; Takahashi et al., 2017a). Most reports studying PGRN loss have focused on PGRN's role in neuroinflammation with $Grn^{-/-}$ mice exhibiting increased proinflammatory cytokines and increased microglial activation (Yin et al., 2010b; Martens et al., 2012; Petkau et al., 2012). Increased inflammation has long been implicated in the pathogeneses of AD and other neurodegenerative diseases, with PGRN expression being positively correlated with both dense-core and amyloid plaques in surrounding microglia (Akiyama et al., 2000; Wyss-Coray, 2006; Pereson et al., 2009). Regarding amyloid pathology, conflicting reports exist with the effect of PGRN loss. In one study, an increase in Aβ plaques was observed in transgenic AD mice after microglial specific PGRN loss, and a reduction in plaque load was observed after the overexpression of total PGRN levels suggesting that loss of PGRN exacerbated Aβ pathology (Minami et al., 2014). However, in another study, an unexpected reduction of diffuse Aβ plaques was observed after PGRN loss via upregulation of TYROBP network genes suggesting that loss of PGRN may be beneficial (Takahashi et al., 2017a). The effect of PGRN loss on tau pathology is equally not well understood. In the same study, loss of PGRN loss was shown to increase tau AT8 and AT180 phosphorylation in $Grn^{-/-}$ mice compared to non-

transgenic (NTg) mice that expressed human P3001L tau 1-441 via an adeno-associated virus vector. This result is supported by a previous report showing increased tau phosphorylation in the same mouse model with partial loss of PGRN (Hosokawa et al., 2015). However, how the loss of PGRN modifies AD amyloid and tau pathology is unknown.

In this dissertation, we investigated the role of PGRN in AD pathology and specifically how haploinsufficient, rather than complete loss, PGRN affects tau and amyloid pathology. The central hypothesis is that haploinsufficiency loss of PGRN in neurons and microglia worsens AD-associated behavioral abnormalities, the accumulation of NFTs composed of hyperphosphorylated tau, and extracellular amyloid plaque deposition. We examined three hypotheses: (1) Happloinsufficient loss of PGRN causes FTD-related behavioral deficits during aging in the absence of neuroinflammation, (2) PGRN haploinsufficiency worsens motor deficits and increases tau phosphorylation in the P301S tau transgenic mouse model, and (3) haploinsufficiency loss of PGRN worsens amyloid-related behavioral deficits and increases amyloid plaque deposition in the APdE9 amyloid transgenic mouse model.

To test these hypotheses, we crossed $Grn^{+/-}$ mice, which have a global herterozygous reduction of PGRN with the P301S tau transgenic mouse model overexpressing the P301S mutant human tau associated with clinical cases of neurodegenerative tauopathy and the APP_{Swe}/PSEN1dE9 (APdE9) amyloid mouse model expressing human APP with the Swedish mutant and human PSEN1 lacking exon 9. While $Grn^{-/-}$ mice have predominately been used to study PGRN

deficiency we opted to use a $Grn^{+/-}$ mouse model instead. Although $Grn^{-/-}$ mice replicate some FTLD-related pathology, such as microgliosis, both $Grn^{-/-}$ and $Grn^{+/-}$ mice display key FTD-related behavior abnormalities (Yin et al., 2010b; Roberson, 2012; Filiano et al., 2013). In humans, mutations causing PGRN haploinsufficiency have only been shown to cause FTLD, whereas mutations causing complete loss of PGRN causes neuronal ceroid lipofuscinosis suggesting different disease outcomes, which has been corroborated with mouse studies (Smith et al., 2012; Tanaka et al., 2014). Behavioral and signaling differences have been reported between the two models with $Grn^{+/-}$, but not $Grn^{-/-}$ mice, showing social dominance and mTORC2/Akt signaling abnormalities (Arrant et al., 2016). Therefore, $Grn^{+/-}$ mice may be a better mouse model for modeling human PGRN-related FTD.

In this study, we first phenotypically characterized a novel $Grn^{+/-}$ mouse model across aging looking at critical cognitive and non-cognitive FTLD-related behaviors and FTLD-related pathology. We then studied PGRN haploinsufficiency's effect on AD by crossing the $Grn^{+/-}$ mouse model with the P301S tau transgenic model and the APdE9 tau transgenic mouse model. We measured AD-related cognitive and non-cognitive behaviors associated with respect to tau and amyloid pathologies for both models. We then investigated the effect of PGRN loss on tau and amyloid pathology using western blots, immunohistochemistry, and immunofluorescence techniques. *In vitro* extracellular

recordings were performed in the hippocampal slices to determine the effect of PGRN loss on long-term potentiation (LTP).

The research presented here aims to elucidate further the role of PGRN in AD and neurodegenerative disease in general. By understanding the effects of PGRN haploinsufficency on AD pathophysiology and identifying mechanisms by which PGRN modulates AD disease progression, we may help develop novel strategies that will improve the treatment of patients with AD and other neurodegenerative diseases.

CHAPTER 2: REVIEW OF LITERATURE

2.1 Alzheimer's Disease

In 1907 the first of two reports describing two patients with pre-senile dementia, "*A Characteristic Disease of the Cerebral Cortex,"* was published by the German psychiatrist Alois Alzheimer(Alzheimer, 1907). This two-page article and his later publication *"On Certain Peculiar Diseases of Old Age"* described the clinical and neuropathological history of Auguste D. and Johann F., who were both patients that were admitted to Alzheimer's care for pre-senile dementia (Alzheimer, 1911). In both patients, Alzheimer described profound memory impairment coupled with agnostic, aphasic, and apractic deficits. In addition to behavioral abnormalities, both patients also had pathological hallmarks, including small extracellular "military foci" and dense intracellular "bundles of fibrils" (Alzheimer, 1907, 1911).

Alzheimer's disease (AD) is a chronic neurodegenerative disease and the most common type of dementia, accounting for approximately 70% of all cases and affecting more than 35 million people worldwide (Burns, 2009; Prince et al., 2013). Behaviorally AD is marked by progressive memory loss with neuropsychiatric symptoms including depression, apathy, aggression, and psychosis appearing later as the disease progresses (Lyketsos et al., 2011; Li et al., 2014). Neuropathologically, AD is characterized by two hallmark lesions: the accumulation of intracellular neurofibrillary tangles (NFTs) composed of hyperphosphorylated tau and extracellular amyloid plaques composed of amyloid-

beta (Aβ) in the central nervous system (Bertram et al., 2010). The degree of cognitive decline parallels with the propagation and pathological distribution of the hallmark lesions that characterize AD (Braak and Braak, 1994; Gomez-Isla et al., 1996). For instance, during the early stages of AD, lesions are primarily confined to the transentorhinal area and CA region of the hippocampus and selectively impair recognition, language comprehension, and visuospatial perceptions while sparing motoric and sensory functions (McKhann et al., 1984). However, in the later stages of AD, legions extend to the isocortex leading to motoric and sensory deficits.

2.2 Tau Pathology in AD and tauopathies

2.2.1 Tau in the healthy brain

Tau is one of three major microtubule-associated proteins, and its primary function in the normal brain is the promotion of the assembly of tubulin into microtubules and the stabilization of the resulting structure (Weingarten et al., 1975). In the human brain, tau has six different molecular isoforms coded by a single gene on chromosome 17 and generated by alternative splicing (Goedert et al., 1989; Himmler et al., 1989). Tau isoforms differ from each other only by the exclusion or inclusion of exon 10 in the carboxy-terminal half and the presence or absence of a 29 amino acid or 58 amino acid insert in the amino-terminal half. The exclusion of exon 10 in tau results in three isoforms with three repeats each, and the inclusion of exon 10 results in the three different isoforms with four repeats each. The repeats are the primary microtubule-binding domain for tau, and experimentally the four repeat isoforms better promote microtubule assembly

versus three repeat isoforms (Goedert and Jakes, 1990). In non-diseased brain there are similar levels of both three and four repeat isoforms.

2.2.2 Genetics of tau in tauopathies

To date, there no known reported tau mutations in AD, but mutations in tau have been reported in other tauopathies. Mutations in tau are predominately limited to frontotemporal dementias, characterized by neurodegeneration in only the frontal and temporal lobes of the cerebral cortex. In 1994, an autosomal dominantly inherited form of frontotemporal dementia with Parkinsonism was linked to chromosome 17q21.2, which later combined with the observations of other familial forms of frontotemporal dementia being linked to this region resulting in frontotemporal dementia and parkinsonism linked to chromosome 17 (FTDP-17) (Wilhelmsen et al., 1994). The pathological accumulation of hyperphosphorylated tau marks all cases of FTDP-17. Over 32 different tau mutations were reported in more than 100 families with FTDP-17, with the first being reported in 1998 (Hutton et al., 1998; Poorkaj et al., 1998; Spillantini et al., 1998). Mutations in tau consist of either missense, deletion, or silent mutations.

Mutations in tau can be broadly separated into two categories: mutations that have a primary effect at the protein level and ones that affect tau pre-mRNA's alternative splicing. Except for mutations in exon 10 of Tau, which affect both the protein and RNA levels, most Tau mutations only affect one (D'Souza et al., 1999; Yoshida et al., 2002). Most missense mutations decrease tau's ability to bind to microtubules, which results in mutant tau's reduced ability to promote microtubule assembly (Hasegawa et al., 1998; Hong et al., 1998). While a few missense

mutations have been shown to increase tau's ability to promote microtubule assembly, the vast majority of missense mutations cause varying degrees of reduced microtubule binding and stability (Delobel et al., 2002). Missense mutations in tau have also been suggested to cause FTDP-17 by promoting tau protein aggregation (Nacharaju et al., 1999). A growing number of studies have demonstrated that missense mutations in tau promote tau hyperphosphorylation, with P301L and P301S mutations being the most prominent (Goedert et al., 1999).

2.2.3 Hyperphosphorylation of tau

In AD and other tauopathies, tau protein is abnormally hyperphosphorylated, and this phosphorylated tau is the major component of neurofibrillary tangles and is associated with neurodegeneration (Grundke-Iqbal et al., 1986; Lee et al., 1991). The hyperphosphorylation of tau is thought to precede the accumulation of tau protein into neurofibrillary tangles with different phosphorylation sites have been identified and used as markers for progression of tau pathology (**Fig. 1**) (Grundke-Iqbal et al., 1986). Pre-neurofibrillary tangles are primarily comprised by phosphorylation at Thr231 stained by the antibody AT180, while neurofibrillary tangles composed of filamentous tau is marked by phosphorylation at Thr212/Ser214 (AT100) and Ser202/Thr205 (AT8) in AD (Augustinack et al., 2002). Quantitative immunohistochemistry studies have revealed tau deposits of only abnormally phosphorylated tau, but not normal tau in AD brains, suggesting phosphorylation is a prerequisite for aggregation (Bancher et al., 1989; Bancher et al., 1991). Pathogenically, hyperphosphorylation is believed to make tau more resistant to proteolysis, making phosphorylated tau's

turnover severalfold slower than wild type tau and promoting aggregation (Wang et al., 1995; Wang et al., 1996).

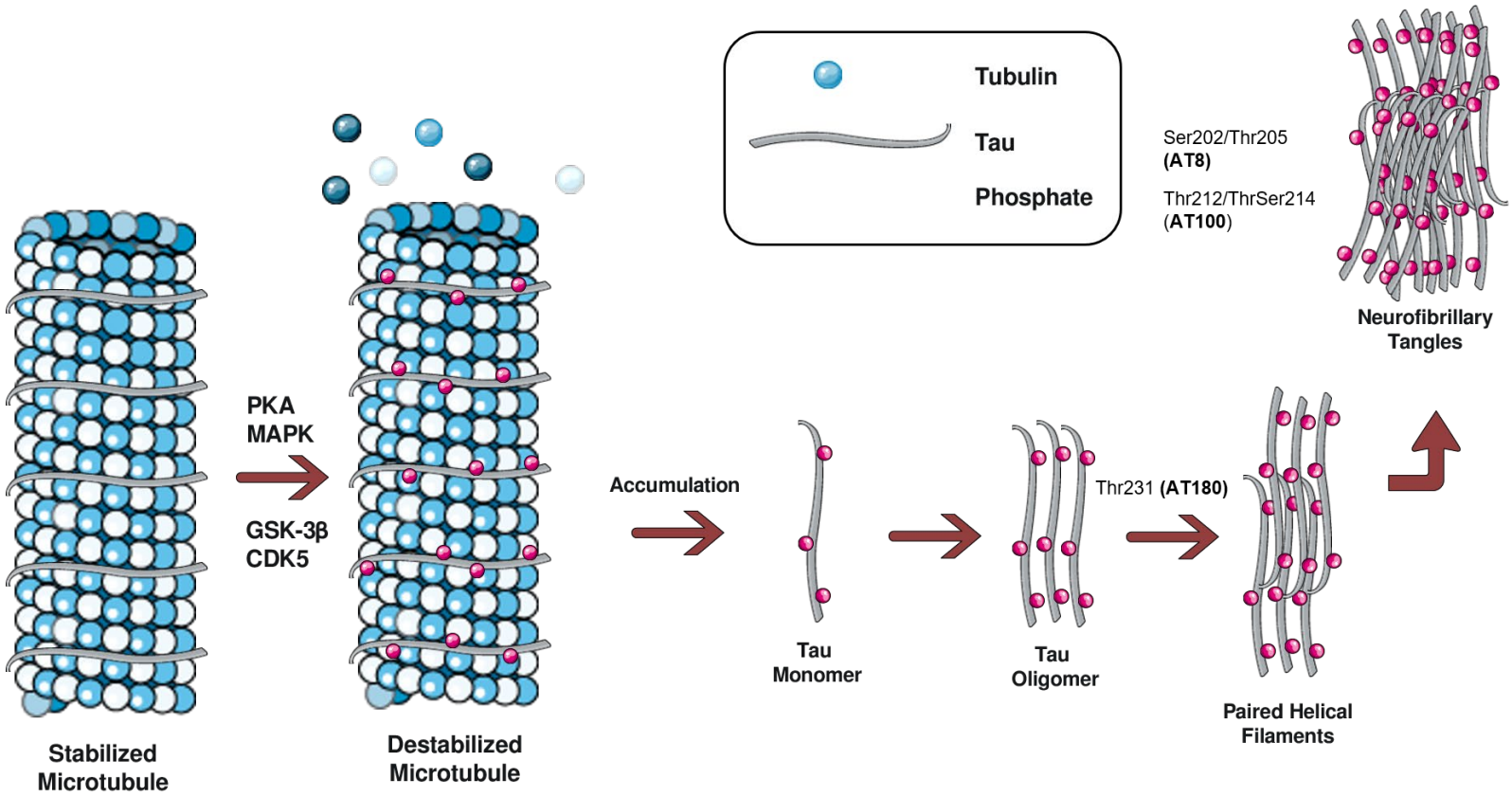
Tubulin
Tau
Phosphate
Ser202/Thr205
(AT8)
Thr212/ThrSer214
(AT100)
Neurofibrillary
Tangles
PKA
MAPK
GSK-3β
CDK5
Stabilized
Microtubule
Destabilized
Microtubule
Accumulation
Tau
Monomer
Tau
Oligomer
Thr231 (AT180)
Paired Helical
Filaments

Fig. 1. Illustration of neurofibrillary tangle formation by tau hyperphosphorylation. Stabilization of microtubule-associated tau protein is controlled by kinases. Hyperphosphorylation of tau proteins results in destabilized microtubules due to the detachment of phosphorylated tau monomers. Phosphorylated tau monomers aggregate into cytoplasmic insoluble tau oligomers, which then accumulate to form paired helical filaments and is associated with phosphorylation at threonine 231 (AT180). Paired helical filaments then begin to aggregate ultimately leading to the formation of neurofibrillary tangles associated with phosphorylation at serine 202 and threonine 205 (AT8) and threonine 212 and serine 214 (AT100).

Like other phosphoproteins, the level of phosphorylation of tau is a function of the activity levels of kinases and phosphatases that regulate phosphorylation. In non-diseased states, normal tau contains two or three phosphate groups. however, in AD, hyperphosphorylated tau contains between 5 and 9 mol of phosphate per mole of the protein (Tomlinson et al., 1970). Over 45 different serine/threonine residues have been reported to be phosphorylated in AD, and several essential protein kinases have been identified (Singh et al., 1994; Morishima-Kawashima and Kosik, 1996; Hanger et al., 1998). Among the identified kinases involved in the abnormal hyperphosphorylation of tau, the most prominent is glycogen synthase kinase-3 beta (GSK-3β), cyclin-dependent protein kinase-5 (CDK5), protein kinase A (PKA), mitogen-activated protein kinase ERK ½, calcium and calmodulin-dependent protein kinase-II (CaMKII) (Pei et al., 2003). Tau is primarily phosphorylated at proline-directed sites consisting of a serine/threonine followed by proline sites for proline-directed protein kinases (PDPKs). All major PDPKs, GSK3-β, CDK5, and ERK ½, have been shown to phosphorylate tau at many phosphorylation sites seen in the AD brain (Wang et al., 2013).

The two most prominent PDPKs in phosphorylating tau are GSK-3β and CDK5, which share many of the same phosphorylation sites (Wang et al., 1998; Liu et al., 2002). The expression for both GSK-3β and cdk5 is high in the brain, and activity is associated with all neurofibrillary pathology stages (Woodgett, 1990; Tsai et al., 1993; Pei et al., 1998; Pei et al., 1999). In both cell cultures and transgenic mouse models, the overexpression of GSK-3β has been shown to increase tau phosphorylation in similar patterns seen in AD (Lovestone et al., 1996;

Spittaels et al., 2000; Lucas et al., 2001). Additionally, the inhibition of GSK-3β activity by lithium chloride has been shown to attenuate tau phosphorylation, further iterating the importance of GSK-3β activity on tau hyperphosphorylation (Stambolic et al., 1996; Hong et al., 1997; Perez et al., 2003). Cdk5 phosphorylates approximately 9-13 sites, and its activation requires the interaction of its regulatory subunit p39 or p35 or their proteolytic products p29 or p25 (Lew et al., 1994; Tsai et al., 1994). Phosphorylation of tau by cdk5-p35 is generally considered physiological, but phosphorylation by cdk5-p25 is considered pathological (Kimura et al., 2014). Incongruence with this, the overexpression of p25 in transgenic mice has been reported to increase the activity of cdk5 and the hyperphosphorylation of tau (Cruz et al., 2003; Noble et al., 2003).

Unlike GSK-3β and cdk5, non-PDKs have been shown only to phosphorylate tau at a few sites. PKA and MARK kinase has been reported to phosphorylate tau at Ser-262 and PKA additionally at Ser-214, Ser-217, Ser-396/404, and at Ser-416 (Brandt et al., 1994; Litersky et al., 1996; Drewes et al., 1997). Additionally, CaMKII has been reported to phosphorylate tau at Ser-262/356 and at Ser-416 (Singh et al., 1996; Sironi et al., 1998; Bennecib et al., 2001). Interestingly, while non-PDPKs phosphorylate tau at fewer sites than PDPKs the phosphorylation of tau by non-PDPKs appears to prime tau for

phosphorylation tau by the PDPKs GSK-3β and cdk5 (Singh et al., 1995; Wang et al., 1998; Cho and Johnson, 2003).

2.2 Amyloid Pathology in AD

Amyloid precursor protein (APP) is a glycoprotein embedded in the membrane of neuronal cells, protruding both outside and inside the cell. APP comprises a large N-terminal extracellular domain, a short hydrophobic transmembrane domain, and a short intracellular C-terminal domain. APP's exact role in the normal brain is unclear, but a growing amount of evidence suggests that APP is important in developmental and postnatal neurological functions (Pearson and Peers, 2006). While the normal function of APP is unknown mutations in APP and proteins that process APP suggest that alterations in APP processing and Aβ production is an essential aspect of familial Alzheimer's disease (FAD) pathophysiology (Drewes et al., 1997) and is the primary component of amyloid plaques (Yankner and Mesulam, 1991; Haass et al., 1992; Seubert et al., 1992; Shoji et al., 1992).

APP is a type 1 integral membrane protein and undergoes alternative splicing to produce eight APP isoforms. The most abundant and amyloidogenic isoforms are APP695, APP751, and APP770, possibly due to all three containing the same Aβ, intracellular and transmembrane domains (Kitaguchi et al., 1988; Palmert et al., 1988; Sandbrink et al., 1994). The relative expression of the APP splice forms varies from tissue to tissue, indicating differential regulation of mRNA processing and stability (Ponte et al., 1988). For example, the APP751 isoform is

distributed among various brain regions, and the APP695 isoform is predominately expressed in neuronal cells in the cortex (Tanzi et al., 1988).

2.2.1 Amyloid processing and plaque formation

APP is processed by two different sets of enzymes, leading to a non-pathogenic pathway and the other set leading to a pathogenic pathway (**Fig.2**). Approximately 90% of APP is processed through the non-pathogenic pathway with the remaining 10% entering the pathogenic pathway (Thinakaran and Koo, 2008). Mutations in APP and related processing proteins and environmental factors can alter these ratios.

In the non-pathogenic pathway, APP is cleaved first by the α-secretase resulting in a soluble N-terminal fragment (sAPPα) and a C-terminal fragment (CTFα). The function of sAPPα is unclear but may involve synaptogenesis, neurite outgrowth, and neuronal survival (Selkoe, 2001). The CTFα fragment is retained in the membrane where it is cleaved by the presenilin-containing γ-secretase yielding a

Amyloid Plaques
Aβ
AICD
γ-secretase
sAPPβ
CTFβ
β-secretase
APP
α-secretase
CTFα
sAPPα
γ-secretase
AICD
p3

Fig. 2. Illustration of the amyloid precursor protein (APP) processing pathway. The APP protein can by processed by two pathways depending on the proteinase: the nonamyloidogenic pathway if processed first by α-secretase and the amyloidogenic pathway if processed first by β-secretase. In the nonamyloidogenic pathway, α-secretase cleaves in the middle of amyloid beta (Aβ) region releasing the soluble APP-fragment (sAPP-α), followed by the γ-secretase resulting in the release of the P3 fragment and APP intracellular domain (AICD). In the amyloidogenic pathway, β-secretase cleaves APP above the Aβ region releasing the soluble APP-fragment (sAPP-β) resulting APP-CTF99 (CTFβ). CTFβ is then cleaved by γ-secretase resulting in various Aβ species (Aβ40, Aβ42, etc.) which then aggregate ultimately resulting in amyloid plaques.

soluble N-terminal fragment (p3) and a membrane-bound C-terminal fragment (AICD).

In the pathogenic pathway, APP is instead first cleaved by the β-secretase resulting in a soluble N-terminal fragment (sAPPβ) and a membrane-bound C-terminal fragment (CTFβ). The CTFβ fragment is then cleaved by the γ-secretase resulting in an AICD fragment and a soluble N-terminal fragment (Aβ). Although Aβ is necessary for neuronal function and inhibition of long-term potentiation, it can accumulate in blood vessels and the brain's parenchymal, where it can aggregate into amyloid plaques found in AD. Interestingly, β-secretase activity has been reported to increase with aging in human, monkey and mouse brains suggesting that aging alone increases the pathogenic processing of APP (Fukumoto et al., 2004).

Unlike other APP fragments, Aβ considered 'sticky' and can self-aggregate into extracellular plaques by a multi-step polymerization process (Thinakaran and Koo, 2008). First, Aβ aggregates into oligomers, which in turn cluster together with a β-sheet structure forming fibrils. Lastly, fibrils aggregate together, making mats, which further aggregate with other proteins, forming diffuse then dense-core amyloid plaques (Sheng et al., 1997). The aggregation of Aβ into amyloid plaques is influenced by several factors, including the concentration of Aβ, neuronal activity and synaptic release, and the activity of level of α-secretase and β-secretase, among others (Selkoe, 2001).

Aβ cleavage products can differ in length between 36 and 43 amino acids. While a variety of Aβ fragments are generated, the two most important with regards

to AD is the Aβ fragment ending at amino acid 42 ($A\beta_{42}$) and Aβ fragment ending at amino acid 40 ($A\beta_{40}$). $A\beta_{42}$ is considered the most pathogenic of Aβ species with mutations favoring the production of $A\beta_{42}$ linked to familial AD (Thinakaran and Koo, 2008).

2.2.2 Genetic evidence implicating Aβ in AD

Unlike mutations in tau there is a considerable and growing amount of genetic evidence suggesting that either the increase in amyloid production or aberrant processing of APP is linked to AD's development. Initial genetic evidence linking amyloid to familial causes of dementia was not in patients with AD but patients with Down's syndrome. The APP gene is located on chromosome 21, and patients with Down's syndrome having a third copy of chromosome 21 develop typical AD neuropathology, presumably due to the increased production of Aβ. Interestingly, individuals with translocation Down's syndrome with only the distal part of chromosome 21 not containing the APP gene have Down's features but not AD neuropathology (Prasher et al., 1998). Furthermore, individuals who have the APP gene segment duplicated but not the rest of chromosome 21 do not develop Down's features but typically develop AD in their 50's (Rovelet-Lecrux et al., 2006). Conversely, the APP missense mutation A673T results in the lifelong decrease of APP cleavage by the β-secretase resulting in the decrease of the amyloidogenic cleavage of APP, effectively decreasing the production of Aβ (Jiang et al., 2014).

Patients with the A673T mutation have a lower risk of developing AD neuropathology and cognitive decline (Kero et al., 2013).

The first mutation discovered in APP capable of causing dementia is the E693Q Dutch missense mutation, where mutation carriers develop a severe hereditary form of cerebral amyloid angiopathy (CAA) that is separate from AD (Levy et al., 1990). A handful of mutations in APP causative for FAD were discovered one year later, including V7171 London and V717F Indiana mutations (Goate et al., 1991; Murrell et al., 1991). In general, APP mutations can be categorized either as causative for CAA or FAD with several unique differences. Mutations causative for CAA is located in the central region of APP and promote fibril formation by changing the charge distribution, likely affecting peptide structure (Miravalle et al., 2000; Baumketner et al., 2008). Unlike FAD mutations, CAA causative APP mutations do not increase the production of Aβ, but some mutations, most notably the Dutch mutation, have been reported to make the APP peptide less efficiently degraded (Morelli et al., 2003). Unlike CAA causative mutations, FAD mutations are typically clustered around the proteolytic processing of APP into Aβ by the β-secretase and γ-secretase enzymes (Weggen and Beher, 2012). Possibly the most well described APP FAD mutation at the β-secretase site is the KM670/671NL Swedish mutation, which increases total Aβ secretion (Citron et al., 1992; Cai et al., 1993; Citron et al., 1994) . Mechanistically the Swedish mutation and other mutations associated with the β-secretase increase APP's affinity for the beta-secretase resulting in increased Aβ species' increased production (Vassar et al., 1999). FAD mutations that occur distal to the γ–

secretase, unlike mutations occurring around the β–secretase cleavage site, typically elevate the Aβ42/Aβ40 ratio (Bergman et al., 2003; Hecimovic et al., 2004). Although it is not clear exactly how FAD mutations increase the Aβ42/Aβ40 ratio, the γ–secretase cleaves APP into a variety of different Aβ peptide species (Aβ38, Aβ39, Aβ40, Aβ42, and Aβ43), and it has been postulated that the FAD mutations make the production of the Aβ42 cleavage more favorable (Weggen and Beher, 2012). Interestingly, the A673T APP missense mutation decreases the affinity for APP cleavage by the γ–secretase resulting in a lower risk of clinical AD and age-related cognitive decline (Jonsson et al., 2012).

Most identified FAD mutations are in the *PSEN1* gene on chromosome 14. Since the first mutations identified in *PSEN1* and *PSEN2* in 1995, over 180 different pathogenic mutations have been identified (Sherrington et al., 1995; Weggen and Beher, 2012). PSEN proteins form the catalytic core of γ-secretase which catalyzes the last step in the cleavage and generation of Aβ peptides from APP (De Strooper, 2010). While PSEN mutations have been postulated to have both γ-secretase-dependent and –independent effects the most consistent feature of PSEN mutations is the increase ratio of Aβ42/Aβ40 that is caused by either increase in Aβ42 levels with decreased A40, increased A42 with unchanged A40 or unchanged A42 with decreased A40 (Weggen and Beher, 2012). Although PSEN mutations were at first considered to be gain-of-function due to the elevation of Aβ42 production subsequent work has shown that overall γ-secretase activity

may be decreased compared to wild type as evidenced by PSEN mutations reducing NICD production representing a loss-of-function (Song et al., 1999).

Several genome-wide association studies have highlighted new genes that might be risk factors for late-onset AD (LOAD). Specifically, three types of processes have emerged as biologically relevant to AD's pathogenesis including cholesterol/sterol metabolism, endosomal vesicle recycling, and the brain's innate immune system and inflammation. Of importance is the role of the immune system in AD pathophysiology. The immune system has long been implicated in AD due to the early observation that multiple components of the classical complement cascade are present in and around amyloid plaques most likely due to the presence of microglia (McGeer et al., 1989). Only recently have genetic reports emerged implicating genetic variability in microglia-specific genes associated with LOAD implicating microglial clearance of Aβ as an essential function; genetic risk factors for AD included polymorphisms in CD33 (Bertram et al., 2008; Hollingworth et al., 2011b; Naj et al., 2011), CLU, complement receptor 1 (Lambert et al., 2009), TREM2 (Guerreiro et al., 2013; Jonsson et al., 2013) and the HLA-DRB4-DRB1 region (Lambert et al., 2013). The risk genes for CR1, CD33, and TREM2 have been the most studied and are involved in microglia response to Aβ. The inactivation or blockade of either CR1 or CD33 inhibits microglial activation and increases microglial phagocytosis of Aβ (Crehan et al., 2013; Griciuc et al., 2013), and TREM2 is responsible for maintaining microglial phagocytosis (Wang 2015). TREM2 expression is upregulated in microglia surrounding amyloid, and the overexpression of TREM2 in hAPP Tg mice decreases amyloid plaque burden

(Karakaya et al., 2012). Taken together, all of these data suggest strongly that the innate immune system and specifically the phagocytosis of Aβ by microglia play an essential role in the pathogeneses of LOAD.

2.2.3 Neuroinflammation and Amyloid Pathology

Even before genome-wide association studies, inflammation has long been associated with the pathological progression in AD (Rogers et al., 1996). Systemic infection and severe head injury, which are both causes of increased inflammation, have been reported to be risk factors for AD (Tanaka et al., 2014). Additionally, epidemiological studies suggest that people taking anti-inflammatory drugs have a significantly lower AD incidence (McGeer et al., 1990). Taken together with prior literature, supports the idea that chronic inflammation exacerbates AD's progression, and blunting the immune response may benefit AD. Initial attempts at manipulating the immune response in transgenic mice led to the surprising finding that the inflammatory response initiation increased the clearance of amyloid plaques suggesting that inflammation attenuated AD pathophysiology (Birch et al., 2014). However, the overexpression of pro-inflammatory mediators increased disease progression supporting the initial hypothesis that increased inflammation exacerbated AD disease progression (Colton et al., 2006). These seemingly paradoxical results underlie the complexity of the role of inflammation and, specifically, the role microglia play in AD's progression. Microglia's role in AD disease progression is further complicated when taking into consideration aging as an important etiological factor. A growing body of evidence from Streit and colleagues have shown microglia are subjected to replicative senescence and

show age related decline in structure and function (Streit, 2006; Streit and Xue, 2013; Streit et al., 2021).

Despite these paradoxical results, general themes have emerged between the genetic manipulations of multiple inflammatory pathways versus studies administering compounds that promote inflammation (Colton et al., 2006; Kummer et al., 2011). In general, the genetic ablation of pro-inflammatory mediators tends to decrease inflammation and AD disease progression. For example, inhibiting pro-inflammatory cytokines IL-12 and IL-23 by deleting their standard subunit p40 decreased amyloid plaque burden and cognitive decline (Vom Berg et al., 2012). Additionally, inhibiting IFNγ signaling by deleting the IFNγ receptor results in reduced neuroinflammation and amyloid plaque burden (Yamamoto et al., 2007). Both results are taken together with other studies genetically ablating inflammatory pathways, enforce the notion that inflammation exacerbates AD's progression. Therefore, a positive correlation generally exists between inflammatory levels and increased AD pathology after genetic manipulation.

In contrast to genetic ablation experiments, most studies increasing inflammation, either by the administration of lipopolysaccharide (LPS) or IL-1β, result in increased gliosis and paradoxically decreased in amyloid plaque burden, suggesting that inflammation may be beneficial. This reduction in amyloid plaques is primarily associated with microglial activation (Shaftel et al., 2008; Jaeger et al., 2009; Matousek et al., 2012). For example, in one study seven days after the administration of LPS reduced the amyloid plaque burden (Herber et al., 2007). However, another study's chronic administration of LPS for two weeks resulted in

increased amyloid plaque burden (Qiao et al., 2001). The discrepancy in these results may be due to microglial activity during short- and long-term inflammatory processes activation. For example, three days after APP/PS1 transgenic mice were injected with LPS had decreased amyloid levels, but after 28 days, amyloid levels rebounded (Herber et al., 2004). This change coincided with changes in microglia morphology during the same period. Taken together, data suggest that at least initially, the activation of inflammatory processes, specifically microglial activation, decreases amyloid pathology. Therefore, a negative correlation is generally seen with increased inflammatory levels and decreased pathology after stimulation.

The dichotomy between how the inflammatory pathway is manipulated, genetically modified versus stimulation, and the concurrent effect on pathology suggests that microglia's various functions are being activated. Like macrophages, microglia exist in various phenotypes (M1, M2a, M2b, and M2c) associated with various functions (Mantovani et al., 2004; Boche et al., 2013). The M1 phenotype is characterized as a classically activated state and is involved in recruiting other immune cells and phagocytic activity (Szekanecz and Koch, 2007). The M2 phenotypes are considered to be alternatively activated states with the M2a phenotype associated with wound-healing and tissue remodeling, M2b a mix of M1 and M2a phenotypes and involved in immunoregulation, and M2c involved with immunoregulation and tissue remodeling (Mantovani et al., 2004; Edwards et al., 2006). Notably, in AD patients, the neuroinflammatory phenotype changes with disease's progression (Sudduth et al., 2013). Early-stage AD patients microglia

are typically clustered into either an M1 or M2a inflammatory phenotype, while late-stage AD displays a mixed phenotype. This mixed microglial phenotype is associated with a significant increase in neuritic amyloid plaques, and early-stage AD patients with an M2a phenotype are associated with a higher degree of cardiovascular disease than in patients with the M1 phenotype. This heterogeneous population of microglial activation in AD patients is also seen in transgenic mouse models, with reports suggesting that the M1 phenotype is associated with a lower amyloid burden due to increased phagocytic activity. For example, overexpressing IL-1β, a well-characterized M1 cytokine, resulted in a decrease in amyloid burden (Shaftel et al., 2007). The mixed microglial phenotype is generally associated with the increased amyloid burden with the Tg2576 AD transgenic mouse models typically having a mixed M2a and M2c inflammatory phenotype (Wilcock et al., 2011). The transition away from an M1 to an M2 phenotype is associated with increased disease progression. For example, the overexpression of IFNγ initially induces an M1 inflammatory phenotype 4-months post-infection, but at six months, a mixed M2 microglial phenotype is observed (Weekman et al., 2014). While no changes in amyloid burden were observed at four months, a significant increase was observed after six months. The different effects of the microglial phenotype on AD pathology suggest that microglial have

a multi-faceted role in AD, and specifically, the manipulation of microglia's phagocytic activity plays a vital role in AD disease progression.

2.3 Progranulin's role in neurodegenerative disease

PGRN is a multifunctional protein expressed in both neurons and microglia with neurotrophic and neuroprotective functions (Pereson et al., 2009; Petkau et al., 2010). Although the exact function of PGRN in the central nervous system (CNS) is not well-understood loss-of-function mutations in the PGRN gene (*GRN)* are a significant cause of familial frontotemporal dementia (FTD), and genetic variation in PGRN has been linked to multiple neurodegenerative diseases (Baker et al., 2006; Cruts et al., 2006b). PGRN's association with a large number of different neurodegenerative diseases has led many to hypothesize that it plays an important role in neurodegenerative disease as a whole and has made it an attractive and potential therapeutic target for a wide range of neurodegenerative diseases.

2.3.1 Progranulin and FTLD

FTLD is a devastating neurodegenerative disease and is the leading cause of dementia in people under 65 (McKhann et al., 2001; Vossel and Miller, 2008). FTLD is a collective term used to describe a group of pathologically heterogeneous neurodegenerative disorders that result in selective atrophy of the brain's frontal and temporal lobes. Clinically, FTLD is referred to as frontotemporal dementia (FTD) can be subdivided into three distinct subtypes based on clinical features, including behavioral variant, which is marked by a progressive decline in behavior and executive function; semantic dementia, which is characterized by a loss of

semantic memory in verbal and non-verbal domains; and progressive non-fluent aphasia, which is characterized by deficits in either expressive or motor speech.

FTLD can be further classified into three different histological subtypes based on the main components of aggregated protein. The earliest pathology to be recognized was hyperphosphorylated tau protein deposits in both neurons and astrocytes called FTLD-Tau (Pickering-Brown, SM 2002). In most cases where tau deposits are absent, neuronal cytoplasmic inclusions that are immunoreactive for ubiquitin are present and referred to as FTLD-U (Neumann et al., 2009). Ubiquitin is a small regulatory protein that among other roles marks proteins for degradation. Withing the context of neurodegenerative disease the presence of ubiquinated protein inclusions are thought to represent a failure to successfully degrade the specific protein (Basisty et al., 2018). Depending on the significant ubiquitinated protein present, FTLD-U can be further subdivided into either FTLD-TDP, FTLD-FUS or FTLD-UPS (Mackenzie and Rademakers, 2007). FTLD due to autosomal dominant loss-of-function mutations in *GRN* is a major cause of familial FTLD-TDP(Baker et al., 2006; Cruts et al., 2006a). The major ubiquitinated protein in many cases of FTLD is made up of trans-activating DNA binding protein with a molecular weight of 43kDa (TDP-43)(Cairns et al., 2007) . Notably, TDP-43 pathology is not unique to just FTLD but is also commonly reported in amyotrophic lateral sclerosis (ALS) and as high as 50% of cases with AD (Wilson et al., 2011).

Unlike in most neurodegenerative disorders, where mutations result in a toxic gain-of-function, FTLD with *GRN* mutations is thought to be caused by a global decrease in the levels of expressed and secreted PGRN. The majority of

reported *GRN* mutations result in nonsense-mediated mRNA decay, which is a eukaryotic mechanism for eliminating mutant transcripts containing premature stop codons, resulting in the complete loss of mRNA expression from one allele (Rademakers and Rovelet-Lecrux, 2009). Over 69 familial mutations in *GRN* have been described; the most common involves the premature insertion of stop codons or frame shifts that destroy mRNA through nonsense-mediated decay. Given that a wealth of mutations has been discovered and all with a similar mode of actions strongly supports the hypothesis that *GRN* haploinsufficiency results in an insufficient level of PGRN that leads to FTLD.

FTLD patients with loss-of-function mutations in *GRN* are highly heterogeneous in disease duration, clinical presentations, and age of onset (Seelaar et al., 2011). FTLD patients with *Grn* mutations have heterogeneous clinical syndromes with patients present with all of the defined clinical syndromes of FTLD, including primary progressive aphasia, FTLD with Parkinsonism, concomitant MND, and corticobasal syndrome (Galimberti and Scarpini, 2012). By far, the most consistent neuroimaging feature of patients with *Grn* mutations is asymmetric brain atrophy (Whitwell and Josephs, 2012), with asymmetric damage to white mater (Bozzali et al., 2013), severe cortical atrophy, and parietal (Whitwell et al., 2009) lobe involvement are additional clinical features associated with *Grn* mutations.

2.3.2 Sex differences in *GRN*-related FTLD

In general, FTD affects men and women equally but sex differences have not been well characterized. For example, with respect to clinical prevalence some

studies have reported sex differences (Bernardi et al., 2012; Goodman et al., 2017), while others have not(Rosso et al., 2003; Borroni et al., 2010). More recent studies suggest that there may be sex differences with specific FTD subtypes compared to FTD overall. An early study by Ratnavalli and colleagues reported that men were four times more likely than women to develop the bvFTD subtype (Ratnavalli et al., 2002). Although this initial study used a small sample size a later study also found similar sex differences (Johnson et al., 2005). In this study, men were more likely to have bvFTD and SD, whereas women were more likely to have progressive nonfluent aphasia.

In support of sex differences in FTD, the prevalence of *GRN* mutations have been reported to be 33% higher in females (Curtis et al., 2017). In support of the notion PGRN may drive sex differences in the prevalence of FTD, PGRN has been implicated in sexual differentiation of the developing brain and estrogen-induced neurogenesis (Chiba et al., 2007; Suzuki et al., 2009). Furthermore, sex differences in behavior have also reported in $Grn^{-/-}$ mice, with elevated levels of aggression and anxiety-like behavior observed (Chiba et al., 2009).

2.3.3 PGRN variability and other degenerative disorders

Because the penetrance of *GRN* mutations is incomplete, the striking variability associated with *GRN* mutations, and variability in wild type *GRN* allele other genes are considered to contribute to disease pathogenesis (Gass et al., 2006; Rademakers et al., 2007). Evidence that genetic background plays a significant role in disease comes from one report that analyzed 30 different families, all with the Arg493X nonsense mutation in GRN that found four clinical

presentations and 25-year age range of onset among the families (Rademakers et al., 2007). also, monozygotic twins with FTLD due to *GRN* mutations were reported to have striking similar clinical and neuroimaging features, further suggesting the importance of genetic background on disease progression (McDade et al., 2012).

Recently the gene *TMEM106B* was identified in a genome-wide association study as a potential disease modifier for *Grn* FTLD mutation carriers (Van Deerlin et al., 2010). *THEM106B* codes for a transmembrane protein associated with PGRN in endo-lysosomes, and increased expression of *TMEM106B* reportedly increases intracellular PGRN (Chen-Plotkin et al., 2012; Lang et al., 2012). A minor allele of *TMEM106B* is associated with lower plasma PGRN levels in both patients, and health Individuals and genetic variability in *TMEM106B* has been shown to affect disease penetrance and age of onset in *Grn* mutation carriers (Cruchaga et al., 2011; Finch et al., 2011; van der Zee et al., 2011).

There is growing evidence that genetic variability in *Grn* acts as a risk factor for other neurodegenerative diseases other than FTLD. Variability in the micro-RNA binding site of the 3' untranslated region of *Grn* (rs5848) has been shown to affect levels of PGRN and increase the risk for FTLD in one study (Rademakers et al., 2008). For unclear reasons, another study did not see an increase in risk with rs5848 (Rollinson et al., 2011). This discrepancy may further illustrate the importance of other factors, including genetic background and environment, affect the loss of PGRN. Regardless, the frisk allele's functional consequences for rs5848 are reduced levels of circulating PGRN, and the risk allele is over-represented in hippocampal sclerosis cases (Dickson et al., 2010; Hsiung et al.,

2011; Pao et al., 2011; Kamalainen et al., 2013). Additionally, four tagging single nucleotide polymorphism in the *Grn* gene was significantly associated with the development of sporadic FTLD in patients who do not carry *Grn* causal mutations (Galimberti et al., 2010) further linking a connection between genetic variability and sporadic FTLD a subsequent study identified increased methylation of the PGRN promoter with a concurrent decrease in PGRN mRNA levels (Galimberti et al., 2012).

Additionally, a growing number of gene association studies assessing *Grn* gene variability in various neurodegenerative diseases have identified associations between disease duration, risk, and age of onset of disease with *Grn* variants in AD (Fenoglio et al., 2009; Lee et al., 2011), multiple sclerosis (Fenoglio et al., 2010), ALS (Sleegers et al., 2008) and bipolar disorder and schizophrenia (Galimberti et al., 2010; Momeni et al., 2010). Interestingly, *Grn* variability as a disease modifier is often small and not consistently reproducible, suggesting complex interactions between PGRN and genetic and environmental factors (Rollinson et al., 2011). Taken together, growing clinical data suggests that PGRN plays an essential role in brain function and neuronal health.

2.4 Progranulin's role in the central nervous system (CNS)

2.4.1 Expression of PGRN in the CNS

While the function of PGRN is still not well defined, clues can be gained from where it is expressed within the CNS. PGRN is primarily expressed in only neurons and microglia in the brain, with relatively low expression during development that increases with age (Petkau et al., 2010; Matsuwaki et al., 2011). Evidence exists

that PGRN may also be present at low levels in astrocytes, but there are conflicting reports (Ahmed et al., 2010; Petkau et al., 2010).

In microglia, PGRN is dynamically regulated, with PGRN expression being upregulated in response to injury or insult. Increased PGRN immunoreactivity in activated microglia has been found in patients and mouse models of multiple diseases, including Lewy body dementia (Revuelta et al., 2008), ALS (Malaspina et al., 2001; Irwin et al., 2009; Philips et al., 2010), multiple sclerosis (Vercellino et al., 2011) and AD (Gliebus et al., 2009; Pereson et al., 2009). PGRN levels have been shown to increase in microglia and macrophages after sciatic axotomy, spinal cord injury, and traumatic brain injury (Moisse et al., 2009; Naphade et al., 2010; Byrnes et al., 2011; Tanaka et al., 2013).

In neurons, it is unclear if PGRN expression is regulated in a similar way as microglial PGRN. An increase in PGRN immunoreactivity has been reported in neurons associated with dense-core plaques in the Tg2576 and APPPS1 AD transgenic mouse models (Pereson et al., 2009). However, other studies have reported either no change in PGRN expression (Moisse et al., 2009) or a decrease (Petkau et al., 2010) after injury. Regardless of how PGRN is regulated during injury under normal conditions, PGRN generally exists at low but stable levels in neurons.

Because *GRN* mutations that cause FTLD result in loss-of-function, and subsequent haploinsufficient loss of PGRN, one would expect PRN expression in patients with mutations to be reduced compared to normal controls. While this is true for histopathologically spared regions, surprisingly, in regions that are

histopathologically involved, such as the frontal and temporal cortex, one study found that *GRN* mRNA levels were increased and not decreased as would be expected (Chen-Plotkin et al., 2010). The increase in PGRN expression in the frontal and temporal lobes was caused by the remaining functional allele and increased in both the number and the activation state of microglia. Taken together with other reports on PGRN expression in the brain, the bulk of PGRN expressed during injury is contributed by the microglial population, while there appears to be little or no change in the expression of PGRN in the neuronal population. Despite a significant increase in PGRN from the microglial population during injury, the increased level of PGRN does little to compensate for the loss of PGRN expression during disease pathophysiology, suggesting that the specific reduction of PGRN in the neuronal population drives disease progression (Eriksen, 2010).

2.4.2 PGRN's function in neurons

As loss of PGRN is implicated in numerous neurodegenerative disorders indicating PGRN may be a crucial neurotrophic factor in the brain, a handful of studies have examined the potential role of PGRN in neurite outgrowth (Toh et al., 2011). In zebrafish models, PGRN is essential for motor neuron development and neurite outgrowth and branching. In one study, knockdown of PGRN was shown to generate truncated caudal primary motor neurons, with co-injection of PGRN partially rescued these effects (Chitramuthu et al., 2010). Similar results were reported in a separate study, which showed knockdown of the two PGRN homologs *GRNa* and *GRNb* resulted in a substantial decrease in axonal length, with the *GRN*a homolog producing a more significant reduction in axon length

(Laird et al., 2010). In the same study, PGRN overexpression rescued the axonopathy induced by PGRN knockdown. In rat cortical and motor neurons, full-length PGRN and the granulin E peptide have been reported to promote neuronal survival and enhance neurite outgrowth (Van Damme et al., 2008; Ryan et al., 2009).

Additionally, in rat hippocampal neurons, small interfering RNA-mediated knockdown of PGRN resulted in reduced neurite arborization and dendritic protrusions (Tapia et al., 2011). In primary hippocampal cultures from $Grn^{-/-}$ mice, decreased neurite outgrowth was observed, which could be partially rescued by the treatment of recombinant full-length PGRN and granulin peptides (Gass et al., 2012). How PGRN regulates neuronal outgrowth remains poorly understood, but one study using cultures of primary mouse neurons showed that treatment with PGRN resulted in an increase in neurite outgrowth by regulating glycogen synthase kinase-3β (GSK-3β) (Gao et al., 2010). Furthermore, a study recently generated transgenic mice with inducible neuronal PGRN overexpression and found that PGRN accelerated axonal outgrowth and restoration of neuromuscular synapses after an injury to the sciatic nerve (Altmann et al., 2016). While few reports exist studying neurotrophic properties of PGRN *in vivo*, one study reported decreased dendritic length in the apical dendritic arbor of CA1 pyramidal neurons in the hippocampus of $Grn^{-/-}$ mice (Petkau et al., 2012). Another study examining

$Grn^{+/-}$ mice reported changes in the dendritic arbors in the basomedial amygdala and the prelimbic cortex (Arrant et al., 2016).

Because the partial loss of PGRN results in gross neuronal loss, several studies have evaluated the role of PGRN in response to exogenous stressors. In cultures of primary mouse neurons, PGRN knockdown increased sensitivity to hydrogen peroxide and n-methyl-D-aspartic acid (NMDA) (Guo et al., 2010). Another study using differentiated neurons derived from induced pluripotent stem cells from a patient with a heterozygous *GRN* mutation had an increased sensitivity to kinase inhibitors (Almeida et al., 2012). Specifically, sensitivity was found for inhibitors for the phosphatidylinositide 3-kinase (PI3K)/protein kinase B (Akt) and mitogen-activated protein/extracellular signal-regulated kinase (MEK)/mitogen-activated protein kinase signaling pathways. Interestingly, PGRN overexpression rescued axonopathy from TDP-43-induced toxicity in zebrafish but not from SOD1-induced toxicity (Laird et al., 2010). Selective increase sensitivity has been reported *in vivo* PGRN mouse models. Against cerebral artery occlusion, lentiviral overexpression of PGRN had a protective effect suggesting neuroprotective effects of PGRN against ischemia and stress-induced cell death (Tao et al., 2012). In $Grn^{-/-}$ mice, increased neuronal cell death was observed in the substantia nigra administering of the toxin 1-methyl-4-phenyl-1,2,3,6-tetrahydropyridine (MPTP) (Martens et al., 2012). However, loss of PGRN has not been shown to increase sensitivity to all stressors in $Grn^{-/-}$ mice with 3-nitropropionic acid, quinolinic acid, kainic acid, and pilocarpine hydrochloride all not affecting neuronal cell death in the striatum and hippocampus compared NTg mice (Petkau et al., 2013).

Collectively, evidence from both cell cultures and PGRN mouse models suggests PGRN has a neurotrophic effect on select toxins.

Despite growing evidence that PGRN may be a crucial neurotrophic factor, one major impediment to understating how PGRN promotes survival and neurite outgrowth in neurons is the lack of a definitive receptor that interacts with PGRN and initiates signal transduction (Kao et al., 2017). Currently, tumor necrosis factor (TNF) receptors and sortilin have been reported to be receptors for PGRN, but their interaction and function remain unclear (Hu et al., 2010; Tang et al., 2011). Sortilin has been shown to traffic extracellular PGRN to the lysosome for degradation and is unlikely to regulate PGRN mediated neuronal survival and neurite outgrowth. Recombinant PGRN has been shown to promote neurite outgrowth in hippocampal neurons despite lacking sortilin *in vitro* (Gass et al., 2012). Similar results were also seen for granulin E promotion of neurite outgrowth despite inhibition of the granulin E-sortilin interaction (De Muynck et al., 2013). Interactions between PGRN and TNF receptors are still controversial, with one study unable to reproduce the interaction by co-immunoprecipitation or surface plasmon resonance (Chen et al., 2013). Therefore, it is unclear how PGRN could regulate neuronal survival and neurite outgrowth through TNF receptors.

There is a growing amount of evidence that PGRN plays a vital role in synapse and synaptic plasticity. A role of PGRN in synapse biology was first proposed after a screen of dysregulated genes from FTLD patients with *GRN* haploinsufficient mutations (Kocerha et al., 2011). Changes in both the number of synaptic vesicles and vesicle release probability have been observed in primary

hippocampal cells after siRNA-mediated knockdown of PGRN (Tapia et al., 2011). An increase in the number of synaptic vesicles has also been reported in FTLD patients carrying haploinsufficient *GRN* mutations, further suggesting that PGRN levels' changes cause changes in synaptic function. PGRN has also been shown to colocalize with dense-core vesicle markers and is secreted in an activity-dependent manner with neuronal activity increasing the recruitment of PGRN to synapses and increasing the density of PGRN (Petoukhov et al., 2013). The same study also that the treatment of recombinant PGRN increased the synapse density while decreasing the size and number of synaptic vesicles.

Contrary to data from hippocampal cultures, postmortem brain sections from FTD patients with *GRN* mutations and $Grn^{-/-}$ mice had decreased synaptic vesicles per synapse number(Tapia et al., 2011; Petkau et al., 2012). In the same paper, complete loss of PGRN decreased LTP in the Schaffer collateral of $Grn^{-/-}$ mice. Decreased LTP has not been shown in $Grn^{+/-}$ mice; however, studies have only been reported in mice up to eleven months (Filiano et al., 2013). Regardless of the various methodologies and models used, growing evidence suggests that PGRN plays a vital role in synaptic function and neuronal connectivity.

2.4.3 Progranulin's function in microglia

Only a few studies have directly investigated the role of PGRN in microglia, however, due to a growing number of studies reporting gross neuroinflammation in $Grn^{-/-}$ mouse models (Ahmed et al., 2010; Yin et al., 2010b; Petkau et al., 2012) and in FTLD patients (Chen-Plotkin et al., 2010) there is a renewed interest in the role of PGRN in microglia about neurodegeneration. The bulk of the existing

evidence strongly suggests that PGRN has an anti-inflammatory function with complete loss of PGRN resulting in overactive microglia (Ahmed et al., 2007). $Grn^{-/-}$ mice exposed to MPTP exhibited an increased microglial inflammatory response resulting in the increased neuronal loss (Martens et al., 2012). The same study also showed an increased inflammatory response marked by increased inflammatory cytokines in $Grn^{-/-}$ isolated microglia after treatment with LPS/IFN-γ. Similarly, microglia from $Grn^{-/-}$ mice exhibited increased inflammatory response compared to wildtype mice after exposure to bacterial lipopolysaccharide (LPS) exhibited by decreased release of the anti-inflammatory cytokine interleukin-10 and increased release of inflammatory cytokines (Yin et al., 2010b). However, another study using siRNA-mediated knockdown of PGRN in human fetal microglia reported decreased inflammatory cytokine production in response to the activation of different TLR receptors via LPS and poly IC suggesting that loss of PGRN did not result in an exaggerated inflammatory phenotype after stimulation (Suh et al., 2012). Although contradictory, this may suggest various regulations of PGRN in mouse versus human microglia. Additionally, because this study involved siRNA-mediated knockdown of PGRN versus the latter using $Grn^{-/-}$ mice, this may reflect differences in acute versus chronic PGRN deficiency in regulating microglial activity.

Under specific conditions, PGRN is a chemoattractant for microglia. The first evidence came from a report that showed that intracortical administration of human PGRN by lentiviral construct in mice increased the number of activated microglia localized to the site injection site (Pickford et al., 2011). However, in a

second paper, the administration of recombinant PGRN to the hippocampus in rats did not alter the microglia number (Zhu et al., 2013). However, the same study did see an increase in the number of CD11b-positive microglia after administration of recombinant PGRN in mice with pilocarpine-induced status epilepticus suggesting that exogenous PGRN acts as a chemoattractant only under specific conditions. Another study investigating the recruitment of microglia to amyloid plaques found no difference in the number of Iba1-positive microglia surrounding amyloid plaques in mice with 50% reduced microglial expression of PGRN versus wild-type mice (Minami et al., 2014). Interestingly, two of the studies that examined PGRN's chemoattractant ability for activated microglial in $Grn^{-/-}$ mice, found that complete loss of PGRN did not affect microglial migration to the site of injury suggesting that while exogenous PGRN can increase microglial chemotaxis microglial PGRN is not required for chemotaxis.

There is growing evidence that PGRN plays a role in endocytosis in microglia and macrophages. In one study, the addition of recombinant PGRN enhanced the endocytosis of $A\beta_{1-42}$ peptide in primary mouse microglial cells (Pickford et al., 2011). Further evidence supporting the role of PGRN in microglial phagocytic activity comes from observations that *Caenorhabditis elegans* were deficient for the gene homologous to the human *Grn* gene, which exhibited increased phagocytic removal of apoptotic cells (Kao et al., 2011). In the same study, macrophages isolated from $Grn^{-/-}$ mice also exhibited an enhanced apoptotic cell phagocytosis rate. Furthermore, a separate study using LysM-cre $Grn^{flox/flox}$ mice reported fewer PGRN-deficient microglia than wild-type microglia

phagocytosed fluorescent beads, suggesting reducing phagocytic activity after the loss of PGRN (Minami et al., 2014). Like PGRN as a chemoattractant, it appears that altered levels of PGRN modulate phagocytic activity but not wholly dependent on PGRN in microglia and macrophages due to differences in rates of phagocytic activities in $Grn^{+/+}$ and $Grn^{-/-}$ cells.

2.5 Mouse models of progranulin deficiency

Several unique lines of $Grn^{-/-}$ and $Grn^{+/-}$ mouse lines have been generated and have been histopathologically and behaviorally characterized (Kayasuga et al., 2007; Ahmed et al., 2010; Petkau et al., 2010; Yin et al., 2010b; Yin et al., 2010a; Ghoshal et al., 2012; Wils et al., 2012; Filiano et al., 2013). To date, $Grn^{-/-}$ mice have predominately been studied as a model for *Grn* caused FTLD over $Grn^{+/-}$ mice due to initial reports suggesting $Grn^{-/-}$ mice have more robust behavioral and pathological phenotypes.

2.5.1 Pathology in PGRN mouse models

Although FTLD patients with *Grn* mutations exhibit robust TDP-43 pathology, both $Grn^{-/-}$ and $Grn^{+/-}$ mouse models show little or no signs of TDP-43 pathology (Roberson, 2012). In FTLD patients with TDP-43 proteinopathy, TDP-43 is pathologically cleaved, translocated to the cytoplasm, and is a significant constituent of ubiquitinated inclusions. While there has been no evidence of pathologically cleaved TDP-43 in either $Grn^{-/-}$ and $Grn^{+/-}$ mouse models, abnormally phosphorylated TDP-43 has been observed in several $Grn^{-/-}$ mouse models (Ahmed et al., 2010; Yin et al., 2010b; Wils et al., 2012), but not in $Grn^{+/-}$ mice. Similarly, unlike FTLD patients that exhibit a gross neuronal loss in the frontal

and temporal lobes, neurodegeneration has not been observed in either $Grn^{-/-}$ and $Grn^{+/-}$ mice (Roberson, 2012).

The most consistent neuropathological change observed in PGRN mouse models is increased inflammation in the brain. Increased microgliosis and astrogliosis is consistently observed in $Grn^{-/-}$ mouse lines between 12 and 18 months of age (Ahmed et al., 2010; Yin et al., 2010b; Yin et al., 2010a; Ghoshal et al., 2012; Petkau et al., 2012; Filiano et al., 2013), but not in $Grn^{+/-}$ mice (Filiano et al., 2013). In addition to neuroinflammation $Grn^{-/-}$ mouse models have consistently shown early and exaggerated deposition of lipofuscin in the brain (Ahmed et al., 2010; Petkau et al., 2010; Yin et al., 2010b; Ghoshal et al., 2012; Wils et al., 2012), but not in $Grn^{+/-}$ mice (Filiano et al., 2013). Lipofuscin is an autofluorescent pigment that accumulates in the brain with age, suggesting that loss of PGRN may lead to accelerated aging (Kelley et al., 2010).

2.5.2 Behavior deficits in PGRN mouse models

Most behavioral abnormalities in $Grn^{-/-}$ and $Grn^{+/-}$ mice are usually subtle and variable between studies. Most reports have only focused on $Grn^{-/-}$ mice, which develop an FTD-like behavioral disturbances pattern, including social and emotional abnormalities and deficits in hippocampal-dependent memory. By far the most commonly reported behavioral abnormality is in social behavior, with $Grn^{-/-}$ displaying impaired social behavior in the three-chamber sociability test (Yin et al., 2010a; Filiano et al., 2013) and the resident/intruder test (Ghoshal et al., 2012; Petkau et al., 2012). Both $Grn^{-/-}$ and $Grn^{+/-}$ mice have shown deficits in impaired emotional behavior with a decrease in freezing time during fear conditioning

(Filiano et al., 2013). Only $Grn^{-/-}$ mice have been shown to exhibit increase aggressive and sexual behaviors (Kayasuga et al., 2007) as well as increased depression-like behavior (Yin et al., 2010a). Generally, $Grn^{-/-}$ mice do not exhibit any differences in non-cognitive behavior, but a few papers have reported sex-differences within the $Grn^{-/-}$ genotype in the motorized rotarod and open field test (Petkau et al., 2012; Roberson, 2012). In $Grn^{-/-}$ mice hippocampus-dependent learning and memory, tested via the Morris water maze (MWM), has been shown to only be impacted in aged mice. With mice between twelve and eighteen months showing impaired learning and memory (Yin et al., 2010a; Ghoshal et al., 2012). The presence or absence of learning and memory deficits in $Grn^{+/-}$ mice is less clear, with only one studying showing no effects at nine months in the MWM (Filiano et al., 2013). However, given that learning and memory deficits are only present in aged $Grn^{-/-}$ mice older than twelve months, they may be present in $Grn^{+/-}$ at older ages.

2.5.3 Differences between $Grn^{-/-}$ and $Grn^{+/-}$ mice

Historically, studies investigating murine PGRN deficiency have primarily focused on the homozygous loss of PGRN versus a haploinsufficient loss of PGRN. While $Grn^{-/-}$ mice replicate some FTLD-related pathology, such as microgliosis, both models have recently been shown to replicatd key FTLD-related behavior abnormalities including social and emotional behavior deficits (Yin et al., 2010b; Roberson, 2012; Filiano et al., 2013). Growing evidence suggests that patients with complete loss of PGRN may be significantly different from patients who have a haploinsufficient loss of PGRN. While *Grn* mutations causing

haploinsufficient loss of PGRN have only been observed in FTLD patients, recently a mutation causing complete loss of PGRN was identified in siblings. However, unexpectedly instead of having FTLD, the siblings have neuronal ceroid lipofuscinosis (NCL), a lysosomal storage disorder (Smith et al., 2012). This has been confirmed in $Grn^{-/-}$ mice, which recapitulate pathological features of Grn-associated-FTLD and NCL, such as elevated lysosomal proteins cathepsin D, lysosomal-associated membrane protein 1 and transmembrane protein 106B (Gotzl et al., 2014; Tanaka et al., 2014). Interestingly, while $Grn^{-/-}$ mice display pathological features of NCL, $Grn^{+/-}$ mice do not suggest that NCL is specific to complete loss of PGRN and not haploinsufficient loss of PGRN (Smith et al., 2012). Besides, recent evidence from $Grn^{+/-}$ mice suggests that critical FTLD-related behavioral deficits resulting from haploinsufficient loss of PGRN can develop in the absence of neuroinflammation (Filiano et al., 2013). This disassociation between behavioral deficits and neuroinflammation suggests that FTLD-related behavioral deficits are independent to the increase of microgliosis and astrogliosis.

There is a growing body of evidence suggesting divergent effects between partial and complete loss of PGRN. In addition to differences in pathological features, the emergence of behavioral and signaling differences in $Grn^{-/-}$ and $Grn^{+/-}$ mice suggesting divergent effects of partial and complete loss of PGRN. While most studies reporting abnormal behavior in $Grn^{-/-}$ mice did not compare them to $Grn^{+/-}$ mice, there have been several instances of divergent behavior (Yin et al., 2010a; Ghoshal et al., 2012). In one study, increased aggressive behavior was observed in $Grn^{-/-}$ mice but not in $Grn^{+/-}$ mice (Kayasuga et al., 2007). Although

studies previously did not observe differences between $Grn^{+/-}$ and $Grn^{-/-}$ mice in social behavior via the three-chamber sociability test (Filiano et al., 2013), recently, differences were observed in the social dominance tube test (Arrant et al., 2016). In this study, $Grn^{+/-}$, but not $Grn^{-/-}$ mice displayed age-dependent abnormalities in the social dominance tube test. In the same study, signaling differences were also reported in the MTORC2/Akt signaling pathway in $Grn^{+/-}$ and $Grn^{-/-}$ mice. Between six and nine months of age, increased phosphorylated ribosomal protein S6 at phosphosites Ser235/236 and Akt at phosphosites Ser473 was observed in the amygdala of $Grn^{+/-}$, but not in $Grn^{-/-}$ mice and this correlated with changes in social dominance behavior (Arrant et al., 2016). Taken together, the mounting behavioral, pathological, and signaling differences between complete and partial PGRN deficiency as well as divergent clinical data suggest that $Grn^{-/-}$ and $Grn^{+/-}$ model different disease pathways.

2.6 Role of progranulin in Alzheimer's disease

Given the high societal and economic cost of AD and dementia, there is a significant societal need to develop new treatments that delay or prevent AD disease progression. PGRN is a secreted pleiotropic growth factor and has been implicated in both Aβ, and NFT AD pathophysiology, with a growing number of studies, suggest that PGRN is a risk factor for AD (Brouwers et al., 2008; Cortini et al., 2008; Viswanathan et al., 2009). Polymorphisms in PGRN, which can cause up to a 20% reduction in PGRN levels, have been shown to increase the risk for AD (Rademakers et al., 2008; Lee et al., 2011; Sheng et al., 2014; Xu et al., 2016). In contrast with FTLD, AD is typically associated with early memory loss whereas

FTLD is associated with early executive behavioral differences. Despite *GRN* mutations being a major cause of FTLD there have been patients with a frameshift mutation in *GRN* due to a single base-pair deletion that have been reported to have clinical presentations to similar to AD (Kelley et al., 2010). Moreover, *Grn* mutation carriers with the apolipoprotein E4 isoform have been reported to exhibit both amyloid plaques and tau-positive NFTs (Perry et al., 2013).

2.6.1 Expression of PGRN in AD

Although there is an increasing number of studies reporting that loss of PGRN is associated with a higher risk for AD, precisely how PGRN loss modifies AD pathophysiology remains poorly understood. Currently, only three studies explore the loss of PGRN in AD transgenic mouse models, with two focusing on PGRN's role in neuroinflammation (Minami et al., 2014; Hosokawa et al., 2015; Takahashi et al., 2017b). A growing number of studies have suggested that increased neuroinflammation contributes to AD's pathogenesis and neurodegenerative disease in general. Recently, two genome-wide association studies linked complement component receptor 1, CD33, and triggering receptor expressed on myeloid cells 2 to an elevated risk for late-onset AD (Seshadri et al., 2010; Hollingworth et al., 2011a).

Much of PGRN's interest in neuroinflammation and specifically in microglia is due to PGRN's expression in the AD brain. PGRN levels are elevated in AD patients and are co-localized with microglia surrounding dense-core amyloid plaques (Gliebus et al., 2009; Pereson et al., 2009; Minami et al., 2014). Interestingly, in three different AD amyloid transgenic mouse models, PGRN is

significantly decreased compared to controls where amyloid pathology is either minimal or absent but elevated with extensive plaque deposition, suggesting that PGRN is differentially regulated during AD pathophysiology (Minami et al., 2014). While the upregulation of PGRN is most likely due to increased transcription via increased activation of microglia, it is not clear how PGRN is downregulated. One possible explanation that has been suggested is that Aβ oligomers may downregulate PGRN in neurons and microglia (Minami et al., 2014). While Aβ fibrils associated with amyloid plaques have been shown to increase PGRN expression in microglia, Aβ oligomers have been shown to signaling pathways that have previously been reported to decrease PGRN expression (Suh et al., 2012).

2.6.2 PGRN and amyloid pathology

Currently, two studies have focused on PGRN's role in modulating inflammation concerning Aβ pathology but have conflicting results (Minami et al., 2014; Takahashi et al., 2017a). In one study a protective role of PGRN was reported with an increase in Aβ plaques in transgenic AD mice with microglial specific loss of PGRN and a reduction of Aβ plaque load with the overexpression of PGRN (Minami et al., 2014). However, paradoxically another study reported a reduction of Aβ plaques after complete PGRN loss in transgenic AD mice via upregulation of the TYROBP network of genes instead of an expected increase in Aβ plaque load (Takahashi et al., 2017a). One possible explanation for the discrepancy in the two studies is that the first study utilized LysM-cre mice lacking endogenous *Lyz2,* which is a gene that is upregulated in $Grn^{-/-}$ mice and *Lyz2* is increased in the CSF of AD and has been suggested to have a protective role in

Aβ aggregation (Ganz et al., 2003; Helmfors et al., 2015; Lui et al., 2016). Regardless of the conflicting reports, both papers strongly suggest that complete loss of PGRN is modulating AD pathophysiology through microglial activity. The first study showed impaired phagocytosis of fluorescent beads in brain slices of *Grn*$^{flox/flox}$ mice compared to wild-type mice, and the addition of recombinant PGRN increases the endocytosis of Aβ in primary microglia cultures (Minami et al., 2014). In the other study, complete loss of PGRN enhanced microglial Aβ phagocytosis caused by increased expression of the TYROBP network of genes, including the AD risk factor *Trem2* (Takahashi et al., 2017b).

2.6.3 PGRN and tau pathology

The effect of PGRN deficiency on tau pathology is even less understood, with only two studies investigating PGRN's effect on tau pathology. Tau pathology has been observed in FTLD patients with *Grn* mutations suggesting an association with Grn mutations and tau pathology (Leverenz et al., 2007; Rademakers et al., 2007; Perry et al., 2013). Recently the *Grn* rs5848 T allele was shown to increase cerebrospinal fluid (CSF) tau levels, but interestingly no changes in CSF p-tau$_{181}$ were observed. While tau protein has been reported to be decreased in FTLD patients with PGRN missense mutations (Papegaey et al., 2016) only changes in tau phosphorylation have been reported in mouse models (Hosokawa et al., 2015; Papegaey et al., 2016; Takahashi et al., 2017b). In the first study, heterozygous loss of PGRN resulted in increased AT8, pT181, and pS422 tau phosphorylation Tris-soluble fractions and AT8 in sarkosyl-insoluble fractions (Hosokawa et al., 2015). Unlike in previous reports suggesting PGRN was modulating amyloid

pathology via microglia it is unlikely that PGRN affected tau phosphorylation through alterations in inflammation, with no changes in Iba1 immunoreactivity observed. Instead, the study reported increased phosphorylated cyclin-dependent kinases. In another study using the same P301L tau transgenic mouse model, an increase in AT8 and AT180 tau phosphorylation was observed in P301L mice with complete loss of PGRN (Takahashi et al., 2017b).

CHAPTER 3: EFFECT OF PGRN LOSS ACROSS AGE

3.1 Introduction

The present chapter examined whether heterozygous loss of PGRN in mice is sufficient to cause behavioral deficits related to FTLD. Behavior and neuropathology were examined in a novel $Grn^{+/-}$ mouse model between six and eighteen months. Several experimental approaches of behavior modeling, histology, and electrophysiology demonstrated that the heterogeneous loss of PGRN resulted in significant behavioral abnormalities in the absence of FTLD-related neuropathology. Electrophysiological alterations accompanied by a loss of GABAergic interneurons were observed in aged $Grn^{+/-}$ mice. These findings suggest that the dissociation, previously reported, is between behavioral abnormalities, loss of interneurons, and synaptic deficits in the absence of inflammation and TDP-43 proteinopathy.

3.2 Materials and Methods

3.2.1 Animal Models

All studies were conducted following the University of Houston-approved Institutional Animal Care and Use Committee protocols. PGRN mutant mice were created by deleting exons 5-12 of the *Grn* gene by homologous recombination. Two clones containing the recombined alleles were isolated and injected into C57BL/6J blastocytes, resulting in 16 chimeric mice. Chimeric males were crossed with C57BL/6J females, and the mutated allele was transmitted to their progeny. The heterozygous mutant mice had normal fertility and did not exhibit any visible

differences compared to their wild-type littermates. $Grn^{+/-}$ and non-transgenic mice (NTg) were used at six, twelve, and eighteen months of age in this study.

3.2.2 Tissue processing

Animals from both genotypes were euthanized with CO_2 and brains were harvested. One hemibrain was flash-frozen in 2-methylbutane and dry ice and stored for long-term storage at -80°C. The other hemibrain was fixed in Accustain (Sigma) for three days and then transferred to 70% ethanol solution and stored at 4°C for long-term storage. Accustain fixed brains were subjected to paraffin processing (Leica TP1020) and then sectioned using a Leica microtome at 10-µm intervals.

3.2.3 Behavioral Tests

3.2.3.1 Open Field

The open field test assessed non-cognitive behavior at six, twelve, and eighteen months. Mice were placed in the center of a 60x40 cm Plexiglas box and allowed to explore the novel environment for 30 minutes in standard lighting conditions. Activity was measured using a computer-operated Opto-Varimex Micro Activity Meter v2.00 system (Optomax Columbus Instruments; OH) as previously described (Vollert et al., 2013). The Plexiglas box contained sensors consisting of eight infrared light emitting diodes and eight phototransistors that emit and detect infrared light beams. Movement was detected by beam breaks and the Opto-Varimex program recorded total time spent moving (MOVE), time spent resting (REST), and stereotypic behavior (STEREO). Time spent in the center and periphery was analyzed by defining a 25 cm x 25 cm square zone in the center of

the Plexiglas box so that the program defined this space as the center and the remaining outside space as the periphery. The Plexiglass box was cleaned with 70% ethanol between mice.

3.2.3.2 Motorized Rotarod

Motor learning, motor coordination, and balance was evaluated by an accelerating cylindrical drum Rotamex Rotarod machine (Columbus Instruments; Columbus, OH) at six and eighteen months as previously described (Vollert et al., 2013). Mice underwent 4 trials with 15-minute inter-trial intervals per day, for a total of 2 days. Each trial consisted of placing the mouse on the horizontal accelerating rod (4-40 rpm) and a trial ended whenever the mouse fell of the rod, the trial time elapsed 300 seconds, or if the mouse became inverted twice in the same trial without falling. The length of time each mouse was able to stay on the rod was recorded by the observer blinded to genotype. The motorized rotarod was cleaned with 70% ethanol between each trial.

3.2.3.3 Light Dark Transition

Anxiety-like behavior was evaluated using the light dark transition test at six, twelve, and eighteen months as described (Vollert et al., 2011). The test consisted of a Plexiglas box with a light compartment made from clear Plexiglas (27 cm x 27 cm x 27 cm) and a dark compartment made from black non-clear Plexiglass (27 cm x 18 cm x 27 cm) that blocked light. Both compartments were separated by a partition with a single opening (7 cm x 7 cm) to allow passage between the compartments. Each test consisted of placing the mouse in the center of the light compartment and allowing the mouse to explore the Plexiglas box for

5 minutes. Transitions between the light and dark compartments was defined as once the mouse's head and forelimbs crossed the opening between compartments. Each test was observed blinded to the genotype and manually documented the time each mouse spent in the light and dark compartments and the number of transitions between the compartments. The Plexiglas box was cleaned with 70% ethanol between mice.

3.2.3.4 Elevated Plus Maze

Building upon the light dark transition test, the elevated plus maze was used to assess fear and anxiety-like behavior at six, twelve, and eighteen months as previously described (Vollert et al., 2011; Butler et al., 2013). Compared to the light dark transition test the elevated plus maze introduces the additional elements of height and openness in the form of an X-shaped apparatus. The apparatus consists of four 5 cm x 30 cm runways arranged perpendicularly to each other and elevated approximately 1 meter above the floor. Two opposing arms are open with the other two opposing arms having tall grey Plexiglas walls (15.5 cm height) and a central open area connecting the four arms. Each test consisted of placing the mouse in the center area facing one of the open arms and allowing the mouse to explore the apparatus for 5 minutes. Each test was observed blinded to the genotype and manually documented the time spent in the open and closed arms

and number of transitions between arms. The elevated plus maze was cleaned with 70% ethanol between mice.

3.2.3.5 Social Dominance Tube

Social behavior was measured by the social dominance tube test as previously described (Lindzey et al., 1961; Filiano et al., 2013). The social dominance tube test consists of a clear Plexiglas tube (3.5 cm ID x 30 cm in length). Mice of the same sex but opposite genotype ($Grn^{+/-}$ vs. NTg) and from different cages were paired for testing. Mice of each genotype were assigned evenly to the left and right sides of the tubes to avoid potential side bias. Each trial consisted of placing mice into either end of the tube and released simultaneously when both mice were completely inside. A trial was considered over when two paws of one mouse left the tube deemed the 'loser' or less dominant and the mouse deemed the 'winner' or more dominant (**Fig. 3**). Tests longer than 2 minutes or if mice crossed paths in the tube were ended and run again at the end of the testing session. All tests were manually recorded by the observer who was blind to genotype. The social dominance tube was cleaned with 70% ethanol between every trial.

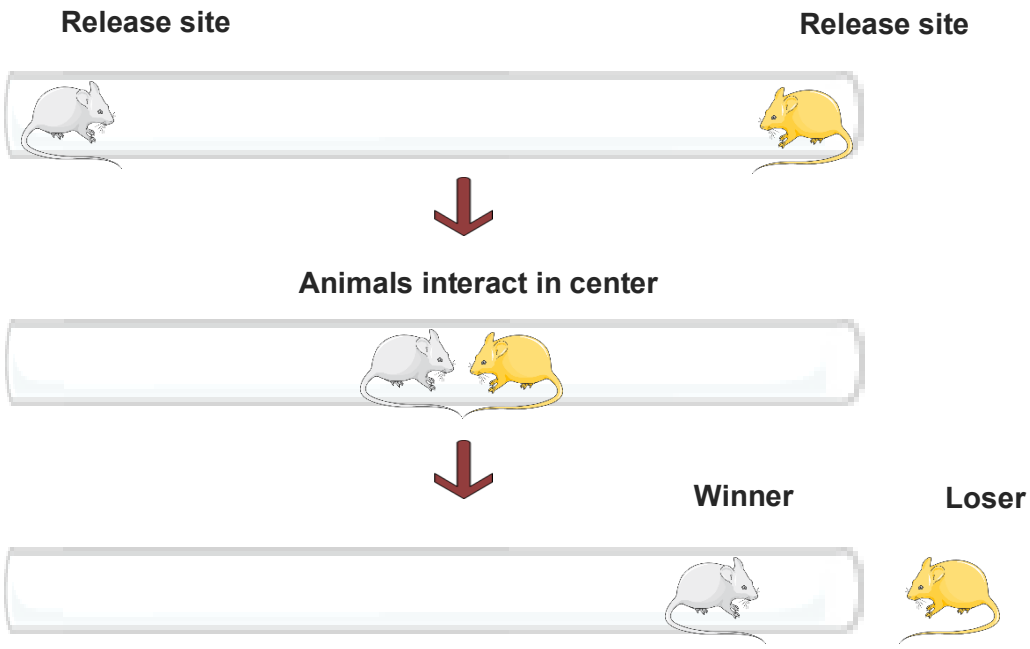

Figure 3. Illustration of the social dominance tube test. Mice of different genotypes ($Grn^{+/-}$ vs. NTg) are released into opposite ends of the clear narrow acrylic tube. The mice will then interact in the middle of the tube with the more dominant mouse forcing the less dominant mouse out of the tube. A mouse is declared the loser when all four paws are outside of the tube while the mouse remaining inside the winner.

3.2.3.6 Cued Fear Conditioning

Amygdala-dependent short-term associative learning was assessed at six months by cued fear conditioning as previously described (Butler et al., 2013). In this test mice are conditioned to freeze to an auditory cue that is associated with a foot shock and/or tone. Short-term associative learning is measured by the ability for the mouse to learn and remember the association of the auditory cue with the aversive stimulus one hour after the conclusion of the training trial. A training trial was used for the acquisition of fear conditioning consisting of a 13 cm x 10.5 cm x 13 cm conditioning chamber containing a 28 V house light, loudspeaker, and a metal rod floor with 19 equally placed rods (2.8 mm diameter). For the training session, mice were placed in the conditioning chamber and were able to explore the environment for 2 minutes. Subsequently, three pairings of a 30 second tone (80 dB, 2kHz) preceded by a 2 second foot shock (0.75 mA) occurred at 3, 4, and 6 minutes. The training session lasted 7 minutes (60 seconds after the last shock). The amount of time the mouse spent freezing, defined as immobility, was detected by infrared cameras within the conditioning chamber and measured automatically using computer software (FreezeFrame, Med Associates/Actimetrics). At the end of the training session mice were returned to their home cage.

One hour after the training session mice were tested for short-term cued fear conditioning. This consisted of placing the mouse back into the same conditioning chamber used in the training session but modified (different olfactory, spatial, tactile, and visual characteristics) to stimulate a novel environment. During the cue trial mice could explore the modified conditioning chamber for 7 minutes

with the tone presented for 3 minutes in the middle of the trial. As before in the training session freezing behavior was measured automatically using computer software. The conditioning chamber was cleaned with 70% ethanol between mice during the training trials and with isopropanol during cued testing.

3.2.3.7 Hot Plate Analgesia

Nociception was measured in mice using the hot plate analgesia meter (Columbus Instruments, OH). The plate was heated to 55C, and each mouse was placed in the center. Latency was defined as the period from being placed on the meter to when the mouse either licked its paw or jumped as an indicator of a nociceptive threshold. A trial was aborted if the mouse stayed on the meter for longer than twenty seconds without a response.

3.2.3.8 Pre-Pulse Inhibition

Sensorimotor gating was measured using the pre-pulse inhibition (PPI) test by assessing the startle response to a sudden loud sound. This test is based on the observation that the startle response is diminished when a softer sound is given before the loud sound. The diminished startle response is a neurobiological process of filtering out redundant and/or unnecessary stimuli and is a form of sensorimotor gating. PPI was measured using the SR-LAB Startle Response System (San Diego Instruments, San Diego, CA) as previously described (Spencer et al., 2006). The testing apparatus consists of a Plexiglas cylinder enclosed in a sound-attenuated startle chamber. The startle response was measured by an electrostatic sensor located directly below the Plexiglas cylinder. Each test last for 15 minutes and consists of placing the mouse in the Plexiglas cylinder with the first

5 minutes for acclimation and the last 10 minutes for the test session. The test session consisted of the following trials in a pseudorandom manner with an inter-trial interval of 10-20 seconds: a) no stimulus trial to measure baseline movement; b) startle only trial (40 ms, 120 dB) to measure the maximum startle response and c) 5 additional trial types (20 ms each; 78, 82, 86, or 90 dB) that preceded 100 ms before the 120 dB startle stimulus (Paylor and Crawley, 1997). The testing apparatus was cleaned with 70% ethanol between mice.

The percent PPI was calculated by using the maximum startle response averaged over 6 trials and used in the following formula:

100 – [(startle response on acoustic prepulse + startle stimulus trials/startle response) x 100]

3.2.3.9 Morris Water Maze

The Morris water maze (MWM) was used to assess hippocampal-dependent spatial learning and memory in $Grn^{+/-}$ at eighteen months-of-age. The MWM is a spatial navigation task requiring the mouse to learn the location of a hidden “escape” platform in a circular pool divided into four quadrants (**Fig. 4**). The water is made opaque with white tempura powder requiring the mouse to rely only on four visual cues outside of the pools as a guide to locate the hidden escape platform located in the 4^{th} quadrant. The MWM consists of a training phase for spatial learning followed by probe trials for short-term and long-term memory trials. The training phase consists for four trials a day with a thirty-minute inter-trial

interval for four days where the mouse is trained to locate the hidden platform. Each trial consisted of releasing the mouse into the pool from one of the four starting quadrants, with the hidden platform location remaining constant. The time taken for the mouse to find the hidden platform is measured as the latency to escape and each trial lasted a maximum of 60 seconds or until the mouse successfully discovered the hidden platform. Over the course of the four training days the starting position for each trial was changed so that each mouse started from a different position each day and the starting position of each trial within each day also changed.

One and twenty-four hours after the last training trial (trial number 16; day 4 and 5) each mouse underwent a probe trial, where the hidden platform was removed, and the mouse could search the pool for 60 seconds. Time spent in each quadrant was measured to assess if the mouse remembered the location of the hidden platform during the training trials. After the last probe trial on day 5, a visual acuity test was performed to rule out potential visual differences between $Grn^{+/-}$ and NTg mice as a potential confounding variable. The visual acuity test consisted of three trials where a visual platform (consisting of a black box on top of a 10 cm post extending above the water) was positioned at different locations within the circular pool excluding the position for the hidden platform. Mice were allowed a maximum of 60 seconds to find the visual platform measured as escape latency. The swimming speed was also recorded automatically by software for each mouse during the training trials to rule out hyperactivity as a confounding variable. All tests

were assessed using Ethovision XT software and track system (Noldus, Leesburg, VA, USA).

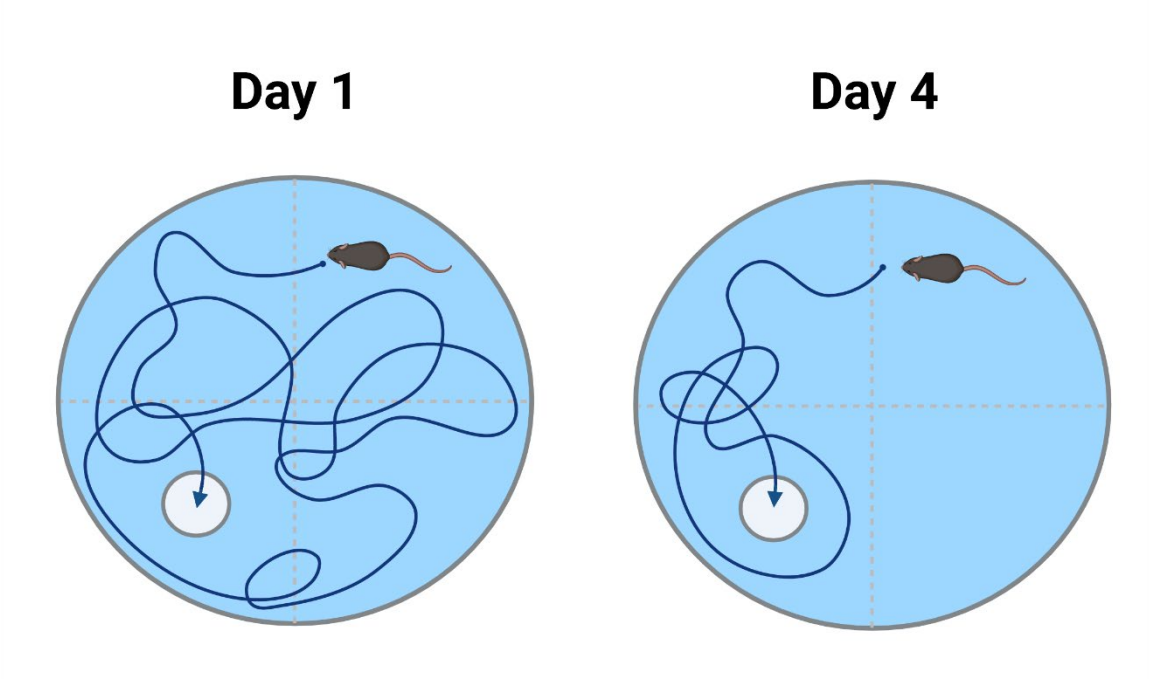

Figure 4. Illustration of the Morris Water Maze. Example swim paths from Day 1 and Day 4 illustrating spatial learning. On the first day mice swim aimlessly around the pool until eventually finding the hidden platform (white circle). Over the course of each trial and day mice will get better at locating with the hidden platform. Eventually, on day 4 mice exhibiting spatial learning will have a more direct path to and faster time finding the hidden platform. Created with BioRender.com

3.2.4 Electrophysiology

Male mice between eighteen and twenty months of age were sacrificed, and brains immediately and briefly transferred to ice-cold carboxygenated (95%O2/5%CO2) cutting solution: (5 mM glucose, 110 mM sucrose, 60 mM NaCl, 28 mM $NaHCO_3$, 3 mM KCl, 1.25 mM NaH_2PO_4, 7 mM $MgCl_2$, and 0.5 mM $CaCl_2$, 0.6 mM ascorbate). Sagittal hippocampal slices (400 μm) were prepared in an ice-cold cutting solution using a 1000Plus Vibratome sectioning system (Vibratome Co., St. Louis, Missouri). Slices were transferred to room temperature (1:1) cutting solution/artificial cerebral spinal fluid (aCSF; 25 mM glucose, 125 mM NaCl, 2.5 mM KCl, 1.25 mM NaH_2PO_4, 25 mM $NaHCO_3$, 1 mM $MgCl_2$, and 2 mM $CaCl_2$), for 20 minutes and then to 100% aCSF at room temperature for a minimum of 1 hr prior to recordings. Recordings were carried out in an interface chamber (Harvard Apparatus, Holliston, MS) at room temperature, perfused continuously with carboxygenated ACSF (perfusion rate: 1-2 ml/min). A bipolar enamel-coated platinum stimulating electrode was placed in CA3 Schaffer collateral/commissural fibers, and a borosilicate glass recording electrode (resistance 1-4 MΩ) filled with aCSF was placed into stratum radiatum of area CA1 (**Fig. 5**). Field excitatory postsynaptic potentials (fEPSP) were collected every twenty seconds and averaged over two-minute intervals using a stimulus intensity that produced 30-50% of the maximum initial slope fEPSP obtained during input/output measurements. Baseline fEPSPs were monitored for at least 20 min for stability. For LTP induction, two high-frequency stimuli (HFS) trains were delivered at 100Hz for 1 sec with an inter-train interval of 5 min. The stimulus intensity of the HFS

pulses was matched to that used during baseline recordings. Data was collected and analyzed using pClamp version 10 (Molecular Devices, Sunnyvale, CA). Recordings were normalized to the baseline mean before introduction of LTP.

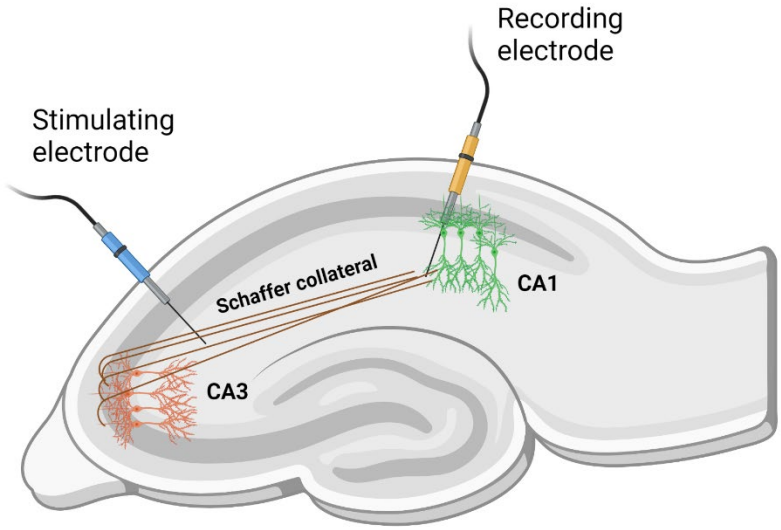

Figure 5: Illustration of a sagittal hippocampal slice with electrodes in place for measuring long-term potentiation. The bipolar enamel-coated platinum stimulating electrode (left; blue) is placed into the CA3 Schaffer collateral axons (orange). The borosilicate glass recording electrode (right; yellow) is placed into the stratum radiatum dendrites of the CA1 region. Created with BioRender.com.

3.2.5 Immunohistochemistry and Immunofluorescence

Coronal sections (10μm) were deparaffinized and subjected to antigen retrieval using 10mM sodium citrate, pH 6.0, in a Decloaking Chamber system (Biocare Medical). Following antigen retrieval, sections were blocked with 5% normal goat serum in TBST for 1 hr. Sections were incubated with IBA1 (1:1000 dilution, Wako Chemicals) and GFAP (1:1000 dilution, DAKO) primary antibodies overnight and washed with TBST. Sections were then incubated with species-specific HRP-goat antibody (Vector Laboratories) for 30 min, washed with TBST 3 times, and developed with chromogenic substrate diaminobenzidine tetrahydrochloride (DAB; Vector Laboratories). Slides were viewed under an Olympus IX61 DSU confocal microscope, and the images were processed with Neurolucida (MicroBrightField Inc., Williston, VT).

For immunofluorescence staining, coronal sections (10μm) were deparaffinized and subjected to antigen retrieval using 10mM sodium citrate, pH 6.0, in a Decloaking Chamber system (Biocare Medical). Following antigen retrieval, sections were blocked with 5% normal goat serum in TBST for one hour and then washed with TBST 3 times. Sections were then blocked using mouse-on-mouse (MOM) reagent for one hour at room temperature and then washed with TBST 3 times. Sections were then incubated with mouse anti-GAD67 (1:500 dilution, Millipore) primary antibody overnight and subsequently washed with TBST. Following washing, sections were incubated with biotinylated secondary (1:200 dilution, Vector) for 30 min at room temperature and then washed with TBST 3 times. Sections were then incubated with avidin fluorophore (1:100

dilution, Vector) for 10 min at room temperature, washed with TBST, and mounted using Fluoro-Gel II (EMS).

3.2.6 Image analysis

For image analysis of IBA1, GFAP, and GAD67, four montage photomicrographs, spaced 50 μm apart, were taken for each mouse with a 20x objective. Thresholds were set to include only GFAP, Iba1, and GAD67 positive cells. The total number of GFAP or Iba-1 positive cells were counted and averaged for the four montage photomicrographs by a blind observer using NIH ImageJ software in the cortex and hippocampus between Paxinos plate numbers 42 and 52 (Filiano et al., 2013).

3.2.7 Western blot and image analysis

Brain lysates were prepared using radioimmune precipitation buffer (RIPA; Thermo Scientific) supplemented with 2% SDS followed by extraction of RIPA insoluble pellets with urea buffer (7M urea, 2M thiourea, 4% CHAPS, 30 mM Tris, pH 8.5) as previously described (Wils et al., 2012). Hemibrain homogenate protein extracts were separated using SDS-PAGE, transferred to a polyvinylidene difluoride membrane, and probed for protein expression. The membranes were put into SuperBlock T20 (PBS) blocking buffer (Thermo Scientific) for one hour at room temperature. Blots were then incubated in primary antibody PGRN (R&D Systems, 1:2000) and TDP-43 (Proteintech, 1:2000) in Tris-buffered saline containing 0.5% Tween 20 (TBST) overnight at 4°C. Membranes were then washed three times in TBST and incubated for one hour at room temperature with appropriate HRP secondary antibody (Jackson Laboratories, 1:10000) and processed with an

enhanced chemiluminescence reagent kit (Amersham ECL plus kit, GE Healthcare). Blots were imaged by a Fluorchem 8900 imaging system with the intensity of each immunoreactive band quantified using ImageJ and normalized to GAPDH (Millipore, 1:3000)

3.2.8 Data analysis

All experiments were conducted by observer's blind to genotype. All data are expressed as mean ± standard error mean. Data was analyzed using Staistica (TIBCO Software, Pal Alto, CA) and statistical comparisons were made using a two-sample t-test to compare $Grn^{+/-}$ and NTg mice. A two-way analysis of variance (ANOVA) was used to compare main effect of sex and genotype followed by a Fisher LSD *post-hoc* for behavioral tests (Buccafusco, 2009). For the motorized rotarod a two-way repeated measures ANOVA, with the $Grn^{+/-}$ genotype and age (six and eighteen months) as between-subject factors and trials as within-subject factor was used, followed by two-way ANOVA and Fisher LSD *post hoc* to analyze the effect of PGRN haploinsufficiency effect on rotarod performance at each of the eight trials at six and eighteen months of age. $p < 0.05$ was considered significant. For the tube test of social dominance statistical comparisons were made with a two-tailed binomial test against an expected outcome of 50%.

3.3 Results

3.3.1 Progranulin haploinsufficiency causes cognitive and non-cognitive behavioral abnormalities in $Grn^{+/-}$ mice

First, Western blotting's relative levels of PGRN were detected using a polyclonal antibody against full-length PGRN in brain homogenates of $Grn^{+/-}$ and

NTg mice to confirm genotype. Consistent with genotypes, a two-sample t-test revealed a significant reduction (50%; $p<0.001$) of PGRN protein in whole brain homogenates of $Grn^{+/-}$ mice compared to NTg littermates **(Fig.6)**.

Differences in non-cognitive behavior have previously been reported in $Grn^{-/-}$ mice; therefore, non-cognitive behavior was next investigated in $Grn^{+/-}$ mice (Petkau et al., 2012). The open-field test was used to assess exploratory activity in $Grn^{+/-}$ mice and their NTg littermates at six, twelve, and eighteen months. No abnormalities were observed in $Grn^{+/-}$ mice by measuring time spent moving (MOVE), resting (REST), and stereotypic (STEREO) behavior at six and twelve months **(Fig. 7A-B)**. At eighteen months two-way ANOVA revealed a main interaction between sex and genotype, [$F(2, 14)=4.6348$, $p<0.05$]. Newman-Keuls *post-hoc* indicated that male $Grn^{+/-}$ mice spent significantly more time moving (MOVE) compared to NTg mice ($p<0.05$; **Fig. 7C**). Additionally, Newman-Keuls *post-hoc* indicated male $Grn^{+/-}$ mice spent significantly less time resting (REST) compared to NTg mice ($p<0.05$; **Fig. 7C**). These experiments suggest that PGRN reduction may have a protective effect on age-related decline in spontaneous exploratory behavior.

Motor coordination, learning, and balance was next assessed in $Grn^{+/-}$ mice across aging by using a motorized rotarod at six and eighteen months by measuring the latency to fall over the course of two days with each day consisting of 4 trials totaling a total of 8 trials **(Fig. 8A and B)**. Two-way repeated measures ANOVA applied to the latency to fall over the 8 trials revealed a main effect of trials with a significant increase in latency to fall over the course of the 8 trials

[F(7,196)=15.552, p=0.000] indicating mice exhibited motor learning. Repeated measures ANOVA also revealed age as a main effect with eighteen months significantly decreasing overall latency to fall compared to six months [F(1,28)=22.180; p<0.0001], but the $Grn^{+/-}$ genotype did not have a main effect on overall rotarod performance [F(1,28)=0.0035, p=0.954]. Fisher LSD *post hoc* test indicated six-month-old $Grn^{+/-}$ mice had a significantly decreased latency to fall compared to NTg mice on trial 1 (p<0.05; **Fig. 8A**). These results indicate PGRN haploinsufficiency does not affect motor coordination, learning, or balance at either six or eighteen months.

Anxiety-like behavior was next assessed in $Grn^{+/-}$ and NTg littermates by the light dark transition and the elevated plus-maze test, which have been previously reported to be affected in $Grn^{-/-}$ mice (Roberson, 2012). Two-sample t-test indicated no significant differences in time spent in the light compartment between $Grn^{+/-}$ and NTg mice at ages six (p>0.05; **Fig. 9A**), twelve (p>0.05; **Fig. 9B**), and eighteen months (p>0.05; **Fig. 9C**) in the light-dark test indicating PGRN haploinsufficiency did not affect anxiety-like behavior across age. Anxiety-like behavior was further evaluated by the elevated plus maze. At six months a sex specific difference was observed in percent time spent in the open arms **(Fig. 9D)**. Two-way ANOVA did not reveal a main effect of $Grn^{+/-}$ genotype [F(1,27)=2.5572, p=0.1214] or sex [F(1,27)=2.6580, p=0.115] nor a significant interaction effect between $Grn^{+/-}$ and sex [F(1,27)=3.5938, p=0.069]. Two-sample t-test indicated female $Grn^{+/-}$ spent significantly less time in the open arms compared to female NTg mice (p=0.033; **Fig. 9D**). Significant differences between $Grn^{+/-}$ and NTg mice

and sex were not seen at twelve ($p>0.05$; **Fig. 9E**) and eighteen ($p>0.05$; **Fig. 9F**) months. Taken together these results suggest that PGRN haploinsufficiency results in task- and sex-dependent effects on anxiety-like behavior.

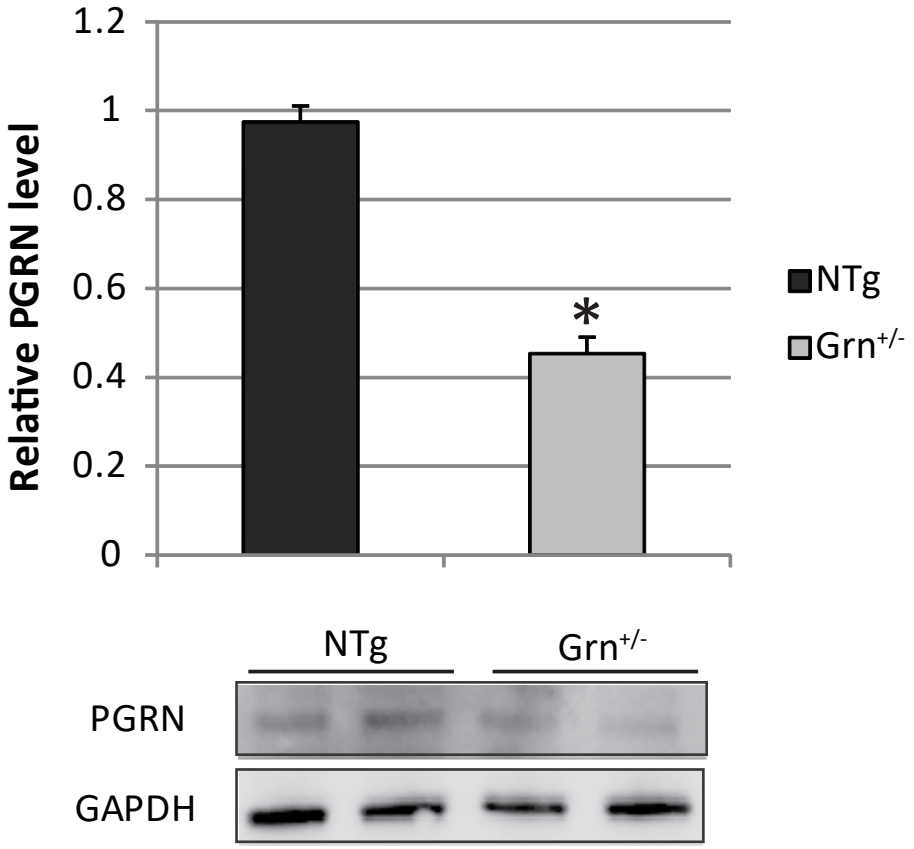

Figure 6. Progranulin expression in NTg and Grn$^{+/-}$ mice. Western blot analysis of relative PGRN levels in whole brain homogenates (*p<0.05; n=5 mice per genotype; age eighteen months).

A.

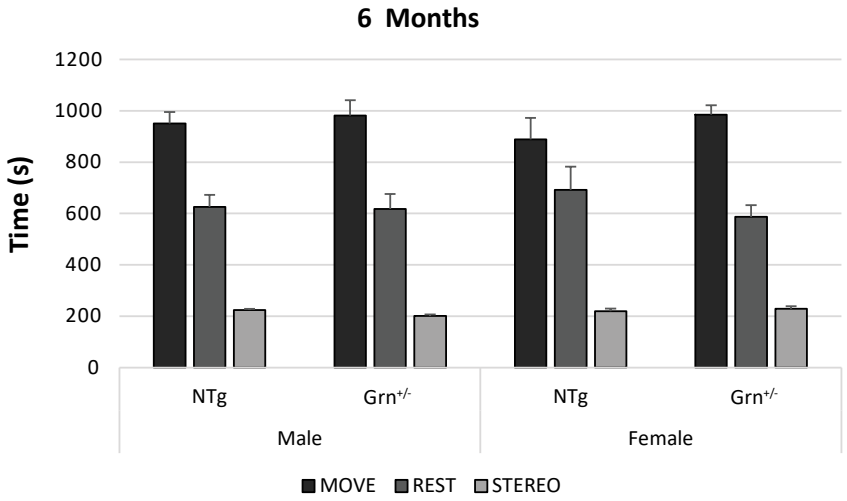
6 Months
Time (s)
1200
1000
800
600
400
200
0
NTg
Grn+/-
NTg
Grn+/-
Male
Female
MOVE
REST
STEREO

B.

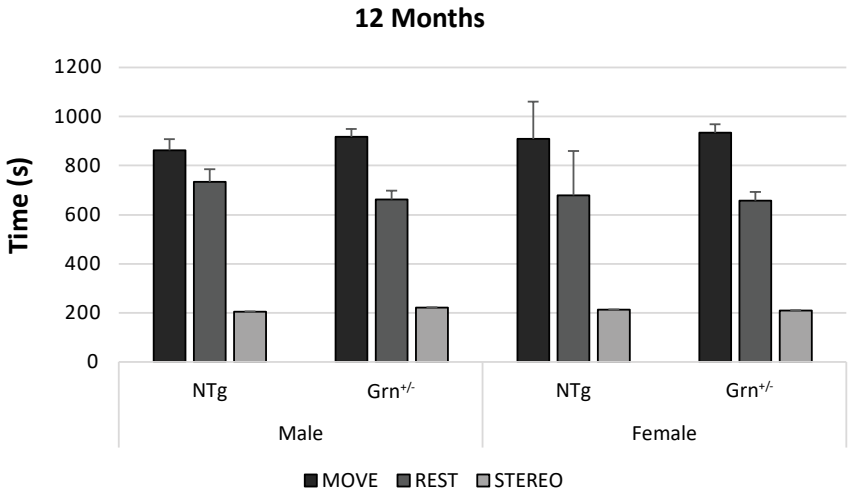
12 Months
Time (s)
1200
1000
800
600
400
200
0
NTg
Grn+/-
NTg
Grn+/-
Male
Female
MOVE
REST
STEREO

C.

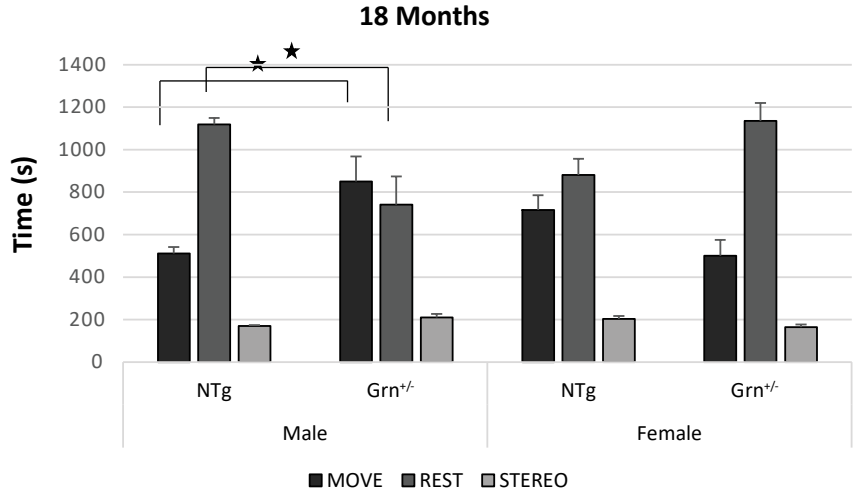
18 Months
Time (s)
1400
1200
1000
800
600
400
200
0
NTg
Grn+/-
NTg
Grn+/-
Male
Female
MOVE
REST
STEREO

Figure 7. Male Grn$^{+/-}$ mice displayed increased exploratory behavior at eighteen months. (A and B) Grn$^{+/-}$ and NTg mice spent similar time moving (MOVE), resting (REST), and stereotypic behavior (STEREO) at six and twelve months. **(C)** However, at eighteen months Grn+/- mice had an increased time moving and decreased time resting compared to NTg littermates. (*$p<0.05$; 6 months N = 7 male NTg, 9 male Grn$^{+/-}$, 10 female NTg, and 12 female Grn$^{+/-}$; 12 months N = 4 male NTg, 13 male Grn$^{+/-}$, 3 female NTg, and 11 female Grn$^{+/-}$; 18 months N = 5 male NTg, 6 male Grn$^{+/-}$, 4 female NTg, and 4 female Grn$^{+/-}$).

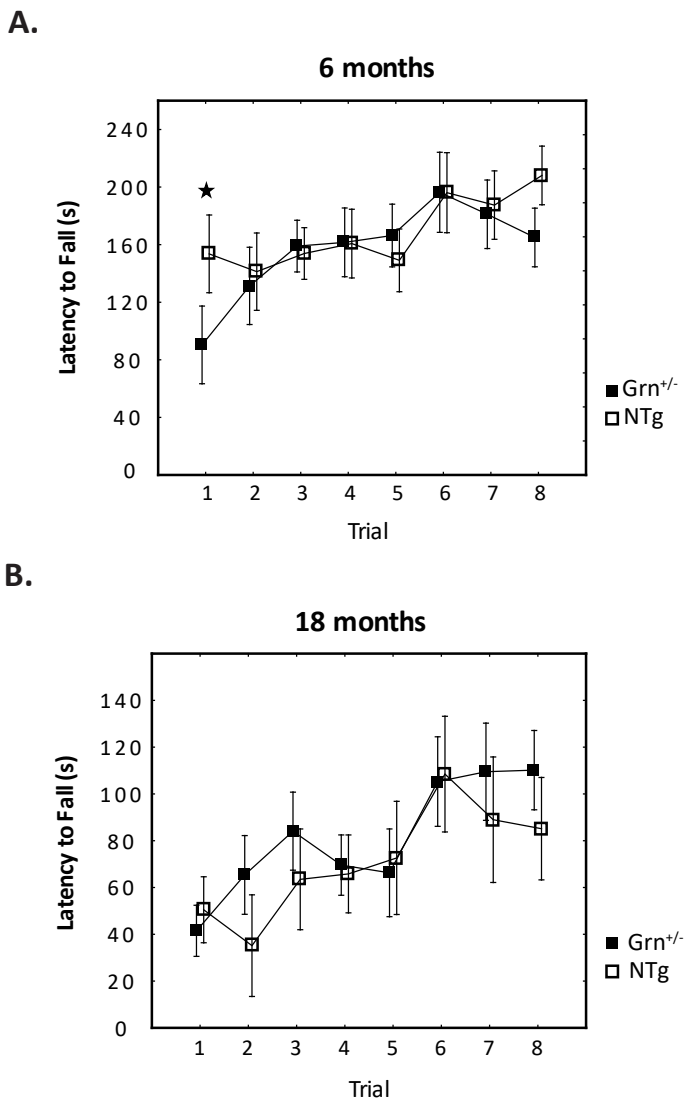

Figure 8. Progranulin haploinsufficiency had a mild impact on motor coordination and balance. (A) $Grn^{+/-}$ mice had a signficant increase in latency to fall on the first trial but otherwise normal on the following seven trials compared to NTg littermates at six months. **(B)** No significant differences were observed between $Grn^{+/-}$ and NTg mice at eighteen months. (*$p<0.05$; N = 6-10 mice per genotype).

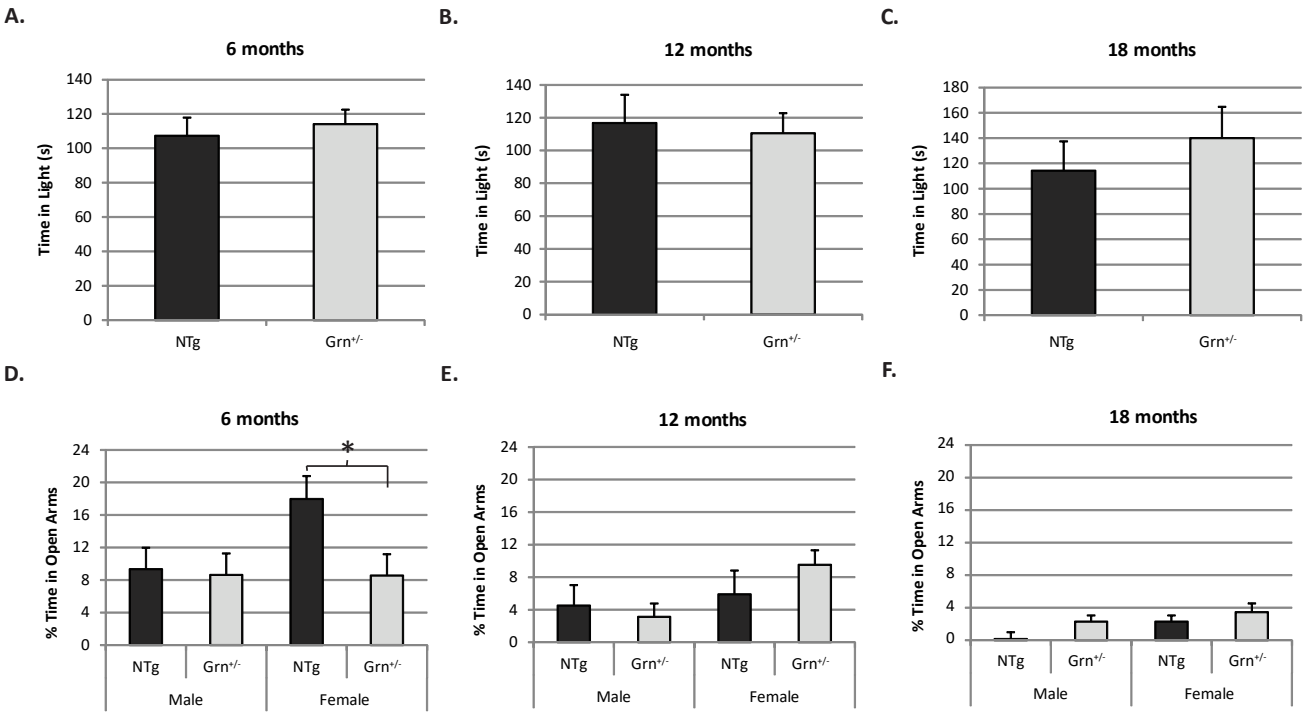

Figure 9. Progranulin haploinsufficiency had a task, age and sex-specific effect on anxiety-like behavior. (A) At six months of age, female $Grn^{+/-}$ mice spent significantly less time time in the open arm compared to female NTg mice exhibiting anxiety-like behavior in the elvated plus maze. **(B and C)** Time spent in the open arms is similar between $Grn^{+/-}$ and NTg mice at twelve and eighteen months of age. **(D, E, and F)** $Grn^{+/-}$ had no signfiicant difference with NTg mice in the time spent in the light/dark test at ages six, twelve, and eighteen months. (*p<0.05; 6m *N* = 16 NTg and 24 $Grn^{+/-}$; 12m *N* = 9 NTg and 16 $Grn^{+/-}$; 18m *N* = 8 NTg and 10 $Grn^{+/-}$; *N* = 4-8 mice per sex and genotype).

Behavioral and emotional changes often precede cognitive alterations in FTD effect of heterozygous loss of PGRN on fear conditioning and were assessed by performing short-term cued-fear conditioning at six months of age. Cued-fear conditioning requires an association between an aversive foot shock and an auditory cue. The amount of time a mouse is frozen after an auditory cue 1-hour post-training is a measure of fear memory. A two-sample t-test was used to compare NTg and $Grn^{+/-}$ mice in short-term cued fear conditioning. Percentage spent freezing was significantly reduced (29.71%; $p<0.05$) in male $Grn^{+/-}$ mice compared to NTg littermates indicating PGRN haploinsufficiency impaired short-term associate learning **(Fig. 10A)**. There were no significant differences between $Grn^{+/-}$ and NTg in the hot plate analgesia test indicating PGRN haploinsufficiency did not affect pain sensitivity and ruling out pain sensitivity as a potential confounding variable ($p>0.05$; **Fig. 10B**).

Abnormalities in social behavior, which are a common symptom of FTLD and have been reported in several different mouse lines, were next studied (Roberson, 2012). To test social impairments in $Grn^{+/-}$ mice, the social dominance tube test was used because of its prior use to assess social dysfunction in $Grn^{-/-}$ mice (Filiano et al., 2013). In the absence of social impairment, each genotype would be expected to win 50% of trials. When paired against NTg mice, $Grn^{+/-}$ mice won 75% of the time at eight months of age (12 of 16 trials; $p=0.278$; **Fig. 11**).

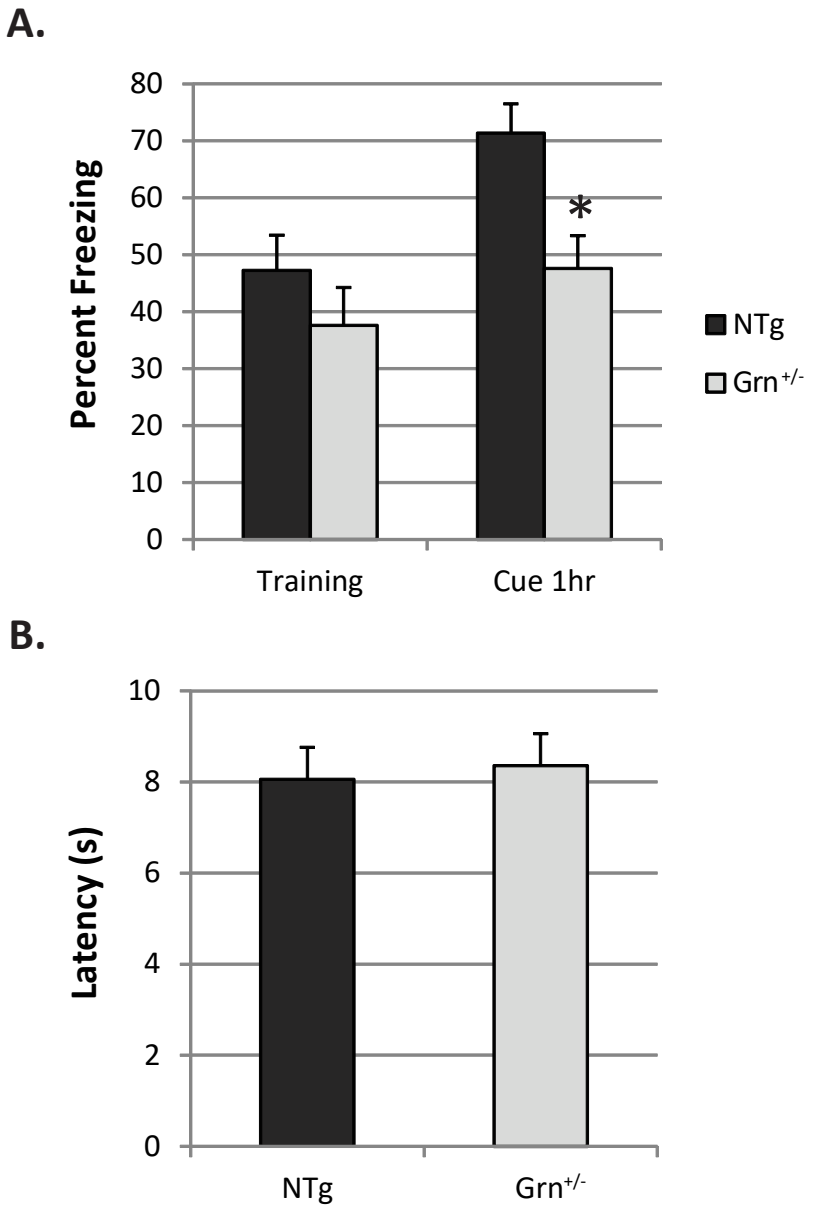

Figure 10. Grn$^{+/-}$ mice exhibited impaired associative learning. (A) At six months male Grn$^{+/-}$ had a signifcantly reudced percent freezing compared to NTg mice in short-term cued-fear conditioning. **(B)** Grn$^{+/-}$ did not exhibit a significant difference in nocieptive response in the hot plate analgesia test. (*p<0.05; NTg = 8; Grn$^{+/-}$ N = 10).

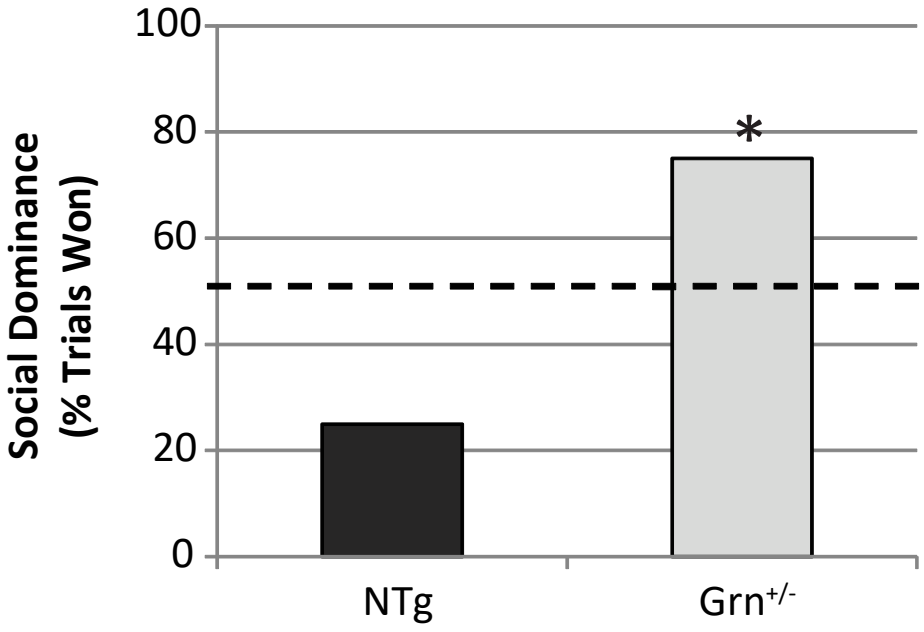

Figure 11. Progranulin haploinsufficiency causes impairment in social behavior. Eight-month-old $Grn^{+/-}$ mice exhibited increased social dominance behavior in the social dominance tube test. $Grn^{+/-}$ mice won 75% (12 of 16) of trials against NTg littermates (exact p = 0.0278).

This result agrees with past reports that PGRN haploinsufficiency causes impaired social behaviors evidenced by increased social dominance behavior (Filiano et al., 2013).

Deficits in PPI have been widely reported in various psychotic disorders, including schizophrenia (Anand et al., 2014). Because FTLD and schizophrenia may share common etiological mechanisms, pre-pulse inhibition changes were tested in $Grn^{+/-}$ mice, a test used to measure the ability to filter out unnecessary information sensorimotor gating (Jankowsky et al., 2004; Galimberti et al., 2012). A two-sample t-test was used to compare $Grn^{+/-}$ and NTg mice revealed no significant differences in either the startle amplitude at 120 dB or percent of inhibition at 74 dB ($p>0.05$; **Fig. 12A and B**). However, a two-sample t-test did reveal significant decreases in the percent of inhibition was observed at 78 (19.32%; $p<0.05$), 82 (21.68%; $p<0.05$), 86 (12.83%; $p<0.01$), and 90 dB (17.72%; $p<0.05$) in $Grn^{+/-}$ mice compared to NTg littermates indicating PGRN haploinsufficiency impaired sensorimotor gating **(Fig. 12B)**.

Deficits in spatial cognitive memory have only been reported in only a few of the published $Grn^{-/-}$ mouse models and none of the $Grn^{+/-}$ mouse models (Roberson, 2012). Therefore, we used a MWM test previously validated in Dr. Eriksen's lab to see if PGRN haploinsufficiency impaired spatial learning and memory as old as eighteen months (Vollert et al., 2013). Using two-sample t-test to compare NTg and $Grn^{+/-}$ mice revealed $Grn^{+/-}$ took significantly longer to find the hidden platform (latency to platform) on day 4 but not days 1, 2, or 3 indicating

impaired spatial learning ($p<0.05$; **Fig. 13A**). However, no significant differences were observed in either the short- (1hr) or long-term (24hr) memory probe test, suggesting that PGRN haploinsufficiency did not impact spatial memory ($p>0.05$; **Fig. 13B**). Additionally, no differences were observed in either the visual cue test or swim speeds ruling out visual and activity levels as potential confounding variables ($p>0.05$; **Fig. 13C and D**).

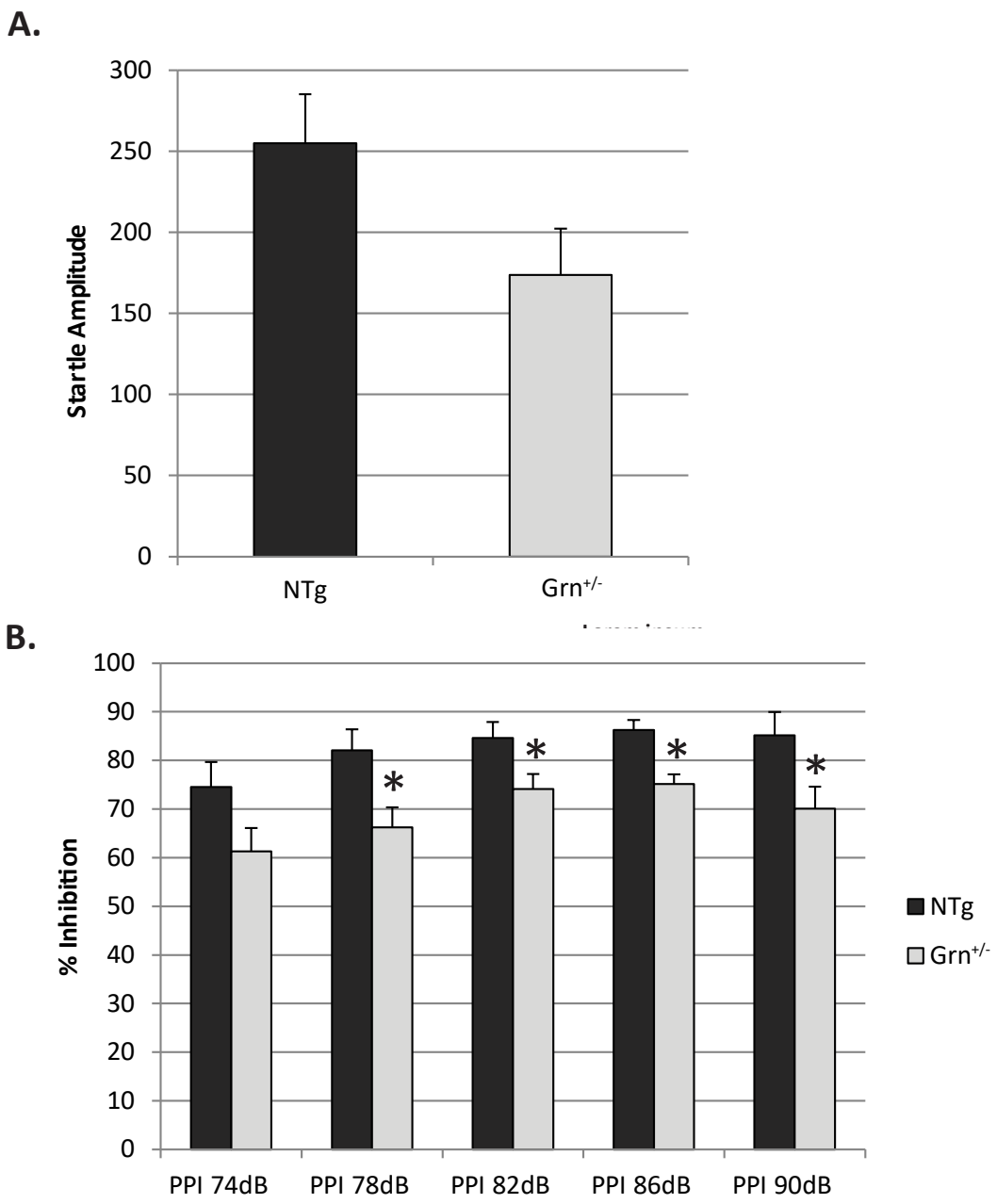

Figure 12. Progranulin haploinsufficiency causes impairment in sensorimotor gating. (A) No differences were observed in startle amplitudes at 120 dB. **(B)** $Grn^{+/-}$ had statistically lower % prepulse inhibition (PPI) at 78, 82, 86 and 90 dB. (*$p<0.05$; NTg N = 8 mice; $Grn^{+/-}$ N = 9 mice).

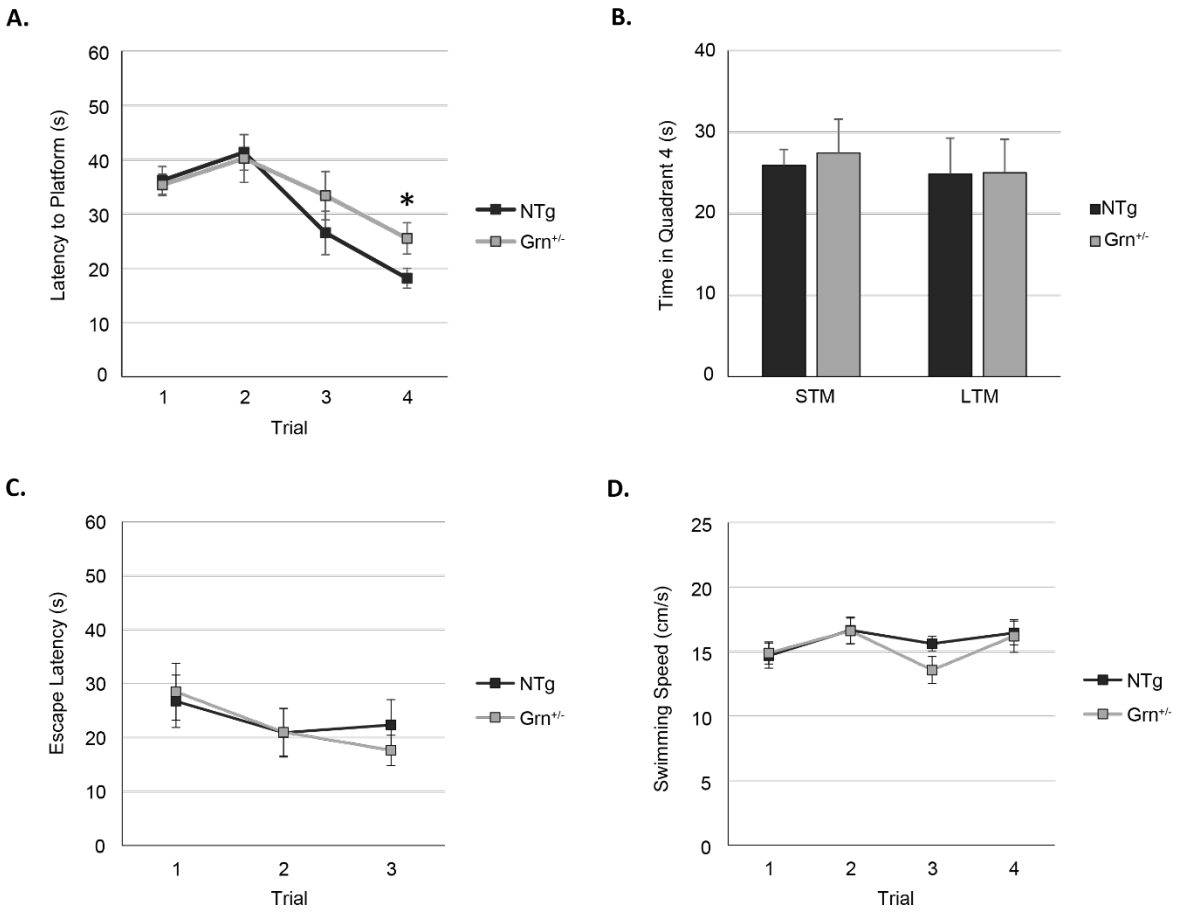

Figure 13. Loss of progranulin worsened spatial learning in eighteen-month-old mice. (A) Grn$^{+/-}$ mice took longer to find the hidden platform on training day 4. **(B)** There were no differences in time spent in quadrant 4 in either the short-term memory (STM) or long-term memory (LTM) probe test. **(C)** No differences were observed in escape latency between genotypes in the visual acuity trials. **(D)** No differences were observed in the swim speed between genotypes during acquisition trials. (*$p<0.05$; NTg = 8 mice, Grn$^{+/-}$ = 8 mice).

3.3.2 Absence of FTD-related neuropathology in $Grn^{+/-}$ mice

Due to observed behavioral differences, the presence of FTD-related neuropathology was next investigated in $Grn^{+/-}$ mice. Neuroinflammation in the hippocampus of $Grn^{+/-}$ mice was assessed at 18 months of age using immunohistochemistry for allograft inflammatory factor 1 (Iba1) and glial fibrillary acidic protein (GFAP), which are markers for resting and activated microglia and astroglia, respectively **(Fig. 14A and B)** (Shapiro et al., 2009). Quantitative image analysis of Iba-1 positive cells to evaluate microgliosis and GFAP as a marker of astrogliosis revealed no differences in the number of either cells between $Grn^{+/-}$ and NTg littermates in the hippocampus indicating the absence of neuroinflammation **(Fig. 15A and B)**.

In humans with FTLD, PGRN-haploinsufficiency results in the pathological aggregation and fragmentation of C-terminal fragments (CTFs) of TDP-43 (Neuman et al., 2006). Using a polyclonal antibody against full-length TDP-34 (Proteintech), no differences were observed in the levels of RIPA soluble TDP-43 and CTFs in eighteen-month-old $Grn^{+/-}$ and NTg littermates indicating TDP processing was not impaired **(Fig. 16A)**. Urea soluble TDP-43 was further studied and observed no significant differences between $Grn^{+/-}$ and NTg mice, suggesting the absence of pathological aggregation of TDP-43 **(Fig. 16B)**.

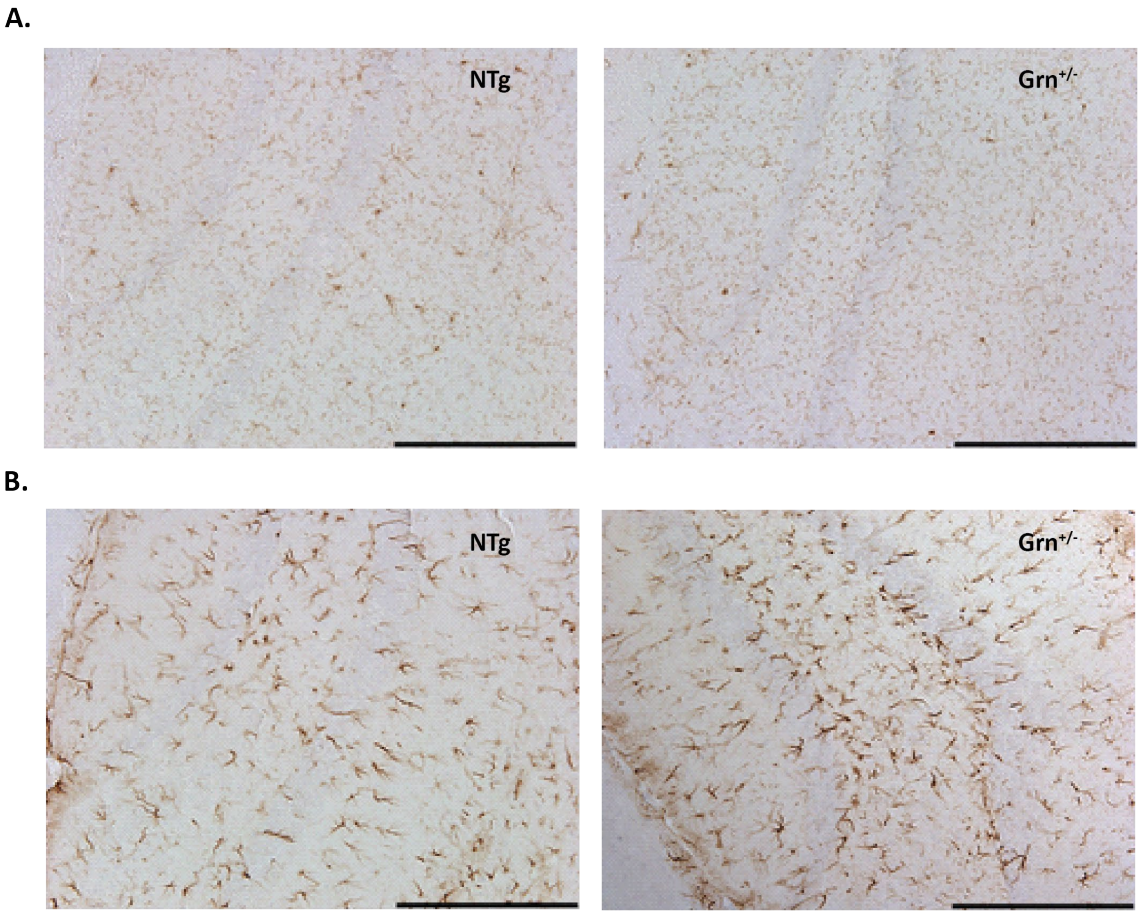

Figure 14. Representative images of Iba1 and GFAP immunoreactivity in the hippocampus of eighteen-month-old Grn$^{+/-}$ mice. (A) Grn$^{+/-}$ mice NTg littermates displayed similar levels of Iba1 immunoreactivity in the hippocampus. **(B)** Grn$^{+/-}$ mice NTg littermates displayed similar levels of GFAP immunoreactivity in the hippocampus. Scale bar represents 200μm. (Brown = Iba1 and GFAP; Blue = hematoxylin counterstain)

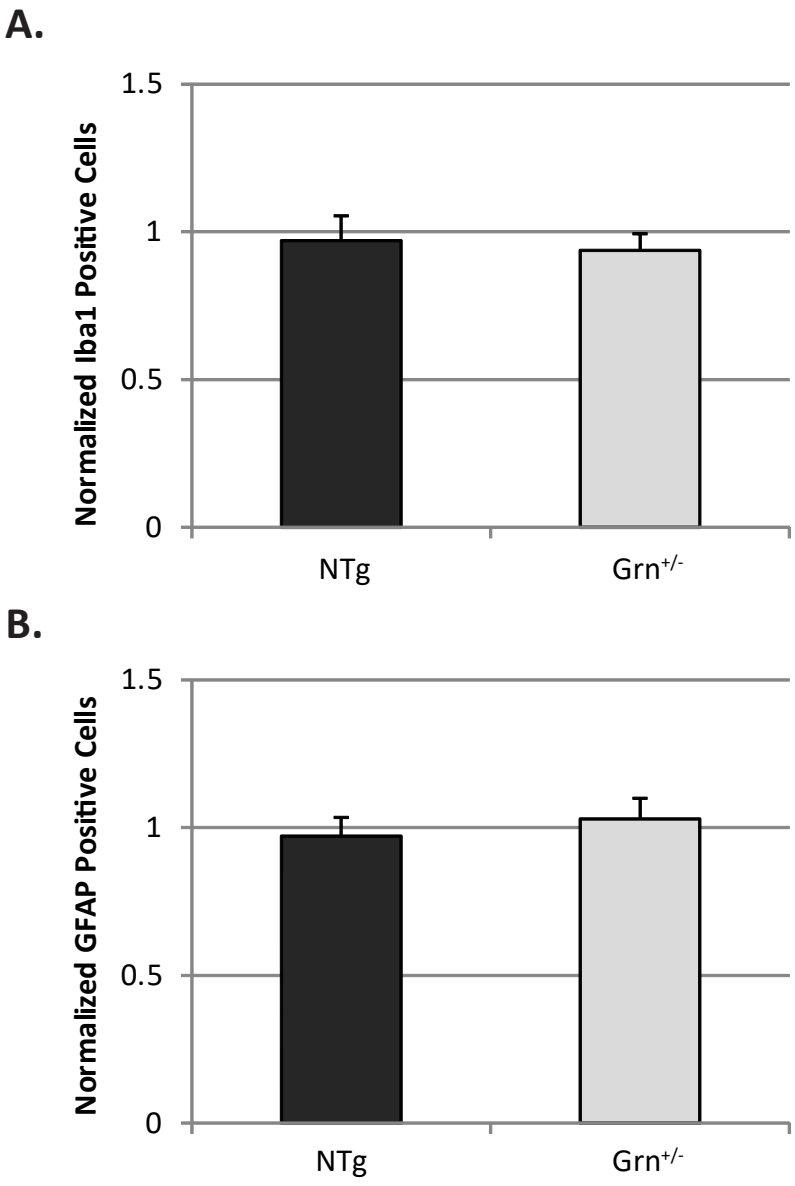

Figure 15. Absence of neuroinflammation in the hippocampi of eighteen-month-old Grn$^{+/-}$ mice. (A) Absence of microgliosis, indicated by Iba1 immunoreactivity in the hippocampi of Grn$^{+/-}$ mice compared to NTg mice. **(B)** Absence of astrogliosis, indicated by GFAP immunoreactivty in the hippocampi of Grn$^{+/-}$ mice compared to NTg littermates. (N = 3 mice per genotype; 18 months of age).

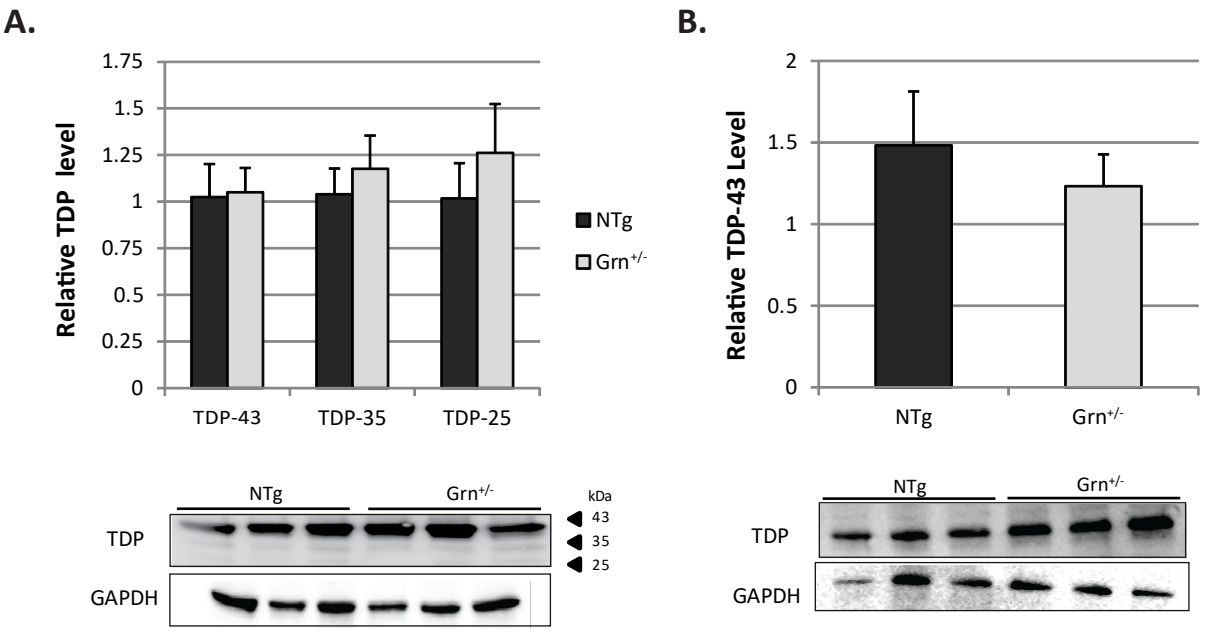

Figure 16. Absence of TDP-43 proteinopathy in eighteen-month-old Grn$^{+/-}$ mice. (A) Immunoblotting of whole brain homogenates did not show any differences in the fragmentation pattern of RIPA-soluble TDP-43 between Grn$^{+/-}$ mice ang NTg littermates. **(B)** Differences were also not observed in urea-soluble TDP-43. (N = 3-5 per genotype; 18 months of age).

3.3.3 Impaired synaptic plasticity and loss of hippocampal GABAergic interneurons in $Grn^{+/-}$ mice

Hippocampal field excitatory post-synaptic potentials (fEPSPs) were next studied in $Grn^{+/-}$ mice at eighteen – twenty months of age (NTg = 4 mice, 11 slices: $Grn^{+/-}$ = 4 mice, 15 slices). Alterations in LTP have previously been reported in some but not all PGRN transgenic mouse models (Petkau et al., 2012; Filiano et al., 2013). Hippocampal neurons from both NTg and $Grn^{+/-}$ exhibited normal responses to increasing stimulation intensities exhibited by the input-output curve **(I/O Fig. 17A)**. Long-term potentiation (LTP) was induced by two brief bursts of high-frequency stimuli (HFS, 100 shocks at 100 Hz) **(Fig. 17B)**. A two-sample t-test revealed significant decrease in post-tetanic potentiation 1 (PTP1) (42.59%; $p<0.05$) and post-tetanic potentiation 2 (PTP2) (46.47%; $p<0.01$) was observed in $Grn^{+/-}$ mice compared to NTg littermates **(Fig. 17C).** Additionally, a significant decrease in the resultant mean of LTP 45-minute post-HFS conditioning (53.29%; $p<0.001$) was observed in $Grn^{+/-}$ mice compared to NTg littermates indicating PGRN haploinsufficiency impaired LTP at eighteen months **(Fig. 17D)**.

One explanation for the cognitive behavioral results is that hippocampal and cortical GABAergic interneurons are either reduced or lost in $Grn^{+/-}$ mice. Immunofluorescence staining was used to quantify the number of GAD67-positive cells (GABAergic neuron marker) in the hippocampus and the posterior parietal cortex. Significantly fewer GAD67-positive cells were observed in $Grn^{+/-}$ compared to NTg littermates. A two-sample t-test a significant reduction of GAD67-positive cells in the DG (30.3%; $p<0.05$) and CA1 (18%; $p<0.05$) hippocampi regions but

not significant in the posterior parietal cortex (0.7%; $p>0.05$) of $Grn^{+/-}$ mice compared to NTg littermates **(Fig. 18)**.

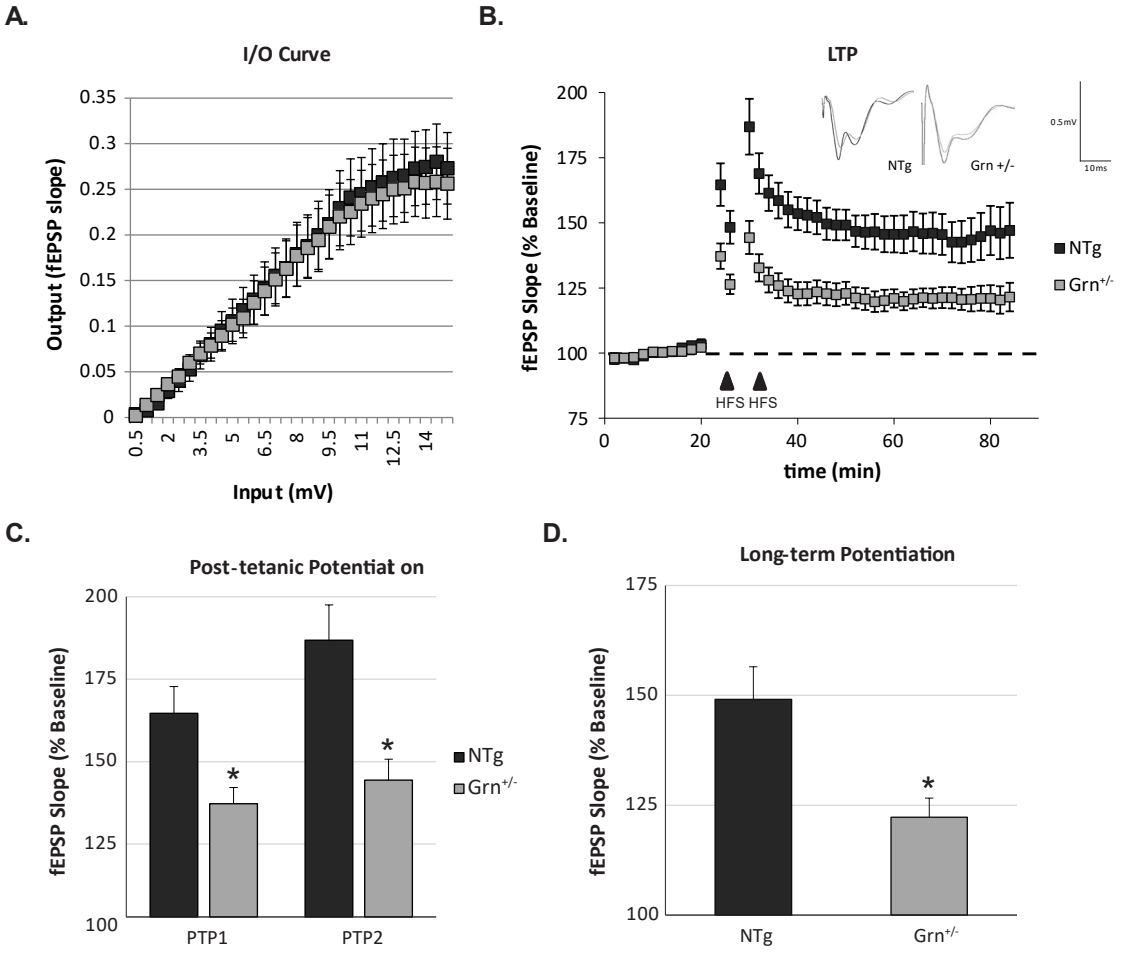

Figure 171. Impaired long-term potentiation (LTP) in Grn$^{+/-}$ mice at eighteen-twenty months. (A) No differences in fEPSPs were observed with increasing stimulus intensities. **(B)** LTP was induced by two bursts of high-frequency stimuli (HFS, 100 shocks at 100 Hz). **(C)** Quantification of post-tetanic potentiation (PTP) after both bursts of HFS and **(D)** LTP, measured 45 minutes after HFS, was significantly reduced in Grn$^{+/-}$ mice compared to NTg mice. (*p< 0.05; NTg = 4 mice, 11 slices; Grn$^{+/-}$ = 4 mice, 15 slices).

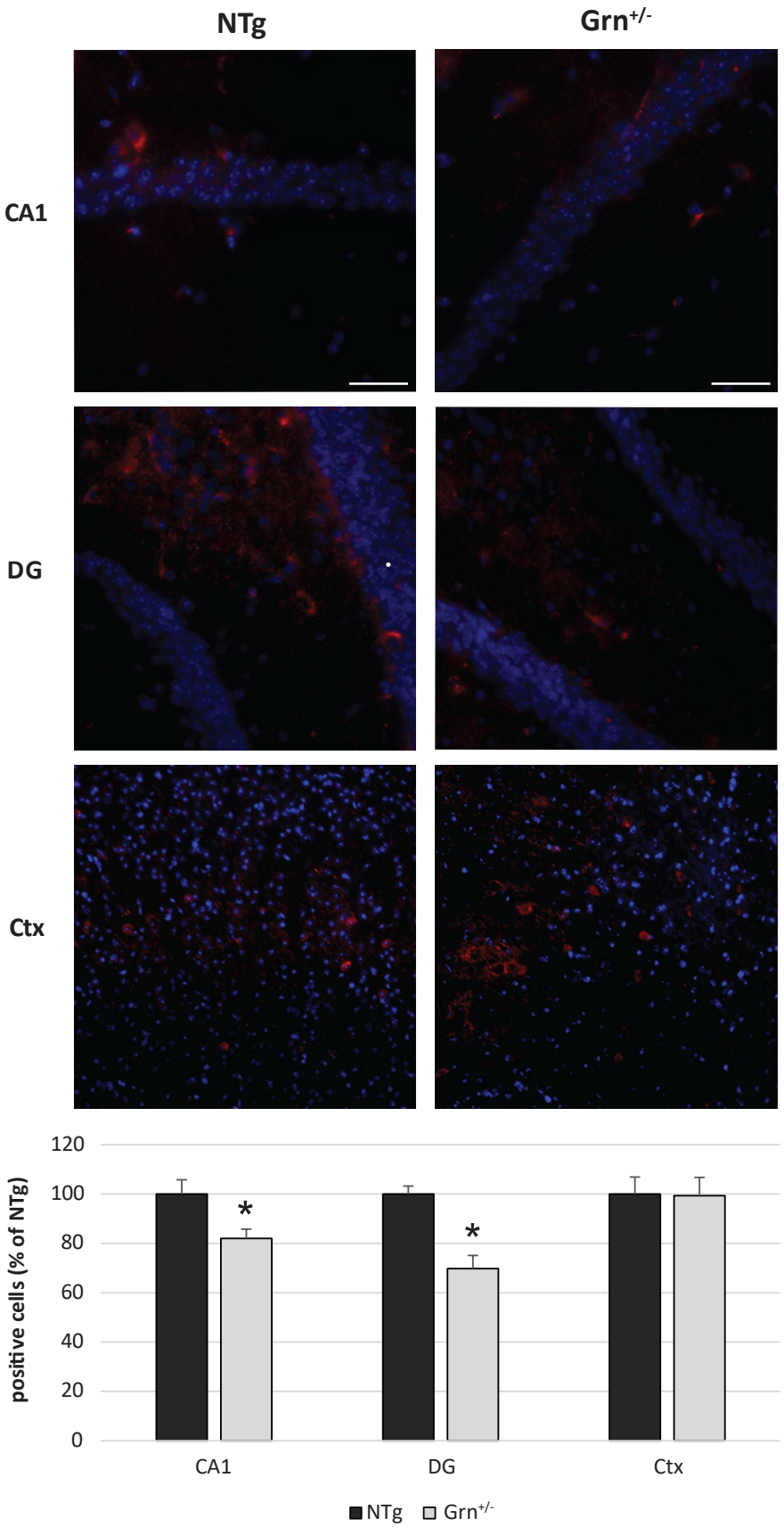
NTg
Grn+/-
CA1
DG
Ctx
positive cells (% of NTg)
120
100
80
60
40
20
0
*
*
CA1
DG
Ctx
NTg
Grn+/-

Figure 182. Loss of GABAergic interneurons in hippocampal area DG in $Grn^{+/-}$ mice. (A) Fluorescent immunostaining of the GABAergic marker GAD67 in the CA1 and DG regions of the hippocampus and the posterior parietal cortex of $Grn^{+/-}$ and Ntg mice. **(B)** $Grn^{+/-}$ mice showed a significant reduction in the number of GAD67-positive neurons in the DG and CA1 regions of the hippocampus compared to NTg littermates. (*$p < 0.05$; n=5 mice, 14 sections per genotype; 18 months). The scale bar is 100 uM.

3.4 Discussion

In this Chapter, behavior and neuropathology were evaluated in a novel $Grn^{+/-}$ mouse line across age. The combined results confirm and expand upon a recent report indicating PGRN haploinsufficiency in mice recapitulate key FTD-related behavioral deficits in the absence of neuropathology (Filiano et al., 2013). In agreement with previous reports, our work demonstrates that $Grn^{+/-}$ mice show social and emotional deficits in the absence of neuroinflammation (microgliosis and astrogliosis). These results also extend the previous behavioral reports to include impaired short-term cued-fear conditioning at six months in male $Grn^{+/-}$ mice, sex-specific increases in anxiety-like behavior in the elevated-plus maze, and impaired decreased sensorimotor gating. We also observed mild cognitive impairment in eighteen-month-old $Grn^{+/-}$ mice which is FTD-related behavioral deficit that has been noticeably absent in previous studies behaviorally characterizing PGRN haploinsufficiency. In addition to behavioral abnormalities, synaptic dysfunction and reduced GABAergic interneurons were also observed in old $Grn^{+/-}$ mice. Despite these observed behavioral and functional deficits, we did not observe FTD-related neuropathology including neuroinflammation and TDP-43 proteinopathy contrary to previous studies using transgenic mice with a complete loss of PGRN.

Most reports modeling murine PGRN deficiency have focused on homozygous knock-out mice due to the presence of FTD-related neuropathology, specifically neuroinflammation, that is not seen in PGRN haploinsufficient mouse models (Garcia-Alloza et al., 2006). The most consistent and robust behavioral

deficit seen across the previously published mouse lines is social dysfunction (Leverenz et al., 2007; Yin et al., 2010a; Petkau et al., 2012). Emotional dysfunction including anxiety-like and depression-like behavior is another key feature of FTD and has been reported in PGRN knock-out mice (Chiba et al., 2009; Yin et al., 2010a; Petkau et al., 2012). Memory loss is seen in late-stage FTLD and has been reported in only some mouse lines (Leverenz et al., 2007; Yin et al., 2010a; Vollert et al., 2013). Recently, it has been shown that PGRN haploinsufficiency in mice recapitulate many of the behavioral deficits seen in the knock-out mouse models, including social and emotional deficits but without changes in spatial memory suggesting a dissociation between FTD-related behavioral deficits and neuroinflammation (Filiano et al., 2013). This section confirms and expands upon the previous observation that PGRN haploinsufficiency reproduces key behavioral deficits related to FTLD in a novel $Grn^{+/-}$ mouse line.

Social deficits are the most consistently observed behavior deficit in the four published $Grn^{-/-}$ mouse lines (Garcia-Alloza et al., 2006) and represent a key symptom of FTLD patients (Rascovsky et al., 2011). Patients with FTD often exhibit diminished social interest and diminished empathy (Garcia-Alloza et al., 2006). Multiple tests have been used, including the three-chamber sociability test (Yin et al., 2010a; Filiano et al., 2013), resident-intruder test (Kayasuga et al., 2007; Leverenz et al., 2007; Petkau et al., 2012), and the social dominance tube test (Filiano et al., 2013; Arrant et al., 2016) to measure different aspects of the social phenotype found in FTD in mouse modes. In this study, social deficits in

$Grn^{+/-}$ mice were observed at eight months of age indicated by increased social dominance using the social dominance tube test which has been reported to be a robust behavioral phenotype unique to $Grn^{+/-}$ and not seen in $Grn^{-/-}$ mice (Filiano et al., 2013; Arrant et al., 2016; Arrant et al., 2017). This is in agreement with a previous paper reporting social dominance behavior using a different $Grn^{+/-}$ mouse line with the social dominance tube test between six and eight months (Filiano et al., 2013). In agreement with past studies, PGRN haploinsufficiency was sufficient to cause social deficits in the social dominance tube test a key FTD-related behavior.

Abnormalities in anxiety-like behavior have been reported in multiple studies examining behavior in PGRN-deficient mice. Two studies reported an increase in anxiety-like behavior (Kayasuga et al., 2007; Petkau et al., 2012), and one reporting a decrease in anxiety-like behavior, which they attributed to increased risk-taking behavior (Yin et al., 2010a). In this study, PGRN haploinsufficiency did not affect anxiety-like behavior in the light-dark test. However, young female $Grn^{+/-}$ mice exhibited increased anxiety-like behavior in the elevated-plus maze exhibited by reduced time spent in the open arms. PGRN loss has previously been shown to affect some sexually dimorphic behaviors including aggression and sexual behavior, and *Grn* has been hypothesized to be an androgen-inducible gene (Kayasuga et al., 2007; Suzuki et al., 2009). Fluctuations in the estrogen cycle are known to affect in the elevated plus maze (Walf and Frye, 2007). These results extend the observation of sex differences in

PGRN-deficient mice's behavior, including anxiety-like behavior as seen in the elevated plus maze.

Disturbances in emotion are a common feature of FTLD(Werner et al., 2007; Kipps et al., 2009), and impairments in fear conditioning have been observed in patients with behavioral variant FTD (Hoefer et al., 2008). Progranulin haploinsufficiency has previously been shown to impair cued-fear conditioning at twelve months but not at four months (Filiano et al., 2013). Because $Grn^{+/-}$ mice in the same study was observed to have social deficits as early as six months of age, we tested short-term cued-fear conditioning in $Grn^{+/-}$ mice at six months. Cued fear conditioning is an amygdala-dependent and hippocampus-independent associative learning behavior requiring an association to be made between an auditory cue and an aversive stimulus. In agreement with past reports, we observed a significant reduction in the percentage time spent immobile in $Grn^{+/-}$ mice compared to NTg littermates indicating PGRN haploinsufficiency impaired cued fear conditioning as early as six months

FTD has been suggested to share similar etiological mechanisms with schizophrenia (Lalonde et al., 2005; Galimberti et al., 2012) and loss-of-function *GRN* mutations have been observed in patients with schizophrenia (Momeni et al., 2010). Because deficits in pre-pulse inhibition (PPI) are widely reported in patients with schizophrenia and neurodegenerative diseases (Janus et al., 2015) , PPI was tested in nine-month-old $Grn^{+/-}$ mice. PPI is considered to reflect the automatic inhibitory process sensorimotor gating where irrelevant sensory and/or cognitive stimuli are filtered out and prevented from influencing behavior. PPI is measured

by presenting a weaker auditory prestimulus (prepulse) which inhibits the startle response of an organism to a subsequent stronger auditory stimulus (pulse). We observed significantly reduced percent inhibition in $Grn^{+/-}$ mice at nine months indicating PGRN haploinsufficiency impaired sensorimotor gating.

Mild deficits in spatial learning and memory assayed by the MWM have been observed in only a few of the $Grn^{-/-}$ mice and none of the $Grn^{+/-}$ mouse lines (Roberson, 2012). In general, spatial memory deficits have been observed in older (> sixteen months) (Leverenz et al., 2007; Vollert et al., 2013; Papegaey et al., 2016), but not younger (< twelve months) $Grn^{-/-}$ mice (Petkau et al., 2012). Spatial deficits have not been observed in $Grn^{+/-}$ mice although previous reports have only looked at nine months (Filiano et al., 2013). Because FTD patients do not exhibit cognitive deficits until late into the disease progression (Cruts et al., 2006a) and the previous behavioral work, this study focused on testing spatial memory at eighteen months of age in $Grn^{+/-}$ mice. Following previous literature, only mild spatial deficits were observed exhibited by a significant decrease in the latency to find the platform on Day 4 of the acquisition trials in $Grn^{+/-}$ compared to NTg littermates, but no differences in the probe trials.

Two studies have reported impaired locomotor activity in separate $Grn^{-/-}$ mouse lines, with relatively normal exploratory behavior. Petaku and colleagues observed a significant increase in latency to fall on an accelerating rotarod in male $Grn^{-/-}$ mice indicating impaired locomotor activity (Petkau et al., 2012). In another study, $Grn^{-/-}$ mice were observed to significantly slower swim speed, indicating impaired locomotor activity (Ghoshal et al., 2012). It is worth noting that $Grn^{-/-}$ mice

were reported to have an increased susceptibility to collagen-induced arthritis (Tang et al., 2011), suggesting complete loss of PGRN may affect non-cognitive behavior through peripheral effects. In this study, no biologically significant locomotor activity differences were observed in young or old $Grn^{+/-}$ suggesting locomotor impairment is unique to $Grn^{-/-}$ mice. Additionally, the opposite was observed with old $Grn^{+/-}$ mice exhibiting hyperactivity compared to NTg mice in the open field test.

Several reports suggest that PGRN knockdown alters neuronal connectivity. In one study, the knockdown of PGRN in hippocampal neurons resulted in an increased number of vesicles per synapse and an increase in the frequency of mEPSCs (Tapia et al., 2011). In the same study, the increased number of vesicles per synapse was observed in FTLD patients with PGRN mutations, suggesting PGRN knockdown alters synaptic plasticity. A recent study from the same lab showed that PGRN is secreted at synapses in an activity-dependent manner, suggesting a possible role in regulating activity-dependent changes in neuronal connectivity (Takahashi et al., 2017b). In another study $Grn^{-/-}$ mice exhibited impaired LTP and abnormal neuronal morphology at ten to twelve months of age (Petkau et al., 2012), but not in $Grn^{+/-}$ mice at the same age (Filiano et al., 2013). Because mild spatial cognitive deficits were previously observed at eighteen months of age, LTP was next studied in $Grn^{+/-}$ mice between eighteen and twenty months. A significant decrease in both the post-tetanic potentiation and

LTP were observed in $Grn^{+/-}$ compared to NTg mice, suggesting PGRN haploinsufficiency significantly altered synaptic connectivity at eighteen months.

Our LTP results are inconsistent with a previous study using a different $Grn^{+/-}$ mouse model (Filiano et al., 2013). There are several potential explanations for this apparent contradiction. It is possible that PGRN haploinsufficiency only affects induction of LTP in the Schaffer collateral at eighteen months or older since the previous study measured LTP at twelve months. Another potential explanation is that PGRN haploinsufficiency's effect on LTP is temporally sensitive. The temporal spacing between high frequency stimuli trains have been reported to involve different singling processes and intracellular singling pathways (Woo et al., 2003). For example, trains separated between 3-20 seconds (massed) regulates PKA-dependent LTP (Scharf et al., 2002; Woo et al., 2003), whereas trains separated between 300-600 seconds (spaced) requires PKA for induction of LTP(Kim et al., 2010). The protocol used to induce LTP in the previous study and ours was nearly identical except for the intertrain interval used between HFS's, with the previous study using an intertrain interval of 20 seconds (massed) versus our study utilizing a 300s (spaced) intertrain interval. Therefore, PGRN haploinsufficient effect on the induction of LTP in the Schaffer collateral of the hippocampus is maybe temporally sensitive to spaced intervals only.

Several neuropathological hallmarks present in FTLD patients carrying *GRN* mutations have been reported in multiple $Grn^{-/-}$ mouse lines, including increased microgliosis, increased astrogliosis, and TDP-43 proteinopathy (Garcia-Alloza et al., 2006). Under pathological conditions, TDP-43 is cleaved, translocated

to the cytoplasm, and becomes the main protein constituent of the ubiquitinated inclusions FTLD-U patients with *GRN* mutations (Neumann et al., 2006). The most consistent neuropathological change observed in $Grn^{-/-}$ mouse lines is increased neuroinflammation, in microglia and astrocytes, in the brain. In this chapter, no changes were observed in neuroinflammation in the hippocampus of $Grn^{-/-}$ mice at eighteen months of age, despite observed behavioral changes consistent with the literature (Filiano et al., 2013). Alterations in TDP-43 expression was also observed, but no differences were observed between insoluble full-length TDP-43 and cleavage of RIPA soluble TDP-43 in eighteen-month-old $Grn^{+/-}$ mice despite behavioral abnormalities; these findings are consistent with previous reports in $Grn^{-/-}$ mice (Yin et al., 2010b; Yin et al., 2010a; Ghoshal et al., 2012; Wils et al., 2012). These findings demonstrate that functional deficits of PGRN loss are independent of FTLD-associated neuropathology.

The initial findings that $Grn^{+/-}$ mice lacked FTD-related neuropathology seen in in $Grn^{-/-}$ mice coupled with a lack of robust behavioral phenotypes led to $Grn^{-/-}$ mice being viewed as the superior model for studying PGRN's role in FTD and other neurovegetative diseases. However, the findings in this aim in conjunction with previous reports modeling behavior more extensively in $Grn^{+/-}$ mice calls this initial view into question and suggests that $Grn^{+/-}$ may in fact be the better model for evaluating PGRN's role in neurodegenerative disease. Our findings further strengthen the dissociation between not just FTD-related behavioral deficits and FTD-related neuropathology but also deficits in synaptic plasticity and loss of interneurons. Our results extend previous reports and show $Grn^{+/-}$ mice exhibit a

more complete range of key FTD-related behavioral deficits including learning to previously identified social and emotional deficits. Although initial research did not identify clear behavioral and physiological phenotypes in $Grn^{+/-}$ mice, our results in accordance with past studies suggest social dominance and fear conditioning are robust behavioral phenotypes, having been reproduced in multiple $Grn^{+/-}$ mouse models, and the significant decrease in induction of LTP utilizing a spaced inter-train interval is potentially a novel physiological phenotype. In addition to recapitulating key-FTD behaviors and functional deficits the greatest advantage of $Grn^{+/-}$ mice over $Grn^{-/-}$ is that because one PGRN allele remains the interplay between different pools of PGRN including neuronal, extracellular, and the dynamic expression in microglia are retained. Therefore, $Grn^{+/-}$ may be a more useful tool in evaluating PGRN's role in neurodegenerative diseases and evaluating potential therapies.

CHAPTER 4: PGRN LOSS AND TAU PATHOLOGY

4.1 Introduction

In this chapter, we explore the role of heterozygous loss of PGRN on the development of tau-associated pathologies with the hypothesis PGRN haploinsufficiency exacerbates tau-related behavioral deficits and increases tau phosphorylation. Behavior and neuropathology were examined in the P301S transgenic mouse model, which overexpresses the P301S mutant human tau associated with clinical cases of neurodegenerative tauopathy, with the previously described $Grn^{+/-}$ mouse model. Several experimental approaches of behavior modeling, histology, and western blotting were used to evaluate the effect of PGRN haploinsufficiency on tau-related behavioral deficits and tau pathology. Contrary to previous reports, heterozygous loss of PGRN in the P301S transgenic mouse model has a protective effect on tau pathology indicated by a decrease in AT8 tau phosphorylation that was associated with increased inhibitory phosphorylation of several proteins in the Akt signaling pathway including GSK-3β which is a key proline-directed serine-threonine kinase involved in tau phosphorylation. We also observed a significant decrease in motor coordination and balance in P301S but not P301S-$Grn^{+/-}$ mice further suggesting a protective effect of PGRN haploinsufficiency on tau. These changes were observed with the absence of gross changes in neuroinflammation suggesting a dissociation between

haploinsufficient loss of PGRN's protective effect on tau pathophysiology and neuroinflammation.

4.2 Materials and Methods

4.2.1 Animal models

The P301S tau transgenic (P301S) mouse model expressing human tau (1N4R) with a P301S mutation and develops progressive neurofibrillary tangle (NFT) pathology and neurodegeneration in the brain and spinal cord (Yoshiyama et al., 2007). In addition to neuropathology, they develop lower-limb weakness starting at six months of age. The P301S tau transgenic mouse model was crossed with a $Grn^{+/-}$ mouse model producing P301S tau transgenic mice harboring the *GRN* hemizygote (P301S-$Grn^{+/-}$). Offspring were backcrossed to C57BL/6J mice. All male and female mice used in this study were ten – eleven months of age.

Mice were housed in the animal facility at the University of Houston and housed in a climate-controlled room (25°C) on a 12/12 h light/dark cycle and given food and water ad libitum. All studies were conducted following the University of Houston approved Institutional Animal Care and Use Committee and implemented following the National Research Council's Guide of The Care and Use of Laboratory Animals.

4.2.2 Tissue processing

Animals from both genotypes were euthanized with CO_2, and brains were harvested. One hemibrain was flash-frozen in 2-methylbutane and dry ice and stored for long-term storage at -80°C. The other hemibrain was fixed in Accustain

(Sigma-Aldrich) and stored at 4°C for long-term storage. Accustain fixed brains were subjected to paraffin processing (Leica TP1020) and then sectioned using a Leica microtome at 10-μm intervals. The other half of each brain and cervical spinal cord were snap-frozen and stored at -80°C for biochemical processing. Tissues were homogenized in cold RIPA lysis and extraction buffer (Thermo-Fisher Scientific) containing protease and phosphatase inhibitors. Samples were then centrifuged at 20,000 x g for twenty minutes at 4°C. The pellet was discarded, and a portion of the RIPA lysate was used for biochemical analysis. Sarkosyl–insoluble tau was isolated following previous reports, with RIPA supernatants adjusted to 1% sarkosyl. Samples were incubated for one hour at room temperature and then spun at 100,000 x g at room temperature. The supernatants were discarded, and the pellets were resuspended in O+ buffer (62.5 mM Tris-HCL, 10% glycerol 5%

2-mercaptoethanol, 0.1% SDS phosphatase, and protease inhibitors). Samples were then boiled for 3 min and kept at -20°C for Western blot analysis.

4.2.3 Behavioral tests

4.2.3.1 Open Field

Procedures were performed as described in Section 3.2.3.1.

4.2.3.2 Motor Coordination and Balance

Procedures were performed as described in Section 3.2.3.2

4.2.3.3 Light Dark Transition

Procedures were performed as described in Section 3.2.3.3.

4.2.4 Immunohistochemistry and image analysis

Brain and lumbar spinal cord tissue were paraffin processed and sectioned at 10 um thickness and the same brain plate and spinal cord regions used in immunofluorescence analysis were used. Immunohistochemistry was performed on equidistant sections from the lumbar spinal cord n > 3 sections per animal) and hemibrain (n > 3 sections per animal) using anti-NeuN (1:1000, Millipore), anti-Iba1 (1:500, Wako), and anti-GFAP (1:500, Abcam). Sections were incubated in primary antibody overnight at 4°C, incubated with horseradish peroxidase-labeled secondary antibody, and stained with DAB. The number of positively stained neurons with an identifiable nucleus was quantified by a blinded observer using NIH Image J software to determine the number of alpha motor neurons in the spinal cord's ventral horn and neurons in the cortex. A 200 μm x μ1000 m rectangular region of the CA3 and CA1 was quantified manually for the hippocampus. For Iba1

and GFAP analysis, three sections per mouse were collected and thresholds were set to include only Iba1 and GFAP positive pixels per image and averaged using Image J in the hippocampus between Paxinos plate numbers 42 and 52.

4.2.5 Western blot and image analysis

Tau from the spinal cord, hippocampus, and cortex samples from RIPA and sarkosyl extractions were resolved using SDS-PAGE or dot blot. Blots were probed with tau antibodies [TAU5, (1:1000), AT8 (1:1000), AT100 (1:1000) and AT180 (1:250)]. After overnight incubation at 4°C, blots were incubated in horseradish peroxidase-labeled secondary antibodies and visualized with an ECL substrate kit (Amersham). Band densities were analyzed with NIH Image J software, and band values were normalized to glyceraldehyde-3-phosphate dehydrogenase (GAPDH). Dot blots were prepared by pipetting 1.2 ul of each sample in each square of a nitrocellulose membrane and allowed to dry for 30 minutes. Blots were incubated with T22 (1:250, kindly donated by Dr. R. Kayed) overnight at 4°C, followed by incubation with a horseradish peroxidase-labeled secondary and visualization with ECL. Dot intensities were analyzed with NIH Image J software.

4.2.6 Analysis of Akt signaling pathway

The PathScan Akt Signaling array kit (Cell Signaling Technology, MA) was used according to the manufacturer's instructions to detect phosphorylated proteins in the Akt signaling pathway. The kit detects 16 signaling proteins when phosphorylated, including Akt (Thr308), Akt (Ser473), S6 Ribosomal Protein (Ser235/236), AMPKa (Thr172), PRAS40 (Thr246), mTOR (Ser2481), GSK-3a (Ser21), GSK-3b (Ser9), p70 S6 Kinase (Thr389), p70 S6 Kinase (Thr421/Ser424),

Bad (Ser380), RSK1 (Ser380), PTEN (Ser380), PDK1 (Ser241), Erk ½ (Thr202/Tyr204) and 4E-BP1 (Thr37/46).

4.2.7 Data Analysis

All experiments were conducted by observer's blind to genotype. All data are expressed as mean ± standard error mean. Data was analyzed using Staistica (TIBCO Software, Pal Alto, CA) and statistical comparisons were made using a two-sample t-test to compare P301S and P301S-Grn$^{+/-}$ mice. A two-way analysis of variance (ANOVA) was used to compare all four groups (NTg, Grn$^{+/-}$, P301S, and P301S-Grn$^{+/-}$). After ANOVA, a Fisher LSD *post-hoc* was used for behavioral tests and Tukey's HSD *post-hoc* was used to compare the significant effects between groups. For the motorized rotarod test a two-ways repeated measures ANOVA, with the Grn$^{+/-}$ and P301S genotype as between-subject factors and trials as within-subject factor was used followed by two-way ANOVA and Fisher LSD *post hoc* to analyze the effect of genotype on rotarod performance at each of the 8 trials. $p < 0.05$ was considered significant.

4.3 Results

4.3.1 Heterozygous loss of PGRN affects both motor coordination and anxiety-like behavior in P301S mice

To test the hypothesis that PGRN haploinsufficiency worsened tau pathology motor coordination, learning, and balance assessed using the motorized rotarod was first investigated. Two-way repeated measures ANOVA applied to the latency to fall over the 8 trials revealed a main effect of trials with a significant increase in latency to fall over the course of the 8 trials [F(7,168)=6.8047, p=0.000]

indicating mice exhibited motor learning **(Fig. 19)**. Two-way ANOVA did not reveal main effects by either the $Grn^{+/-}$ [$F(1,24)=0.0533$, $p=0.816$] or P301S genotypes [$F(1,24)=1.4252$, $p=0.244$] or an interaction effect between the two genotypes [$F(1,24)=0.6057$, $p=0.444$]. Fisher LSD *post hoc* indicated P301S mice had a significantly decreased latency to fall on the rotarod for trials 5 ($p<0.05$) and 6 ($p<0.05$) on day two compared to NTg littermates indicating the P301S genotype impacted motor coordination and balance **(Fig. 19A and B)**. P301S-$Grn^{+/-}$ mice on the other hand were not significantly different from NTg mice on trials 5 ($p>0.05$) and 6 ($p>0.05$) suggesting that PGRN haploinsufficiency decreased the effect of the P301S genotype on motor coordination and balance or delayed the onset of motor coordination and balance impairment.

Non-cognitive behavior was further investigated using the open field test. PGRN haploinsufficiency resulted in increased exploratory activity (MOVE) and decreased time spent resting (REST) while exploring the open field **(Fig. 20)**. Two-way ANOVA analysis did not reveal a main effect from either the $Grn^{+/-}$ [$F(2,23)=0.002$, $p=0.998$] or P301S genotypes [$F(2,23)=1.667$, $p=0.211$] nor a significant effect between the two genotypes [$F(2,23)=1.772$, $p=0.192$]. Fisher LSD *post hoc* test indicated P301S-$Grn^{+/-}$ mice spent more time moving (MOVE) and significantly less time moving (REST) compared to $Grn^{+/-}$ mice ($p<0.05$; **Fig. 20**). There were no significant differences in stereotypic behavior (STERO) between P301S-$Grn^{+/-}$ and $Grn^{+/-}$ mice nor any differences in exploratory behavior between NTg and $Grn^{+/-}$ mice and P301S and P301S-$Grn^{+/-}$ mice.

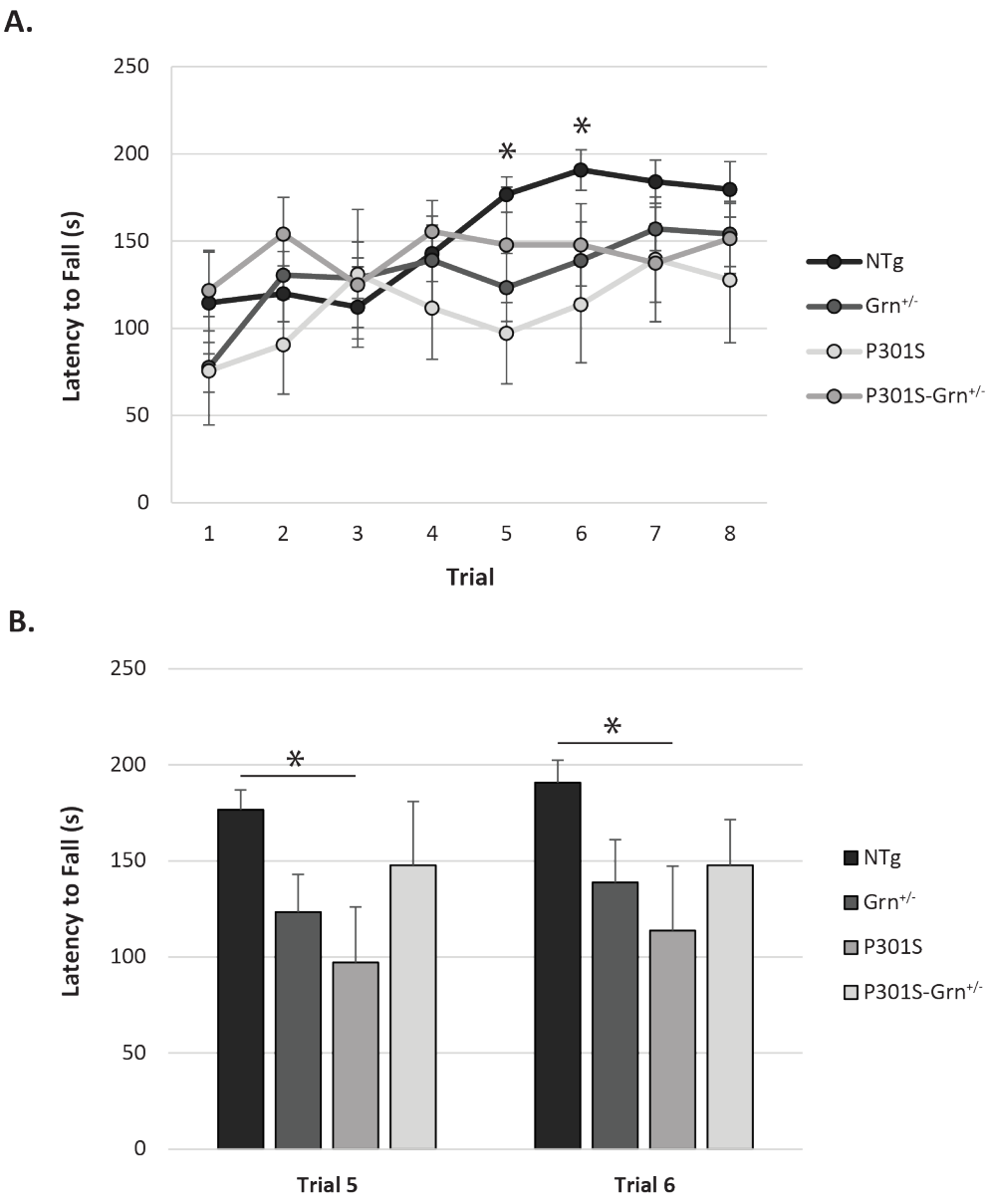

Figure 19. P301S mice exhibit significantly impaired motor coordination and balance. (A) The motorized rotarod across eight trials measured motor coordination and learning for two days**. (B)** P301S-Grn$^{+/-}$ mice exhibited impaired motor coordination on trials five and six of the motorized rotarod compared to NTg mice. (*p<0.05; N = 7 per genotype).

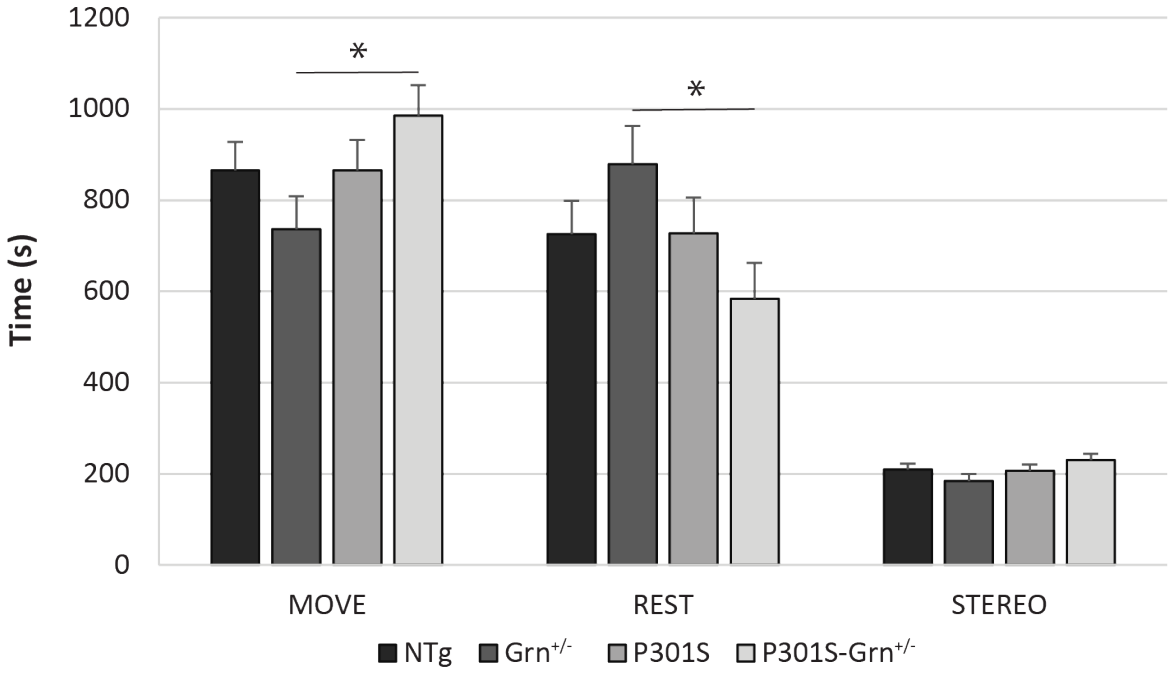

Figure 20. Open field locomotor performance enhanced in P301S-Grn$^{+/-}$ mice. P301S-Grn$^{+/-}$ mice showed increased exploratory behavior indicated by the increased time moving (MOVE) and decreased time resting (REST) compared to Grn$^{+/-}$ mice. No differences in stereotypic behavior (STEREO) were observed in either genotype. (*$p<0.05$; N = 7 – 9 per genotype).

Anxiety-like behaviors were also investigated with previously reported alterations in both $Grn^{+/-}$ and AD mouse models (Kayasuga et al., 2007; Petkau et al., 2012). The light-dark transition test was used to assess whether PGRN haploinsufficiency affected anxiety-like behavior in P301S mice. Two-way ANOVA revealed a significant effect between the $Grn^{+/-}$ and P301S genotypes [$F(1,27)=7.2479$, $p=0.1204$] but not a main effect of either $Grn^{+/-}$ [$F(1,27)=1.3707$, $p=0.252$] or P301S [$F(1,27)=1.7434$, $p=0.198$] genotypes **(Fig. 21)**. A Fisher LSD *post hoc* test indicated P301S mice spent significantly less time in the light compartment compared to NTg indicating tau pathology increased anxiety-like behavior ($p<0.05$; **Fig. 21**). This significant decrease seen in time spent in the light compartment of P301S mice, however, was not seen in P301S-$Grn^{+/-}$ mice and a Fisher LSD *post hoc* test indicated instead a significant increase compared to P301S mice ($p<0.05$; **Fig. 21**). These findings suggest that PGRN haploinsufficiency may attenuate or decrease the onset of anxiety-like behavior seen in the P301S tau transgenic mouse model.

4.3.2 Heterozygous loss of PGRN reduces hyperphosphorylated tau in P301S mice

Previously, two studies have reported that loss of PGRN increases tau phosphorylation in the P301L mouse model (Hosokawa et al., 2015; Takahashi et al., 2017b). Therefore, whether PGRN haploinsufficiency affected tau pathology in the brain and spinal cord of P301S transgenic mice was next examined.

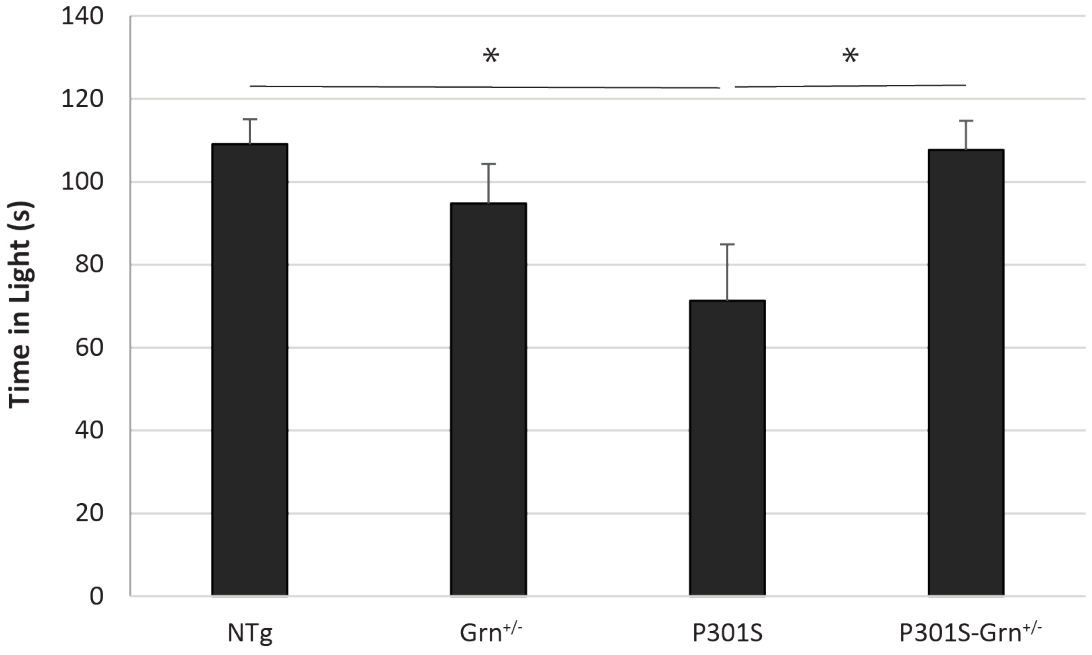

Figure 21. Progranulin haploinsufficiency rescues anxiety-like behavior in P301S mice in the light dark transition test. P301S mice spent significantly less time on the light side compared to NTg, indicating increased anxiety-like behavior. However, P301S-Grn$^{+/-}$ spent significantly more time in the light than P301S, suggesting loss of PGRN reduced anxiety-like behavior. (*$p<0.05$; N = 7 – 9 per genotype).

Sequential RIPA and sarkosyl-extractions to quantify soluble and insoluble levels of tau protein in the cortex, hippocampus, and spinal cord was used to assess the impact of PGRN haploinsufficiency (Planel et al., 2009). A Student's t-test was used to analyze differences between P301S and P301S-Grn$^{+/-}$ genotypes. A significant reduction in soluble tau (p=0.031; **Fig. 22C**) was observed in the cortex and reduced soluble AT8 phosphorylation in the spinal cord (p=0.005; **Fig. 22A**) and cortex (p=0.027; **Fig. 22C**) of P301S-Grn$^{+/-}$ versus P301S mice. Although not significant, reductions in insoluble tau (36% decrease) and soluble AT8 phosphorylation (47% decrease) in the hippocampus were observed in P301S-Grn$^{+/-}$ compared to P301S mice **(Fig. 22B)**. Loss of PGRN did not significantly affect the levels of soluble AT100 or AT180 in the spinal cord, hippocampus, or cortex of P301S mice **(Fig. 22A, B, and C)**. No significant effects on either insoluble tau or insoluble phosphorylated tau were observed in the spinal cord, hippocampus, or cortex in the sarkosyl extractions **(Fig. 23A, B, and C)**. Next soluble tau oligomeric tau in the spinal cord and brain was investigated by dot blot analysis. Two-sample t-test revealed that PGRN haploinsufficiency did not affect the levels of tau oligomers in either the spinal cord or brain; mice from the P301S-Grn$^{+/-}$ mice displayed similar levels of oligomer tau in the spinal cord (p=0.611) and brain (p=0.699) **(Fig. 24)**. Taken together, our results, contrary to previous reports suggest that PGRN haploinsufficiency reduces site-specific (AT8) tau phosphorylation.

RIPA-Soluble Tau

A.

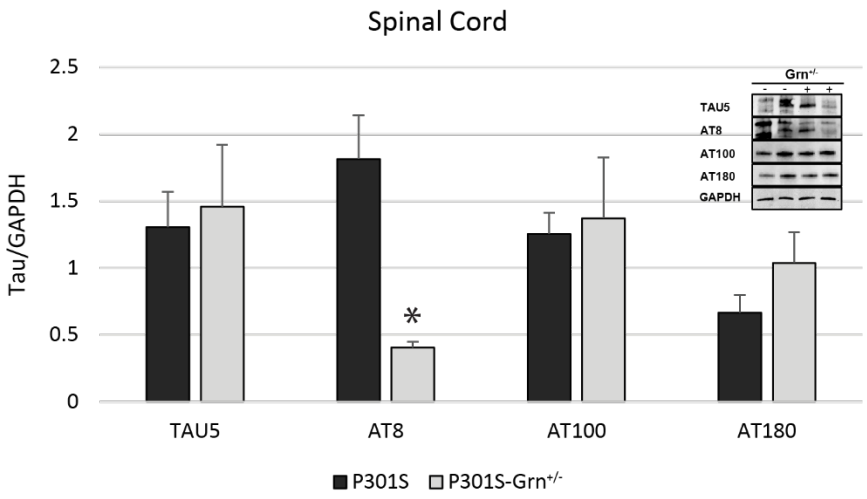

B.

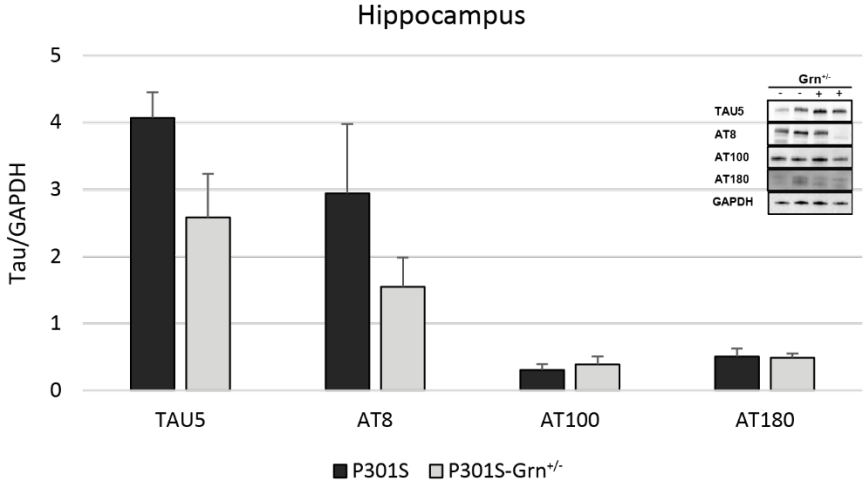

C.

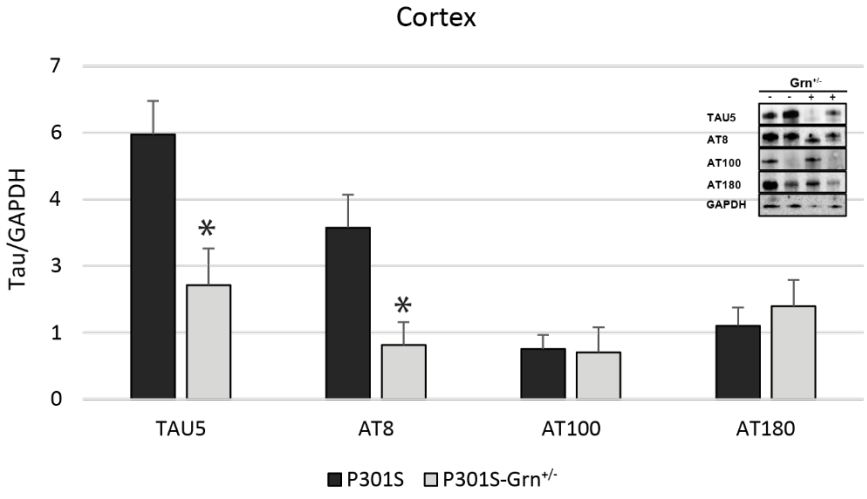

Figure 22. RIPA-soluble tau levels in the spinal cord, cortex, and hippocampus of P301S transgenic mice with progranulin haploinsufficiency. RIPA-soluble total (TAU5) and phosphorylated (AT8, AT100, and AT180) tau protein quantification via western blot analysis of the **(B)** hippocampus revealed no significant reductions in P301S-Grn$^{+/-}$ versus P301S mice. However, the **(A)** spinal cord revealed a significant reduction in AT8-tau phosphorylation and the **(C)** cortex revealed a significant reduction in total tau and AT8-tau phosphorylation in P301S-Grn$^{+/-}$ versus P301S mice. (*$p<0.05$; n = 4 mice per Genotype)

Sarkosyl-Insoluble Tau

A.

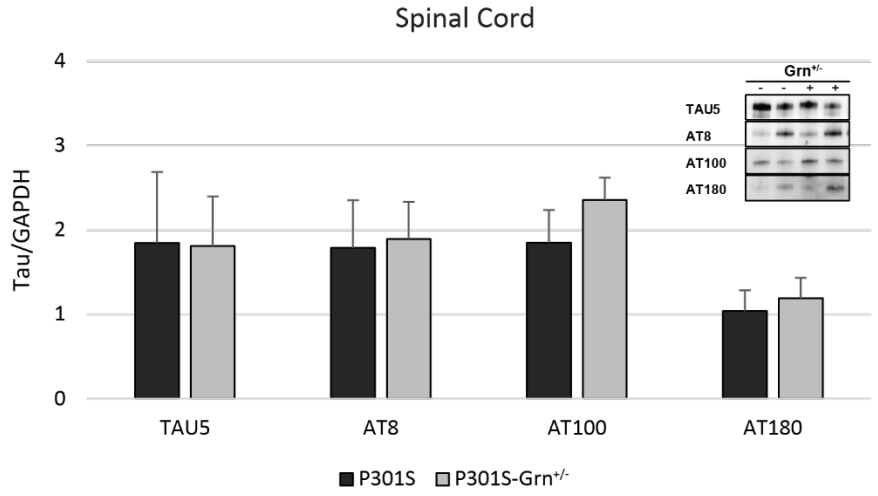

B.

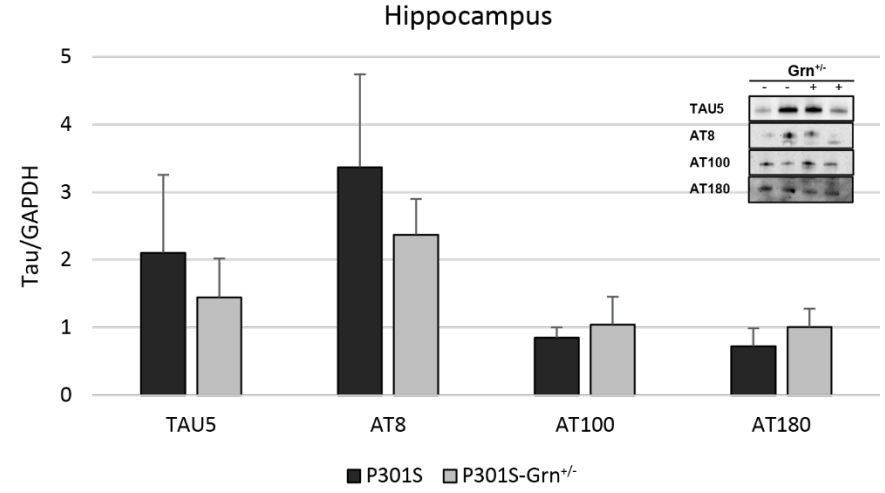

C.

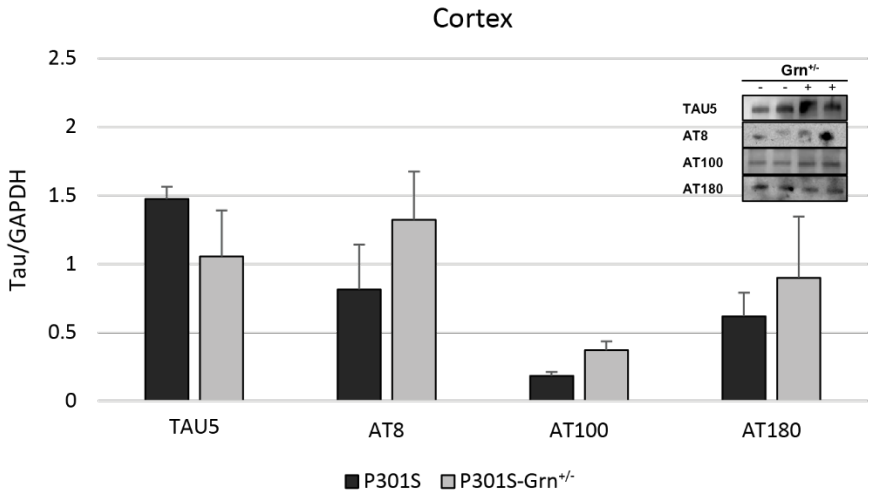

Figure 23. Sarkosyl-insoluble tau levels in the spinal cord, cortex, and hippocampus of P301S transgenic mice with progranulin haploinsufficiency. Sarkosyl-insoluble total and phosphorylated Western blot analysis of the **(A)** spinal cord, **(B)** cortex and **(C)** hippocampus revealed no significant reductions in P301S-$Grn^{+/-}$ versus P301S mice. (*$p<0.05$; n = 4 mice per Genotype)

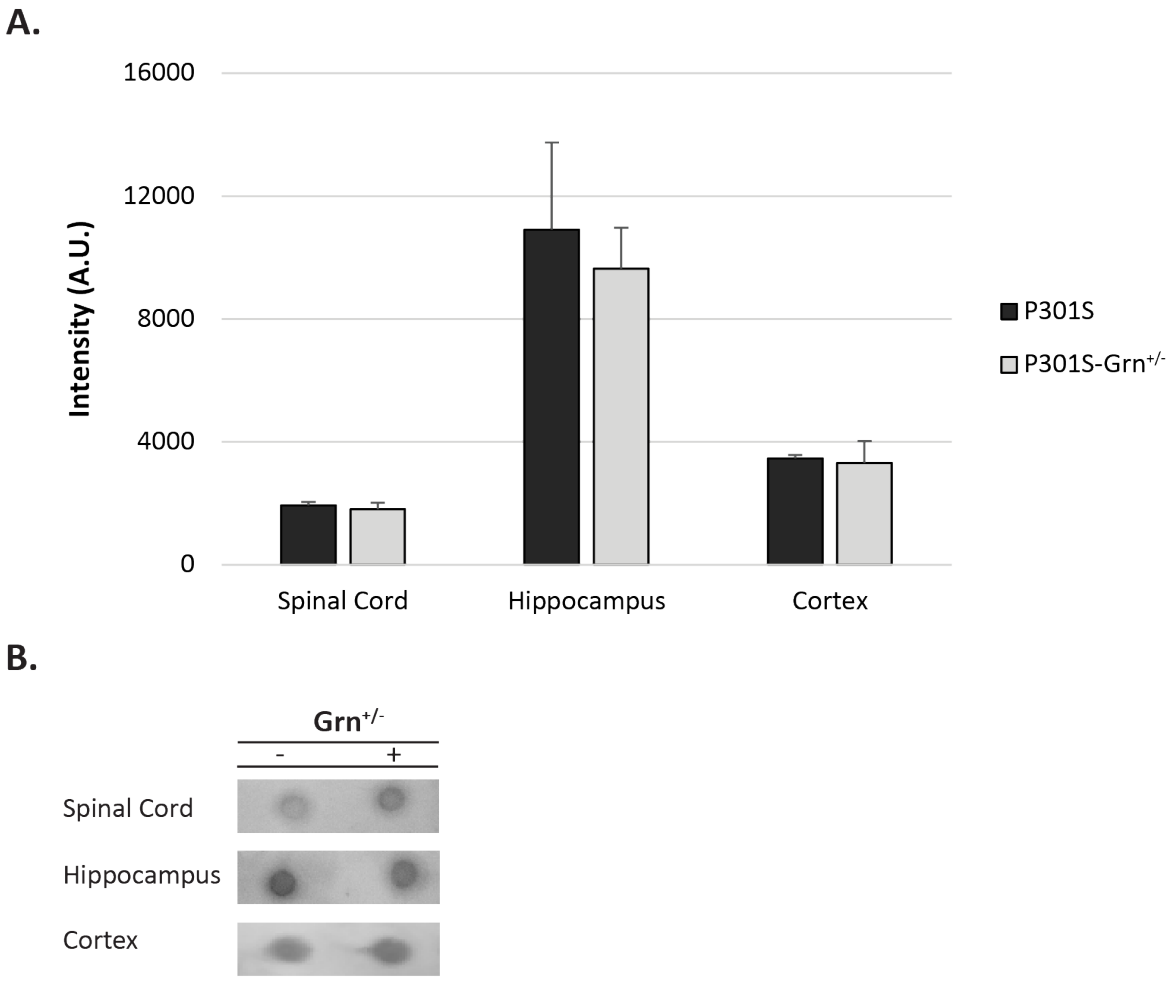

Figure 24. Soluble tau oligomers are present in the spinal cord and brain of progranulin haploinsufficient P301S mice. (A) Dot blot analysis indicates similar levels of oligomeric tau in the spinal cord, cortex, and hippocampus. **(B)** Represenative dot blot images of T22 in the spinal cord, cortex, and hippocampus. (N = 4 per genotype).

4.3.3 PGRN haploinsufficiency does not alter neurodegeneration or neuroinflammation in the brain of P301S mice

Neurodegeneration in P301S and P301S-Grn$^{+/-}$ mice was assessed by quantifying motor neurons in the spinal cord and neurons in the brain by NeuN immunohistochemistry. Neurodegeneration was observed in the cortex and CA1 and CA3 regions of the hippocampus but not in the spinal cord **(Fig. 25A, B, C, and D)**. A main effect from the P301S genotype [$F(4,9)=21.386$, $p=0.001$] but not from the Grn$^{+/-}$ genotype [$F(4,9)=2.4303$, $p=0.124$] nor an interactive effect between the two genotypes [$F(4,9)=1.2357$, $p=0.362$] indicated by two-way ANOVA analysis. In the spinal cord, Tukey HSD *post hoc* did not indicate any significant differences in number of motor neurons in any of the groups ($p>0.05$; **Fig. 25A**). In the cortex, Tukey HSD *post hoc* test indicated P301S and P301S-Grn$^{+/-}$ mice had significantly fewer NeuN-positive cells compared to NTg ($p<0.01$) and Grn$^{+/-}$ mice ($p<0.01$) in the cortex **(Fig. 25B)**. In the hippocampus, P301S and P301S-Grn$^{+/-}$ mice had significantly fewer NeuN-positive cells compared to NTg ($p<0.01$) and Grn$^{+/-}$ mice ($p<0.01$) in the CA1 and CA3 regions **(Fig. 25C and D)**. However, no differences in NeuN-positive cells were observed between P301S and P301S-Grn$^{+/-}$ mice in the spinal cord, cortex and CA1 and CA3 hippocampal regions indicating PGRN haploinsufficiency did not affect neurodegeneration in the P301S transgenic mouse model **(Fig. 25A, B, C, and D)**.

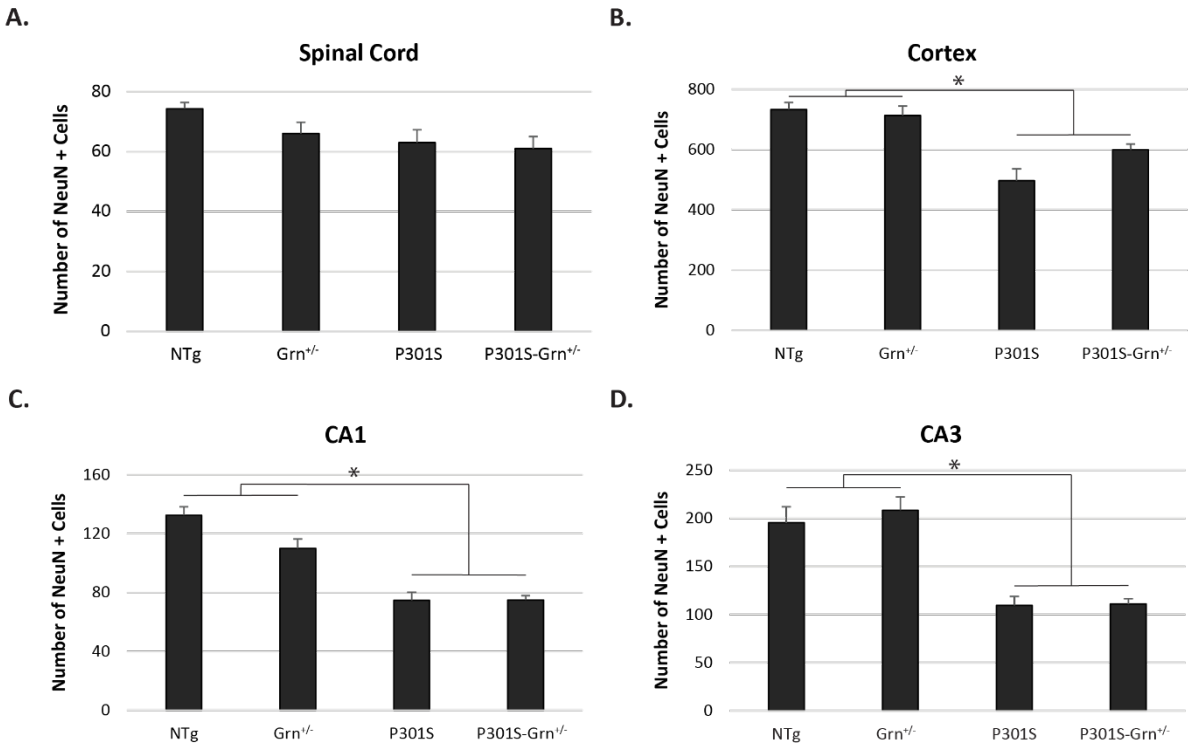

Figure 25. Heterozygous loss of progranulin does not affect neurodegeneration in the spinal cord or brain of P301S transgenic mice. (A) The number of spinal cord motor neurons was not significantly different across all groups. **(B, C, and D)** P301S transgenic mice displayed significant neurodegeneration in the posterior parietal cortex and the CA1 and CA3 region of the hippocampus compared NTg and $Grn^{+/-}$ mice controls regardless of Grn genotype. (*$p<0.05$; N = 3 – 5 per genotype).

Whether PGRN loss affected neuroinflammation in P301S mice was next evaluated by Iba1 and GFAP immunoreactivity. Microgliosis was measured by the percent area of Iba1 positive pixels by immunohistochemistry. A significant increase in Iba1 positive pixels was observed in the spinal cord, hippocampus, and cortex of P301S and P301S-Grn$^{+/-}$ mice compared to NTg and Grn$^{+/-}$ mice. Two-way ANOVA revealed a main effect of the P301S genotype [$F(3,8)=27.828$, $p=0.0001$]. Tukey HSD *post hoc* test revealed significant increase in Iba1 immunoreactivity in P301S mice compared to NTg mice and P301S-Grn$^{+/-}$ mice compared to Grn$^{+/-}$ mice in the spinal cord ($p<0.001$; **Fig. 26A**), hippocampus ($p<0.001$; **Fig. 26B**), and cortex ($p<0.001$; **Fig. 26C**). Next astrogliosis was measured by the percent area of GFAP positive pixels by immunohistochemistry. A significant increase in GFAP positive pixels was observed in the spinal cord, hippocampus, and cortex of P301S and P301S-Grn$^{+/-}$ mice compared to NTg and Grn$^{+/-}$ mice. Two-way ANOVA revealed a main effect of the P301S genotype [$F(3,8)=27.828$, $p=0.0001$]. Tukey HSD *post hoc* test revealed significant increase in Iba1 immunoreactivity in P301S mice compared to NTg mice and P301S-Grn$^{+/-}$ mice compared to Grn$^{+/-}$ mice in the spinal cord ($p<0.001$; **Fig. 26D**), hippocampus ($p<0.001$; **Fig. 26E**), and cortex ($p<0.001$; **Fig. 26F**). No differences were observed between the P301S and P301S-Grn$^{+/-}$ for both Iba1 and GFAP immunoreactivity mice indicating PGRN haploinsufficiency did not affect neuroinflammation in the

spinal cord, hippocampus or cortex of P301S mice, despite observed changes in total and hyperphosphorylated tau.

4.3.4 PGRN haploinsufficiency dysregulates GSK-3β and Akt signaling pathway in P301S mice

Sixteen phosphorylated proteins that belong to the Akt signaling network were investigated using the PathScan Akt Signaling array kit (Cell Signaling Technology; #9700) in the spinal cord to characterize how PGRN haploinsufficiency might decrease phosphorylated tau in the P301S mouse model. Within the Akt signaling network, a two-sample t-test revealed significant increases in the inhibitory phosphorylation sites for GSK-3β (Ser9), PTEN (Ser380), and 4E-BP1 (Thr37/46) in P301S-Grn$^{+/-}$ mice compared to P301S mice ($p<0.05$; **Fig. 27**). Furthermore, a two-sample t-test revealed a significant increase in GSK-3β phosphorylation at Ser9 in the spinal cord of P301S-Grn$^{+/-}$ mice compared to P301S mice via western blot indicating increased inhibition of GSK-3β activity in P301S mice with PGRN haploinsufficiency **(Fig. 28A and B)**. Taken together, these results suggest that PGRN haploinsufficiency dysregulates the Akt signaling pathways and increases inhibitory phosphorylation of GSK-3β (Ser9).

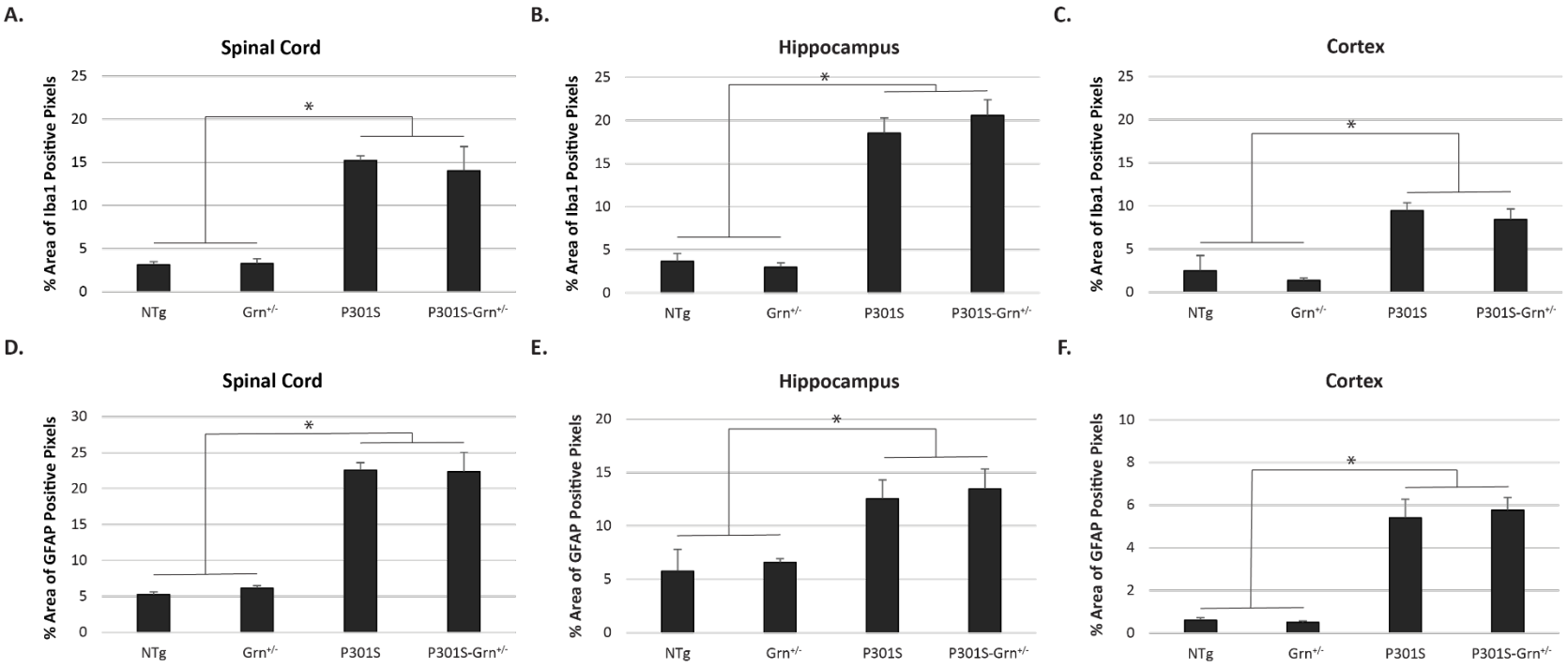
A.
Spinal Cord
% Area of Iba1 Positive Pixels
25
20
15
10
5
0
*
NTg
Grn+/-
P301S
P301S-Grn+/-
B.
Hippocampus
% Area of Iba1 Positive Pixels
25
20
15
10
5
0
*
NTg
Grn+/-
P301S
P301S-Grn+/-
C.
Cortex
% Area of Iba1 Positive Pixels
25
20
15
10
5
0
*
NTg
Grn+/-
P301S
P301S-Grn+/-
D.
Spinal Cord
% Area of GFAP Positive Pixels
30
25
20
15
10
5
0
*
NTg
Grn+/-
P301S
P301S-Grn+/-
E.
Hippocampus
% Area of GFAP Positive Pixels
20
15
10
5
0
*
NTg
Grn+/-
P301S
P301S-Grn+/-
F.
Cortex
% Area of GFAP Positive Pixels
10
8
6
4
2
0
*
NTg
Grn+/-
P301S
P301S-Grn+/-

Figure 26. Heterozygous loss of Progranulin does not affect neuroinflammation in the spinal cord or brain of P301S transgenic mice. (A, B, and C) P301S mice displayed significant microgliosis in the spinal cord, hippocampus, and posterior parietal cortex compared to NTg and $Grn^{+/-}$ mice regardless of Grn genotype. **(D, E, and F)** P301S mice displayed significant astrogliosis in the spinal cord, hippocampus, and cortex compared to NTg and $Grn^{+/-}$ mice regardless of Grn genotype. (*<0.05; N = 3 – 5 per genotype).

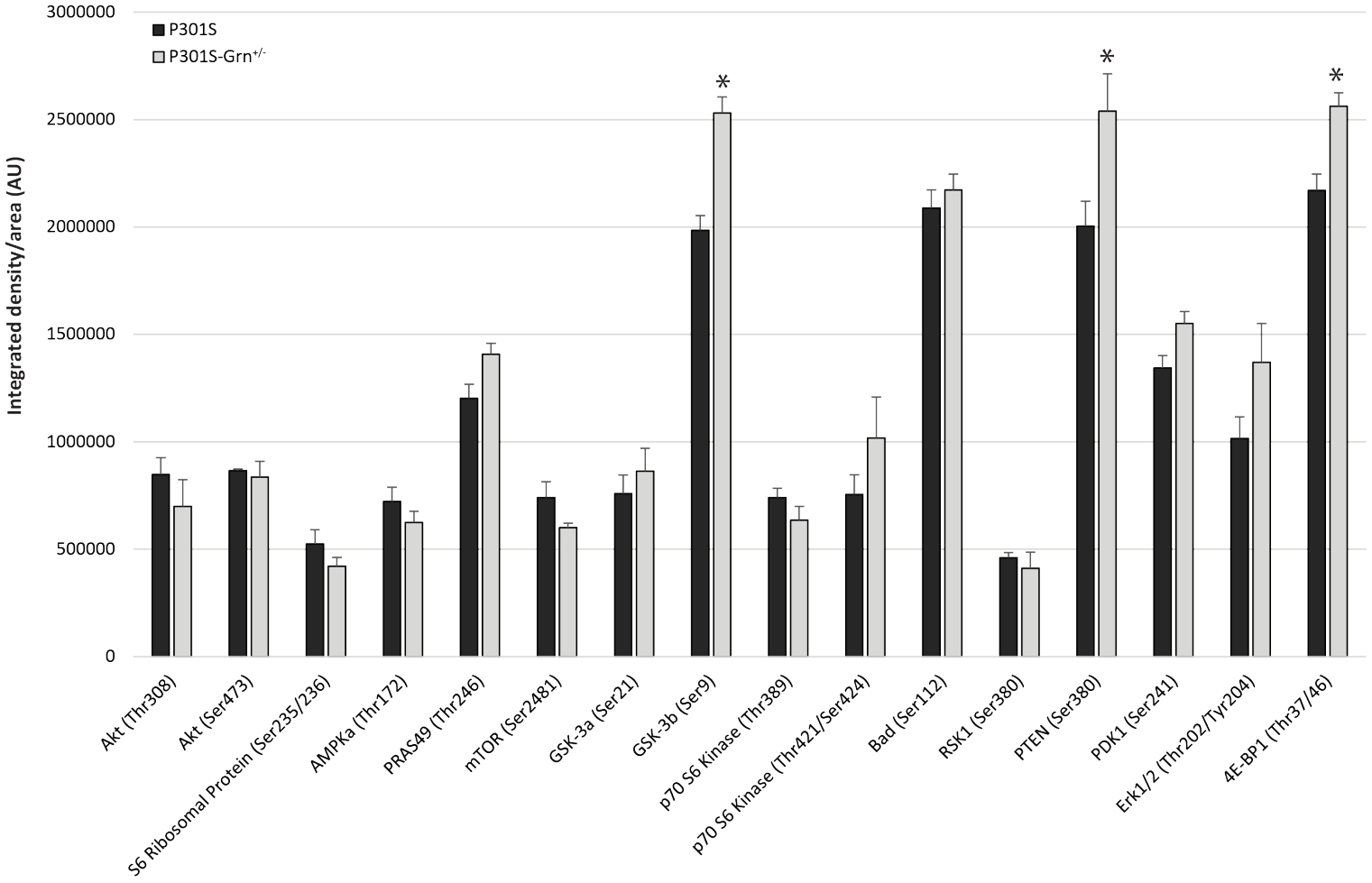
P301S
P301S-Grn+/-
Integrated density/area (AU)
3000000
2500000
2000000
1500000
1000000
500000
0
*
*
*
Akt (Thr308)
Akt (Ser473)
S6 Ribosomal Protein (Ser235/236)
AMPKa (Thr172)
PRAS49 (Thr246)
mTOR (Ser2481)
GSK-3a (Ser21)
GSK-3b (Ser9)
p70 S6 Kinase (Thr389)
p70 S6 Kinase (Thr421/Ser424)
Bad (Ser112)
RSK1 (Ser380)
PTEN (Ser380)
PDK1 (Ser241)
Erk1/2 (Thr202/Tyr204)
4E-BP1 (Thr37/46)

Figure 273. Akt signaling and GSK-3β are dysregulated in P301S-Grn$^{+/-}$ mice. Analysis of the Akt signaling network by the PathScan® Akt Signaling Antibody Array Kit P301S-Grn$^{+/-}$ mice showed increased phosphorylation of GSK-3b (Ser9), PTEN (Ser380), and 4E-BP1 (Thr37/46) . (*$p<0.05$; N = 4 per genotype).

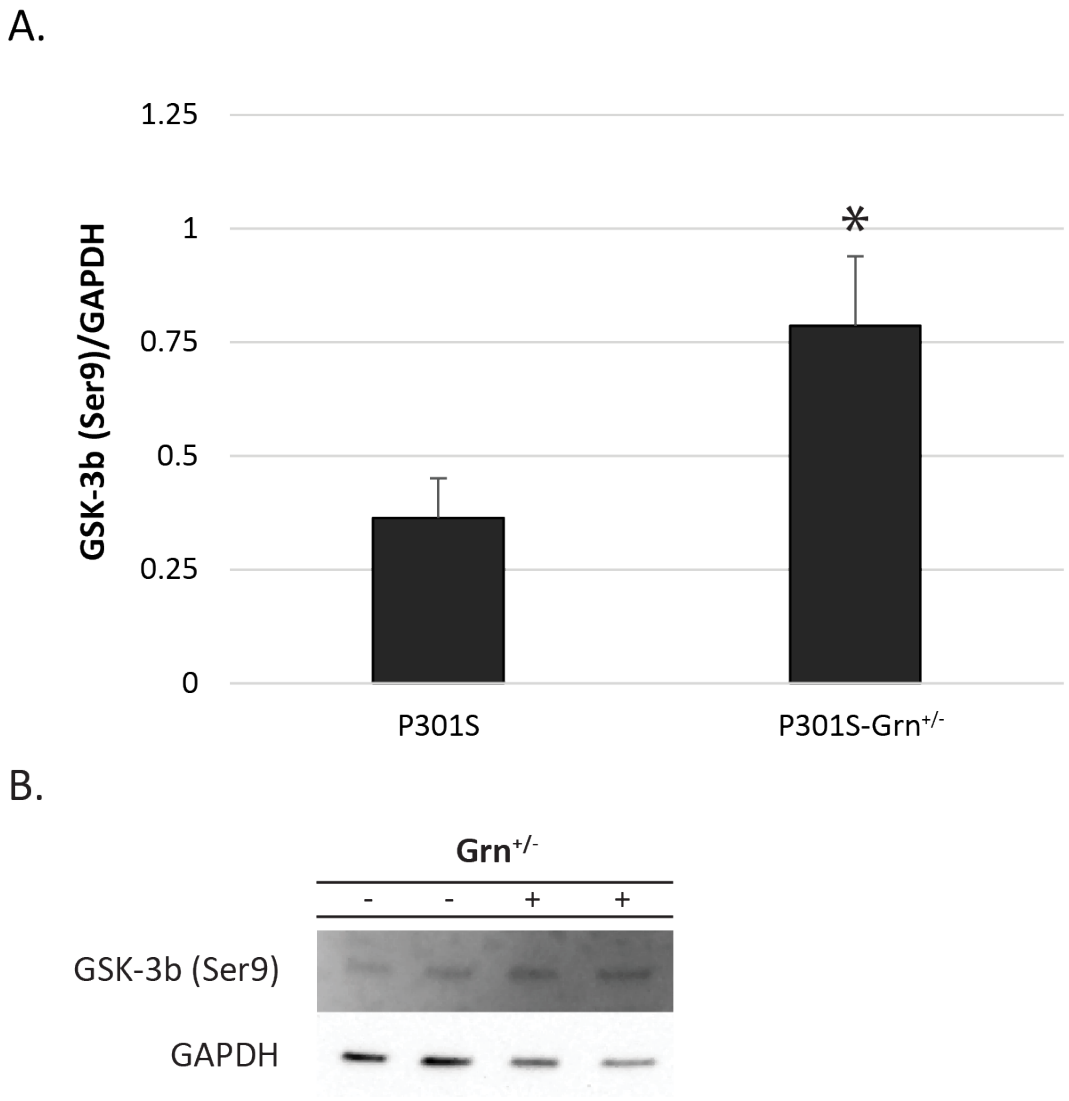

Figure 284. Increased inhibitory phosphorylation (Ser9) of GSK-3β in P301S-Grn$^{+/-}$ mice. (A) Western blot analysis indicates increased inhibiotry phosphorylation of GSK-3β (Ser9) in the spinal cord of P301S-Grn$^{+/-}$ mice. **(B)** Representative western blots of GSK-3β (Ser9) in the spinal cord. (*$p<0.05$; N = 4 per genotype).

4.4 Discussion

In this series of experiments, whether heterozygous loss of PGRN worsened the AD-related behavior and pathology in mice that overexpress human P301S mutation was investigated. In the P301S transgenic mouse model, heterozygous loss of PRGN improved non-cognitive tau-related behavioral deficits, which was accompanied by reduced tau phosphorylation in the brain and spinal cord. However, despite these changes' partial loss of PGRN did not affect neurodegeneration or neuroinflammation. Moreover, PGRN haploinsufficiency in the P301S transgenic mouse model altered cell signaling in the Akt signaling pathways. These findings suggest new roles of PGRN in AD and neurodegenerative disease in general and that loss of PGRN attenuates tau-related pathology, at least with respect to P301S tau mutation, which is contrary to previous reports evaluating PGRN loss on tau pathology.

The P301S mutation has been shown to increase hyperphosphorylation, aggregation, and filament formation of tau associated with FTD forms (Bugiani et al., 1999; Lossos et al., 2003; Goedert and Jakes, 2005). By six months of age, P301S tau transgenic mice develop extensive tau pathology in the spinal cord, accompanied by neurogenic muscle atrophy resulting in a progressive decline in locomotor function (Scattoni et al., 2010; Schaeffer et al., 2012). While there was no observed decline in general activity levels of P301S mice in the open field test, a significant reduction in motor coordination was observed during the rotarod test in P301S mice compared to NTg littermates. However, no significant reduction was observed in P301S-Grn$^{+/-}$, suggesting that heterozygous loss of PGRN may have

attenuated decline in motor coordination of P301S mice. P301S mice have previously been reported to exhibit decrease in anxiety-like behavior with the progression of tau pathology (Takeuchi et al., 2011). In this study, P301S mice spent significantly less time in the light compartment during the light-dark test compared to NTg mice, suggesting an increase in anxiety-like behavior, which contrasts with the previous study. Although increased anxiety-like behavior in P301S mice was observed, this was absent P301S-Grn$^{+/-}$ mice which spent significantly more time in the light compartment compared to P301S mice, suggesting ` haploinsufficiency reduced anxiety-like behavior in P301S mice. A lack of a distinct general locomotor phenotype and discrepancy in anxiety-like behavior in our P301S mice may potentially be due to phenotypic drift, which has been previously reported in the P301S mouse line (Iba et al., 2013; Maruyama et al., 2013).

Pre-neurofibrillary tangles are composed predominately of phosphorylated Ther231 (AT180) tau, with later-stage neurofibrillary tangles made up of filamentous tau that are characterized by phosphorylation at sites Ser202/Thr205 (AT8) and Thr212/Ser214 (AT100). In this study, a significant reduction was observed in only AT8 phosphorylated tau in the lumbar spinal cord and hippocampus of P301S-Grn$^{+/-}$ mice, with no differences in AT180 or AT100 phosphorylation or total tau. This finding suggests that PGRN haploinsufficiency

attenuates the progression of neurofibrillary tangle formation in the spinal cord and hippocampus in P301S mice.

Despite evidence that loss of PGRN affects soluble tau phosphorylation in mice (Hosokawa et al., 2015; Takahashi et al., 2017a), it is not clear if PGRN loss affects insoluble tau accumulation which represents another pathological characteristic of tauopathies (Hasegawa, 2006). Therefore, RIPA-soluble and sarkosyl-insoluble forms of tau were analyzed in the brain and spinal cord of P301S and P301S-Grn$^{+/-}$ mice. While RIPA is commonly used to detect pre-aggregated tau, sarkosyl extractions are commonly used to isolate aggregated paired helical filaments of tau, which are the primary constituents of insoluble NFT's (Julien et al., 2012). Significant reductions of both total and hyperphosphorylated tau for RIPA-soluble tau in the brain and spinal cord of P301S-Grn$^{+/-}$ mice were observed but did not observe any differences in sarkosyl-insoluble tau. In the brain, significant reductions of RIPA-soluble total tau and AT8-tau phosphorylation were observed in the cortex of P301S-Grn$^{+/-}$ mice, with similar but not significant reductions in the hippocampus. No differences were observed in AT100, or AT180 phosphorylated tau. Levels of soluble tau oligomers were analyzed, which is a toxic species of tau and has been suggested to initiate toxicity before forming NFTs (Lasagna-Reeves et al., 2012; Gerson and Kayed, 2013). Although differences were observed in RIPA-soluble tau, no significant effects of

PGRN loss were observed on tau oligomer's levels in the brain or spinal cord of P301S mice.

These reported results of tau phosphorylation after the heterozygous loss of PGRN contrast with two previous studies that used a different tau transgenic mouse model with either complete or partial loss of PGRN (Hosokawa et al., 2015; Takahashi et al., 2017a). In both studies, complete and partial loss of PGRN increased and not decreased tau phosphorylation in the P301L transgenic tau mouse model. One possible explanation for this discrepancy could be the different choice of transgenic tau mouse models, where P301S and P301L mutations may affect strain-specific signaling pathways; phenotypic differences between the P301S and P301L tau mouse models have been previously reported. Neuronal loss was observed to be more pronounced in P301S mice than in the P301L mice, which is consistent with FTD patients carrying the P301S mutation (Allen et al., 2002). Unlike the P301L tau line, which shows increased DNA fragmentation and apoptosis (Gotz et al., 2001; Ho et al., 2001), the P301S tau line showed no evidence for apoptosis based on DNA fragmentation and increased activation of caspase-3, which is also consistent with tauopathies in humans (Migheli et al., 1994; Atzori et al., 2001; Ferrer et al., 2001). Our data, in context with previous reports, suggest that the effect of PGRN haploinsufficiency on tau pathology maybe mutation specific.

Although these results suggest the heterozygous loss of PGRN reduces total and phosphorylated tau in the brain of P301S mice, no changes were observed in neuronal loss between P301S and P301S-Grn$^{+/-}$ mice, indicating a

reduction in PGRN expression did not affect the rate of neurodegeneration in P301S mice. Consistent with previous studies, significant neurodegeneration was observed in the CA1 and CA3 regions of the hippocampus and cortex of P301S mice (Yoshiyama et al., 2007; Crescenzi et al., 2014; Koga et al., 2014), but not in the spinal cord (Ohia-Nwoko et al., 2014). Even though, PGRN loss leads to neurodegeneration in humans, it is not surprising that there was no observed increase in neuronal loss in P301S-Grn$^{+/-}$ compared to P301S mice. While PGRN has been shown to be neuroprotective and a neurotrophic factor for some stressors (Guo et al., 2010; Martens et al., 2012; Tao et al., 2012), it has also been reported not to be for others (Petkau et al., 2013). Differences between different neurotoxic stressors in Grn$^{-/-}$ mice suggest a complex role of PGRN as a neurotrophic factor suggesting that PGRN deficiency may only exacerbate specific stressors. Taken together, the data reported here suggest that PGRN-dependent neurotrophic pathways are independent of tau-induced toxicity in the P301S transgenic mouse model.

How PGRN reduction modulates AD and specifically tau phosphorylation is not well understood. One possible explanation is changes in the inflammatory pathway, which has been reported to increase tau phosphorylation in tau transgenic mouse models (Kitazawa et al., 2005; Lee et al., 2010; Maphis et al., 2015). Previous reports studying the effect of PGRN on AD pathology have largely focused on PGRN's role in regulating inflammation and, more specifically, microglial activity (Minami et al., 2014; Takahashi et al., 2017a). Despite the strong relationship between inflammation and complete loss of PGRN, the finding in this

study that PGRN haploinsufficiency did not affect neuroinflammation in P301S mice and prior literature suggests that PGRN haploinsufficiency is likely affecting tau phosphorylation through a mechanism independent of changes in the inflammatory pathway. No differences were observed in either the total number of microglia or astrocytes in both the brain and spinal cord of P301S-$Grn^{+/-}$ compared to P301S mice, despite observed reductions in total and phosphorylated tau. This is consistent with previous studies of $Grn^{+/-}$ mice showing that they do not develop neuroinflammation (Filiano et al., 2013), unlike $Grn^{-/-}$ mice (Filiano et al., 2013). This is also consistent with a recent study that also found no changes in neuroinflammation, indicated by cytokine levels, despite observing changes in tau phosphorylation in the P301L tau mouse model with PGRN loss (Hosokawa et al., 2015).

To better understand how PGRN haploinsufficiency reduces total and phosphorylated tau signaling pathways that play a key role in tau phosphorylation was next investigated. Many different kinases and phosphatases regulate tau's phosphorylation with glycogen synthase kinase 3β (GSK-3β), a proline-directed serine/threonine kinase, being a key kinase in AT8 phosphorylation (Stoothoff et al., 2005). Increased expression of GSK-3β has been observed in AD, and the dysregulation of GSK-3β has also been suggested to play a key role in AD's pathogenesis. Overexpression of GSK-3β in cells and mice enhance tau phosphorylation and promotes tau aggregation (Lucas et al., 2001; Goldbaum et al., 2003; Johnson and Stoothoff, 2004; Rankin et al., 2008). Furthermore, overexpression of GSK3β was shown to increase AT8 phosphorylation (Braak

and Braak, 1995), and AT8 phosphorylation could not be detected in the absence of GSK3β in SK-N-SH cells (Richet et al., 2012). GSK-3β activity is known to be regulated by phosphorylation, with phosphorylation of Ser9 inhibiting GSK-3β function and phosphorylation of Tyr216 increasing function (Jope and Johnson, 2004). In this study we observed a significant increase in p-GSK-3β (Ser9) in P301S-Grn$^{+/-}$ mice versus P301S littermates and is consistent with the previous observation of a significant reduction in AT8 phosphorylation in the brain and spinal cord of P301S-Grn$^{+/-}$ mice. To the best of our knowledge, this is the first report showing that heterozygous loss of PGRN haploinsufficiency dysregulates GSK-3β activity in a transgenic mouse model.

This observed dysregulation of GSK-3β in P301S-Grn$^{+/-}$ mice is consistent with previous studies reporting changes GSK-3β phosphorylation. PGRN was first shown to increase phosphorylation of GSK-3β (Ser9) in neurons treated with exogenous PGRN which was associated with PGRN's neurotrophic effects (Gao et al., 2010). Another study also observed increased phosphorylation of GSK-3β (Ser9) and proliferation in neural progenitor cells from Grn$^{-/-}$ mice treated with PGRN (Nedachi et al., 2011). However, although previous studies show an increase p-GSK-3β (Ser9) after an increase in PGRN, in this study we observed an increase with PGRN haploinsufficiency. This discordance maybe due to differential effects on GSK-3β between neuronal and exogenous PGRN or PGRN's

effect maybe disease-dependent. Regardless, our results suggest PGRN haploinsufficiency increases p-GSK-3β (Ser9) in the P301S mice.

How exactly PGRN is modulating GSK-3β activity is not clear. One possible explanation is that PGRN haploinsufficiency is modulating GSK-3β through the *Wnt* signaling pathway. PGRN deficiency has been implicated in *Wnt* signaling with an increased *Wnt* signaling observed after loss of PGRN (Rosen et al., 2011; Alquezar et al., 2014). The stabilization of free β-catenin by the inactivation of GSK-3β is a critical step in *Wnt* signaling (Xu et al., 2016). Another possibility is through increased mTORC2/Akt signaling which has been observed in $Grn^{+/-}$ mice (Arrant et al., 2016). In this study phosphorylation of Akt at Ser473, which is associated with increased activity, mTORC1 was increased in $Grn^{+/-}$ mice, but not $Grn^{-/-}$ mice, between six and eight months. Although not investigated in this study p-Akt (Ser473) has been shown to increase p-GSK-3β (Endo, et al., 2006). Another possibility is that PGRN haploinsufficiency increases p-GSK-3β through the PI3K/Akt signaling pathway. This is supported by our results where an increase in phosphorylated PTEN at Ser380 was observed. PTEN is a primary regulator of the PI3K/Akt signaling pathway and phosphorylation of Ser380 is known to reduce PTEN function (Vazquez et al., 2000). Loss or inactivation of PTEN is correlated with an increase in p-Akt (Ser473) and increased p-GSK-3β (Ser9) (Mulholland et al., 2006). Given that we report an increase in p-PTEN (Ser380) and p-GSK-3β (Ser9) our results suggest that PGRN haploinsufficiency decreases tau

phosphorylation through dysregulating the PI3K/Akt signaling pathway in P301S mice.

Although previous reports suggest that PGRN loss worsens tau pathology in the P301L transgenic mouse model, the findings in this aim suggests PGRN haploinsufficiency has a protective role in the P301S transgenic mouse model. Our findings further strengthen the dissociation between PGRN's functional effects on behavior disease pathology independent to changes in neuroinflammation. Contrary to previous reports showing complete and haploinsufficient loss of PGRN increased AT8 tau phosphorylation, we observed a decrease in AT8 phosphorylation of RIPA-soluble, but not sarkosyl-soluble, tau. Furthermore, we observed impairments in motor coordination and balance and increase in anxiety-like behavior only in P301S mice suggesting PGRN haploinsufficiency had a protective effect with disease progression in P301S mice. In agreement with a decrease in AT8 phosphorylation we observed increased inhibitory phosphorylation of both PTEN and GSK-3β indicating decreased PI3K/Akt signaling in P301S-Grn$^{+/-}$ mice. Taken together, the results of this aim suggest PGRN haploinsufficiency may differentially affect tau pathology depending on the mutation present and with respect to the P301S mutation PGRN loss has a protective role.

CHAPTER 5: PGRN LOSS AND AMYLOID PATHOLOGY

5.1 Introduction

In this chapter, the role of PGRN in AD pathology with respect to Aβ pathology was investigated with the hypothesis that PGRN haploinsufficiency would exacerbate cognitive behavioral deficits and Aβ pathology. To test this, the APPSwe/PSEN1dE9 (APdE9) amyloid mouse model, which expresses human APP with the Swedish mutant and human PSEN1 lacking exon 9, was crossed with a global heterozygous loss of PGRN mouse model (Jankowsky et al., 2004). Although previous studies have predominately used $Grn^{-/-}$ mice to recapitulate PGRN loss, a $Grn^{+/-}$ mouse model was used instead as a more analogous model of typical FTLD carriers. While only $Grn^{-/-}$ mice replicate some FTLD-related pathology, such as microgliosis, both models exhibit key FTD-related behavior abnormalities (Yin et al., 2010b; Roberson, 2012; Filiano et al., 2013). Growing evidence suggests that patients with a complete loss of PGRN may be significantly different from patients who have haploinsufficiency. With mutations causing complete loss of PGRN causing neuronal ceroid lipofuscinosis and only partial loss resulting in FTD (Smith et al., 2012; Tanaka et al., 2014). Additionally, behavioral and signaling differences have been reported between the $Grn^{+/-}$ and $Grn^{-/-}$ mice suggesting that complete and partial loss of PGRN are maybe affecting different disease and signaling pathways (Arrant et al., 2016). Utilizing several experimental approaches of behavior modeling, histology, and electrophysiology we demonstrated heterozygous loss of PGRN exacerbated deficits in spatial learning and memory, synaptic plasticity, modulated Aβ-related pathology, and decreased

the number of GABAerigc interneurons in the APdE9 transgenic mouse model in absence of increased neuroinflammation suggesting PGRN haploinsufficiency worsens Alzheimer's disease progression with respect to amyloid pathology.

5.2 Materials and Methods

5.3.1 Animal models

The APP_{Swe}/PS1dE9 amyloid transgenic (APdE9) mouse model expressing human APP with the Swedish mutation and human PSEN1 lacking exon 9. The APdE9 mouse model begins to develop amyloid plaques as early as six months of age, with abundant plaques in the hippocampus and cortex seen at nine months (Jankowsky et al., 2004; Garcia-Alloza et al., 2006). In addition to amyloid pathology, they develop impaired contextual memory and spatial learning by 12 months of age (Lalonde et al., 2005; Janus et al., 2015). The APdE9 mice were crossed with a $Grn^{+/-}$ mouse model producing APdE9 amyloid transgenic mice harboring the *GRN* hemizygote (APdE9-$Grn^{+/-}$). Both mouse models were backcrossed using C57BL/6J mice. All mice used in this study were behaviorally screened at twelve months and electrophysiology was performed at fourteen months.

Mice were housed in the animal facility at the University of Houston and housed in a climate-controlled room (25°C) on a 12/12 h light/dark cycle and given food and water ad libitum. All studies were conducted following the University of Houston approved Institutional Animal Care and Use Committee and implemented

following the National Research Council's Guide to The Care and Use of Laboratory Animals.

5.3.2 Tissue Processing

Animals from both genotypes were euthanized with CO_2 and brains were harvested. One hemibrain was flash-frozen in 2-methylbutane and dry ice and stored for long-term storage at -80°C. The other hemibrain was fixed in Accustain (Sigma-Aldrich) and stored at 4°C for long-term storage. Accustain fixed brains were subjected to paraffin processing (Leica TP1020) and then sectioned using a

Leica microtome at 10-μm intervals. The other half of each brain and cervical spinal cord were snap-frozen and stored at -80°C for biochemical processing.

5.3.3 Behavior tests

5.3.3.1 Open Field

Exploratory and non-cognitive behavior was evaluated by the open field test at twelve months-of-age. Procedures were performed as described in Section 3.2.3.1.

5.3.3.2 Motor Coordination and Balance

Motor learning, coordination, and balance were evaluated by a motorized rotarod at twelve months-of-age. Procedures were performed as described in Section 3.2.3.2.

5.3.3.3 Light Dark Transition

Anxiety-like behavior was assessed by the light dark transition test at twelve months-of-age. Procedures were performed as described in Section 3.2.3.3.

5.3.3.4 Elevated Plus Maze

Anxiety-like behavior and fear was assessed by the elevated plus maze at twelve-months of age. Procedures were performed as described in Section 3.2.3.4.

5.3.3.5 Contextual Fear Conditioning

Contextual fear conditioning was used to test short-term associative learning at twelve months-of-age as previously described (Butler et al., 2013). Like cued fear conditioning, mice were conditioned to freeze to visual cues that are associated with a foot shock and/or tone. Mice were measured on their ability to

learn and remember the association of the environment cues with the aversive stimulus. For the learning trial, mice were placed in a 13 cm x 10.5 cm x 13 cm conditioning chamber with a loudspeaker, 28V house light, and a metal floor consisting of 19 equally spaced rods (2.8 mm diameter) for 7 minutes. For the first 2 minutes mice were to explore the environment. At the 3rd, 4th, and 6th minute mark a 30-second tone (80 dB, 2 kHz) followed by a 2 second foot shock (0.75 mA) was presented. Sixty seconds after the last shock the session ended. Each mouse spent freezing (defined as immobility) was detected by infrared cameras within the conditioning chamber and automatically measured using computer software (FreezeFrame, Med Associates/Actimetrics). Percentage freezing for post-conditioning was measured by averaging the percentage freezing of the 6th and 7th minute of the learning trial. Mice were returned to their home cage and the conditioning chamber was cleaned between mice with 70% ethanol.

To evaluate short-term and long-term associate learning mice were placed back into the test chamber 1 and 24 hours after the last learning trial. The contextual trial consisted of placing the mice back into the conditioning chamber and allowed to explore the environment for 7 minutes. No shocks or tone were presented to evaluate the mouses contextually conditioned fear, which was evaluated as associative learning and memory behavior. As with the learning trials the time spent freezing the conditioning chamber was automatically measured using computer software (FreezeFrame, Med Associates/Actimetrics). Percentage freezing for the 1-hour and 24-hour context trials was calculated by averaging the

percentage freezing (%) of the final 3 minutes (minutes 5, 6, and 7). The conditioning chamber was cleaned with 70% ethanol between mice.

5.3.3.6 Morris Water Maze

Spatial learning and memory were assessed by the MWM at twelve-months-of-age. Procedures were performed as described in Section 3.2.3.9.

5.3.4 Electrophysiology

Mice fourteen months of age were sacrificed, and brains immediately and briefly transferred to ice-cold carboxygenated (95%O2/5%CO2) cutting solution: (5 mM glucose, 110 mM sucrose, 60 mM NaCl, 28 mM $NaHCO_3$, 3 mM KCl, 1.25 mM NaH_2PO_4, 7 mM $MgCl_2$, and 0.5 mM $CaCl_2$, 0.6 mM ascorbate). Sagittal hippocampal slices (400 μm) were prepared in an ice-cold cutting solution using a 1000Plus Vibratome sectioning system (Vibratome Co., St. Louis, Missouri). Slices were transferred to room temperature (1:1) cutting solution/artificial cerebral spinal fluid (aCSF; 25 mM glucose, 125 mM NaCl, 2.5 mM KCl, 1.25 mM NaH_2PO_4, 25 mM $NaHCO_3$, 1 mM $MgCl_2$, and 2 mM $CaCl_2$), for twenty minutes and then to 100% aCSF at room temperature for a minimum of one hour prior to recordings. Recordings were carried out in an interface chamber (Harvard Apparatus, Holliston, MS) at room temperature, perfused continuously with carboxygenated ACSF (perfusion rate: 1-2 ml/min). A bipolar enamel-coated platinum stimulating electrode was placed in CA3 Schaffer collateral/commissural fibers and a borosilicate glass recording electrode (resistance 1-4 MΩ) filled with aCSF was placed into stratum radiatum of area CA1. Field excitatory postsynaptic potentials (fEPSP) were collected every twenty seconds and averaged over a two-minute

interval using a stimulus intensity that produced 30-50% of the maximum initial slope fEPSP obtained during input/output measurements. Baseline fEPSPs were monitored for at least 20 min for stability. For LTP induction, two high-frequency stimuli (HFS) trains were delivered at 100Hz for 1 sec with an inter-strain interval of 5 min. The stimulus intensity of the HFS pulses was matched to that used during baseline recordings. Data was collected and analyzed using pClamp version 10 (Molecular Devices, Sunnyvale, CA). Recordings were normalized to the baseline mean before induction of LTP.

5.3.5 Aβ Sandwich ELISA

Mouse hemibrains for NTg, $Grn^{+/-}$, APdE9, and APdE9-$Grn^{+/-}$ were homogenized in PBS extraction buffer and centrifuged at 20,800 x g for 30 min at 4C to separate PBS-soluble and PBS-insoluble fractions. The insoluble proteins were then extracted using RIPA buffer. RIPA fractions were sonicated then centrifuged at 20,800 x g for thirty minutes at 14C to separate RIPA-soluble and RIPA-insoluble fractions. Aβ levels were then determined by end-specific sandwich ELISAs as previously described (Kukar et al., 2005; Murphy et al., 2007). Briefly, Ab9 (anti-Aβ1-16 of Aβ) was used as the capture antibody and 21.3.1 (anti-Aβ 35-42) or 13.1.1 (anti-Aβ 35-40) as the detection antibodies for Aβ40 and Aβ42.

5.3.6 Immunohistochemistry and Image Analysis

Coronal sections (10μm) were deparaffinized and subjected to antigen retrieval using 10mM sodium citrate, pH 6.0, in a Decloaking Chamber system (Biocare Medical, CA). Following antigen retrieval, sections were blocked with 5% normal goat serum in TBST for one hour. Sections were incubated with IBA1

(1:1000 dilution, Wako Chemicals) and 4G8 (1:1000 dilution, DAKO) primary antibodies overnight and washed with TBST. Sections were then incubated with a species-specific HRP-goat antibody (Vector Laboratories) for 30 min, washed with TBST 3 times, and developed with chromogenic substrate diaminobenzidine tetrahydrochloride (DAB; Vector Laboratories). Slides were viewed under an Olympus IX61 DSU confocal microscope, and the images were processed with Neurolucida (MicroBrightField Inc., Williston, VT).

For image analysis of IBA1 and GAD67, four montage photomicrographs, spaced 50 μm apart, were taken from each sample using a 20x objective. Thresholds were set to include only Iba1 and GAD67 positive cells. The total number of Iba-1 positive pixels were counted and averaged for the four montage photomicrographs by a blind observer using NIH ImageJ software in the cortex and hippocampus between Paxinos plate numbers 42 and 52 (Filiano et al., 2013). For GAD67, the total numbers of GAD67 positive cells were counted and averaged for the four montage micrographs.

5.3.7 Data Analysis

All experiments were conducted by observer's blind to genotype. All data are expressed as mean ± standard error mean. Data was analyzed using Staistica (TIBCO Software, Pal Alto, CA) and statistical comparisons were made using a two-sample t-test to compare APdE9 and APdE9-Grn$^{+/-}$ mice. Two-way analysis of variance (ANOVA) was used to compare all four groups (NTg, Grn$^{+/-}$, APdE9, and APdE9-Grn$^{+/-}$). After two-way ANOVA analysis, a Fisher LSD *post hoc* was used for behavioral tests and Tukey's HSD *post hoc* was used to compare the significant

effects between groups for LTP, Aβ sandwich ELISA, and immunohistochemistry data. A two-way repeated measures ANOVA with $Grn^{+/-}$ and APdE9 genotypes as between-subject factors and trials as within-subject factor was used for analyzing the motorized rotarod behavioral test. Two-way repeated measures ANOVA was then followed by two-way ANOVA and Fisher LSD *post hoc* for analyzing the effect of PGRN haploinsufficiency on single trials of the motorized rotarod in the APdE9 transgenic mouse model. $p < 0.05$ was considered significant.

5.3 Results

5.3.1 Heterozygous loss of PGRN exacerbates AD-related cognitive and non-cognitive behavior deficits in APdE9 mice

To test the hypothesis that PGRN haploinsufficiency worsens AD pathogenesis and disease progression, the effect of PGRN haploinsufficiency on AD-related behaviors was first investigated. For assessing spatial learning and memory, the Morris water maze (MWM) was used and evaluated mice at twelve months of age. Two-way ANOVA revealed a main effect of the APdE9 genotype [$F(6,41)=2.5699$, $p<0.033$] but not a main effect by the $Grn^{+/-}$ genotype [$F(6,41)=1.3901$, $p=0.242$] or an interaction effect between the two genotypes [$F(6,41)=2.0646$, $p=0.079$] **(Fig. 29)**. During the training trials, Fisher LSD *post hoc* test indicated APdE9-$Grn^{+/-}$ mice, but not APdE9 mice, spent significantly more time to find the hidden escape platform (latency to platform) on day 3 and day 4 compared to NTg mice indicating impaired spatial learning ($p<0.05$; **Fig. 29A**). During long-term memory trial, Fisher LSD *post hoc* test indicated APdE9-$Grn^{+/-}$ mice, but not APdE9 mice, spent significantly less time in quadrant 4, the quadrant

containing the hidden “escape” platform during training trials, indicating impaired long-term spatial memory ($p<0.01$; **Fig. 29B**). No differences were observed in either the latency to find the visible platform during the acuity trials or swim speed during the training trials across all genotypes ruling out activity levels or visual issues as potential confounding variables **(Fig. 29C and D)**. Taken together, the results from the MWM indicate PGRN haploinsufficiency increases the onset of spatial learning and long-term memory deficits in the APdE9 transgenic mouse model.

Learning and memory was futher investigated by contextual fear-conditioning to evaluate the effect of PGRN haploinsufficiency on associative learning and memory. A two-way ANOVA revealed a main effect of the APdE9 genotype [$F(4,39)=4.7946$, $p=0.003$] but not a main effect of the $Grn^{+/-}$ genotype [$F(4,39)=0.9873$, $p=0.426$] or an interaction effect between genotypes [$F(4,39)=0.1747$, $p=0.95$] **(Fig. 30)**. For the training trial, Fisher LSD *post hoc* test indicated both $Grn^{+/-}$ and APdE9-$Grn^{+/-}$ mice had significantly lower percentage freezing compared to NTg ($p<0.05$; **Fig. 30**) and APdE9 mice ($p<0.05$; **Fig. 30**). For the context 1 hour trial, Fisher LSD *post hoc* indicated APdE9-$Grn^{+/-}$ mice, but not APdE9 mice, had significantly lower percentage freezing compared to NTg mice ($p<0.05$) suggesting PGRN haploinsufficiency worsened short-term hippocampal-dependent associate memory in the APdE9 transgenic mouse model **(Fig. 30)**.

Anxiety-like behavior was next investigated, which has been previously reported in both $Grn^{+/-}$ and APdE9 mouse models (Kayasuga et al., 2007; Petkau

et al., 2012). In the light dark transition test, a two-way ANOVA showed no main effect between either the $Grn^{+/-}$ genotype [$F(1,47)=1.8702$, $p=0.178$] or APdE9 genotype [$F(1,47)=0.1037$, $p=0.748$] as well as no interaction effect between the two genotypes [$F(1, 47)=2.361$, $p=0.131$] **(Fig. 31)**. Fisher LSD *post hoc* test revealed a significant decrease in the time $Grn^{+/-}$ spent in the light compartment compared to NT g mice ($p<0.05$), while no significant difference was observed between APdE9 and APdE9-$Grn^{+/-}$ mice ($p>0.05$) **(Fig. 31)**. This result suggests PGRN haploinsufficiency increases anxiety-like behavior in the absence of the APdE9 genotype.

Anxiety-like behavior was further evaluated with the elevated plus maze which introduces the added elements of height and openness compared to the light dark transition test. A two-way ANOVA revealed a main effect from the $Grn^{+/-}$ genotype [$F(1,43)=6.9535$, $p=0.012$] but not a main effect from the APdE9 genotype [$F(1,43)=0.1460$, $p=0.708$] or an interaction effect between the two genotypes [$F(1,43)=0.8397$, $p=0.365$] **(Fig. 32)**. Fisher LSD *post hoc* test revealed APdE9-$Grn^{+/-}$ mice spent significantly less time in the open arms compared to APdE9 mice ($p<0.05$) indicating PGRN haploinsufficiency increased anxiety-like fear in the APdE9 mouse model **(Fig. 32)**. Additionally, anxiety-like behavior was examined in the open field test but did not observe any differences in time spent in the periphery versus center across all genotypes ($p>0.05$; **Fig. 34B**). These

results suggest that PGRN haploinsufficiency increases anxiety-like behavior in a task-specific manner independent of Aβ pathology.

AD-related pathology has also been shown to affect non-cognitive behaviors in transgenic mouse models (Kuwabara et al., 2014). Therefore, the effect of haploinsufficient loss of PGRN was also assessed with non-cognitive behaviors in the APdE9 transgenic mouse model. The motorized rotarod test and open field test were used to measure motor coordination and activity levels in all genotypes at twelve months. The latency to fall off the rotarod for eight trials split over two days was measured in the motorized rotarod test. Repeated measures ANOVA applied to the latency to fall all over the 8 trials showed a significant main effect of trials [$F(7,301)=10.705$, $p=0.000$] and the APdE9 genotype [$F(1,43)=5.4077$, $p=0.0248$] but not the $Grn^{+/-}$ genotype [$F(1,43)=0.7784$, $p=0.383$] or interaction effect between the two the genotypes [$F(1,43)=1.3704$, $p=0.248$]. No significant interactions were observed between trials and either the $Grn^{+/-}$ [$F(7,301)=1.662$, $p=0.118$] or APdE9 genotype [$F(7,301)=0.9335$, $p=0.485$] were observed indicating neither genotype impacted motor learning **(Fig. 33A)**. Fisher LSD *post hoc* test indicated a significant decrease in latency to fall for APdE9-$Grn^{+/-}$ mice compared to NTg mice on trials 1 ($p<0.05$), 3 ($p<0.05$), and 5 ($p<0.05$) **(Fig. 33B)**. This result suggests PGRN haploinsufficiency worsens motor coordination and balance but not learning in the APdE9 transgenic mouse model.

In the open field test, similar levels of activity were observed across all genotypes, with no differences in time spent moving (MOVE), resting (REST), or stereotypic behavior (STEREO) **(Fig. 34A)**. Two-way ANOVA revealed no main

effect from either the $Grn^{+/-}$ [F(2,53)=0.225, p=0.800] or APdE9 [F(2,53)=0.040, p=0.0961] genotype as well as no interaction effect from both genotypes [F(2,53)=0.441, p=0.0646]. While motor coordination deficits were observed in the motorized rotarod neither the $Grn^{+/-}$ or APdE9 genotype affected overall exploratory activity levels.

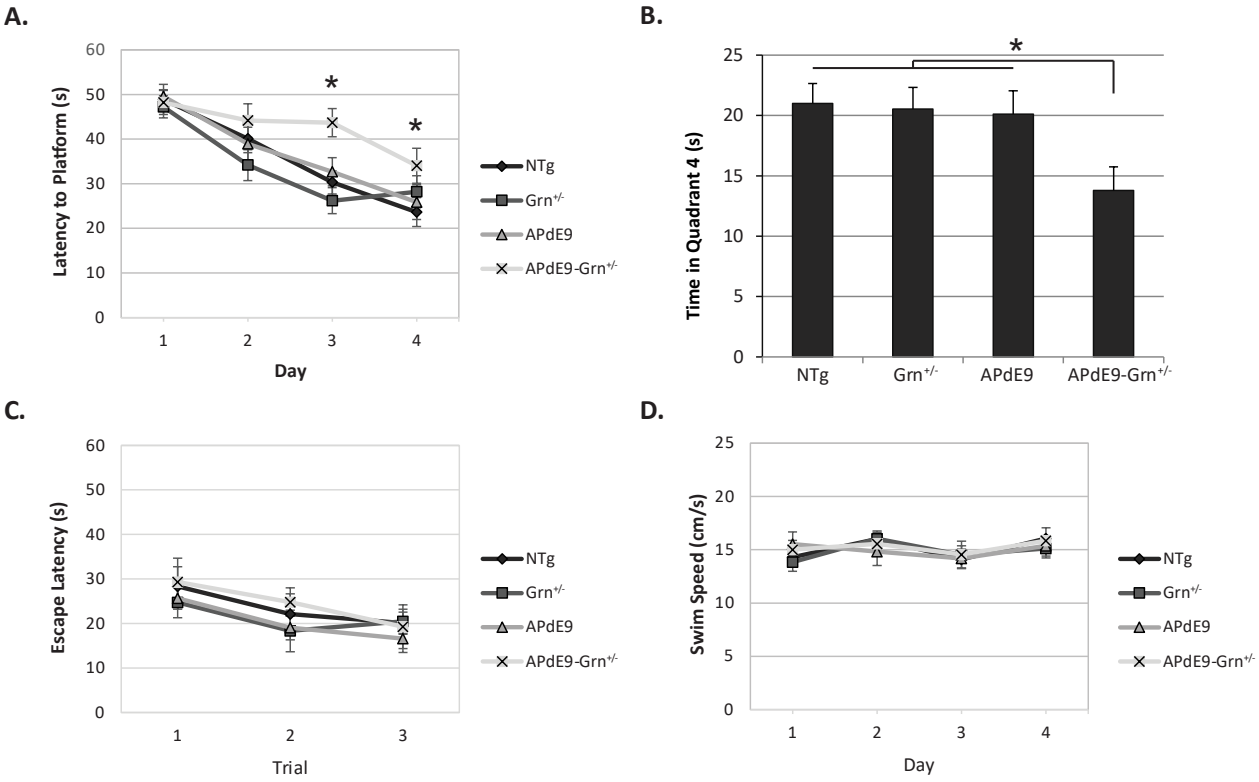

Figure 29. Heterozygous loss of progranulin exacerbated spatial learning and memory in the APdE9 mouse model (A) APdE9-Grn$^{+/-}$, but not APdE9 mice, took longer to find the hidden platform during the third and fourth acquisition trials of the Morris water maze. **(B)** APdE9-Grn$^{+/-}$ spent significantly less time in the target quadrant during the long-term memory trial. **(C)** No differences were observed in the swim speed between all genotypes during the acquisition trials. **(D)** No differences were observed in escape latency between all genotypes in the visual acuity trials. (*p<0.05; N = 7-9 mice per genotype).

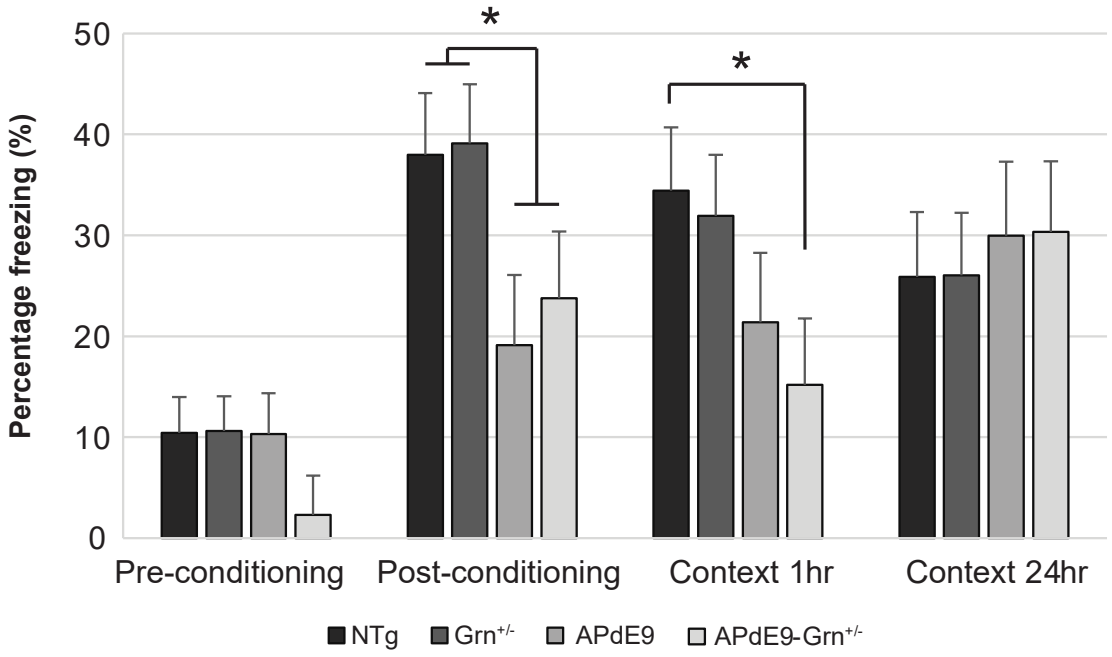

Figure 30. Progranulin haploinsufficiency exacerbated associative learning in the APdE9 mouse model. Both APdE9 and APdE9-Grn$^{+/-}$ mice had impaired freezing response in post-conditioning but only APdE9-Grn$^{+/-}$ mice exhibited significantly decreased freezing in the 1-hour contextual trial. (*$p<0.05$; N = 7-9 mice per genotype).

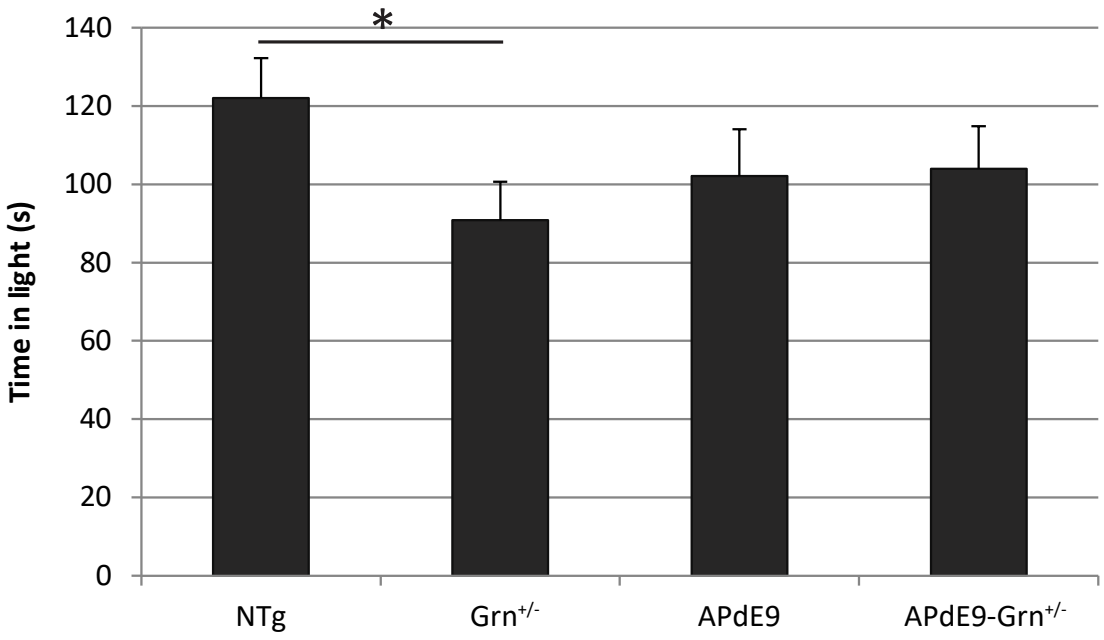

Figure 31.5 Heterozygous loss of progranulin increases anxiety-like behavior in NTg mice in the light dark transition test. $Grn^{+/-}$ mice spent significantly less time in the light compartment compared NTg mice, indicating increased anxiety-like behavior, but no differences were observed in the APdE9 or APdE9-$Grn^{+/-}$ mice (*$p<0.05$; N = 7-9 mice per genotype).

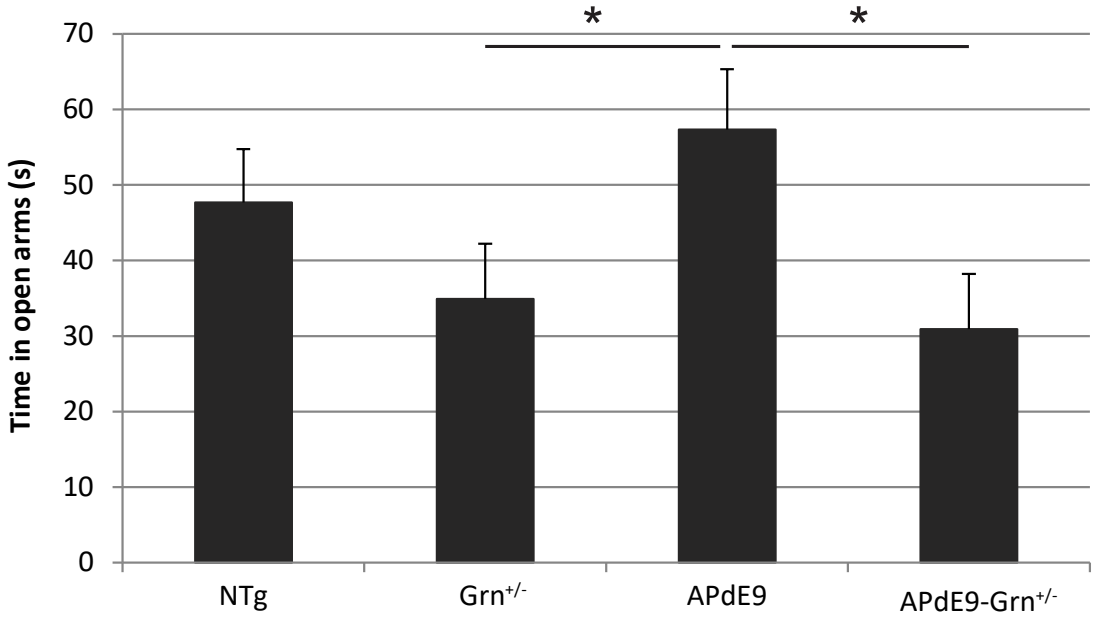

Figure 326. Heterozygous loss of progranulin increases anxiety-like behavior in APdE9 mice in the elevated plus maze. APdE9-Grn$^{+/-}$ mice spent significantly less time in the open arms compared to APdE9 mice indicating increased anxiety-like behavior. (*$p<0.05$; N = 7-9 mice per genotype).

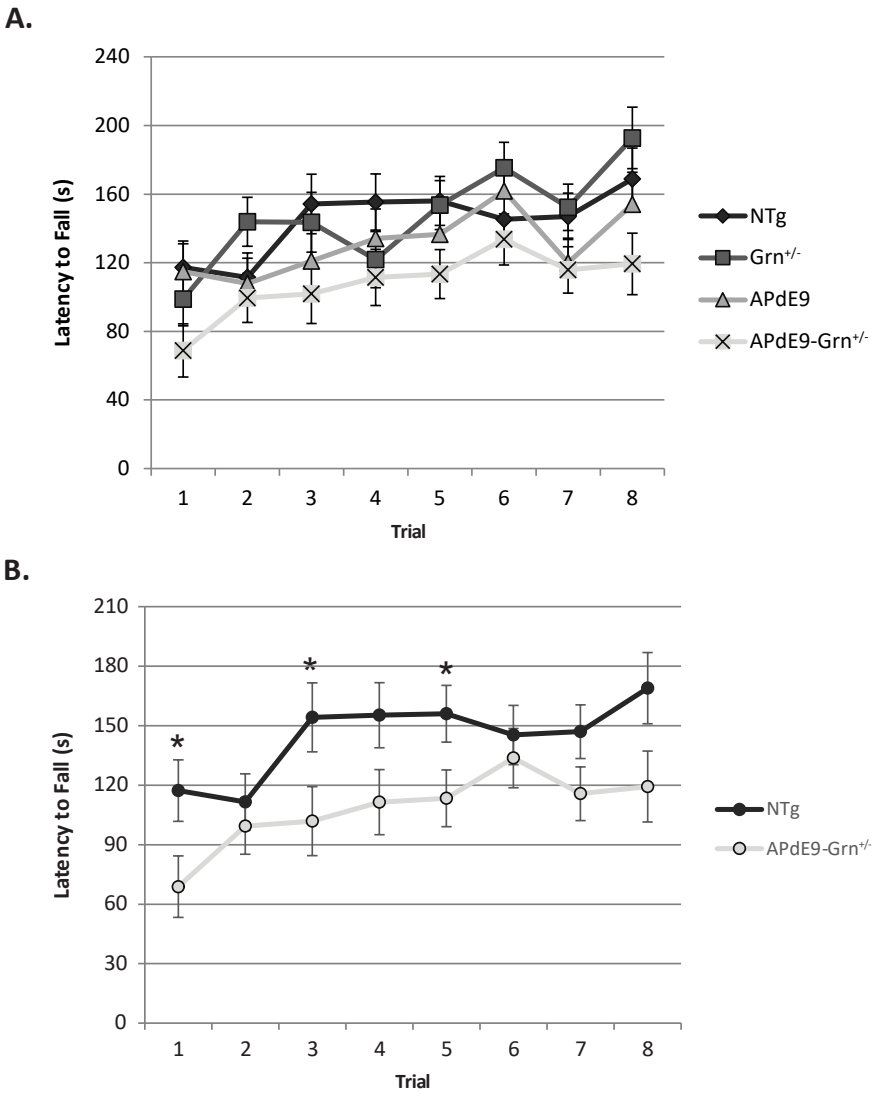

Figure 33. Heterozygous loss of progranulin impairs motor coordination in the APdE9 mouse model. (A and B) APdE9-Grn$^{+/-}$ mice exhibited impaired motor coordination on trials 1, 3, and 5 of the motorized rotarod. (*$p<0.05$; N = 7-9 mice per genotype).

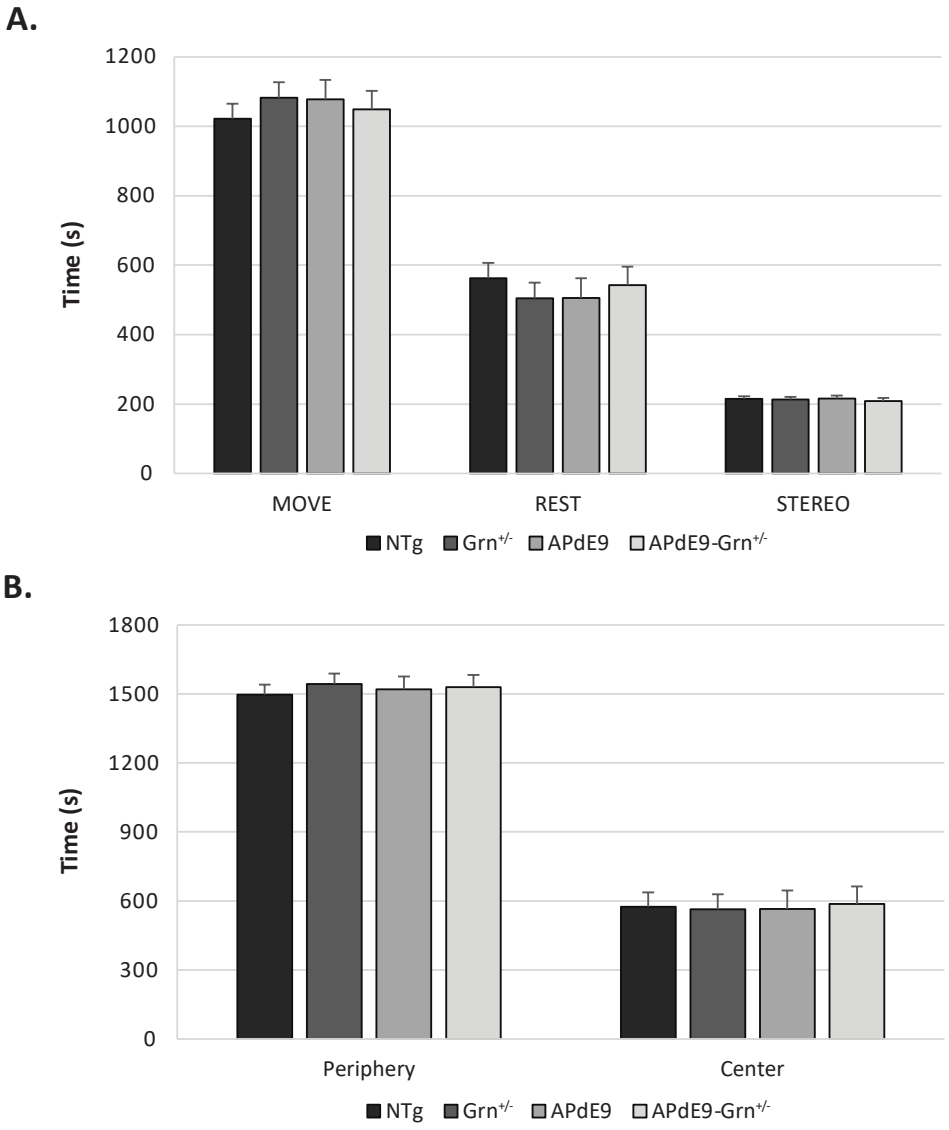

Figure 34. Progranulin haploinsufficiency does not affect exploratory behavior. (A) Time spent moving (MOVE) and resting (REST), or stereotypic behavior (STEREO) were not different between $Grn^{+/-}$ and NTg mice while exploring the open-field chamber. **(B)** Time spent in the periphery versus the center of the open-field chamber were similar between genotypes. (*$p<0.05$; N = 7-9 mice per genotype).

5.3.2 Heterozygous loss of PGRN modulates amyloid pathology but not neuroinflammation in APdE9 mice

Previously, conflicting reports exist whether complete loss of PGRN impacts amyloid pathology, with one report showing exacerbation of plaque deposition and another showing complete loss of PGRN surprisingly reduced diffuse amyloid(Minami et al., 2014; Takahashi et al., 2017b). In both papers, only the effect of the complete loss of PGRN was studied on amyloid pathology. Therefore, whether haploinsufficient loss of PGRN affected amyloid pathology in the brain of twelve-month-old APdE9 mice was next examined. Quantification of RIPA-soluble Aβ40 and Aβ42 in the whole brain by ELISA revealed PGRN haploinsufficiency increased Aβ40 and Aβ42 in APdE9 mice **(Fig. 35A)**. Two-way ANOVA revealed a main effect of $Grn^{+/-}$ genotype [$F(2, 15)=8.7105$, $p<0.003$)], APdE9 genotypes [$F(2,15)=0.06264$, $p<0.000$)], and interaction effect between $Grn^{+/-}$ and APdE9 genotypes [$F(2,15)=10.081$, $p<0.0017$] **(Fig. 35A)**. Tukey HSD *post hoc* test indicated that APdE9-$Grn^{+/-}$ mice had significantly higher levels of RIPA-soluble Aβ40 and Aβ42 compared to APdE9 mice ($p<0.001$; **Fig. 35A**).

Whether PGRN haploinsufficiency the aggregation and distribution of Aβ plaques was next investigated using an immunostaining method with the anti-human-Aβ mouse monoclonal antibody 4G8 **(Fig. 35B)**. A two-sample t-test was used to compare the number of and average area size of 4G8-positive amyloid plaques in the posterior parietal cortex and hippocampus between APdE9 and APdE9-$Grn^{+/-}$ mice. In the cortex, significantly fewer ($p<0.05$; **Fig. 35C**), but larger amyloid plaques ($p<0.01$; **Fig. 35D**) were observed in APdE9-$Grn^{+/-}$ mice

compared to APdE9 mice. Although a similar trend was observed in the hippocampus it was not significantly different in either the number of ($p>0.05$; **Fig. 35C**) or size ($p<0.05$; **Fig.35D**) of amyloid plaques between APdE9 and APdE9-$Grn^{+/-}$ mice. Both results suggest that the PGRN haploinsufficiency modulates the production and aggregation of Aβ in the APdE9 transgenic mouse model.

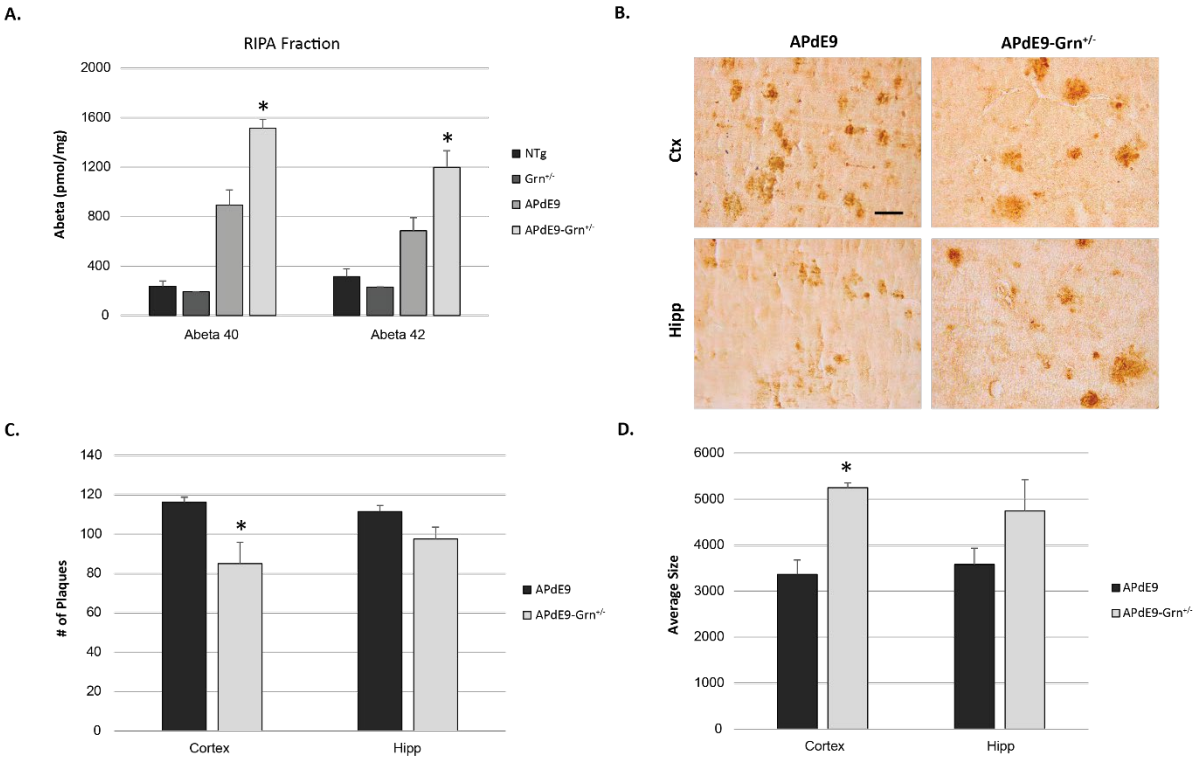

Figure 35. Heterozygous loss of progranulin modulates Aβ plaque deposition in APdE9 mice. (A) RIPA-soluble Aβ40 and Aβ42 measured by sandwich ELISA were significantly increased in APdE9-Grn$^{+/-}$ mice compared to APdE9 mice. **(B)** Representative images of 4G8 immunostaining in the cortex and hippocampus. **(C)** Loss of progranulin decreased the number of 4G8 immunostained plaques in the cortex of APdE9-Grn$^{+/-}$ mice. **(D)** Loss of progranulin increased the average size of 4G8 immunostained plaques in the cortex of APdE9 mice. Scale bars represent 100 um. (*$p<0.05$; N = 4 mice per genotype).

Previous reports studying the effect of complete loss of PGRN on amyloid pathology have focused on PGRN's relationship with microglial function(Minami et al., 2014; Takahashi et al., 2017b). Given that altered amyloid deposition was observed in APdE9-Grn$^{+/-}$ mice, microgliosis was investigated using an immunostaining method for allograft inflammatory factor 1 (Iba1) (**Fig. 36**), which is a marker for both resting and activated microglia (Shapiro et al., 2009). Quantification of microgliosis by Iba1 immunoreactivity revealed a significant increase in the number of microglia in the cortex and hippocampus of APdE9 and APdE9-Grn$^{+/-}$ mice compared to NTg and Grn$^{+/-}$ mice **(Fig. 37A and B)**. Two-way ANOVA revealed a main effect of the APdE9 genotype [$F(2,11)=39.059$, $p<0.001$]. Tukey HSD *post hoc* test revealed significant increase in % area positive pixels of Iba1 immunostaining between APdE9 and NTg mice ($p<0.001$; **Fig. 37A and B**) and APdE9-Grn$^{+/-}$ and Grn$^{+/-}$ mice ($p<0.001$; **Fig. 37A and B**) in both the posterior parietal cortex and hippocampus. However, no differences were observed between APdE9 and APdE9-Grn$^{+/-}$ mice indicating PGRN haploinsufficiency did not affect microgliosis in APdE9 mice ($p>0.05$; **Fig. 37A and B**). These results suggest that unlike with complete loss of PGRN, PGRN haploinsufficiency impacts AD-related behavior and amyloid pathology independent to changes in microgliosis.

APdE9-Grn+/-
APdE9
Grn+/-
NTg
Ctx
Hipp

Figure 36. Iba1 immunoreactivity in the cortex and hippocampus of APdE9-Grn$^{+/-}$ mice. Representative images of Iba1 immunoreactivity in the cortex and hippocampus of NTg, Grn$^{+/-}$, APdE9, and APdE9-Grn$^{+/-}$ mice (Brown = Iba1; N = 3– 5 mice per genotype). Scale bars represent 100 um.

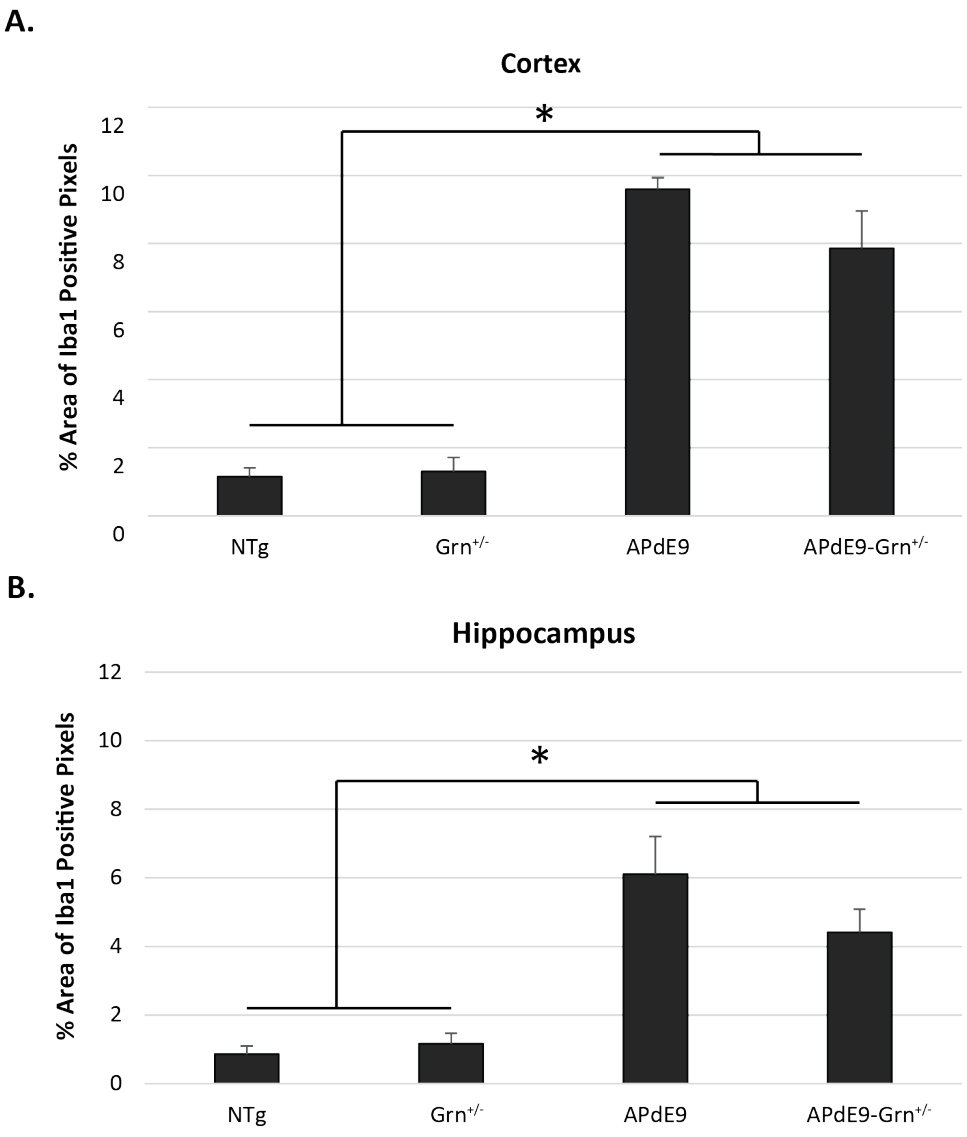

Figure 37. Heterozygous loss of progranulin does not affect microgliosis in the cortex or hippocampus of APdE9 transgenic mice. (A and B) APdE9 and APdE9-Grn$^{+/-}$ displayed significant microgliosis in the cortex and hippocampus compared to NTg and Grn$^{+/-}$ mice regardless of Grn$^{+/-}$ genotype. (*$p<0.05$; N = 3–5 mice per genotype).

5.3.3 Loss of PGRN Impaired synaptic plasticity and loss of hippocampal GABAergic interneurons in APdE9 mice

One explanation for the hippocampus-dependent memory deficits observed in the MWM and contextual fear conditioning is changes in long-term potentiation (LTP) (Campbell et al., 2002). Therefore, the effect of heterozygous loss of PGRN on hippocampal field excitatory post synaptic potentials (fEPSPs) in the Schaffer collaterals of APdE9 at fourteen months of age was next tested. LTP was induced by two brief bursts of high-frequency stimuli (HFS, 100 shocks at 100 Hz) **(Fig. 38A)**. Two-way ANOVA revealed a main effect of the $Grn^{+/-}$ genotype [$F(3,33)=7.1001$, $p=0.001$] but not a main effect of the APdE9 genotype [$F(3,33)=0.5659$, $p=0.641$] or an interaction effect between $Grn^{+/-}$ and APdE9 genotypes [$F(3,33)=0.2988$, $p=0.8259$] **(Fig. 38)**. Tukey HSD *post hoc* test revealed no significant differences in either the post-tetanic potentiation 1 and 2 (PTP1 and PTP2) across all genotypes ($p>0.05$; **Fig. 38C**). For LTP, Tukey HSD *post hoc* test revealed a significant decrease in LTP in APdE9-$Grn^{+/-}$ mice compared to APdE9 mice ($p<0.01$), as well as a significant decrease in LTP in $Grn^{+/-}$ mice compared to NTg ($p<0.05$) and APdE9 mice ($p<0.01$) **(Fig. 38D**). This data is consistent with electrophysiology results from Chapter 3 and reiterates the finding that haploinsufficient loss of PGRN is sufficient to impair LTP in the Schaffer collateral pathway and in the context of APdE9 mice impairs synaptic plasticity in the hippocampus independent to amyloid pathology. Furthermore, because changes were only observed in LTP and not in either PTP1 or PTP2 suggests PGRN haploinsufficiency impacts synaptic plasticity through either post-

translational mechanisms or gene transcription and protein syntheses rather than through changes in the buildup of calcium in the axon terminals of presynaptic neurons during HFS.

A possible explanation for both the cognitive and electrophysiology deficits observed in APdE9 transgenic mice is that heterozygous loss of PGRN impacts GABAergic interneurons in the hippocampus. Recently, complete loss of PGRN was shown to increase preferential elimination of inhibitory synapses of parvalbumin-positive interneurons(Lui et al., 2016) and loss of interneurons have previously been reported in AD transgenic mouse models(Levenga et al., 2013). Immunohistochemistry was used to quantify the number of GAD67-positive interneurons, a general marker for counting GABAergic interneurons(Rudy et al., 2011), in the CA1 and DG regions of the hippocampus and posterior parietal cortex to determine if PGRN haploinsufficiency impacts GABAergic interneurons in APdE9 mice. Two-way ANOVA revealed a main effect of the $Grn^{+/-}$ genotype [$F(3,9)=7.4098$, $p=0.008$)] significantly decreasing GAD67-positive interneurons but not with the APdE9 genotype [$F(3,9)=2.5125$, $p=0.124$)] or an interaction between the two genotypes [$F(3,9)=0.3923$, $p=0.761$] **(Fig. 39)**. In the CA1 region of the hippocampus, Tukey HSD *post hoc* test revealed a significant decrease in GAD67-positive cells in APdE9-$Grn^{+/-}$ mice compared NTg ($p<0.01$) and APdE9 mice ($p<0.05$) as well as a significant decrease in GAD67-positive cells in $Grn^{+/-}$ mice compared to NTg mice ($p<0.05$) **(Fig. 39)**. In the DG regions of the hippocampus, Fisher LSD *post hoc* test revealed a significant decrease in GAD67-positive cells in APdE9-$Grn^{+/-}$ mice compared to NTg ($p<0.01$) and APdE9 mice

($p<0.05$) **(Fig. 39)**. Although not statistically significant a similar trend was seen in $Grn^{+/-}$ mice compared to NTg mice ($p=0.076$). Unlike in the hippocampus, no significant differences were seen in the posterior parietal cortex across genotypes. In agreement with results in Chapter 3, PGRN haploinsufficiency decreases the number of GAD67-positive interneurons in the hippocampus but not posterior parietal cortex of APdE9 mice.

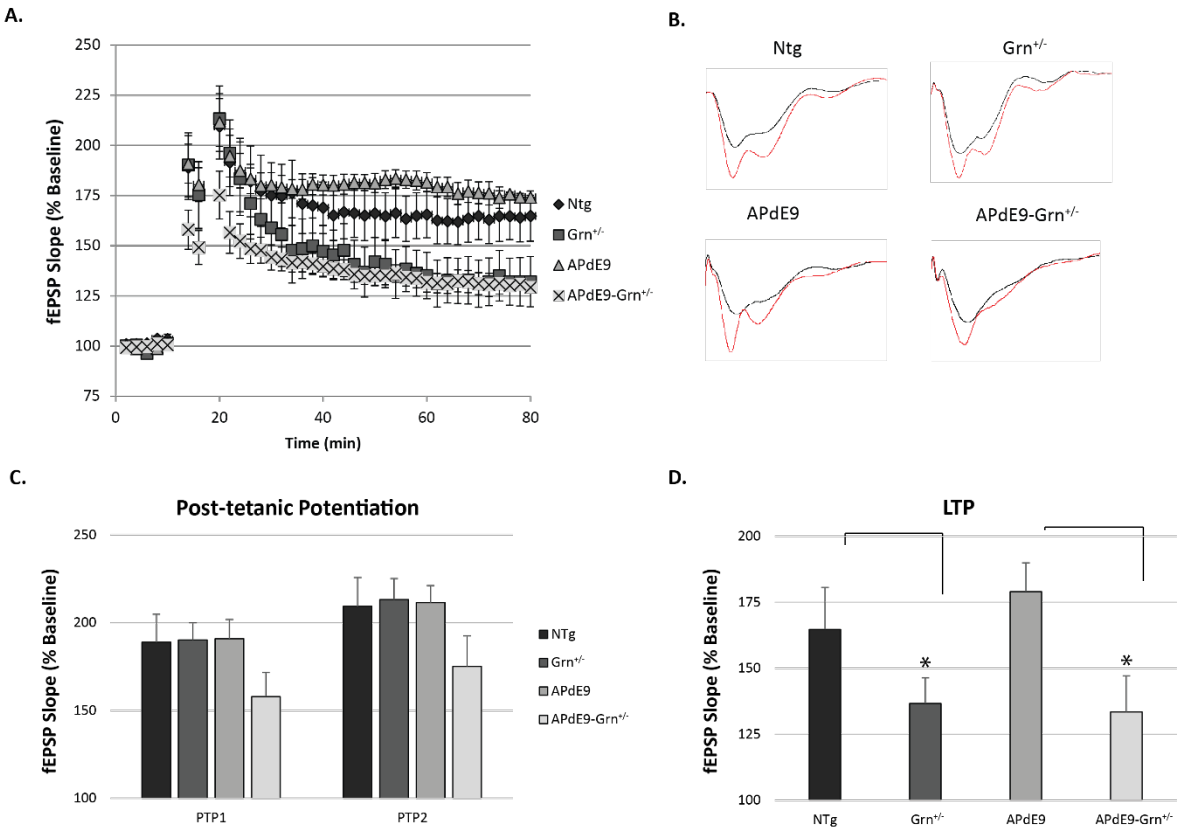

Figure 38. Heterozygous loss of progranulin impairs long-term potentiation in APdE9 mice. (A) LTP was induced by two bursts of high-frequency stimuli (HFS, 100 shocks at 100 Hz). **(B)** Representative LTP traces for NTg, Grn$^{+/-}$, APdE9 and APdE9-Grn$^{+/-}$ traces. **(C)** Quantification of post-tetanic potentiation (PTP) after both bursts of HFS was significantly reduced in APdE9-Grn$^{+/-}$ mice, and **(D)** LTP, measured 45 minutes after HFS, was significantly reduced in both Grn$^{+/-}$ and APdE9-Grn$^{+/-}$ mice. (*$p<0.05$; NTg = 4 mice, 11 slices; Grn$^{+/-}$ = 4 mice, 15 slices; APdE9 = 3 mice, 8 slides; APdE9-Grn$^{+/-}$ = 4 mice, 12).

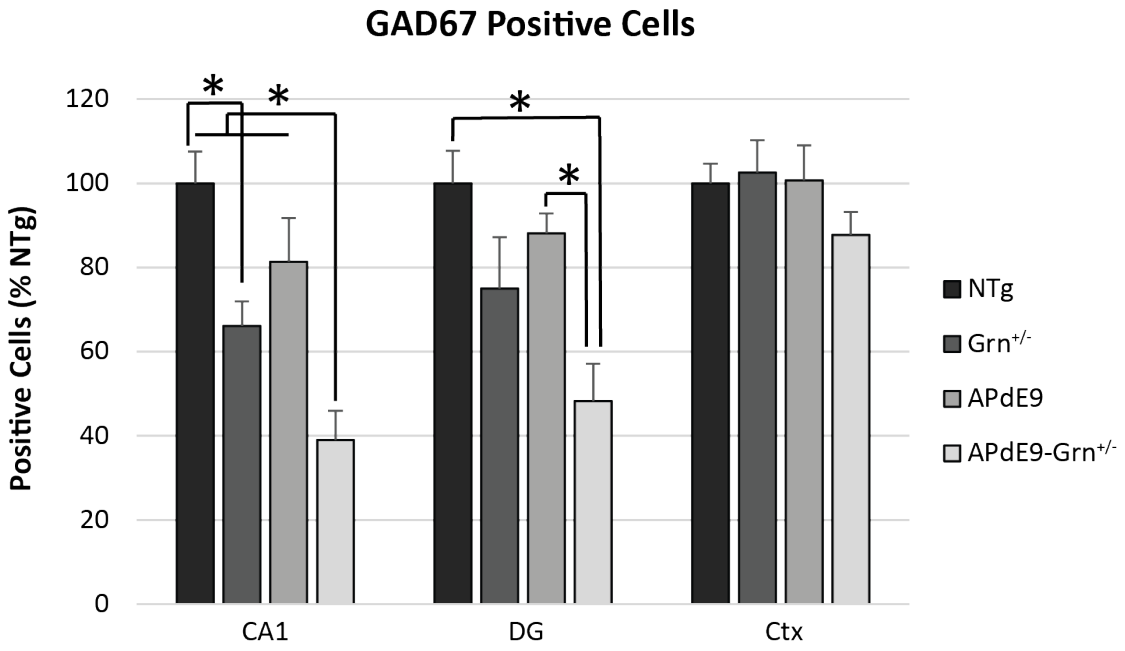

Figure 39. Heterozygous loss of progranulin results in loss of GABAergic interneurons in the hippocampus. Significant decrease in GAD-67 immunostained cells in the CA1 and DG regions of the hippocampus but not in the posterior parietal cortex (Ctx) in $Grn^{+/-}$ and APdE9-$Grn^{+/-}$ mice. (*$p<0.05$; N = 4 mice per genotype).

5.4 Discussion

In this series of experiments, whether PGRN haploinsufficiency exacerbated AD-related behavior and pathology progression in mice that overexpress mutant human APP_{SWE} and PS1-dE9 genes were investigated. The major conclusions of this section are that heterozygous loss of PGRN exacerbated cognitive and non-cognitive AD-related behaviors that was accompanied by changes in amyloid plaque morphology and increased RIPA-soluble Aβ42. Moreover, PGRN haploinsufficiency disrupted LTP and significantly reduced the number of interneurons in the hippocampus. Importantly, these changes were observed without gross changes in microglia which is seen in models with complete loss of PGRN suggesting PGRN haploinsufficiency may be affecting disease progression through neuronal-dependent affects instead. These findings extend previous studies suggesting that changes in PGRN levels affects behavior and amyloid pathology and suggests new roles of PGRN in AD and neurodegenerative disease.

To evaluate the role PGRN haploinsuffiency in AD disease progression the APdE9 transgenic mouse model containing the APP KM670/671NL (Swedish mutation) and the PS1-dE9 mutation was used. The Swedish mutation is located immediately adjacent to the β-secretase site in APP and biases β-secretase processing of APP resulting in the increase production of Aβ40 and Aβ42 but does not affect the ratio of Aβ40/Aβ42. The PS1-dE9 mutation on the other hand is located on one of the four core proteins comprising the γ-secretase complex and has been shown to increase the pool of Aβ42 without changing levels of Aβ40,

resulting in significantly increased plaque load. By six months of age, APdE9 mice begin to deposit Aβ with amyloid plaques forming in the hippocampus and cortex between nine and twelve months accompanied by cognitive and non-cognitive behavior deficits (Lui et al., 2016). We and others have previously shown that the APdE9 transgenic mouse line show spatial deficits signifincatnly later at sixteen months of age when backcrossed on a C57Bl/6J mouse line (Vollert et al., 2013; Takahashi et al., 2017b). Due to the late onset of amyloid pathology and cognitive deficits seen in the APdE9 transgenic mouse model made it uniquely suitable for assessing the effects of PGRN haploinsufficiency on AD disease progression.

Because $Grn^{+/-}$ and APdE9 mice do not show disturbances in spatial learning and memory until sixteen and eighteen months-of-age spatial learning and memory was tested at twelve months to determine if PGRN haploinsufficiency increased the onset of learning and memory deficits in APde9 mice. Utilizing the MWM, significant increases in the latency to find the hidden platform on learning days three and four was observed for APde9-$Grn^{+/-}$, but not APdE9 mice indicating PGRN haploinsufficiency impaired spatial learning in APdE9 mice. Furthermore, a significant decrease in time spent in the target quadrant of the 1hr probe trial was also observed in APdE9-$Grn^{+/-}$ mice, but not APdE9 mice indicating PGRN haploinsufficiency also impaired short-term spatial memory. Differences were not observed in either the visual acuity trials or swim speed throughout the learning trials ruling out vision and hyperactivity as potential confounding variables. In addition to the findings in the MWM, APdE9-$Grn^{+/-}$ mice had a significant decrease in the percent freezing during the 1hr context trial, which was absent in APdE9

mice, indicating PGRN haploinsufficiency also impaired short-term contextual memory in APdE9. Together, these results indicate that PGRN haploinsufficiency increases the onset of contextual and spatial learning and memory deficits in the APdE9 transgenic mouse model and is consistent with the hypothesis that heterozygous loss of PGRN exacerbates AD disease progression and a previous report showing complete loss of PGRN exacerbates Aβ-related behavioral deficits (Minami et al., 2014).

Anxiety-like behavior has also been shown to be affected in both AD and PGRN mouse models (Kayasuga et al., 2007; Petkau et al., 2012). Although no differences were observed in anxiety-like behavior in APdE9 mice in either the elevated plus-maze or light-dark test, a task-specific effect was observed with $Grn^{+/-}$ genotype. In the elevated plus-maze, a significant reduction was observed in time spent in the open arms of both $Grn^{+/-}$ and APde9-$Grn^{+/-}$ mice compared to APdE9 mice suggesting that the partial loss of PGRN increased anxiety-like behavior in APdE9-$Grn^{+/-}$ mice. In the light-dark test, a reduction in time spent in the light compartment was only observed in $Grn^{+/-}$ mice compared to NTg littermates indicating increased anxiety-like behavior only in the $Grn^{+/-}$ genotype but was not seen in the APdE9 mice.

Non-cognitive behaviors including exploratory behavior and motor coordination have also been shown to be affected by increases in amyloid plaque deposition (Lomoio et al., 2012; Kuwabara et al., 2014). Although no differences were observed in activity levels across all genotypes in the open field, motor coordination impairment was observed using the rotarod test. APdE9-$Grn^{+/-}$ mice

had a decreased latency to fall on three of the eight trials compared to NTg mice, suggesting that heterozygous loss of PGRN impaired motor coordination in APdE9 mice. These observations are consistent with previous studies that have reported motor deficits in patients with the PS1-dE9 mutation and the APdE9 transgenic mouse model (Crook et al., 1998; Kuwabara et al., 2014). The cerebellum is well known to be essential for motor coordination, and Aβ pathology has been shown to accumulate in the cerebellum of APdE9 mice (Kuwabara et al., 2014). Impairment in motor coordination is consistent with the cognitive behavioral data suggesting that PGRN haploinsufficiency exacerbates AD-related cognitive and non-cognitive behavior.

Amyloid plaques are composed of both Aβ40 and Aβ42 peptides that aggregate into oligomers and, in turn combine to form fibrils and ultimately into plaques. In normal brains soluble pools of Aβ40 and Aβ42 are the largest fractions of total Aβ but are the smallest in the AD brain suggesting the insoluble pool of Aβ correlates with amyloid plaque deposition (Wang., et al. 1999). Aβ42 is the main species of Aβ peptide deposited in plaques, with even small changes of Aβ42 can significantly modulate the rate of amyloid deposition and plaque formation. In this study, differences in both biochemical and morphological changes in Aβ pathology were observed in APdE9 mice with heterozygous loss of PGRN. Biochemically, an increase in RIPA-soluble Aβ42 and Aβ40 was observed in the whole brain. Morphological changes in amyloid plaque deposition were also observed with heterozygous loss of PGRN, resulting in fewer but larger plaques in the cortex.

These findings show that heterozygous loss of PGRN modulates the deposition of Aβ pathology in APdE9 mice.

The progressive impairment in hippocampal-based spatial learning and memory in AD transgenic mouse lines has been associated with Aβ associated synaptic dysfunction (Walsh et al., 2002; Palop and Mucke, 2010). The majority of AD mouse models have focused on the long-term form of synaptic plasticity induced by high-frequency stimulation with Aβ pathology resulting in synaptic depression and reduced synaptic facilitation (Walsh et al., 2002). In this study, synaptic plasticity and LTP were investigated in APdE9-Grn$^{+/-}$ mice at 14 months. A significant reduction in LTP was observed in APdE9-Grn$^{+/-}$ and Grn$^{+/-}$ mice and a significant reduction in post-tetanic potentiation was only seen in APdE9-Grn$^{+/-}$ mice. Because no significant differences were observed in either the post-tetanic potentiation or LTP in the APdE9 mice, our data suggest that the heterozygous loss of PGRN is driving the decreased LTP rather than an effect associated with Aβ pathology. Although our study did not evaluate in greater detail how PGRN haploinsuffieincy impaired LTP in Grn$^{+/-}$ and APdE9-Grn$^{+/-}$ mice this observation is consistent with the prior literature where several reports have observed altered neuronal connectivity after complete loss of PGRN (Petkau et al., 2012; Lui et al., 2016). In hippocampal neurons, the knockdown of PGRN increased the number of vesicles per synapse and the frequency of mEPSCs (Tapia et al., 2011). Moreover, in the same study, an increase in the number of vesicles per synapse was confirmed in FTLD patients with PGRN mutations. Abnormal neuronal morphology

has also been seen in $Grn^{+/-}$ mice exhibiting decreased LTP in the Schaffer (Petkau et al., 2012).

Exactly how the loss of PGRN is impacting learning and memory and specifically synaptic plasticity, is unclear. Earlier reports have reported differences in the number of vesicles per synapse and altered synaptic morphology (Petkau et al., 2012). Recently, it has been suggested that loss of PGRN impacts inhibitory synapses of parvalbumin-positive interneurons driven by microglia (Lui et al., 2016). Supporting the idea that loss of PGRN impacts inhibitory synapses, a significant reduction of GAD67-positive cells was observed in this study in both $Grn^{+/-}$ and APdE9-$Grn^{+/-}$ mice with APdE9-$Grn^{+/-}$ having significantly fewer GAD-67 positive interneurons compared to NTg, $Grn^{+/-}$ and ApdE9 mice. These results suggest that alterations in interneurons are not only driven by the $Grn^{-/-}$ genotype, but that heterozygous loss of PGRN is impacting GAD-67 positive interneurons independent of amyloid pathology.

The observed reduction of interneurons is consistent with the reported behavioral and synaptic plasticity deficits observed in APdE9-$Grn^{+/-}$, which have been observed in other mouse models with similar phenotypes (Li et al., 2009; Andrews-Zwilling et al., 2010; Loreth et al., 2012). In contrast to the previous report which showed a preferential loss of inhibitory synapses in parvalbumin-positive interneurons in $Grn^{-/-}$ mice due to aberrant microglia activation, no significant differences in either number or morphology were seen in microglia in our experiments suggesting that loss of PGRN maybe impacting GABAergic differently in heterozygous versus a complete loss of PGRN. Furthermore, the previous study

looked specifically at the number of synapses of parvalbumin-positive interneurons, whereas our study looked at the total number of interneurons and not at the synapse level. It is unclear if the loss of interneurons seen in $Grn^{+/-}$ and ApdE9-$Grn^{+/-}$ mice is also accompanied by a loss of inhibitory synapses or if the loss of inhibitory synapses is specific only to increased microgliosis seen in the $Grn^{-/-}$ phenotype. While it is unclear how PGRN haploinsufficiency impacts GABAergic interneurons, further study would help better understand how loss of PGRN impacts specific subpopulations of GABAergic interneurons such as parvalbumin and somatostatin expressing interneurons and whether this loss occurs during development or through aging.

How PGRN haploinsufficiency modulates AD pathophysiology, specifically amyloid pathology and synaptic plasticity, is not well understood. One possible explanation is that the reduction of PGRN is impacting the inflammatory pathway, which has been reported to both increase and decrease amyloid pathology in AD transgenic mouse models depending on how it is manipulated (DiCarlo et al., 2001; Qiao et al., 2001; Herber et al., 2004; Vom Berg et al., 2012). An increase in a pro-inflammatory state has been suggested to contribute to the pathogenesis of multiple neurodegenerative diseases, including AD (Akiyama et al., 2000; Wyss-Coray, 2006; Frank-Cannon et al., 2009). The relationship of PGRN with inflammation has been extensively studied in PGRN transgenic mouse models, with $Grn^{-/-}$ mice displaying a marked age-dependent increase in both microgliosis and astrogliosis across multiple transgenic mouse models (Ahmed et al., 2010; Yin et al., 2010b; Ghoshal et al., 2012). The reduction of PGRN has been reported to

act as a chemoattractant to recruit microglia and increase the endocytosis of amyloid β (Pickford et al., 2011). Moreover, in cell cultures, $Grn^{-/-}$ macrophages have been reported to cause an exaggerated release of cytokines after stimulation (Yin et al., 2010b), increased inflammatory response (Martens et al., 2012), and increased phagocytosis activity (Kao et al., 2011).

Although there is a strong connection between the complete loss of PGRN and inflammation, both findings in this report and prior literature suggest that the heterozygous loss of PGRN may affect Aβ pathology and synaptic plasticity through mechanisms that are independent of changes in neuroinflammation. Despite observed changes in both AD-related behavior and pathology, no differences were observed in the total number of microglia in APdE9-$Grn^{+/-}$ mice suggesting haploinsufficient loss of PGRN did not exacerbate neuroinflammation in APdE9 mice. This is contrary to a previous study that reported reduced diffuse Aβ plaque growth attributed to enhanced microglial Aβ phagocytosis caused by increased expression of TYROBP network genes in APdE9-$Grn^{-/-}$ mice (Takahashi et al., 2017). One potential explanation is the lack of a neuroinflammatory phenotype in $Grn^{+/-}$ mice which do not develop neuroinflammation marked by increased microglia and astrocytes seen in their $Grn^{-/-}$ littermates (Ahmed et al., 2010) despite both models showing FTD-related behavioral deficits (Filiano et al., 2013). Furthermore, a recent study evaluating loss of PGRN on tau pathology did not see any changes in inflammatory cytokines suggesting that heterozygous loss of PGRN was modulating AD pathology independent of changes in neuroinflammation (Hosokawa et al., 2015), despite observing increased tau

phosphorylation. However, microglial involvement Instead this group suggested that PGRN loss increased tau phosphorylation through the activation of P cyclin-dependent kinases rather than through the inflammatory pathway.

Our results that haploinsufficient loss of PGRN affects amyloid pathology in lieu of changes in neuroinflammation is in contrast with two other reports investigating the role of PGRN in AD pathology. Both studies used $Grn^{-/-}$ mice and results supported the role of inflammation in PGRN's effect on AD disease progression albeit with conflicting results. In one report, an increase in amyloid plaque deposition was reported in mouse models of both complete loss and partial loss of PGRN specific to microglia suggesting loss of PGRN effect on amyloid pathology was due to impaired phagocytosis in microglia (Minami et al., 2014). Paradoxically, a later study reported a reduction of diffuse Aβ plaques in the APdE9 transgenic mouse model with complete loss of PGRN and this was associated with upregulated expression of microglial genes from the TYROBP network suggesting complete loss of PGRN increased microglial phagocytosis of Aβ (Takahashi et al., 2017a). However, like the previous report studying the role of PGRN and inflammation, $Grn^{+/-}$ mice did not exhibit the same increases in TYROBP gene network as their $Grn^{-/-}$ counterparts, suggesting this may be a unique phenotype to the complete loss of PGRN.

In context with these two studies our results have interesting implications for the role of PGRN in AD disease progression. Our results show that heterozygous loss of PGRN is able to affect amyloid beta and exacerbate behavioral deficits despite the absence of increased neuroinflammation which is

seen with complete loss of PGRN. This is in line with the growing literature that PGRN haploinsufficiency can cause behavioral and neuropathological deficits in the absence of neuroinflammation (Filiano et al., 2013; Arrant et al., 2016; Arrant et al., 2017). Although we did not observe gross changes in the levels of microglia this does not rule out the possibility that PGRN haploinsufficiency still modulated amyloid pathology through effects on microglia. In a previous study examining loss of PGRN on amyloid pathology LysM-cre mice was utilized to selectively reduce levels of PGRN in an AD mouse model. Interestingly, they showed that microglia in this model had an approximately 50% decrease in PGRN mRNA and this reduction was followed by an increase in plaque deposition attributed to a decrease in phagocytic activity in microglia. Therefore, it is possible that although gross changes were not seen in microglia levels in our study, PGRN haploinsufficiency still impaired phagocytic activity in microglia suggesting a dissociation between neuroinflammation and impaired microglial phagocytic activity. This could be an explanation to why we observed increased levels of soluble Aβ and larger plaques in APdE9 mice with haploinsufficient loss of PGRN. Microglia with impaired ability to phagocytize soluble Aβ could result into a larger soluble pool of Aβ available to aggregate to plaques already formed. Although this can only be determined with a more in-depth analysis of the composition of amyloid plaques observed and evaluating primary microglia phagocytic activity from APdE9-Grn$^{+/-}$ mice.

Our results are also inconsistent with a previous study reporting a decrease in number of amyloid plaques after heterozygous loss of PGRN. One potential

explanation for this is the differences in experimental design. In our study we used the APdE9 transgenic mouse model which contains the Swedish mutation increasing the amount of APP processed by the β-secretase and the PS1dE9 mutation which increases the preferential cleavage of Aβ42. On the other hand, the previous study used the Tg2576 transgenic mouse model which only contains the Swedish mutation resulting in increased processing of Aβ species but not altering the preference for the Aβ42 species. It is possible that PGRN haploinsufficiency may exert a mutant-dependent effect on amyloid pathology where different ratios of Aβ40/Aβ42 are present. Another possible explanation is that both studies examined amyloid pathology at different timepoints. In our study, we examined amyloid pathology at twelve months where amyloid plaque deposition is beginning to appear and cognitive deficits are not yet seen, whereas the other study examined amyloid pathology between sixteen and eighteen months where amyloid pathology is more extensive. Therefore, the discrepancy maybe due to PGRN haploinsufficiency having a biphasic effect on amyloid pathology during the initial stages of amyloid plaque development and late stages of amyloid plaque development. However, regardless of the difference in mouse models and stage of disease progression, our results clearly suggest PGRN haploinsufficiency increased RIPA soluble Aβ42 and modulates amyloid plaque deposition in the APdE9 mouse model.

CHAPTER 6: CONCLUDING REMARKS

6.1 Summary and Conclusions

Overall, the work presented in this dissertation highlights an aspect that, until recently, has been largely overlooked in PGRN research – the effect of heterozygous rather than complete loss of PGRN across aging and on AD pathologies. Prior work has focused almost exclusively on the complete loss of PGRN in neurodegeneration, emphasizing PGRN's role in microglia. However, data from this dissertation and a growing body of literature suggests that the heterozygous loss of PGRN recapitulates many of the functional deficits seen with complete loss of PGRN independent of changes in neuroinflammation. Furthermore, the partial loss of PGRN has both positive and negative effects on AD pathophysiology suggesting that therapies that increase global PGRN levels may not be beneficial in treating AD.

Several different *Grn* transgenic mouse lines have been studied as models of FTLD-TDP, with the majority only focused on the effect of complete loss of PGRN due to the initial observation that only full-knockout PGRN mouse models had observable phenotypes (Kayasuga et al., 2007; Ghoshal et al., 2012; Petkau et al., 2012; Wils et al., 2012; Filiano et al., 2013). However, Filiano and colleagues recently reported FTLD-related social and emotional dysfunction in $Grn^{+/-}$ mice in the absence of neuroinflammation, suggesting a dissociation between neuroinflammation and behavioral deficits also observable behavioral deficits in $Grn^{+/-}$ mice (Filiano et al., 2013). In congruence with this finding, using a novel

$Grn^{+/-}$ transgenic mouse line, data from this dissertation confirms and extends the observation that heterozygous loss of PGRN causes key FTLD-related behavioral deficits in the absence of FTLD-related pathology to include deficits in spatial learning and sensorimotor gating **(Fig. 40)**. Our findings extend the initial observations and shows for the first time that heterozygous loss of PGRN results in a reduced number of GABAergic interneurons in the hippocampus of aged $Grn^{+/-}$ mice and impaired LTP, all in the absence of neuroinflammation. This data supports the observation of a dissociation between FTLD-related pathology and the functional effects of PGRN loss, suggesting that PGRN's effect on neurons rather than microglia is the cause for observed functional deficits. Furthermore, this work and others suggest that $Grn^{+/-}$ mice, rather than $Grn^{-/-}$ mice, may be a better mouse model at recapitulating FTLD-TDP and PGRN's role in neurodegeneration.

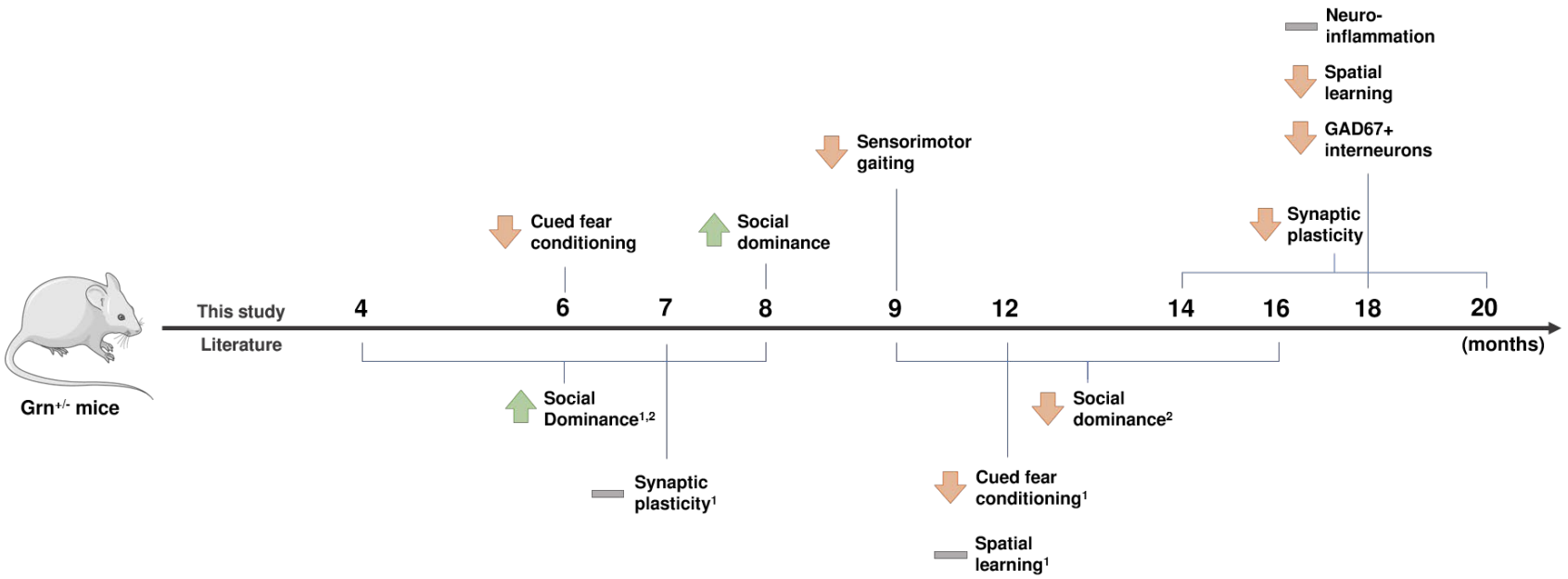

1. Filiano, A.J., et al. 2013 Dissociation of Frontotemporal Dementia-Related Deficits and Neuroinflammation in Progranulin Haploinsufficient Mice. *J Neurosci.* 33(12):5352-5361
2. Arrant, A.E., et al. 2016. Progranulin haploinsufficiency causes biphasic social dominance abnormalities in the tube test. *Genes Brain Behav.*15(6):588-603
3. Arrant, A.E., et al. 2017. Restoring neuronal progranulin reverses deficits in a mouse model of frontotemporal dementia. *Brain.* 140(5):1447-1465

Fig. 40. Schematic diagram of behavioral and neuropathology changes in progranulin haploinsufficient mice across age. Previous studies examining behavior in $Grn^{+/-}$ mice identified social and behavioral abnormalities but not in cognitive behavior or synaptic plasticity. In this study $Grn^{+/-}$ mice exhibited impaired spatial learning and reduced synaptic plasticity at eighteen months which is much later than previously tested.

Epidemiological reports suggest that loss of PGRN may be a risk factor for AD, but transgenic mouse model studies investigating the complete loss of PGRN have resulted in conflicting reports. Concerning tau pathologies, data from this work suggests that heterozygous loss of PGRN results in reduced motor coordination and balance deficits and AT8 tau phosphorylation in the P301S tau transgenic mouse model, which was associated with abnormal cell signaling in the Akt and Wnt signaling pathways (**Fig. 41**). Although significant tau phosphorylation changes were observed, they did not appear to affect the progression of neurodegeneration. This contrasts with two previous studies showing increased tau phosphorylation with complete or partial loss of PGRN in the P301L mouse model suggesting the effect of PGRN loss on tau pathology is mutation dependent. This work suggests that partial loss of PGRN may not worsen all aspects of AD pathology and may be beneficial in attenuating the progression of tau pathology. Additionally, while previous reports have focused on PGRN's function in microglia and potential impact on AD, our data suggests that a partial loss of PGRN modifies tau phosphorylation through the Akt signaling pathway rather than through changes in the activity of microglia.

With regards to amyloid pathology, data from this dissertation show that heterozygous loss of PGRN exacerbated AD-related cognitive and non-cognitive behavior and modulated Aβ pathology in the APdE9 mouse model (**Fig. 41**). Reduced LTP and a significant reduction in GABAergic interneurons in APdE9 mice with heterozygous loss of PGRN were also observed. Despite observing

significant changes in AD-related behavior and pathophysiology, the heterozygous loss of PGRN did not appear to affect the number of microglia activity, which has been reported in AD transgenic mice with complete loss of PGRN. This work further expands on the prior literature and suggests that complete loss and even partial loss of PGRN are enough to exacerbate amyloid-related behavioral and functional deficits. However, unlike with complete loss of PGRN, partial loss of PGRN appears to exacerbate AD-related pathology independent of inflammation and microglial function.

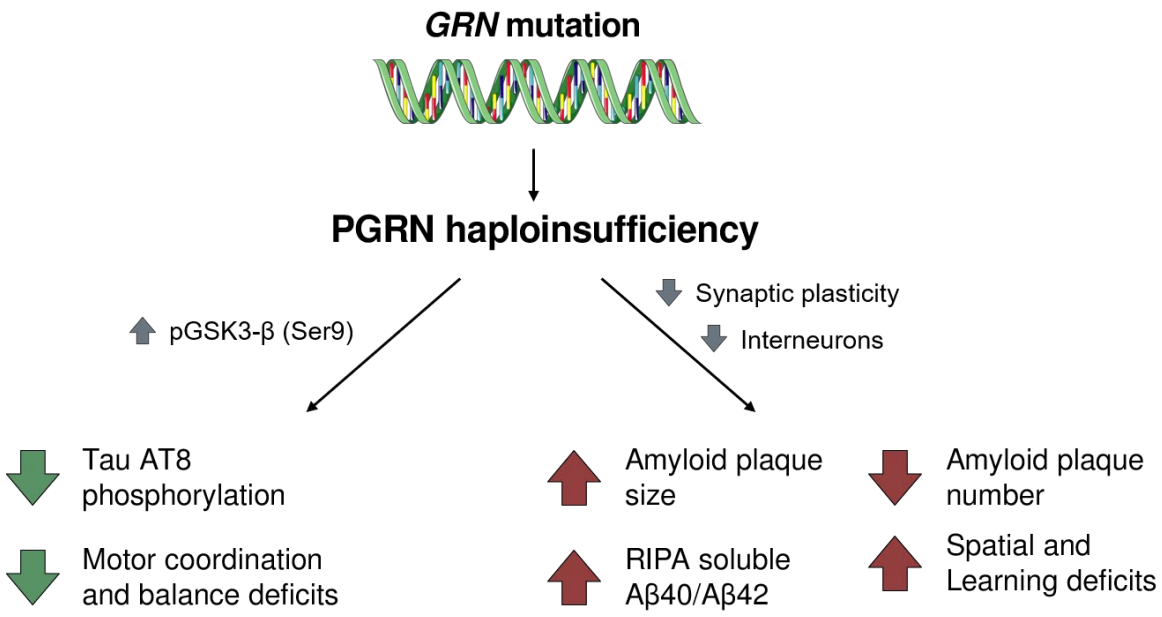

Fig. 41. Schematic diagram of the opposing effects of progranulin haploinsufficiency on Alzheimer's disease neuropathology. Progranulin haploinsufficiency caused by a *GRN* mutation decreased tau AT8 phosphorylation and reduced motor coordination and balance impairment suggesting a possible protective role. Progranulin haploinsufficiency increased RIPA-soluble Aβ40/Aβ42, modulated amyloid plaque formation, and increased spatial and learning cognitive deficits suggesting progranulin haploinsufficiency maybe a risk factor.

6.2 Implications and Future Directions

Future work will be needed to understand the role of PGRN in AD and neurodegeneration fully.

An important implication from this work is the different functional roles of microglial versus neuronal PGRN in neurodegeneration. The bulk of the current literature has focused on PGRN's role in microglia in driving neurodegenerative disease processes. However, this work and others suggest that similar effects on AD disease progression are seen in $Grn^{+/-}$ mice in the absence of apparent changes in microglial function, suggesting a dissociation between loss of PGRN's effect on neurodegenerative disease and microglial function. The present study utilized a global $Grn^{+/-}$ mouse model. However, this model is limited in that PGRN is reduced in both neurons and microglial, making it challenging to separate PGRN loss effects between neuronal and microglial populations. Recently, a group developed two neuronal PGRN-deficient mouse lines to better differentiate effects from neuronal and microglial PGRN loss and reported that both lines developed social behavior abnormalities, a fundamental FTLD behavioral deficit, similar to global $Grn^{+/-}$ mice and that this behavior along with lysosomal abnormalities was corrected after adeno-associated virus-driven expression of neuronal PGRN (Arrant et al., 2017). A potential conclusion from our work regarding PGRN haploinsufficiency effect on tau and amyloid pathology is that neuronal loss and not microglial loss is driving changes in disease progression given a lack of gross changes in microglia. However, given both pools of PGRN were reduced and the possibility that PGRN haploinsufficiency was affecting microglial function

independent of increases in gross markers of activity (number and morphology) it cannot be ruled out. Future studies utilizing neuron specific PGRN-deficient mouse models crossed with AD transgenic mouse models and the rescue of specific neuronal PGRN in mouse models will better elucidate the functional roles of neuronal and microglial PGRN in neurodegenerative disease.

One limitation of the present study is that it only characterized neuroinflammation by histological expression of Iba1-positive cells. Because Iba1 is a gross maker for that the total number of microglial cells and is not specific to activated microglia, partial loss of PGRN may cause more subtle microglia changes that are not detected with a general marker with histology. For example, our observation of changes in amyloid plaque morphology in APdE9-Grn$^{+/-}$ mice could be due to haploinsufficient loss of PGRN affecting microglia phagocytosis despite not observing increases in Iba1 staining. In a previous study, microglial PGRN deficiency was induced using LysM-Cre in high APP expressing model (Minami et al., 2014). Interestingly, these mice were reported to have increased plaque deposition and isolated microglia exhibited impaired phagocytosis with an approximately 50% decline in PGRN mRNA. Therefore, in the context of this study it is possible that PGRN haploinsufficiency may be disrupting microglial function in APdE9-Grn$^{+/-}$ mice accounting for the changes in amyloid pathology. While PGRN-deficient microglia have been thoroughly studied regarding microglial phagocytosis, PGRN-haploinsufficient microglia have not (Pickford et al., 2011; Martens et al., 2012). Future studies should explore microglial function in greater detail. With regards to our study reducing only microglial specific PGRN will be

valuable in better understanding how PGRN haploinsufficiency is affecting amyloid pathology and synaptic plasticity deficits and if these effects are the result of specific populations of PGRN. Furthermore, phenotyping microglial by looking at levels of different inflammatory M1 and M2 markers across AD disease pathology will also build upon the current literature and better elucidate PGRN's role.

PGRN has long been implicated in increasing neuronal susceptibility leading to neurodegeneration, and evidence suggests that PGRN also plays an essential role in neuronal differentiation during neurodevelopment with modulating motor neuron development and the masculinization of the rodent brain (Suzuki et al., 2009; Chitramuthu et al., 2010). An important finding in this dissertation is that the heterozygous loss of PGRN resulted in fewer GAD67-positive interneurons in $Grn^{+/-}$ mice as early as twelve months of age. However, it is unclear if this loss is due to increased susceptibility in interneuron-specific populations during aging or during embryonic development since this study only looked at mice as young as twelve months of age. Furthermore, a recent study showed increased synaptic pruning of parvalbumin positive interneurons in $Grn^{-/-}$ mice due to microglia (Lui et al., 2016). Because we only looked at gross levels of interneurons and not at the level of synapses an important follow-on study for our work is to see if we see a similar effect in $Grn^{+/-}$. If interneuron synapses are not lost this may suggest that synaptic pruning of interneurons by microglia is a unique to $Grn^{-/-}$ and PGRN haploinsufficiency is affecting interneurons at a neuronal level. Therefore, future studies should investigate interneuron populations in PGRN-deficient mice during

embryonic stages to determine if interneurons' loss is due to developmental effects or because of aging as well as corroborate results from $Grn^{-/-}$ mice.

A limitation of the present study is that it only characterized GAD67-positive interneurons, a gross marker for GABAergic interneurons, but not for specific subtypes. Interneurons can be further subdivided by whether they co-express parvalbumin, somatostatin or the serotonin receptor 5HT3a which together account for nearly all neuronal GABAergic interneurons in the cortex (Rudy et al., 2011). Therefore, future studies should further characterize GABAergic interneuron subtypes in $Grn^{+/-}$ mice to determine if the heterozygous loss of PGRN results in a global loss of GABAergic interneurons or rather specific subpopulations.

Another important finding in this study is that PGRN haploinsufficiency dysregulates the Akt signaling pathway through increase inhibitory phosphorylation of PTEN and an increased inhibitory phosphorylation of GSK3β activity in P301S mice. However, it is unclear how exactly PGRN loss perturbs this signaling pathway and if this disruption is unique to PGRN loss in the context of tau pathology or is also seen in $Grn^{+/-}$ mice. To date, only one other publication has reported an increase in GSK3β phosphorylation after treatment with PGRN in cultured neurons (Gao et al., 2010). One critical gap in PGRN biology knowledge is what receptors it interacts with, and a better understanding of PGRN's relationship with these signaling pathways may be essential road marks. Therefore, future studies would be beneficial in further elucidating how PGRN

interacts with the Akt signaling pathway in the context of Alzheimer's disease and PGRN's overall role in the CNS.

Another interesting finding from this study is that heterozygous loss of PGRN decreased tau phosphorylation in the P301S transgenic mouse model, which contrasts with another report showing increased tau phosphorylation in the P301S transgenic mouse model. The discordance between these two results suggests that PGRN may interact with tau differently based on the mutation present. Different signaling pathways have been reported to be perturbed in the P301S and P301L transgenic mouse models, suggesting that PGRN may be interacting with different signaling pathways resulting in either the increase or decrease in tau phosphorylation. Therefore, more detailed studies, would help better understand how PGRN interacts with different tau mutations to better the role of PGRN in Alzheimer's disease and related tauopathies.

7. REFERENCES

Ahmed Z, Mackenzie IR, Hutton ML, Dickson DW (2007) Progranulin in frontotemporal lobar degeneration and neuroinflammation. Journal of neuroinflammation 4:7.

Ahmed Z, Sheng H, Xu YF, Lin WL, Innes AE, Gass J, Yu X, Wuertzer CA, Hou H, Chiba S, Yamanouchi K, Leissring M, Petrucelli L, Nishihara M, Hutton ML, McGowan E, Dickson DW, Lewis J (2010) Accelerated lipofuscinosis and ubiquitination in granulin knockout mice suggest a role for progranulin in successful aging. The American journal of pathology 177:311-324.

Akiyama H et al. (2000) Inflammation and Alzheimer's disease. Neurobiol Aging 21:383-421.

Allen B, Ingram E, Takao M, Smith MJ, Jakes R, Virdee K, Yoshida H, Holzer M, Craxton M, Emson PC, Atzori C, Migheli A, Crowther RA, Ghetti B, Spillantini MG, Goedert M (2002) Abundant tau filaments and nonapoptotic neurodegeneration in transgenic mice expressing human P301S tau protein. The Journal of neuroscience : the official journal of the Society for Neuroscience 22:9340-9351.

Almeida S, Zhang Z, Coppola G, Mao W, Futai K, Karydas A, Geschwind MD, Tartaglia MC, Gao F, Gianni D, Sena-Esteves M, Geschwind DH, Miller BL, Farese RV, Jr., Gao FB (2012) Induced pluripotent stem cell models of progranulin-deficient frontotemporal dementia uncover specific reversible neuronal defects. Cell reports 2:789-798.

Alquezar C, Esteras N, de la Encarnacion A, Alzualde A, Moreno F, Lopez de Munain A, Martin-Requero A (2014) PGRN haploinsufficiency increased Wnt5a signaling in peripheral cells from frontotemporal lobar degeneration-progranulin mutation carriers. Neurobiology of aging 35:886-898.

Altmann C, Vasic V, Hardt S, Heidler J, Haussler A, Wittig I, Schmidt MH, Tegeder I (2016) Progranulin promotes peripheral nerve regeneration and reinnervation: role of notch signaling. Molecular neurodegeneration 11:69.

Alzheimer A (1907) Über eine eigenartige Erkrankung der Hirnrinde. . Allg Zschr Psychiatr Psych gerichtl Med:146-148.

Alzheimer A (1911) Über eigenartige Krankheitsfälle des späteren Alters. Z Ges Neurol Psychiatr:356-385.

Anand R, Gill KD, Mahdi AA (2014) Therapeutics of Alzheimer's disease: Past, present and future. Neuropharmacology 76 Pt A:27-50.

Andrews-Zwilling Y, Bien-Ly N, Xu Q, Li G, Bernardo A, Yoon SY, Zwilling D, Yan TX, Chen L, Huang Y (2010) Apolipoprotein E4 causes age- and Tau-dependent impairment of GABAergic interneurons, leading to learning and

memory deficits in mice. The Journal of neuroscience : the official journal of the Society for Neuroscience 30:13707-13717.
Arrant AE, Filiano AJ, Warmus BA, Hall AM, Roberson ED (2016) Progranulin haploinsufficiency causes biphasic social dominance abnormalities in the tube test. Genes Brain Behav 15:588-603.
Arrant AE, Filiano AJ, Unger DE, Young AH, Roberson ED (2017) Restoring neuronal progranulin reverses deficits in a mouse model of frontotemporal dementia. Brain 140:1447-1465.
Atzori C, Ghetti B, Piva R, Srinivasan AN, Zolo P, Delisle MB, Mirra SS, Migheli A (2001) Activation of the JNK/p38 pathway occurs in diseases characterized by tau protein pathology and is related to tau phosphorylation but not to apoptosis. Journal of neuropathology and experimental neurology 60:1190-1197.
Baker M et al. (2006) Mutations in progranulin cause tau-negative frontotemporal dementia linked to chromosome 17. Nature 442:916-919.
Bancher C, Grundke-Iqbal I, Iqbal K, Fried VA, Smith HT, Wisniewski HM (1991) Abnormal phosphorylation of tau precedes ubiquitination in neurofibrillary pathology of Alzheimer disease. Brain Res 539:11-18.
Bancher C, Brunner C, Lassmann H, Budka H, Jellinger K, Wiche G, Seitelberger F, Grundke-Iqbal I, Iqbal K, Wisniewski HM (1989) Accumulation of abnormally phosphorylated tau precedes the formation of neurofibrillary tangles in Alzheimer's disease. Brain Res 477:90-99.
Basisty N, Schilling B, Rabinovitch PS (2018) Identifying ubiquitinated proteins and aggregates. Aging (Albany NY) 10:2549-2550.
Baumketner A, Krone MG, Shea JE (2008) Role of the familial Dutch mutation E22Q in the folding and aggregation of the 15-28 fragment of the Alzheimer amyloid-beta protein. Proc Natl Acad Sci U S A 105:6027-6032.
Bennecib M, Gong CX, Grundke-Iqbal I, Iqbal K (2001) Inhibition of PP-2A upregulates CaMKII in rat forebrain and induces hyperphosphorylation of tau at Ser 262/356. FEBS Lett 490:15-22.
Bergman A, Religa D, Karlstrom H, Laudon H, Winblad B, Lannfelt L, Lundkvist J, Naslund J (2003) APP intracellular domain formation and unaltered

signaling in the presence of familial Alzheimer's disease mutations. Exp Cell Res 287:1-9.
Bernardi L et al. (2012) Epidemiology and genetics of frontotemporal dementia: a door-to-door survey in southern Italy. Neurobiol Aging 33:2948.e2941-2948.e2910.
Bertram L, Lill CM, Tanzi RE (2010) The genetics of Alzheimer disease: back to the future. Neuron 68:270-281.
Bertram L et al. (2008) Genome-wide association analysis reveals putative Alzheimer's disease susceptibility loci in addition to APOE. Am J Hum Genet 83:623-632.
Birch AM, Katsouri L, Sastre M (2014) Modulation of inflammation in transgenic models of Alzheimer's disease. J Neuroinflammation 11:25.
Boche D, Perry VH, Nicoll JA (2013) Review: activation patterns of microglia and their identification in the human brain. Neuropathol Appl Neurobiol 39:3-18.
Borroni B, Alberici A, Grassi M, Turla M, Zanetti O, Bianchetti A, Dalla Volta G, Rozzini R, Gilberti N, Bellelli G, Padovani A (2010) Is frontotemporal lobar degeneration a rare disorder? Evidence from a preliminary study in Brescia county, Italy. J Alzheimers Dis 19:111-116.
Bozzali M, Battistoni V, Premi E, Alberici A, Giulietti G, Archetti S, Turla M, Gasparotti R, Cercignani M, Padovani A, Borroni B (2013) Structural brain signature of FTLD driven by Granulin mutation. Journal of Alzheimer's disease : JAD 33:483-494.
Braak H, Braak E (1994) Morphological criteria for the recognition of Alzheimer's disease and the distribution pattern of cortical changes related to this disorder. Neurobiol Aging 15:355-356; discussion 379-380.
Braak H, Braak E (1995) Staging of Alzheimer's disease-related neurofibrillary changes. Neurobiology of aging 16:271-278; discussion 278-284.
Brandt R, Lee G, Teplow DB, Shalloway D, Abdel-Ghany M (1994) Differential effect of phosphorylation and substrate modulation on tau's ability to promote microtubule growth and nucleation. J Biol Chem 269:11776-11782.
Brouwers N, Sleegers K, Engelborghs S, Maurer-Stroh S, Gijselinck I, van der Zee J, Pickut BA, Van den Broeck M, Mattheijssens M, Peeters K, Schymkowitz J, Rousseau F, Martin JJ, Cruts M, De Deyn PP, Van Broeckhoven C (2008) Genetic variability in progranulin contributes to risk for clinically diagnosed Alzheimer disease. Neurology 71:656-664.
Buccafusco JJ (2009) Methods of Behavior Analysis in Neuroscience. In.
Bugiani O, Murrell JR, Giaccone G, Hasegawa M, Ghigo G, Tabaton M, Morbin M, Primavera A, Carella F, Solaro C, Grisoli M, Savoiardo M, Spillantini MG, Tagliavini F, Goedert M, Ghetti B (1999) Frontotemporal dementia and

corticobasal degeneration in a family with a P301S mutation in tau. Journal of neuropathology and experimental neurology 58:667-677.
Burns A (2009) Alzheimer's disease: on the verges of treatment and prevention. Lancet Neurol 8:4-5.
Butler K, Martinez LA, Tejada-Simon MV (2013) Impaired cognitive function and reduced anxiety-related behavior in a promyelocytic leukemia (PML) tumor suppressor protein-deficient mouse. Genes Brain Behav 12:189-202.
Byrnes KR, Washington PM, Knoblach SM, Hoffman E, Faden AI (2011) Delayed inflammatory mRNA and protein expression after spinal cord injury. Journal of neuroinflammation 8:130.
Cai XD, Golde TE, Younkin SG (1993) Release of excess amyloid beta protein from a mutant amyloid beta protein precursor. Science 259:514-516.
Cairns NJ et al. (2007) TDP-43 in familial and sporadic frontotemporal lobar degeneration with ubiquitin inclusions. Am J Pathol 171:227-240.
Campbell IG, Guinan MJ, Horowitz JM (2002) Sleep deprivation impairs long-term potentiation in rat hippocampal slices. Journal of neurophysiology 88:1073-1076.
Chen-Plotkin AS, Xiao J, Geser F, Martinez-Lage M, Grossman M, Unger T, Wood EM, Van Deerlin VM, Trojanowski JQ, Lee VM (2010) Brain progranulin expression in GRN-associated frontotemporal lobar degeneration. Acta neuropathologica 119:111-122.
Chen-Plotkin AS, Unger TL, Gallagher MD, Bill E, Kwong LK, Volpicelli-Daley L, Busch JI, Akle S, Grossman M, Van Deerlin V, Trojanowski JQ, Lee VM (2012) TMEM106B, the risk gene for frontotemporal dementia, is regulated by the microRNA-132/212 cluster and affects progranulin pathways. The Journal of neuroscience : the official journal of the Society for Neuroscience 32:11213-11227.
Chen X, Chang J, Deng Q, Xu J, Nguyen TA, Martens LH, Cenik B, Taylor G, Hudson KF, Chung J, Yu K, Yu P, Herz J, Farese RV, Jr., Kukar T, Tansey MG (2013) Progranulin does not bind tumor necrosis factor (TNF) receptors and is not a direct regulator of TNF-dependent signaling or bioactivity in immune or neuronal cells. The Journal of neuroscience : the official journal of the Society for Neuroscience 33:9202-9213.
Chiba S, Suzuki M, Yamanouchi K, Nishihara M (2007) Involvement of granulin in estrogen-induced neurogenesis in the adult rat hippocampus. J Reprod Dev 53:297-307.
Chiba S, Matsuwaki T, Yamanouchi K, Nishihara M (2009) Alteration in anxiety with relation to the volume of the locus ceruleus in progranulin-deficient mice. J Reprod Dev 55:518-522.
Chitramuthu BP, Baranowski DC, Kay DG, Bateman A, Bennett HP (2010) Progranulin modulates zebrafish motoneuron development in vivo and

rescues truncation defects associated with knockdown of Survival motor neuron 1. Mol Neurodegener 5:41.
Cho JH, Johnson GV (2003) Glycogen synthase kinase 3beta phosphorylates tau at both primed and unprimed sites. Differential impact on microtubule binding. J Biol Chem 278:187-193.
Citron M, Oltersdorf T, Haass C, McConlogue L, Hung AY, Seubert P, Vigo-Pelfrey C, Lieberburg I, Selkoe DJ (1992) Mutation of the beta-amyloid precursor protein in familial Alzheimer's disease increases beta-protein production. Nature 360:672-674.
Citron M, Vigo-Pelfrey C, Teplow DB, Miller C, Schenk D, Johnston J, Winblad B, Venizelos N, Lannfelt L, Selkoe DJ (1994) Excessive production of amyloid beta-protein by peripheral cells of symptomatic and presymptomatic patients carrying the Swedish familial Alzheimer disease mutation. Proc Natl Acad Sci U S A 91:11993-11997.
Colton CA, Vitek MP, Wink DA, Xu Q, Cantillana V, Previti ML, Van Nostrand WE, Weinberg JB, Dawson H (2006) NO synthase 2 (NOS2) deletion promotes multiple pathologies in a mouse model of Alzheimer's disease. Proc Natl Acad Sci U S A 103:12867-12872.
Cortini F, Fenoglio C, Guidi I, Venturelli E, Pomati S, Marcone A, Scalabrini D, Villa C, Clerici F, Dalla Valle E, Mariani C, Cappa S, Bresolin N, Scarpini E, Galimberti D (2008) Novel exon 1 progranulin gene variant in Alzheimer's disease. Eur J Neurol 15:1111-1117.
Crehan H, Hardy J, Pocock J (2013) Blockage of CR1 prevents activation of rodent microglia. Neurobiol Dis 54:139-149.
Crescenzi R, DeBrosse C, Nanga RP, Reddy S, Haris M, Hariharan H, Iba M, Lee VM, Detre JA, Borthakur A, Reddy R (2014) In vivo measurement of glutamate loss is associated with synapse loss in a mouse model of tauopathy. NeuroImage 101:185-192.
Crook R, Verkkoniemi A, Perez-Tur J, Mehta N, Baker M, Houlden H, Farrer M, Hutton M, Lincoln S, Hardy J, Gwinn K, Somer M, Paetau A, Kalimo H, Ylikoski R, Poyhonen M, Kucera S, Haltia M (1998) A variant of Alzheimer's disease with spastic paraparesis and unusual plaques due to deletion of exon 9 of presenilin 1. Nat Med 4:452-455.
Cruchaga C, Graff C, Chiang HH, Wang J, Hinrichs AL, Spiegel N, Bertelsen S, Mayo K, Norton JB, Morris JC, Goate A (2011) Association of TMEM106B

gene polymorphism with age at onset in granulin mutation carriers and plasma granulin protein levels. Archives of neurology 68:581-586.
Cruts M, Kumar-Singh S, Van Broeckhoven C (2006a) Progranulin mutations in ubiquitin-positive frontotemporal dementia linked to chromosome 17q21. Curr Alzheimer Res 3:485-491.
Cruts M et al. (2006b) Null mutations in progranulin cause ubiquitin-positive frontotemporal dementia linked to chromosome 17q21. Nature 442:920-924.
Cruz JC, Tseng HC, Goldman JA, Shih H, Tsai LH (2003) Aberrant Cdk5 activation by p25 triggers pathological events leading to neurodegeneration and neurofibrillary tangles. Neuron 40:471-483.
Cummings JL, Morstorf T, Zhong K (2014) Alzheimer's disease drug-development pipeline: few candidates, frequent failures. Alzheimers Res Ther 6:37.
Curtis AF, Masellis M, Hsiung GR, Moineddin R, Zhang K, Au B, Millett G, Mackenzie I, Rogaeva E, Tierney MC (2017) Sex differences in the prevalence of genetic mutations in FTD and ALS: A meta-analysis. Neurology 89:1633-1642.
D'Souza I, Poorkaj P, Hong M, Nochlin D, Lee VM, Bird TD, Schellenberg GD (1999) Missense and silent tau gene mutations cause frontotemporal dementia with parkinsonism-chromosome 17 type, by affecting multiple alternative RNA splicing regulatory elements. Proc Natl Acad Sci U S A 96:5598-5603.
Daniel R, Daniels E, He Z, Bateman A (2003) Progranulin (acrogranin/PC cell-derived growth factor/granulin-epithelin precursor) is expressed in the placenta, epidermis, microvasculature, and brain during murine development. Dev Dyn 227:593-599.
Daniel R, He Z, Carmichael KP, Halper J, Bateman A (2000) Cellular localization of gene expression for progranulin. J Histochem Cytochem 48:999-1009.
De Muynck L, Herdewyn S, Beel S, Scheveneels W, Van Den Bosch L, Robberecht W, Van Damme P (2013) The neurotrophic properties of progranulin depend on the granulin E domain but do not require sortilin binding. Neurobiology of aging 34:2541-2547.
De Strooper B (2010) Proteases and proteolysis in Alzheimer disease: a multifactorial view on the disease process. Physiol Rev 90:465-494.
Delobel P, Flament S, Hamdane M, Jakes R, Rousseau A, Delacourte A, Vilain JP, Goedert M, Buee L (2002) Functional characterization of FTDP-17 tau

gene mutations through their effects on Xenopus oocyte maturation. J Biol Chem 277:9199-9205.
DiCarlo G, Wilcock D, Henderson D, Gordon M, Morgan D (2001) Intrahippocampal LPS injections reduce Abeta load in APP+PS1 transgenic mice. Neurobiology of aging 22:1007-1012.
Dickson DW, Baker M, Rademakers R (2010) Common variant in GRN is a genetic risk factor for hippocampal sclerosis in the elderly. Neuro-degenerative diseases 7:170-174.
Drewes G, Ebneth A, Preuss U, Mandelkow EM, Mandelkow E (1997) MARK, a novel family of protein kinases that phosphorylate microtubule-associated proteins and trigger microtubule disruption. Cell 89:297-308.
Edwards JP, Zhang X, Frauwirth KA, Mosser DM (2006) Biochemical and functional characterization of three activated macrophage populations. J Leukoc Biol 80:1298-1307.
Eriksen JL (2010) The enigmatic roles of microglial versus neuronal progranulin in neurological disease. Acta neuropathologica 119:107-109.
Fenoglio C, Galimberti D, Cortini F, Kauwe JS, Cruchaga C, Venturelli E, Villa C, Serpente M, Scalabrini D, Mayo K, Piccio LM, Clerici F, Albani D, Mariani C, Forloni G, Bresolin N, Goate AM, Scarpini E (2009) Rs5848 variant influences GRN mRNA levels in brain and peripheral mononuclear cells in patients with Alzheimer's disease. Journal of Alzheimer's disease : JAD 18:603-612.
Fenoglio C et al. (2010) Progranulin gene variability increases the risk for primary progressive multiple sclerosis in males. Genes and immunity 11:497-503.
Ferrer I, Blanco R, Carmona M, Ribera R, Goutan E, Puig B, Rey MJ, Cardozo A, Vinals F, Ribalta T (2001) Phosphorylated map kinase (ERK1, ERK2) expression is associated with early tau deposition in neurones and glial cells, but not with increased nuclear DNA vulnerability and cell death, in Alzheimer disease, Pick's disease, progressive supranuclear palsy and corticobasal degeneration. Brain Pathol 11:144-158.
Filiano AJ, Martens LH, Young AH, Warmus BA, Zhou P, Diaz-Ramirez G, Jiao J, Zhang Z, Huang EJ, Gao FB, Farese RV, Jr., Roberson ED (2013) Dissociation of frontotemporal dementia-related deficits and

neuroinflammation in progranulin haploinsufficient mice. J Neurosci 33:5352-5361.
Finch N et al. (2011) TMEM106B regulates progranulin levels and the penetrance of FTLD in GRN mutation carriers. Neurology 76:467-474.
Frank-Cannon TC, Alto LT, McAlpine FE, Tansey MG (2009) Does neuroinflammation fan the flame in neurodegenerative diseases? Molecular neurodegeneration 4:47.
Fukumoto H, Rosene DL, Moss MB, Raju S, Hyman BT, Irizarry MC (2004) Beta-secretase activity increases with aging in human, monkey, and mouse brain. Am J Pathol 164:719-725.
Galimberti D, Scarpini E (2012) Clinical phenotypes and genetic biomarkers of FTLD. J Neural Transm (Vienna) 119:851-860.
Galimberti D et al. (2010) GRN variability contributes to sporadic frontotemporal lobar degeneration. Journal of Alzheimer's disease : JAD 19:171-177.
Galimberti D et al. (2012) Progranulin gene variability and plasma levels in bipolar disorder and schizophrenia. PloS one 7:e32164.
Ganz T, Gabayan V, Liao HI, Liu L, Oren A, Graf T, Cole AM (2003) Increased inflammation in lysozyme M-deficient mice in response to Micrococcus luteus and its peptidoglycan. Blood 101:2388-2392.
Gao X, Joselin AP, Wang L, Kar A, Ray P, Bateman A, Goate AM, Wu JY (2010) Progranulin promotes neurite outgrowth and neuronal differentiation by regulating GSK-3beta. Protein Cell 1:552-562.
Garcia-Alloza M, Robbins EM, Zhang-Nunes SX, Purcell SM, Betensky RA, Raju S, Prada C, Greenberg SM, Bacskai BJ, Frosch MP (2006) Characterization of amyloid deposition in the APPswe/PS1dE9 mouse model of Alzheimer disease. Neurobiology of disease 24:516-524.
Gass J, Lee WC, Cook C, Finch N, Stetler C, Jansen-West K, Lewis J, Link CD, Rademakers R, Nykjaer A, Petrucelli L (2012) Progranulin regulates neuronal outgrowth independent of sortilin. Molecular neurodegeneration 7:33.
Gass J et al. (2006) Mutations in progranulin are a major cause of ubiquitin-positive frontotemporal lobar degeneration. Hum Mol Genet 15:2988-3001.
Gerson JE, Kayed R (2013) Formation and propagation of tau oligomeric seeds. Frontiers in neurology 4:93.
Ghoshal N, Dearborn JT, Wozniak DF, Cairns NJ (2012) Core features of frontotemporal dementia recapitulated in progranulin knockout mice. Neurobiol Dis 45:395-408.
Gliebus G, Rosso A, Lippa CF (2009) Progranulin and beta-amyloid distribution: a case report of the brain from preclinical PS-1 mutation carrier. American journal of Alzheimer's disease and other dementias 24:456-460.
Goate A, Chartier-Harlin MC, Mullan M, Brown J, Crawford F, Fidani L, Giuffra L, Haynes A, Irving N, James L, et al. (1991) Segregation of a missense

mutation in the amyloid precursor protein gene with familial Alzheimer's disease. Nature 349:704-706.
Goedert M, Jakes R (1990) Expression of separate isoforms of human tau protein: correlation with the tau pattern in brain and effects on tubulin polymerization. EMBO J 9:4225-4230.
Goedert M, Jakes R (2005) Mutations causing neurodegenerative tauopathies. Biochimica et biophysica acta 1739:240-250.
Goedert M, Spillantini MG, Jakes R, Rutherford D, Crowther RA (1989) Multiple isoforms of human microtubule-associated protein tau: sequences and localization in neurofibrillary tangles of Alzheimer's disease. Neuron 3:519-526.
Goedert M, Spillantini MG, Crowther RA, Chen SG, Parchi P, Tabaton M, Lanska DJ, Markesbery WR, Wilhelmsen KC, Dickson DW, Petersen RB, Gambetti P (1999) Tau gene mutation in familial progressive subcortical gliosis. Nat Med 5:454-457.
Goldbaum O, Oppermann M, Handschuh M, Dabir D, Zhang B, Forman MS, Trojanowski JQ, Lee VM, Richter-Landsberg C (2003) Proteasome inhibition stabilizes tau inclusions in oligodendroglial cells that occur after treatment with okadaic acid. The Journal of neuroscience : the official journal of the Society for Neuroscience 23:8872-8880.
Gomez-Isla T, Price JL, McKeel DW, Jr., Morris JC, Growdon JH, Hyman BT (1996) Profound loss of layer II entorhinal cortex neurons occurs in very mild Alzheimer's disease. J Neurosci 16:4491-4500.
Goodman RA, Lochner KA, Thambisetty M, Wingo TS, Posner SF, Ling SM (2017) Prevalence of dementia subtypes in United States Medicare fee-for-service beneficiaries, 2011-2013. Alzheimers Dement 13:28-37.
Gotz J, Chen F, Barmettler R, Nitsch RM (2001) Tau filament formation in transgenic mice expressing P301L tau. The Journal of biological chemistry 276:529-534.
Gotzl JK, Mori K, Damme M, Fellerer K, Tahirovic S, Kleinberger G, Janssens J, van der Zee J, Lang CM, Kremmer E, Martin JJ, Engelborghs S, Kretzschmar HA, Arzberger T, Van Broeckhoven C, Haass C, Capell A (2014) Common pathobiochemical hallmarks of progranulin-associated

frontotemporal lobar degeneration and neuronal ceroid lipofuscinosis. Acta neuropathologica 127:845-860.
Griciuc A, Serrano-Pozo A, Parrado AR, Lesinski AN, Asselin CN, Mullin K, Hooli B, Choi SH, Hyman BT, Tanzi RE (2013) Alzheimer's disease risk gene CD33 inhibits microglial uptake of amyloid beta. Neuron 78:631-643.
Grundke-Iqbal I, Iqbal K, Tung YC, Quinlan M, Wisniewski HM, Binder LI (1986) Abnormal phosphorylation of the microtubule-associated protein tau (tau) in Alzheimer cytoskeletal pathology. Proc Natl Acad Sci U S A 83:4913-4917.
Guerreiro R et al. (2013) TREM2 variants in Alzheimer's disease. N Engl J Med 368:117-127.
Guo A, Tapia L, Bamji SX, Cynader MS, Jia W (2010) Progranulin deficiency leads to enhanced cell vulnerability and TDP-43 translocation in primary neuronal cultures. Brain research 1366:1-8.
Haass C, Koo EH, Mellon A, Hung AY, Selkoe DJ (1992) Targeting of cell-surface beta-amyloid precursor protein to lysosomes: alternative processing into amyloid-bearing fragments. Nature 357:500-503.
Hanger DP, Betts JC, Loviny TL, Blackstock WP, Anderton BH (1998) New phosphorylation sites identified in hyperphosphorylated tau (paired helical filament-tau) from Alzheimer's disease brain using nanoelectrospray mass spectrometry. J Neurochem 71:2465-2476.
Hasegawa M (2006) Biochemistry and molecular biology of tauopathies. Neuropathology : official journal of the Japanese Society of Neuropathology 26:484-490.
Hasegawa M, Smith MJ, Goedert M (1998) Tau proteins with FTDP-17 mutations have a reduced ability to promote microtubule assembly. FEBS Lett 437:207-210.
Hecimovic S, Wang J, Dolios G, Martinez M, Wang R, Goate AM (2004) Mutations in APP have independent effects on Abeta and CTFgamma generation. Neurobiol Dis 17:205-218.
Helmfors L, Boman A, Civitelli L, Nath S, Sandin L, Janefjord C, McCann H, Zetterberg H, Blennow K, Halliday G, Brorsson AC, Kagedal K (2015) Protective properties of lysozyme on beta-amyloid pathology: implications for Alzheimer disease. Neurobiology of disease 83:122-133.
Herber DL, Roth LM, Wilson D, Wilson N, Mason JE, Morgan D, Gordon MN (2004) Time-dependent reduction in Abeta levels after intracranial LPS administration in APP transgenic mice. Exp Neurol 190:245-253.
Herber DL, Mercer M, Roth LM, Symmonds K, Maloney J, Wilson N, Freeman MJ, Morgan D, Gordon MN (2007) Microglial activation is required for Abeta

clearance after intracranial injection of lipopolysaccharide in APP transgenic mice. J Neuroimmune Pharmacol 2:222-231.
Himmler A, Drechsel D, Kirschner MW, Martin DW, Jr. (1989) Tau consists of a set of proteins with repeated C-terminal microtubule-binding domains and variable N-terminal domains. Mol Cell Biol 9:1381-1388.
Ho L, Xiang Z, Mukherjee P, Zhang W, De Jesus N, Mirjany M, Yemul S, Pasinetti GM (2001) Gene expression profiling of the tau mutant (P301L) transgenic mouse brain. Neuroscience letters 310:1-4.
Hoefer M, Allison SC, Schauer GF, Neuhaus JM, Hall J, Dang JN, Weiner MW, Miller BL, Rosen HJ (2008) Fear conditioning in frontotemporal lobar degeneration and Alzheimer's disease. Brain : a journal of neurology 131:1646-1657.
Hollingworth P et al. (2011a) Common variants at ABCA7, MS4A6A/MS4A4E, EPHA1, CD33 and CD2AP are associated with Alzheimer's disease. Nature genetics 43:429-435.
Hollingworth P et al. (2011b) Common variants at ABCA7, MS4A6A/MS4A4E, EPHA1, CD33 and CD2AP are associated with Alzheimer's disease. Nat Genet 43:429-435.
Hong M, Chen DC, Klein PS, Lee VM (1997) Lithium reduces tau phosphorylation by inhibition of glycogen synthase kinase-3. J Biol Chem 272:25326-25332.
Hong M, Zhukareva V, Vogelsberg-Ragaglia V, Wszolek Z, Reed L, Miller BI, Geschwind DH, Bird TD, McKeel D, Goate A, Morris JC, Wilhelmsen KC, Schellenberg GD, Trojanowski JQ, Lee VM (1998) Mutation-specific functional impairments in distinct tau isoforms of hereditary FTDP-17. Science 282:1914-1917.
Hosokawa M, Arai T, Masuda-Suzukake M, Kondo H, Matsuwaki T, Nishihara M, Hasegawa M, Akiyama H (2015) Progranulin reduction is associated with increased tau phosphorylation in P301L tau transgenic mice. J Neuropathol Exp Neurol 74:158-165.
Hsiung GY, Fok A, Feldman HH, Rademakers R, Mackenzie IR (2011) rs5848 polymorphism and serum progranulin level. Journal of the neurological sciences 300:28-32.
Hu F, Padukkavidana T, Vaegter CB, Brady OA, Zheng Y, Mackenzie IR, Feldman HH, Nykjaer A, Strittmatter SM (2010) Sortilin-mediated endocytosis determines levels of the frontotemporal dementia protein, progranulin. Neuron 68:654-667.
Hutton M et al. (1998) Association of missense and 5'-splice-site mutations in tau with the inherited dementia FTDP-17. Nature 393:702-705.
Iba M, Guo JL, McBride JD, Zhang B, Trojanowski JQ, Lee VM (2013) Synthetic tau fibrils mediate transmission of neurofibrillary tangles in a transgenic mouse model of Alzheimer's-like tauopathy. The Journal of neuroscience : the official journal of the Society for Neuroscience 33:1024-1037.
Irwin D, Lippa CF, Rosso A (2009) Progranulin (PGRN) expression in ALS: an immunohistochemical study. Journal of the neurological sciences 276:9-13.
Jaeger LB, Dohgu S, Sultana R, Lynch JL, Owen JB, Erickson MA, Shah GN, Price TO, Fleegal-Demotta MA, Butterfield DA, Banks WA (2009)

Lipopolysaccharide alters the blood-brain barrier transport of amyloid beta protein: a mechanism for inflammation in the progression of Alzheimer's disease. Brain Behav Immun 23:507-517.
Jankowsky JL, Fadale DJ, Anderson J, Xu GM, Gonzales V, Jenkins NA, Copeland NG, Lee MK, Younkin LH, Wagner SL, Younkin SG, Borchelt DR (2004) Mutant presenilins specifically elevate the levels of the 42 residue beta-amyloid peptide in vivo: evidence for augmentation of a 42-specific gamma secretase. Human molecular genetics 13:159-170.
Janus C, Flores AY, Xu G, Borchelt DR (2015) Behavioral abnormalities in APPSwe/PS1dE9 mouse model of AD-like pathology: comparative analysis across multiple behavioral domains. Neurobiology of aging 36:2519-2532.
Jiang T, Tan L, Zhu XC, Zhang QQ, Cao L, Tan MS, Gu LZ, Wang HF, Ding ZZ, Zhang YD, Yu JT (2014) Upregulation of TREM2 ameliorates neuropathology and rescues spatial cognitive impairment in a transgenic mouse model of Alzheimer's disease. Neuropsychopharmacology 39:2949-2962.
Johnson GV, Stoothoff WH (2004) Tau phosphorylation in neuronal cell function and dysfunction. Journal of cell science 117:5721-5729.
Johnson JK, Diehl J, Mendez MF, Neuhaus J, Shapira JS, Forman M, Chute DJ, Roberson ED, Pace-Savitsky C, Neumann M, Chow TW, Rosen HJ, Forstl H, Kurz A, Miller BL (2005) Frontotemporal lobar degeneration: demographic characteristics of 353 patients. Arch Neurol 62:925-930.
Jonsson T et al. (2013) Variant of TREM2 associated with the risk of Alzheimer's disease. N Engl J Med 368:107-116.
Jonsson T et al. (2012) A mutation in APP protects against Alzheimer's disease and age-related cognitive decline. Nature 488:96-99.
Jope RS, Johnson GV (2004) The glamour and gloom of glycogen synthase kinase-3. Trends in biochemical sciences 29:95-102.
Julien C, Bretteville A, Planel E (2012) Biochemical isolation of insoluble tau in transgenic mouse models of tauopathies. Methods Mol Biol 849:473-491.
Kamalainen A, Viswanathan J, Natunen T, Helisalmi S, Kauppinen T, Pikkarainen M, Pursiheimo JP, Alafuzoff I, Kivipelto M, Haapasalo A, Soininen H, Herukka SK, Hiltunen M (2013) GRN variant rs5848 reduces plasma and brain levels of granulin in Alzheimer's disease patients. Journal of Alzheimer's disease : JAD 33:23-27.
Kao AW, McKay A, Singh PP, Brunet A, Huang EJ (2017) Progranulin, lysosomal regulation and neurodegenerative disease. Nature reviews Neuroscience 18:325-333.
Kao AW, Eisenhut RJ, Martens LH, Nakamura A, Huang A, Bagley JA, Zhou P, de Luis A, Neukomm LJ, Cabello J, Farese RV, Jr., Kenyon C (2011) A neurodegenerative disease mutation that accelerates the clearance of

apoptotic cells. Proceedings of the National Academy of Sciences of the United States of America 108:4441-4446.
Karakaya T, Fusser F, Prvulovic D, Hampel H (2012) Treatment options for tauopathies. Curr Treat Options Neurol 14:126-136.
Kayasuga Y, Chiba S, Suzuki M, Kikusui T, Matsuwaki T, Yamanouchi K, Kotaki H, Horai R, Iwakura Y, Nishihara M (2007) Alteration of behavioural phenotype in mice by targeted disruption of the progranulin gene. Behav Brain Res 185:110-118.
Kelley BJ, Haidar W, Boeve BF, Baker M, Shiung M, Knopman DS, Rademakers R, Hutton M, Adamson J, Kuntz KM, Dickson DW, Parisi JE, Smith GE, Petersen RC (2010) Alzheimer disease-like phenotype associated with the c.154delA mutation in progranulin. Arch Neurol 67:171-177.
Kero M, Paetau A, Polvikoski T, Tanskanen M, Sulkava R, Jansson L, Myllykangas L, Tienari PJ (2013) Amyloid precursor protein (APP) A673T mutation in the elderly Finnish population. Neurobiol Aging 34:1518 e1511-1513.
Kim M, Huang T, Abel T, Blackwell KT (2010) Temporal sensitivity of protein kinase a activation in late-phase long term potentiation. PLoS Comput Biol 6:e1000691.
Kimura T, Ishiguro K, Hisanaga S (2014) Physiological and pathological phosphorylation of tau by Cdk5. Front Mol Neurosci 7:65.
Kipps CM, Nestor PJ, Acosta-Cabronero J, Arnold R, Hodges JR (2009) Understanding social dysfunction in the behavioural variant of frontotemporal dementia: the role of emotion and sarcasm processing. Brain : a journal of neurology 132:592-603.
Kitaguchi N, Takahashi Y, Tokushima Y, Shiojiri S, Ito H (1988) Novel precursor of Alzheimer's disease amyloid protein shows protease inhibitory activity. Nature 331:530-532.
Kitazawa M, Oddo S, Yamasaki TR, Green KN, LaFerla FM (2005) Lipopolysaccharide-induced inflammation exacerbates tau pathology by a cyclin-dependent kinase 5-mediated pathway in a transgenic model of Alzheimer's disease. The Journal of neuroscience : the official journal of the Society for Neuroscience 25:8843-8853.
Kocerha J, Kouri N, Baker M, Finch N, DeJesus-Hernandez M, Gonzalez J, Chidamparam K, Josephs KA, Boeve BF, Graff-Radford NR, Crook J, Dickson DW, Rademakers R (2011) Altered microRNA expression in frontotemporal lobar degeneration with TDP-43 pathology caused by progranulin mutations. BMC genomics 12:527.
Koga S, Kojima A, Ishikawa C, Kuwabara S, Arai K, Yoshiyama Y (2014) Effects of diet-induced obesity and voluntary exercise in a tauopathy mouse model: implications of persistent hyperleptinemia and enhanced astrocytic leptin receptor expression. Neurobiology of disease 71:180-192.
Kukar T, Murphy MP, Eriksen JL, Sagi SA, Weggen S, Smith TE, Ladd T, Khan MA, Kache R, Beard J, Dodson M, Merit S, Ozols VV, Anastasiadis PZ, Das P, Fauq A, Koo EH, Golde TE (2005) Diverse compounds mimic Alzheimer

disease-causing mutations by augmenting Abeta42 production. Nature medicine 11:545-550.
Kummer MP, Hermes M, Delekarte A, Hammerschmidt T, Kumar S, Terwel D, Walter J, Pape HC, Konig S, Roeber S, Jessen F, Klockgether T, Korte M, Heneka MT (2011) Nitration of tyrosine 10 critically enhances amyloid beta aggregation and plaque formation. Neuron 71:833-844.
Kuwabara Y, Ishizeki M, Watamura N, Toba J, Yoshii A, Inoue T, Ohshima T (2014) Impairments of long-term depression induction and motor coordination precede Abeta accumulation in the cerebellum of APPswe/PS1dE9 double transgenic mice. J Neurochem 130:432-443.
Laird AS, Van Hoecke A, De Muynck L, Timmers M, Van den Bosch L, Van Damme P, Robberecht W (2010) Progranulin is neurotrophic in vivo and protects against a mutant TDP-43 induced axonopathy. PloS one 5:e13368.
Lalonde R, Kim HD, Maxwell JA, Fukuchi K (2005) Exploratory activity and spatial learning in 12-month-old APP(695)SWE/co+PS1/DeltaE9 mice with amyloid plaques. Neuroscience letters 390:87-92.
Lambert JC et al. (2009) Genome-wide association study identifies variants at CLU and CR1 associated with Alzheimer's disease. Nat Genet 41:1094-1099.
Lambert JC et al. (2013) Meta-analysis of 74,046 individuals identifies 11 new susceptibility loci for Alzheimer's disease. Nat Genet 45:1452-1458.
Lang CM, Fellerer K, Schwenk BM, Kuhn PH, Kremmer E, Edbauer D, Capell A, Haass C (2012) Membrane orientation and subcellular localization of transmembrane protein 106B (TMEM106B), a major risk factor for frontotemporal lobar degeneration. The Journal of biological chemistry 287:19355-19365.
Lasagna-Reeves CA, Castillo-Carranza DL, Sengupta U, Guerrero-Munoz MJ, Kiritoshi T, Neugebauer V, Jackson GR, Kayed R (2012) Alzheimer brain-derived tau oligomers propagate pathology from endogenous tau. Scientific reports 2:700.
Lee DC, Rizer J, Selenica ML, Reid P, Kraft C, Johnson A, Blair L, Gordon MN, Dickey CA, Morgan D (2010) LPS- induced inflammation exacerbates phospho-tau pathology in rTg4510 mice. Journal of neuroinflammation 7:56.
Lee MJ, Chen TF, Cheng TW, Chiu MJ (2011) rs5848 variant of progranulin gene is a risk of Alzheimer's disease in the Taiwanese population. Neurodegener Dis 8:216-220.
Lee VM, Balin BJ, Otvos L, Jr., Trojanowski JQ (1991) A68: a major subunit of paired helical filaments and derivatized forms of normal Tau. Science 251:675-678.
Levenga J, Krishnamurthy P, Rajamohamedsait H, Wong H, Franke TF, Cain P, Sigurdsson EM, Hoeffer CA (2013) Tau pathology induces loss of GABAergic interneurons leading to altered synaptic plasticity and behavioral impairments. Acta neuropathologica communications 1:34.
Leverenz JB, Yu CE, Montine TJ, Steinbart E, Bekris LM, Zabetian C, Kwong LK, Lee VM, Schellenberg GD, Bird TD (2007) A novel progranulin mutation

associated with variable clinical presentation and tau, TDP43 and alpha-synuclein pathology. Brain : a journal of neurology 130:1360-1374.
Levy E, Carman MD, Fernandez-Madrid IJ, Power MD, Lieberburg I, van Duinen SG, Bots GT, Luyendijk W, Frangione B (1990) Mutation of the Alzheimer's disease amyloid gene in hereditary cerebral hemorrhage, Dutch type. Science 248:1124-1126.
Lew J, Huang QQ, Qi Z, Winkfein RJ, Aebersold R, Hunt T, Wang JH (1994) A brain-specific activator of cyclin-dependent kinase 5. Nature 371:423-426.
Li G, Bien-Ly N, Andrews-Zwilling Y, Xu Q, Bernardo A, Ring K, Halabisky B, Deng C, Mahley RW, Huang Y (2009) GABAergic interneuron dysfunction impairs hippocampal neurogenesis in adult apolipoprotein E4 knockin mice. Cell stem cell 5:634-645.
Li XL, Hu N, Tan MS, Yu JT, Tan L (2014) Behavioral and psychological symptoms in Alzheimer's disease. Biomed Res Int 2014:927804.
Lindzey G, Winston H, Manosevitz M (1961) Social dominance in inbred mouse strains. Nature 191:474-476.
Litersky JM, Johnson GV, Jakes R, Goedert M, Lee M, Seubert P (1996) Tau protein is phosphorylated by cyclic AMP-dependent protein kinase and calcium/calmodulin-dependent protein kinase II within its microtubule-binding domains at Ser-262 and Ser-356. Biochem J 316 (Pt 2):655-660.
Liu F, Zaidi T, Iqbal K, Grundke-Iqbal I, Merkle RK, Gong CX (2002) Role of glycosylation in hyperphosphorylation of tau in Alzheimer's disease. FEBS Lett 512:101-106.
Lomoio S, Lopez-Gonzalez I, Aso E, Carmona M, Torrejon-Escribano B, Scherini E, Ferrer I (2012) Cerebellar amyloid-beta plaques: disturbed cortical circuitry in AbetaPP/PS1 transgenic mice as a model of familial Alzheimer's disease. Journal of Alzheimer's disease : JAD 31:285-300.
Loreth D, Ozmen L, Revel FG, Knoflach F, Wetzel P, Frotscher M, Metzger F, Kretz O (2012) Selective degeneration of septal and hippocampal GABAergic neurons in a mouse model of amyloidosis and tauopathy. Neurobiology of disease 47:1-12.
Lossos A, Reches A, Gal A, Newman JP, Soffer D, Gomori JM, Boher M, Ekstein D, Biran I, Meiner Z, Abramsky O, Rosenmann H (2003) Frontotemporal dementia and parkinsonism with the P301S tau gene mutation in a Jewish family. Journal of neurology 250:733-740.
Lovestone S, Hartley CL, Pearce J, Anderton BH (1996) Phosphorylation of tau by glycogen synthase kinase-3 beta in intact mammalian cells: the effects on the organization and stability of microtubules. Neuroscience 73:1145-1157.
Lucas JJ, Hernandez F, Gomez-Ramos P, Moran MA, Hen R, Avila J (2001) Decreased nuclear beta-catenin, tau hyperphosphorylation and

neurodegeneration in GSK-3beta conditional transgenic mice. EMBO J 20:27-39.
Lui H et al. (2016) Progranulin Deficiency Promotes Circuit-Specific Synaptic Pruning by Microglia via Complement Activation. Cell 165:921-935.
Lyketsos CG, Carrillo MC, Ryan JM, Khachaturian AS, Trzepacz P, Amatniek J, Cedarbaum J, Brashear R, Miller DS (2011) Neuropsychiatric symptoms in Alzheimer's disease. Alzheimers Dement 7:532-539.
Mackenzie IR, Rademakers R (2007) The molecular genetics and neuropathology of frontotemporal lobar degeneration: recent developments. Neurogenetics 8:237-248.
Malaspina A, Kaushik N, de Belleroche J (2001) Differential expression of 14 genes in amyotrophic lateral sclerosis spinal cord detected using gridded cDNA arrays. Journal of neurochemistry 77:132-145.
Mantovani A, Sica A, Sozzani S, Allavena P, Vecchi A, Locati M (2004) The chemokine system in diverse forms of macrophage activation and polarization. Trends Immunol 25:677-686.
Maphis N, Xu G, Kokiko-Cochran ON, Jiang S, Cardona A, Ransohoff RM, Lamb BT, Bhaskar K (2015) Reactive microglia drive tau pathology and contribute to the spreading of pathological tau in the brain. Brain : a journal of neurology 138:1738-1755.
Martens LH, Zhang J, Barmada SJ, Zhou P, Kamiya S, Sun B, Min SW, Gan L, Finkbeiner S, Huang EJ, Farese RV, Jr. (2012) Progranulin deficiency promotes neuroinflammation and neuron loss following toxin-induced injury. J Clin Invest 122:3955-3959.
Maruyama M et al. (2013) Imaging of tau pathology in a tauopathy mouse model and in Alzheimer patients compared to normal controls. Neuron 79:1094-1108.
Matousek SB, Ghosh S, Shaftel SS, Kyrkanides S, Olschowka JA, O'Banion MK (2012) Chronic IL-1beta-mediated neuroinflammation mitigates amyloid pathology in a mouse model of Alzheimer's disease without inducing overt neurodegeneration. J Neuroimmune Pharmacol 7:156-164.
Matsuwaki T, Asakura R, Suzuki M, Yamanouchi K, Nishihara M (2011) Age-dependent changes in progranulin expression in the mouse brain. The Journal of reproduction and development 57:113-119.
McDade E, Boeve BF, Burrus TM, Boot BP, Kantarci K, Fields J, Lowe VJ, Peller P, Knopman D, Baker M, Finch N, Rademakers R, Petersen R (2012) Similar clinical and neuroimaging features in monozygotic twin pair with mutation in progranulin. Neurology 78:1245-1249.
McGeer PL, Akiyama H, Itagaki S, McGeer EG (1989) Activation of the classical complement pathway in brain tissue of Alzheimer patients. Neurosci Lett 107:341-346.
McGeer PL, McGeer E, Rogers J, Sibley J (1990) Anti-inflammatory drugs and Alzheimer disease. Lancet 335:1037.
McKhann G, Drachman D, Folstein M, Katzman R, Price D, Stadlan EM (1984) Clinical diagnosis of Alzheimer's disease: report of the NINCDS-ADRDA

Work Group under the auspices of Department of Health and Human Services Task Force on Alzheimer's Disease. Neurology 34:939-944.
McKhann GM, Albert MS, Grossman M, Miller B, Dickson D, Trojanowski JQ (2001) Clinical and pathological diagnosis of frontotemporal dementia: report of the Work Group on Frontotemporal Dementia and Pick's Disease. Archives of neurology 58:1803-1809.
Migheli A, Cavalla P, Marino S, Schiffer D (1994) A study of apoptosis in normal and pathologic nervous tissue after in situ end-labeling of DNA strand breaks. Journal of neuropathology and experimental neurology 53:606-616.
Minami SS, Min SW, Krabbe G, Wang C, Zhou Y, Asgarov R, Li Y, Martens LH, Elia LP, Ward ME, Mucke L, Farese RV, Jr., Gan L (2014) Progranulin protects against amyloid beta deposition and toxicity in Alzheimer's disease mouse models. Nat Med 20:1157-1164.
Miravalle L, Tokuda T, Chiarle R, Giaccone G, Bugiani O, Tagliavini F, Frangione B, Ghiso J (2000) Substitutions at codon 22 of Alzheimer's abeta peptide induce diverse conformational changes and apoptotic effects in human cerebral endothelial cells. J Biol Chem 275:27110-27116.
Moisse K, Volkening K, Leystra-Lantz C, Welch I, Hill T, Strong MJ (2009) Divergent patterns of cytosolic TDP-43 and neuronal progranulin expression following axotomy: implications for TDP-43 in the physiological response to neuronal injury. Brain research 1249:202-211.
Momeni P, DeTucci K, Straub RE, Weinberger DR, Davies P, Grafman J, Hardy J, Huey ED (2010) Progranulin (GRN) in two siblings of a Latino family and in other patients with schizophrenia. Neurocase 16:273-279.
Morelli L, Llovera R, Gonzalez SA, Affranchino JL, Prelli F, Frangione B, Ghiso J, Castano EM (2003) Differential degradation of amyloid beta genetic

variants associated with hereditary dementia or stroke by insulin-degrading enzyme. J Biol Chem 278:23221-23226.
Morishima-Kawashima M, Kosik KS (1996) The pool of map kinase associated with microtubules is small but constitutively active. Mol Biol Cell 7:893-905.
Mulholland DJ, Dedhar S, Wu H, Nelson CC (2006) PTEN and GSK3beta: key regulators of progression to androgen-independent prostate cancer. Oncogene 25:329-337.
Murphy MP, Beckett TL, Ding Q, Patel E, Markesbery WR, St Clair DK, LeVine H, 3rd, Keller JN (2007) Abeta solubility and deposition during AD progression and in APPxPS-1 knock-in mice. Neurobiology of disease 27:301-311.
Murrell J, Farlow M, Ghetti B, Benson MD (1991) A mutation in the amyloid precursor protein associated with hereditary Alzheimer's disease. Science 254:97-99.
Nacharaju P, Lewis J, Easson C, Yen S, Hackett J, Hutton M, Yen SH (1999) Accelerated filament formation from tau protein with specific FTDP-17 missense mutations. FEBS Lett 447:195-199.
Naj AC et al. (2011) Common variants at MS4A4/MS4A6E, CD2AP, CD33 and EPHA1 are associated with late-onset Alzheimer's disease. Nat Genet 43:436-441.
Naphade SB, Kigerl KA, Jakeman LB, Kostyk SK, Popovich PG, Kuret J (2010) Progranulin expression is upregulated after spinal contusion in mice. Acta neuropathologica 119:123-133.
Neumann M, Rademakers R, Roeber S, Baker M, Kretzschmar HA, Mackenzie IR (2009) A new subtype of frontotemporal lobar degeneration with FUS pathology. Brain : a journal of neurology 132:2922-2931.
Neumann M, Sampathu DM, Kwong LK, Truax AC, Micsenyi MC, Chou TT, Bruce J, Schuck T, Grossman M, Clark CM, McCluskey LF, Miller BL, Masliah E, Mackenzie IR, Feldman H, Feiden W, Kretzschmar HA, Trojanowski JQ, Lee VM (2006) Ubiquitinated TDP-43 in frontotemporal lobar degeneration and amyotrophic lateral sclerosis. Science 314:130-133.
Noble W, Olm V, Takata K, Casey E, Mary O, Meyerson J, Gaynor K, LaFrancois J, Wang L, Kondo T, Davies P, Burns M, Veeranna, Nixon R, Dickson D, Matsuoka Y, Ahlijanian M, Lau LF, Duff K (2003) Cdk5 is a key factor in tau aggregation and tangle formation in vivo. Neuron 38:555-565.
Ohia-Nwoko O, Montazari S, Lau YS, Eriksen JL (2014) Long-term treadmill exercise attenuates tau pathology in P301S tau transgenic mice. Molecular neurodegeneration 9:54.
Palmert MR, Golde TE, Cohen ML, Kovacs DM, Tanzi RE, Gusella JF, Usiak MF, Younkin LH, Younkin SG (1988) Amyloid protein precursor messenger RNAs: differential expression in Alzheimer's disease. Science 241:1080-1084.
Palop JJ, Mucke L (2010) Amyloid-beta-induced neuronal dysfunction in Alzheimer's disease: from synapses toward neural networks. Nature neuroscience 13:812-818.
Pao WC, Dickson DW, Crook JE, Finch NA, Rademakers R, Graff-Radford NR (2011) Hippocampal sclerosis in the elderly: genetic and pathologic

findings, some mimicking Alzheimer disease clinically. Alzheimer disease and associated disorders 25:364-368.
Papegaey A, Eddarkaoui S, Deramecourt V, Fernandez-Gomez FJ, Pantano P, Obriot H, Machala C, Anquetil V, Camuzat A, Brice A, Maurage CA, Le Ber I, Duyckaerts C, Buee L, Sergeant N, Buee-Scherrer V (2016) Reduced Tau protein expression is associated with frontotemporal degeneration with progranulin mutation. Acta Neuropathol Commun 4:74.
Paylor R, Crawley JN (1997) Inbred strain differences in prepulse inhibition of the mouse startle response. Psychopharmacology (Berl) 132:169-180.
Pearson HA, Peers C (2006) Physiological roles for amyloid beta peptides. J Physiol 575:5-10.
Pei JJ, Gong CX, Iqbal K, Grundke-Iqbal I, Wu QL, Winblad B, Cowburn RF (1998) Subcellular distribution of protein phosphatases and abnormally phosphorylated tau in the temporal cortex from Alzheimer's disease and control brains. J Neural Transm (Vienna) 105:69-83.
Pei JJ, Braak E, Braak H, Grundke-Iqbal I, Iqbal K, Winblad B, Cowburn RF (1999) Distribution of active glycogen synthase kinase 3beta (GSK-3beta) in brains staged for Alzheimer disease neurofibrillary changes. J Neuropathol Exp Neurol 58:1010-1019.
Pei JJ, Khatoon S, An WL, Nordlinder M, Tanaka T, Braak H, Tsujio I, Takeda M, Alafuzoff I, Winblad B, Cowburn RF, Grundke-Iqbal I, Iqbal K (2003) Role of protein kinase B in Alzheimer's neurofibrillary pathology. Acta Neuropathol 105:381-392.
Pereson S, Wils H, Kleinberger G, McGowan E, Vandewoestyne M, Van Broeck B, Joris G, Cuijt I, Deforce D, Hutton M, Van Broeckhoven C, Kumar-Singh S (2009) Progranulin expression correlates with dense-core amyloid plaque burden in Alzheimer disease mouse models. J Pathol 219:173-181.
Perez M, Hernandez F, Lim F, Diaz-Nido J, Avila J (2003) Chronic lithium treatment decreases mutant tau protein aggregation in a transgenic mouse model. J Alzheimers Dis 5:301-308.
Perry DC, Lehmann M, Yokoyama JS, Karydas A, Lee JJ, Coppola G, Grinberg LT, Geschwind D, Seeley WW, Miller BL, Rosen H, Rabinovici G (2013)

Progranulin mutations as risk factors for Alzheimer disease. JAMA Neurol 70:774-778.
Petkau TL, Zhu S, Lu G, Fernando S, Cynader M, Leavitt BR (2013) Sensitivity to neurotoxic stress is not increased in progranulin-deficient mice. Neurobiology of aging 34:2548-2550.
Petkau TL, Neal SJ, Orban PC, MacDonald JL, Hill AM, Lu G, Feldman HH, Mackenzie IR, Leavitt BR (2010) Progranulin expression in the developing and adult murine brain. J Comp Neurol 518:3931-3947.
Petkau TL, Neal SJ, Milnerwood A, Mew A, Hill AM, Orban P, Gregg J, Lu G, Feldman HH, Mackenzie IR, Raymond LA, Leavitt BR (2012) Synaptic dysfunction in progranulin-deficient mice. Neurobiol Dis 45:711-722.
Petoukhov E, Fernando S, Mills F, Shivji F, Hunter D, Krieger C, Silverman MA, Bamji SX (2013) Activity-dependent secretion of progranulin from synapses. Journal of cell science 126:5412-5421.
Philips T, De Muynck L, Thu HN, Weynants B, Vanacker P, Dhondt J, Sleegers K, Schelhaas HJ, Verbeek M, Vandenberghe R, Sciot R, Van Broeckhoven C, Lambrechts D, Van Leuven F, Van Den Bosch L, Robberecht W, Van Damme P (2010) Microglial upregulation of progranulin as a marker of motor neuron degeneration. Journal of neuropathology and experimental neurology 69:1191-1200.
Pickford F, Marcus J, Camargo LM, Xiao Q, Graham D, Mo JR, Burkhardt M, Kulkarni V, Crispino J, Hering H, Hutton M (2011) Progranulin is a chemoattractant for microglia and stimulates their endocytic activity. Am J Pathol 178:284-295.
Planel E, Bretteville A, Liu L, Virag L, Du AL, Yu WH, Dickson DW, Whittington RA, Duff KE (2009) Acceleration and persistence of neurofibrillary pathology in a mouse model of tauopathy following anesthesia. FASEB

journal : official publication of the Federation of American Societies for Experimental Biology 23:2595-2604.
Ponte P, Gonzalez-DeWhitt P, Schilling J, Miller J, Hsu D, Greenberg B, Davis K, Wallace W, Lieberburg I, Fuller F (1988) A new A4 amyloid mRNA contains a domain homologous to serine proteinase inhibitors. Nature 331:525-527.
Poorkaj P, Bird TD, Wijsman E, Nemens E, Garruto RM, Anderson L, Andreadis A, Wiederholt WC, Raskind M, Schellenberg GD (1998) Tau is a candidate gene for chromosome 17 frontotemporal dementia. Ann Neurol 43:815-825.
Prasher VP, Farrer MJ, Kessling AM, Fisher EM, West RJ, Barber PC, Butler AC (1998) Molecular mapping of Alzheimer-type dementia in Down's syndrome. Ann Neurol 43:380-383.
Prince M, Bryce R, Albanese E, Wimo A, Ribeiro W, Ferri CP (2013) The global prevalence of dementia: a systematic review and metaanalysis. Alzheimers Dement 9:63-75 e62.
Qiao X, Cummins DJ, Paul SM (2001) Neuroinflammation-induced acceleration of amyloid deposition in the APPV717F transgenic mouse. Eur J Neurosci 14:474-482.
Rademakers R, Rovelet-Lecrux A (2009) Recent insights into the molecular genetics of dementia. Trends in neurosciences 32:451-461.
Rademakers R et al. (2008) Common variation in the miR-659 binding-site of GRN is a major risk factor for TDP43-positive frontotemporal dementia. Hum Mol Genet 17:3631-3642.
Rademakers R et al. (2007) Phenotypic variability associated with progranulin haploinsufficiency in patients with the common 1477C-->T (Arg493X) mutation: an international initiative. The Lancet Neurology 6:857-868.
Rankin CA, Sun Q, Gamblin TC (2008) Pre-assembled tau filaments phosphorylated by GSK-3b form large tangle-like structures. Neurobiology of disease 31:368-377.
Rascovsky K et al. (2011) Sensitivity of revised diagnostic criteria for the behavioural variant of frontotemporal dementia. Brain : a journal of neurology 134:2456-2477.
Ratnavalli E, Brayne C, Dawson K, Hodges JR (2002) The prevalence of frontotemporal dementia. Neurology 58:1615-1621.
Revuelta GJ, Rosso A, Lippa CF (2008) Association between progranulin and beta-amyloid in dementia with Lewy bodies. American journal of Alzheimer's disease and other dementias 23:488-493.
Richet E, Pooler AM, Rodriguez T, Novoselov SS, Schmidtke G, Groettrup M, Hanger DP, Cheetham ME, van der Spuy J (2012) NUB1 modulation of

GSK3beta reduces tau aggregation. Human molecular genetics 21:5254-5267.
Roberson ED (2012) Mouse models of frontotemporal dementia. Ann Neurol 72:837-849.
Rogers J, Webster S, Lue LF, Brachova L, Civin WH, Emmerling M, Shivers B, Walker D, McGeer P (1996) Inflammation and Alzheimer's disease pathogenesis. Neurobiol Aging 17:681-686.
Rollinson S, Rohrer JD, van der Zee J, Sleegers K, Mead S, Engelborghs S, Collinge J, De Deyn PP, Mann DM, Van Broeckhoven C, Pickering-Brown SM (2011) No association of PGRN 3'UTR rs5848 in frontotemporal lobar degeneration. Neurobiology of aging 32:754-755.
Rosen EY, Wexler EM, Versano R, Coppola G, Gao F, Winden KD, Oldham MC, Martens LH, Zhou P, Farese RV, Jr., Geschwind DH (2011) Functional genomic analyses identify pathways dysregulated by progranulin deficiency, implicating Wnt signaling. Neuron 71:1030-1042.
Rosso SM, Donker Kaat L, Baks T, Joosse M, de Koning I, Pijnenburg Y, de Jong D, Dooijes D, Kamphorst W, Ravid R, Niermeijer MF, Verheij F, Kremer HP, Scheltens P, van Duijn CM, Heutink P, van Swieten JC (2003) Frontotemporal dementia in The Netherlands: patient characteristics and prevalence estimates from a population-based study. Brain 126:2016-2022.
Rovelet-Lecrux A, Hannequin D, Raux G, Le Meur N, Laquerriere A, Vital A, Dumanchin C, Feuillette S, Brice A, Vercelletto M, Dubas F, Frebourg T, Campion D (2006) APP locus duplication causes autosomal dominant early-onset Alzheimer disease with cerebral amyloid angiopathy. Nat Genet 38:24-26.
Rudy B, Fishell G, Lee S, Hjerling-Leffler J (2011) Three groups of interneurons account for nearly 100% of neocortical GABAergic neurons. Dev Neurobiol 71:45-61.
Ryan CL, Baranowski DC, Chitramuthu BP, Malik S, Li Z, Cao M, Minotti S, Durham HD, Kay DG, Shaw CA, Bennett HP, Bateman A (2009)

Progranulin is expressed within motor neurons and promotes neuronal cell survival. BMC neuroscience 10:130.
Sandbrink R, Masters CL, Beyreuther K (1994) Similar alternative splicing of a non-homologous domain in beta A4-amyloid protein precursor-like proteins. J Biol Chem 269:14227-14234.
Scattoni ML, Gasparini L, Alleva E, Goedert M, Calamandrei G, Spillantini MG (2010) Early behavioural markers of disease in P301S tau transgenic mice. Behavioural brain research 208:250-257.
Schaeffer V, Lavenir I, Ozcelik S, Tolnay M, Winkler DT, Goedert M (2012) Stimulation of autophagy reduces neurodegeneration in a mouse model of human tauopathy. Brain : a journal of neurology 135:2169-2177.
Scharf MT, Woo NH, Lattal KM, Young JZ, Nguyen PV, Abel T (2002) Protein synthesis is required for the enhancement of long-term potentiation and long-term memory by spaced training. J Neurophysiol 87:2770-2777.
Seelaar H, Rohrer JD, Pijnenburg YA, Fox NC, van Swieten JC (2011) Clinical, genetic and pathological heterogeneity of frontotemporal dementia: a review. Journal of neurology, neurosurgery, and psychiatry 82:476-486.
Selkoe DJ (2001) Alzheimer's disease results from the cerebral accumulation and cytotoxicity of amyloid beta-protein. J Alzheimers Dis 3:75-80.
Seshadri S et al. (2010) Genome-wide analysis of genetic loci associated with Alzheimer disease. Jama 303:1832-1840.
Seubert P, Vigo-Pelfrey C, Esch F, Lee M, Dovey H, Davis D, Sinha S, Schlossmacher M, Whaley J, Swindlehurst C, et al. (1992) Isolation and quantification of soluble Alzheimer's beta-peptide from biological fluids. Nature 359:325-327.
Shaftel SS, Griffin WS, O'Banion MK (2008) The role of interleukin-1 in neuroinflammation and Alzheimer disease: an evolving perspective. J Neuroinflammation 5:7.
Shaftel SS, Kyrkanides S, Olschowka JA, Miller JN, Johnson RE, O'Banion MK (2007) Sustained hippocampal IL-1 beta overexpression mediates chronic

neuroinflammation and ameliorates Alzheimer plaque pathology. J Clin Invest 117:1595-1604.
Shapiro LA, Perez ZD, Foresti ML, Arisi GM, Ribak CE (2009) Morphological and ultrastructural features of Iba1-immunolabeled microglial cells in the hippocampal dentate gyrus. Brain research 1266:29-36.
Sheng J, Su L, Xu Z, Chen G (2014) Progranulin polymorphism rs5848 is associated with increased risk of Alzheimer's disease. Gene 542:141-145.
Sheng JG, Mrak RE, Griffin WS (1997) Neuritic plaque evolution in Alzheimer's disease is accompanied by transition of activated microglia from primed to enlarged to phagocytic forms. Acta Neuropathol 94:1-5.
Sherrington R et al. (1995) Cloning of a gene bearing missense mutations in early-onset familial Alzheimer's disease. Nature 375:754-760.
Shoji M, Golde TE, Ghiso J, Cheung TT, Estus S, Shaffer LM, Cai XD, McKay DM, Tintner R, Frangione B, et al. (1992) Production of the Alzheimer amyloid beta protein by normal proteolytic processing. Science 258:126-129.
Singh TJ, Grundke-Iqbal I, McDonald B, Iqbal K (1994) Comparison of the phosphorylation of microtubule-associated protein tau by non-proline dependent protein kinases. Mol Cell Biochem 131:181-189.
Singh TJ, Zaidi T, Grundke-Iqbal I, Iqbal K (1995) Modulation of GSK-3-catalyzed phosphorylation of microtubule-associated protein tau by non-proline-dependent protein kinases. FEBS Lett 358:4-8.
Singh TJ, Zaidi T, Grundke-Iqbal I, Iqbal K (1996) Non-proline-dependent protein kinases phosphorylate several sites found in tau from Alzheimer disease brain. Mol Cell Biochem 154:143-151.
Sironi JJ, Yen SH, Gondal JA, Wu Q, Grundke-Iqbal I, Iqbal K (1998) Ser-262 in human recombinant tau protein is a markedly more favorable site for phosphorylation by CaMKII than PKA or PhK. FEBS Lett 436:471-475.
Sleegers K, Brouwers N, Maurer-Stroh S, van Es MA, Van Damme P, van Vught PW, van der Zee J, Serneels S, De Pooter T, Van den Broeck M, Cruts M, Schymkowitz J, De Jonghe P, Rousseau F, van den Berg LH, Robberecht W, Van Broeckhoven C (2008) Progranulin genetic variability contributes to amyotrophic lateral sclerosis. Neurology 71:253-259.
Smith KR, Damiano J, Franceschetti S, Carpenter S, Canafoglia L, Morbin M, Rossi G, Pareyson D, Mole SE, Staropoli JF, Sims KB, Lewis J, Lin WL, Dickson DW, Dahl HH, Bahlo M, Berkovic SF (2012) Strikingly different clinicopathological phenotypes determined by progranulin-mutation dosage. Am J Hum Genet 90:1102-1107.
Song W, Nadeau P, Yuan M, Yang X, Shen J, Yankner BA (1999) Proteolytic release and nuclear translocation of Notch-1 are induced by presenilin-1 and impaired by pathogenic presenilin-1 mutations. Proc Natl Acad Sci U S A 96:6959-6963.
Spencer CM, Serysheva E, Yuva-Paylor LA, Oostra BA, Nelson DL, Paylor R (2006) Exaggerated behavioral phenotypes in Fmr1/Fxr2 double knockout

mice reveal a functional genetic interaction between Fragile X-related proteins. Human molecular genetics 15:1984-1994.
Spillantini MG, Murrell JR, Goedert M, Farlow MR, Klug A, Ghetti B (1998) Mutation in the tau gene in familial multiple system tauopathy with presenile dementia. Proc Natl Acad Sci U S A 95:7737-7741.
Spittaels K, Van den Haute C, Van Dorpe J, Geerts H, Mercken M, Bruynseels K, Lasrado R, Vandezande K, Laenen I, Boon T, Van Lint J, Vandenheede J, Moechars D, Loos R, Van Leuven F (2000) Glycogen synthase kinase-3beta phosphorylates protein tau and rescues the axonopathy in the central nervous system of human four-repeat tau transgenic mice. J Biol Chem 275:41340-41349.
Stambolic V, Ruel L, Woodgett JR (1996) Lithium inhibits glycogen synthase kinase-3 activity and mimics wingless signalling in intact cells. Curr Biol 6:1664-1668.
Stoothoff WH, Cho JH, McDonald RP, Johnson GV (2005) FRAT-2 preferentially increases glycogen synthase kinase 3 beta-mediated phosphorylation of primed sites, which results in enhanced tau phosphorylation. The Journal of biological chemistry 280:270-276.
Streit WJ (2006) Microglial senescence: does the brain's immune system have an expiration date? Trends Neurosci 29:506-510.
Streit WJ, Xue QS (2013) Microglial senescence. CNS Neurol Disord Drug Targets 12:763-767.
Streit WJ, Khoshbouei H, Bechmann I (2021) The Role of Microglia in Sporadic Alzheimer's Disease. J Alzheimers Dis 79:961-968.
Sudduth TL, Schmitt FA, Nelson PT, Wilcock DM (2013) Neuroinflammatory phenotype in early Alzheimer's disease. Neurobiol Aging 34:1051-1059.
Suh HS, Choi N, Tarassishin L, Lee SC (2012) Regulation of progranulin expression in human microglia and proteolysis of progranulin by matrix metalloproteinase-12 (MMP-12). PloS one 7:e35115.
Suzuki M, Lee HC, Kayasuga Y, Chiba S, Nedachi T, Matsuwaki T, Yamanouchi K, Nishihara M (2009) Roles of progranulin in sexual differentiation of the developing brain and adult neurogenesis. J Reprod Dev 55:351-355.
Szekanecz Z, Koch AE (2007) Macrophages and their products in rheumatoid arthritis. Curr Opin Rheumatol 19:289-295.
Takahashi H, Klein ZA, Bhagat SM, Kaufman AC, Kostylev MA, Ikezu T, Strittmatter SM (2017a) Opposing effects of progranulin deficiency on amyloid and tau pathologies via microglial TYROBP network. Acta neuropathologica.
Takahashi H, Klein ZA, Bhagat SM, Kaufman AC, Kostylev MA, Ikezu T, Strittmatter SM, Alzheimer's Disease Neuroimaging I (2017b) Opposing effects of progranulin deficiency on amyloid and tau pathologies via microglial TYROBP network. Acta Neuropathol 133:785-807.
Takeuchi H, Iba M, Inoue H, Higuchi M, Takao K, Tsukita K, Karatsu Y, Iwamoto Y, Miyakawa T, Suhara T, Trojanowski JQ, Lee VM, Takahashi R (2011) P301S mutant human tau transgenic mice manifest early symptoms of

human tauopathies with dementia and altered sensorimotor gating. PloS one 6:e21050.
Tanaka Y, Matsuwaki T, Yamanouchi K, Nishihara M (2013) Exacerbated inflammatory responses related to activated microglia after traumatic brain injury in progranulin-deficient mice. Neuroscience 231:49-60.
Tanaka Y, Chambers JK, Matsuwaki T, Yamanouchi K, Nishihara M (2014) Possible involvement of lysosomal dysfunction in pathological changes of the brain in aged progranulin-deficient mice. Acta Neuropathol Commun 2:78.
Tang W et al. (2011) The growth factor progranulin binds to TNF receptors and is therapeutic against inflammatory arthritis in mice. Science 332:478-484.
Tanzi RE, McClatchey AI, Lamperti ED, Villa-Komaroff L, Gusella JF, Neve RL (1988) Protease inhibitor domain encoded by an amyloid protein precursor mRNA associated with Alzheimer's disease. Nature 331:528-530.
Tao J, Ji F, Wang F, Liu B, Zhu Y (2012) Neuroprotective effects of progranulin in ischemic mice. Brain research 1436:130-136.
Tapia L, Milnerwood A, Guo A, Mills F, Yoshida E, Vasuta C, Mackenzie IR, Raymond L, Cynader M, Jia W, Bamji SX (2011) Progranulin deficiency decreases gross neural connectivity but enhances transmission at individual synapses. The Journal of neuroscience : the official journal of the Society for Neuroscience 31:11126-11132.
Thinakaran G, Koo EH (2008) Amyloid precursor protein trafficking, processing, and function. J Biol Chem 283:29615-29619.
Toh H, Chitramuthu BP, Bennett HP, Bateman A (2011) Structure, function, and mechanism of progranulin; the brain and beyond. Journal of molecular neuroscience : MN 45:538-548.
Tomlinson BE, Blessed G, Roth M (1970) Observations on the brains of demented old people. J Neurol Sci 11:205-242.
Tsai LH, Takahashi T, Caviness VS, Jr., Harlow E (1993) Activity and expression pattern of cyclin-dependent kinase 5 in the embryonic mouse nervous system. Development 119:1029-1040.
Tsai LH, Delalle I, Caviness VS, Jr., Chae T, Harlow E (1994) p35 is a neural-specific regulatory subunit of cyclin-dependent kinase 5. Nature 371:419-423.
Van Damme P, Van Hoecke A, Lambrechts D, Vanacker P, Bogaert E, van Swieten J, Carmeliet P, Van Den Bosch L, Robberecht W (2008) Progranulin functions as a neurotrophic factor to regulate neurite outgrowth and enhance neuronal survival. The Journal of cell biology 181:37-41.
Van Deerlin VM et al. (2010) Common variants at 7p21 are associated with frontotemporal lobar degeneration with TDP-43 inclusions. Nature genetics 42:234-239.
van der Zee J, Van Langenhove T, Kleinberger G, Sleegers K, Engelborghs S, Vandenberghe R, Santens P, Van den Broeck M, Joris G, Brys J, Mattheijssens M, Peeters K, Cras P, De Deyn PP, Cruts M, Van Broeckhoven C (2011) TMEM106B is associated with frontotemporal lobar

degeneration in a clinically diagnosed patient cohort. Brain : a journal of neurology 134:808-815.
Vassar R et al. (1999) Beta-secretase cleavage of Alzheimer's amyloid precursor protein by the transmembrane aspartic protease BACE. Science 286:735-741.
Vazquez F, Ramaswamy S, Nakamura N, Sellers WR (2000) Phosphorylation of the PTEN tail regulates protein stability and function. Molecular and cellular biology 20:5010-5018.
Vercellino M, Grifoni S, Romagnolo A, Masera S, Mattioda A, Trebini C, Chiavazza C, Caligiana L, Capello E, Mancardi GL, Giobbe D, Mutani R, Giordana MT, Cavalla P (2011) Progranulin expression in brain tissue and cerebrospinal fluid levels in multiple sclerosis. Mult Scler 17:1194-1201.
Viswanathan J, Makinen P, Helisalmi S, Haapasalo A, Soininen H, Hiltunen M (2009) An association study between granulin gene polymorphisms and Alzheimer's disease in Finnish population. Am J Med Genet B Neuropsychiatr Genet 150B:747-750.
Vollert C, Forkuo GS, Bond RA, Eriksen JL (2013) Chronic treatment with DCPCX, an adenosine A(1) antagonist, worsens long-term memory. Neuroscience letters 548:296-300.
Vollert C, Zagaar M, Hovatta I, Taneja M, Vu A, Dao A, Levine A, Alkadhi K, Salim S (2011) Exercise prevents sleep deprivation-associated anxiety-like behavior in rats: potential role of oxidative stress mechanisms. Behav Brain Res 224:233-240.
Vom Berg J, Prokop S, Miller KR, Obst J, Kalin RE, Lopategui-Cabezas I, Wegner A, Mair F, Schipke CG, Peters O, Winter Y, Becher B, Heppner FL (2012) Inhibition of IL-12/IL-23 signaling reduces Alzheimer's disease-like pathology and cognitive decline. Nat Med 18:1812-1819.
Vossel KA, Miller BL (2008) New approaches to the treatment of frontotemporal lobar degeneration. Current opinion in neurology 21:708-716.
Walf AA, Frye CA (2007) The use of the elevated plus maze as an assay of anxiety-related behavior in rodents. Nature protocols 2:322-328.
Walsh DM, Klyubin I, Fadeeva JV, Cullen WK, Anwyl R, Wolfe MS, Rowan MJ, Selkoe DJ (2002) Naturally secreted oligomers of amyloid beta protein potently inhibit hippocampal long-term potentiation in vivo. Nature 416:535-539.
Wang JZ, Grundke-Iqbal I, Iqbal K (1996) Glycosylation of microtubule-associated protein tau: an abnormal posttranslational modification in Alzheimer's disease. Nat Med 2:871-875.
Wang JZ, Xia YY, Grundke-Iqbal I, Iqbal K (2013) Abnormal hyperphosphorylation of tau: sites, regulation, and molecular mechanism of neurofibrillary degeneration. J Alzheimers Dis 33 Suppl 1:S123-139.
Wang JZ, Gong CX, Zaidi T, Grundke-Iqbal I, Iqbal K (1995) Dephosphorylation of Alzheimer paired helical filaments by protein phosphatase-2A and -2B. J Biol Chem 270:4854-4860.
Wang JZ, Wu Q, Smith A, Grundke-Iqbal I, Iqbal K (1998) Tau is phosphorylated by GSK-3 at several sites found in Alzheimer disease and its biological

activity markedly inhibited only after it is prephosphorylated by A-kinase. FEBS Lett 436:28-34.
Weekman EM, Sudduth TL, Abner EL, Popa GJ, Mendenhall MD, Brothers HM, Braun K, Greenstein A, Wilcock DM (2014) Transition from an M1 to a mixed neuroinflammatory phenotype increases amyloid deposition in APP/PS1 transgenic mice. J Neuroinflammation 11:127.
Weggen S, Beher D (2012) Molecular consequences of amyloid precursor protein and presenilin mutations causing autosomal-dominant Alzheimer's disease. Alzheimers Res Ther 4:9.
Weingarten MD, Lockwood AH, Hwo SY, Kirschner MW (1975) A protein factor essential for microtubule assembly. Proc Natl Acad Sci U S A 72:1858-1862.
Werner KH, Roberts NA, Rosen HJ, Dean DL, Kramer JH, Weiner MW, Miller BL, Levenson RW (2007) Emotional reactivity and emotion recognition in frontotemporal lobar degeneration. Neurology 69:148-155.
Whitwell JL, Josephs KA (2012) Recent advances in the imaging of frontotemporal dementia. Current neurology and neuroscience reports 12:715-723.
Whitwell JL, Jack CR, Jr., Boeve BF, Senjem ML, Baker M, Rademakers R, Ivnik RJ, Knopman DS, Wszolek ZK, Petersen RC, Josephs KA (2009) Voxel-based morphometry patterns of atrophy in FTLD with mutations in MAPT or PGRN. Neurology 72:813-820.
Wilcock DM, Zhao Q, Morgan D, Gordon MN, Everhart A, Wilson JG, Lee JE, Colton CA (2011) Diverse inflammatory responses in transgenic mouse models of Alzheimer's disease and the effect of immunotherapy on these responses. ASN Neuro 3:249-258.
Wilhelmsen KC, Lynch T, Pavlou E, Higgins M, Nygaard TG (1994) Localization of disinhibition-dementia-parkinsonism-amyotrophy complex to 17q21-22. Am J Hum Genet 55:1159-1165.
Wils H, Kleinberger G, Pereson S, Janssens J, Capell A, Van Dam D, Cuijt I, Joris G, De Deyn PP, Haass C, Van Broeckhoven C, Kumar-Singh S (2012) Cellular ageing, increased mortality and FTLD-TDP-associated neuropathology in progranulin knockout mice. J Pathol 228:67-76.
Wilson AC, Dugger BN, Dickson DW, Wang DS (2011) TDP-43 in aging and Alzheimer's disease - a review. International journal of clinical and experimental pathology 4:147-155.
Woo NH, Duffy SN, Abel T, Nguyen PV (2003) Temporal spacing of synaptic stimulation critically modulates the dependence of LTP on cyclic AMP-dependent protein kinase. Hippocampus 13:293-300.
Woodgett JR (1990) Molecular cloning and expression of glycogen synthase kinase-3/factor A. EMBO J 9:2431-2438.
Wyss-Coray T (2006) Inflammation in Alzheimer disease: driving force, bystander or beneficial response? Nat Med 12:1005-1015.
Xu HM, Tan L, Wan Y, Tan MS, Zhang W, Zheng ZJ, Kong LL, Wang ZX, Jiang T, Yu JT (2016) PGRN Is Associated with Late-Onset Alzheimer's Disease: a

Case-Control Replication Study and Meta-analysis. Molecular neurobiology.
Yamamoto M, Kiyota T, Horiba M, Buescher JL, Walsh SM, Gendelman HE, Ikezu T (2007) Interferon-gamma and tumor necrosis factor-alpha regulate amyloid-beta plaque deposition and beta-secretase expression in Swedish mutant APP transgenic mice. Am J Pathol 170:680-692.
Yankner BA, Mesulam MM (1991) Seminars in medicine of the Beth Israel Hospital, Boston. beta-Amyloid and the pathogenesis of Alzheimer's disease. N Engl J Med 325:1849-1857.
Yin F, Dumont M, Banerjee R, Ma Y, Li H, Lin MT, Beal MF, Nathan C, Thomas B, Ding A (2010a) Behavioral deficits and progressive neuropathology in progranulin-deficient mice: a mouse model of frontotemporal dementia. FASEB J 24:4639-4647.
Yin F, Banerjee R, Thomas B, Zhou P, Qian L, Jia T, Ma X, Ma Y, Iadecola C, Beal MF, Nathan C, Ding A (2010b) Exaggerated inflammation, impaired host defense, and neuropathology in progranulin-deficient mice. J Exp Med 207:117-128.
Yoshida H, Crowther RA, Goedert M (2002) Functional effects of tau gene mutations deltaN296 and N296H. J Neurochem 80:548-551.
Yoshiyama Y, Higuchi M, Zhang B, Huang SM, Iwata N, Saido TC, Maeda J, Suhara T, Trojanowski JQ, Lee VM (2007) Synapse loss and microglial activation precede tangles in a P301S tauopathy mouse model. Neuron 53:337-351.
Zhu S, Tai C, Petkau TL, Zhang S, Liao C, Dong Z, Wen W, Chang Q, Tian Wang Y, MacVicar BA, Leavitt BR, Jia W, Cynader MS (2013) Progranulin promotes activation of microglia/macrophage after pilocarpine-induced status epilepticus. Brain research 1530:54-65.